

ARCH DAM-RESERVOIR INTERACTION MODELING
AND APPLICATION TO KARAKAYA DAM

by

Yasin M. FAHJAN

B.S. in C.E. Eastern Mediterranean University, 1992

M.S. in C.E. Eastern Mediterranean University, 1992

Submitted to the Institute for Graduate Studies in
Science and Engineering in partial fulfillment of
the requirements for the degree of

Doctor

of

Philosophy

Boğaziçi University

1998

Bogazici University Library



39001100104101

14

To my late brother

Dr. Zaki Fahjan

ACKNOWLEDGMENT

It gives me great pleasure here to express my gratitude to all the people who have guided, encouraged and made it possible for me to complete this work.

Words would not suffice to address my cordial gratitude and indebtedness to the thesis supervisor Dr. Osman Breki for his kindness and help which extends beyond my mere academic life. I feel indebted to him for his continued support, encouragement, patience and never-failing friendship in every stage of this study.

My sincere deepest gratitude goes to the thesis co-supervisor Dr. Mustafa Erdik for his continuous guidance and witty criticisms throughout this study. Special thanks goes to Dr. Nuray Aydınođlu for his valuable help and advices for the problems I encountered while developing the numerical model and to the other members of the committee; Dr. Cem Avcı and Dr. Yalın Yksel for their careful and constructive review of the draft.

I would also like to express my best wishes and thanks to all the members of Civil Engineering Department and Kandilli Observatory and Earthquake Research Center for their kindness and endless support. Special thanks goes to Dudu Soysal from Prota Bilgisayar for her neat drawings.

I would like to acknowledge the inspiration of my fiancée Firuze Kaymaz for her endless support, patience and encouragement. I am especially indebted to my family for their continuous emotional and financial support throughout my education. Also special thanks go to my friends and colleagues who have made the life easier in difficult times.

This study was carried out at the Department of Civil Engineering and was supported by the Research Fund of Bođazii University (Project No:96AO429). Acknowledgments goes to Bođazii University Foundation (BVAK) and Arab Student Aid International (ASAI) for their financial support without which it would have been impossible for me to complete this work.

ABSTRACT

An effective analytical model based on the hybrid FEM-DRBEM scheme has been developed to study the fluid-structure interaction and earthquake response of arch dam-reservoir systems. Applying the substructure technique, the finite element method is utilized to model dam structure and the dual reciprocity method is used to model the reservoir domain. Considering the bottom absorption effects, the reservoir domain is idealized as a finite region of irregular geometry adjacent to an infinite domain of uniform cross section. The three-dimensional dual reciprocity method is applied to model the finite domain of the reservoir. The uniform infinite domain is modeled by applying two-dimensional eigenvalue analysis based on the dual reciprocity formulations over the uniform cross section combined with a continuum expression in the upstream direction. Based on the model, a computer code has been developed to calculate the seismic response of a three-dimensional dam-reservoir system of arbitrary geometry to upstream-downstream, cross-stream and vertical harmonic ground motion. The model is verified by comparing the hydrodynamic response of a three-dimensional rectangular reservoir with that from the analytical formulation existing in the literature. The model was applied to investigate the hydrodynamic and structural response of the Karakaya dam-reservoir system. The effects of arch dam-reservoir interaction, the reservoir geometry and the reservoir boundary bottom absorption on the hydrodynamic and structural responses are studied

Key Words: Fluid-structure interaction, dual reciprocity boundary element method, finite element method, arch dam

ÖZET

Bu tezde, deprem etkisiyle kemer baraj-resrvuar sistemlerinde yapı-su etkileşimini incelemiştir. Bu amaçla sonlu elemanlar metodu (SEM) ve karşılıklı sınır elemanları metodu (KSEM) kullanılarak 3-boyutlu bir hibrid nümerik model geliştirmiştir. SEM kemer baraj gövdesinde, KSEM ise rezervuarın modellenmesinde kullanılmıştır. Baraj rezervuarı taban geometrisinin ve tabanın sönümlenme etkisinin hissedildiği sonlu uzunluktaki bir hacim ve enerji radyasyonu etkisiyle sönümlenmenin etkili olduğu üniform kesitli sonsuz bir hacim olarak iki parçada ele alınmıştır. Sonlu hacim için 3-boyutlu KSEM kullanılmıştır. Sonsuz hacimde, düşey düzlemde 2-boyutlu KSEM kullanılırken rezervuar aksı yönünde analitik bir ifadeden yararlanılmıştır. Geliştirilen modelle, istenen geometrideki 3-boyutlu kemer baraj-reservuar sistemlerinin depreme tepkisi elde edilebilmektedir. Model baraj ve rezervuarın depreme tepkilerinin ayrı ayrı hesaplanmasına olanak sağladığı gibi etkileşimlerinin de incelenmesine olanak sağlamaktadır. Model sonuçlarının doğruluğunun araştırılması ise literatürde mevcut olan basitleştirilmiş geometrideki baraj-reservuar sistemleri için elde edilen analitik model sonuçları kullanılarak yapılmıştır. Ayrıca modelin SEM ile geliştirilen kısımlarının sonuçları SAPIV programı sonuçları ile karşılaştırılmıştır. Karşılaştırmalar sonucunda modelin doğruluğu gösterilmiştir. Model Karakaya Barajı ve rezervuarına uygulanmıştır. Sistemin rezervuar aksına paralel veya dik yönlerde uygulanan bir depreme tepkisinin, yapı-su etkileşimi, taban geometrisi ve taban sönümlenmesi ile değişimi incelenmiştir. Model sonuçları baraj gövdesi üzerinde detaylı hidrodinamik basınç ve kuvvet dağılımları olarak sunulmuştur.

TABLE OF CONTENTS

	Page
ACKNOWLEDGMENT	iii
ABSTRACT	v
TABLE OF CONTENTS	vii
LIST OF TABLES	x
LIST OF FIGURES	xi
1. INTRODUCTION	1
1.1. Problem Definition	1
1.2. Literature Survey	4
1.2.1. Concrete Gravity Dam	4
1.2.2. Arch-Dam	6
1.3. Scope of the Study	8
2. ARCH DAM-RESERVOIR SYSTEMS AND GROUND MOTION	10
2.1. The Arch Dam	10
2.2. The Reservoir	12
2.3. Ground Motion	13
3. ANALYSIS OF THE ARCH DAM-RESERVOIR SYSTEM RESPONSE	14
3.1. Equations of Motion for the Dam Structure	14
3.2. Equations of Motion and Boundary Conditions for the Fluid Domain	17
3.2.1. Reservoir Free Surface Boundary Condition	18
3.2.2. Arch Dam-fluid Interface Boundary Condition	18
3.2.3. Reservoir Bottom and Banks Boundary Condition	19
3.2.4. The Radiation Boundary Conditions	19
3.2.5. Hydrodynamic Pressure and Force Responses	20
3.3. Equations of the Arch Dam-reservoir System	21
3.4. Responses to Arbitrary Ground Motion	22
4. THREE-DIMENSIONAL DUAL RECIPROCITY METHOD FOR THE RESERVOIR DOMAIN	23
4.1. Formulations for the Finite Domain of the Reservoir	23
4.2. Dual Reciprocity Method for the Helmholtz Equation	25
4.3. Dual Reciprocity Approximation Functions	28

4.4	Dual Reciprocity Formulations for the Reservoir Domain	30
5.	TWO-DIMENSIONAL DUAL RECIPROCITY METHOD TO MODEL THE INFINITE DOMAIN	33
5.1.	The Boundary Value Problem for the Infinite Region of the Reservoir	34
5.2.	Continuum Expression for the Pressure Along the Upstream Direction	36
5.3.	Dual Reciprocity Formulation for the Pressure Over the Uniform Cross Section	37
5.4.	Formulation of the Radiation Matrix	40
6.	VERIFICATION OF THE HYDRODYNAMIC MODEL	43
6.1.	Case Study: Three-Dimensional Rectangular Reservoir	43
6.2.	Verification of the DRBEM-Radiation Model	45
6.3.	Verification of the DRBEM-Reservoir Model	46
6.3.1.	The Hydrodynamic Pressure	46
6.3.2.	Hydrodynamic Forces	48
7.	CASE STUDY : DYNAMIC RESPONSES OF KARAKAYA DAM	92
7.1.	Idealization of the Karakaya Dam-Reservoir System	92
7.1.1.	The Dam Structure	92
7.1.2.	The Reservoir Domain	95
7.1.3.	The Ground Motion	96
7.2.	Hydrodynamic Responses on the Rigid Arch Dam	96
7.2.1.	Free Vibrations of The Infinite Domain	96
7.2.2.	Effects of Reservoir Geometry Shape	97
7.2.3.	Effects of Reservoir Boundary Absorption	98
7.3.	Dam-Water Interaction Effects	99
7.3.1.	Free Vibration of Karakaya Dam	99
7.3.2.	Hydrodynamic Forces on the Flexible Dam	99
7.3.3.	Structrual Responses	101
8.	CONCLUSIONS	140
8.1.	Hydrodynamic Response in Three-dimensional Rectangular Reservoir ...	141
8.2.	Hydrodynamic Response on the Upstream Face of Karakaya Dam	142
8.3.	Dam-Water Interaction Effects	142
	APPENDIX A: THIN PLATE SPLINE APPROXIMATION FUNCTIONS IN DRBEM ...	144
	APPENDIX B: FINITE ELEMENT FORMULATION OF THE RADIATION MATRIX ...	146

APPENDIX C: COMPUTER PROGRAM DAM3D	149
REFERENCES	151
REFERENCES NOT CITED	158

LIST OF TABLES

	Page
TABLE 6.1. Comparison of natural frequencies of the infinite domain in a three-dimensional rectangular reservoir.	50
TABLE 7.1. Comparison of natural frequencies of the infinite reservoir domain of Karakaya Dam (actual geometry reservoir case).	102
TABLE 7.2. Comparison of the free vibration frequencies of Karakaya Dam	103

LIST OF FIGURES

	Page
FIGURE 2.1. Arch dam-reservoir system	11
FIGURE 4.1 Idealization of arch dam-reservoir system	24
FIGURE 5.1. Infinite domain radiation model	35
FIGURE 6.1. Three-dimensional rectangular infinite reservoir	44
FIGURE 6.2.(a) Hydrodynamic pressure distribution on the upstream face of the rigid dam (harmonic upstream ground motion, reservoir boundary reflection coefficient, $\alpha_r = 1.0$	51
FIGURE 6.2.(b) Hydrodynamic pressure distribution on the upstream face of the rigid dam (harmonic upstream ground motion, reservoir boundary reflection coefficient, $\alpha_r = 1.0$	52
FIGURE 6.3.(a) Hydrodynamic pressure distribution on the upstream face of the rigid dam (harmonic upstream ground motion, reservoir boundary reflection coefficient, $\alpha_r = 0.75$	53
FIGURE 6.3.(b) Hydrodynamic pressure distribution on the upstream face of the rigid dam (harmonic upstream ground motion, reservoir boundary reflection coefficient, $\alpha_r = 0.75$).	54
FIGURE 6.4.(a) Hydrodynamic pressure distribution on the upstream face of the rigid dam (harmonic upstream ground motion, reservoir boundary reflection coefficient, $\alpha_r = 0.5$).	55
FIGURE 6.4.(b) Hydrodynamic pressure distribution on the upstream face of the rigid dam (harmonic upstream ground motion, reservoir boundary reflection	

coefficient, $\alpha_r=0.5$). 56

FIGURE 6.5.(a) Hydrodynamic pressure distribution on the upstream face of the rigid dam (harmonic upstream ground motion, reservoir boundary reflection coefficient, $\alpha_r=0.0$). 57

FIGURE 6.5.(b) Hydrodynamic pressure distribution on the upstream face of the rigid dam (harmonic upstream ground motion, reservoir boundary reflection coefficient, $\alpha_r=0.0$). 59

FIGURE 6.6.(a) Hydrodynamic pressure distribution along the reservoir bottom (rigid dam, harmonic upstream ground motion, boundary reflection coefficient, $\alpha_r=1.0$). 59

FIGURE 6.6.(b) Hydrodynamic pressure distribution along the reservoir bottom (rigid dam, harmonic upstream ground motion, boundary reflection coefficient, $\alpha_r=1.0$). 60

FIGURE 6.7.(a) Hydrodynamic pressure distribution along the reservoir bottom (rigid dam, harmonic upstream ground motion, boundary reflection coefficient, $\alpha_r=0.75$). 61

FIGURE 6.7.(b) Hydrodynamic pressure distribution along the reservoir bottom (rigid dam, harmonic upstream ground motion, boundary reflection coefficient, $\alpha_r=0.75$). 62

FIGURE 6.8.(a) Hydrodynamic pressure distribution along the reservoir bottom (rigid dam, harmonic upstream ground motion, boundary reflection coefficient, $\alpha_r=0.75$). 63

FIGURE 6.8.(b) Hydrodynamic pressure distribution along the reservoir bottom (rigid dam, harmonic upstream ground motion, boundary reflection coefficient, $\alpha_r=0.5$). 64

FIGURE 6.9.(a) Hydrodynamic pressure distribution along the reservoir bottom (rigid dam, harmonic upstream ground motion, boundary reflection coefficient, $\alpha_r=0.0$).	65
FIGURE 6.9.(b) Hydrodynamic pressure distribution along the reservoir bottom (rigid dam, harmonic upstream ground motion, boundary reflection coefficient, $\alpha_r=0.0$).	66
FIGURE 6.10.(a) Hydrodynamic pressures distribution on the upstream face of the rigid dam (harmonic vertical ground motion, reservoir boundary reflection coefficient, $\alpha_r=1.0$).	67
FIGURE 6.10.(b) Hydrodynamic pressures distribution on the upstream face of the rigid dam (harmonic vertical ground motion, reservoir boundary reflection coefficient, $\alpha_r=1.0$).	68
FIGURE 6.11.(a) Hydrodynamic pressures distribution on the upstream face of the rigid dam (harmonic vertical ground motion, reservoir boundary reflection coefficient, $\alpha_r=0.75$).	69
FIGURE 6.11.(b) Hydrodynamic pressures distribution on the upstream face of the rigid dam (harmonic vertical ground motion, reservoir boundary reflection coefficient, $\alpha_r=0.75$).	70
FIGURE 6.12.(a) Hydrodynamic pressures distribution on the upstream face of the rigid dam (harmonic vertical ground motion, reservoir boundary reflection coefficient, $\alpha_r=0.5$).	71
FIGURE 6.12.(b) Hydrodynamic pressures distribution on the upstream face of the rigid dam (harmonic vertical ground motion, reservoir boundary reflection coefficient, $\alpha_r=0.5$).	72

- FIGURE 6.13.(a) Hydrodynamic pressures distribution on the upstream face of the rigid dam (harmonic vertical ground motion, reservoir boundary reflection coefficient, $\alpha_r=0.0$). 73
- FIGURE 6.13.(b) Hydrodynamic pressures distribution on the upstream face of the rigid dam (harmonic vertical ground motion, reservoir boundary reflection coefficient, $\alpha_r=0.0$). 74
- FIGURE 6.14.(a) Hydrodynamic pressures distribution on the upstream face of the rigid dam (harmonic cross-stream ground motion, reservoir boundary reflection coefficient, $\alpha_r=1.0$). 76
- FIGURE 6.14.(b) Hydrodynamic pressures distribution on the upstream face of the rigid dam (harmonic cross-stream ground motion, reservoir boundary reflection coefficient, $\alpha_r=1.0$). 77
- FIGURE 6.15.(a) Hydrodynamic pressures distribution on the upstream face of the rigid dam (harmonic cross-stream ground motion, reservoir boundary reflection coefficient, $\alpha_r=0.75$). 78
- FIGURE 6.15.(b) Hydrodynamic pressures distribution on the upstream face of the rigid dam (harmonic cross-stream ground motion, reservoir boundary reflection coefficient, $\alpha_r=0.75$). 79
- FIGURE 6.16.(a) Hydrodynamic pressures distribution on the upstream face of the rigid dam (harmonic cross-stream ground motion, reservoir boundary reflection coefficient, $\alpha_r=0.5$). 80
- FIGURE 6.16.(b) Hydrodynamic pressures distribution on the upstream face of the rigid dam (harmonic cross-stream ground motion, reservoir boundary reflection coefficient, $\alpha_r=0.5$). 81
- FIGURE 6.17.(a) Hydrodynamic pressures distribution on the upstream face of the rigid

dam (harmonic cross-stream ground motion, reservoir boundary reflection coefficient, $\alpha_r = 0.0$). 82

FIGURE 6.17.(b) Hydrodynamic pressures distribution on the upstream face of the rigid dam (harmonic cross-stream ground motion, reservoir boundary reflection coefficient, $\alpha_r = 0.0$). 83

FIGURE 6.18. Total hydrodynamic force on the upstream face of a rigid dam due to harmonic upstream ground motion. 83

FIGURE 6.19. In-phase hydrodynamic force on the upstream face of a rigid dam due to harmonic upstream ground motion. 84

FIGURE 6.20. Out-of-phase hydrodynamic force on the upstream face of a rigid dam due to harmonic upstream ground motion. 85

FIGURE 6.21. Total hydrodynamic force on the upstream face of a rigid dam due to harmonic vertical ground motion. 86

FIGURE 6.22. In-phase hydrodynamic force on the upstream face of a rigid dam due to harmonic vertical ground motion. 87

FIGURE 6.23. Out-of-phase hydrodynamic force on the upstream face of a rigid dam due to harmonic vertical ground motion. 88

FIGURE 6.24. Total hydrodynamic force on the upstream face of a rigid dam due to harmonic cross-stream ground motion. 89

FIGURE 6.25. In-phase hydrodynamic force on the upstream face of a rigid dam due to harmonic cross-stream ground motion. 90

FIGURE 6.26. Out-of-phase hydrodynamic force on the upstream face of a rigid dam due to harmonic cross-stream ground motion. 91

FIGURE 7.1. The Karakaya Dam and reservoir system	93
FIGURE 7.2. Idealization of the Karakaya dam and reservoir system	94
FIGURE 7.3. Natural vibration modes of Karakaya Dam	104
FIGURE 7.4. Natural vibration modes of Karakaya Dam	105
FIGURE 7.5 Natural vibration modes of Karakaya Dam	106
FIGURE 7.6. The hydrodynamic pressure distribution on the upstream face of Karakaya Dam : without dam-reservoir interaction, symmetrical reservoir, harmonic upstream-downstream ground motion, reservoir boundary reflection coefficient, $\alpha_r=0.75$	107
FIGURE 7.7. The hydrodynamic pressure distribution on the upstream face of Karakaya Dam : without dam-reservoir interaction, symmetrical reservoir, harmonic vertical ground motion, reservoir boundary reflection coefficient, $\alpha_r=0.75$	108
FIGURE 7.8. The hydrodynamic pressure distribution on the upstream face of Karakaya Dam : without dam-reservoir interaction, symmetrical reservoir, harmonic cross-stream ground motion, reservoir boundary reflection coefficient, $\alpha_r=0.75$	109
FIGURE 7.9. The hydrodynamic pressure distribution on the upstream face of Karakaya Dam : without dam-reservoir interaction, actual geometry reservoir, harmonic upstream-downstream ground motion, reservoir boundary reflection coefficient, $\alpha_r=0.75$	110
FIGURE 7.10. The hydrodynamic pressure distribution on the upstream face of Karakaya Dam : without dam-reservoir interaction, actual geometry reservoir,	

harmonic vertical ground motion, reservoir boundary reflection coefficient,
 $\alpha_r=0.75$ 111

FIGURE 7.11. The hydrodynamic pressure distribution on the upstream face of Karakaya Dam : without dam-reservoir interaction, actual geometry reservoir, harmonic cross-stream ground motion, reservoir boundary reflection coefficient, $\alpha_r=0.75$ 112

FIGURE 7.12 The hydrodynamic pressure distribution on the upstream face of Karakaya Dam : with dam-reservoir interaction, symmetrical reservoir, harmonic upstream-downstream ground motion, reservoir boundary reflection coefficient, $\alpha_r=0.75$ 113

FIGURE 7.13. The hydrodynamic pressure distribution on the upstream face of Karakaya Dam : with dam-reservoir interaction, symmetrical reservoir, harmonic vertical ground motion, reservoir boundary reflection coefficient, $\alpha_r=0.75$ 114

FIGURE 7.14. The hydrodynamic pressure distribution on the upstream face of Karakaya Dam : with dam-reservoir interaction, symmetrical reservoir, harmonic cross-stream ground motion, reservoir boundary reflection coefficient, $\alpha_r=0.75$ 115

FIGURE 7.15. The hydrodynamic pressure distribution on the upstream face of Karakaya Dam : with dam-reservoir interaction, actual geometry reservoir, harmonic upstream-downstream ground motion, reservoir boundary reflection coefficient, $\alpha_r=0.75$ 116

FIGURE 7.16. The hydrodynamic pressure distribution on the upstream face of Karakaya Dam : with dam-reservoir interaction, actual geometry reservoir, harmonic vertical ground motion, reservoir boundary reflection coefficient, $\alpha_r=0.75$ 117

FIGURE 7.17. The hydrodynamic pressure distribution on the upstream face of Karakaya

Dam : with dam-reservoir interaction, actual geometry reservoir, harmonic cross-stream ground motion, reservoir boundary reflection coefficient, $\alpha_r=0.75$ 118

FIGURE 7.18. Total hydrodynamic force on the upstream face of Karakaya dam: without dam-reservoir interaction, symmetrical reservoir, harmonic upstream-downstream ground motion, reservoir boundary reflection coefficient, $\alpha_r=0.75$ 119

FIGURE 7.19. Total hydrodynamic force on the upstream face of Karakaya dam: without dam-reservoir interaction, symmetrical reservoir, harmonic vertical ground motion, reservoir boundary reflection coefficient, $\alpha_r=0.75$ 120

FIGURE 7.20. Total hydrodynamic force on the upstream face of Karakaya dam: without dam-reservoir interaction, symmetrical reservoir, harmonic cross-stream ground motion, reservoir boundary reflection coefficient, $\alpha_r=0.75$ 121

FIGURE 7.21. Total hydrodynamic force on the upstream face of Karakaya dam without dam-reservoir interaction for the symmetrical reservoir case due to harmonic the upstream-downstream ground motion. 122

FIGURE 7.22. Total hydrodynamic force on the upstream face of Karakaya dam without dam-reservoir interaction for the symmetrical reservoir case due to harmonic vertical ground motion. 123

FIGURE 7.23. Total hydrodynamic force on the upstream face of Karakaya dam without dam-reservoir interaction for the symmetrical reservoir case due to harmonic cross-stream ground motion. 124

FIGURE 7.24. Total hydrodynamic force on the upstream face of Karakaya dam without dam-reservoir interaction for the actual geometry reservoir case due to harmonic the upstream-downstream ground motion. 125

- FIGURE 7.25. Total hydrodynamic force on the upstream face of Karakaya dam without dam-reservoir interaction for the actual geometry reservoir case due to harmonic vertical ground motion 126
- FIGURE 7.26. Total hydrodynamic force on the upstream face of Karakaya dam without dam-reservoir interaction for the actual geometry reservoir case due to harmonic cross-downstream ground motion 127
- FIGURE 7.27 Total hydrodynamic force on the upstream face of Karakaya dam with dam-reservoir interaction for the symmetrical reservoir case due to harmonic the upstream-downstream ground motion 128
- FIGURE 7.28 Total hydrodynamic force on the upstream face of Karakaya dam with dam-reservoir interaction for the symmetrical reservoir case due to harmonic vertical ground motion. 129
- FIGURE 7.29 Total hydrodynamic force on the upstream face of Karakaya dam with dam-reservoir interaction for the symmetrical reservoir case due to harmonic cross-stream ground motion 130
- FIGURE 7.30 Total hydrodynamic force on the upstream face of Karakaya dam with dam-reservoir interaction for the actual geometry reservoir case due to harmonic the upstream-downstream ground motion. 131
- FIGURE 7.31 Total hydrodynamic force on the upstream face of Karakaya dam with dam-reservoir interaction for the actual geometry reservoir case due to harmonic vertical ground motion. 132
- FIGURE 7.32 Total hydrodynamic force on the upstream face of Karakaya dam with dam-reservoir interaction for the actual geometry reservoir case due to harmonic cross-downstream ground motion. 133
- FIGURE 7.33 The radial acceleration response of the Karakaya Dam structure for the

symmetrical reservoir case due to harmonic upstream-downstream ground motion with reservoir boundary reflection coefficient, $\alpha_r=0.75$	134
FIGURE 7.34 The radial acceleration response of the Karakaya Dam structure for the symmetrical reservoir case due to harmonic vertical ground motion with reservoir boundary reflection coefficient, $\alpha_r=0.75$	135
FIGURE 7.35 The radial acceleration response of the Karakaya Dam structure the symmetrical reservoir case due to harmonic cross-stream ground motion with reservoir boundary reflection coefficient, $\alpha_r=0.75$	136
FIGURE 7.36 The radial acceleration response of the Karakaya Dam structure for the actual geometry case due to harmonic upstream-downstream ground motion with reservoir boundary reflection coefficient, $\alpha_r=0.75$	137
FIGURE 7.37 The radial acceleration response of the Karakaya Dam structure for the actual geometry case due to harmonic vertical ground motion with reservoir boundary reflection coefficient, $\alpha_r=0.75$	138
FIGURE 7.38 The radial acceleration response of the Karakaya Dam structure for the actual geometry reservoir case due to harmonic cross-stream ground motion with reservoir boundary reflection coefficient, $\alpha_r=0.75$	139
FIGURE C.1. Flowchart of DAM3D computer program	150

LIST OF SYMBOLS

a_g	free field earthquake ground acceleration
a_n	component of acceleration normal to the fluid boundary
C	finite element damping matrix for the dam structure
c	velocity of sound waves in water
C_j	generalized damping in the j^{th} mode of the free vibration of the dam
E	vector of inertia loads on the dam due to a unit acceleration of the rigid dam
F	geometrical relation matrix in DRBEM formulation
f_j	global shape function to define the particular solution in DRBEM
F_{st}	x-component of the force on the dam due to the hydrostatic pressure.
G	matrix based on DRBEM formulation
g	acceleration of gravity
$g(x,y)$	fundamental solution of Laplace Equation
g_n	free-field ground acceleration
H	matrix based on DRBEM formulation
J	number of vibration modes included in the analysis of the dam
K	Finite element mass matrix for the dam
K_j	generalized stiffness for j^{th} natural mode of vibration of dam.
L	Generalized load vector
L	number of internal points in DRBEM.
M	number of eigenvalues of the infinite domain
M	finite element mass matrix for the dam
M_j	generalized mass for j^{th} natural mode of vibration of dam.
N	number of boundary nodes in DRBEM
p	hydrodynamic pressure vector acting on the upstream face of the arch dam
\hat{p}	particular solution in DRBEM
p_0	hydrodynamic pressure vector due to ground motion with the rigid dam
\tilde{p}	homogenous solution related with DRBEM formulation
P_j	generalized hydrodynamic load
p_j	hydrodynamic pressure vector due to the dam acceleration in its j^{th} vibration mode
Q	hydrodynamic force vector acting on the upstream face of the arch dam
q	the normal derivative of the hydrodynamic pressure

$\hat{q}(r)$	derivative of the particular solution in DRBEM
\mathbf{Q}_0	static equivalent of \mathbf{p}_0
$\mathbf{Q}^f(t)$	static equivalent of the hydrodynamic pressure on the upstream face of arch dam
\mathbf{Q}_j	static equivalent of \mathbf{p}_j
\mathbf{R}	radiation matrix
r	distance from source to field point in DRBEM formulation
\mathbf{S}	generalized dynamic stiffness matrix for the dam structure
$\dot{\mathbf{u}}$	vector of the translational components of nodal displacement
$\dot{\mathbf{u}}$	corresponding nodal velocity vector
$\ddot{\mathbf{u}}$	corresponding nodal acceleration vector
$\ddot{\mathbf{u}}_g(t)$	harmonic ground motion acceleration
x^*	upstream distance normalized with respect to the length of the finite reservoir
\dot{Y}_j	generalized modal velocity in the j^{th} mode of vibration
\ddot{Y}_j	generalized modal acceleration in the j^{th} mode of vibration
Y_j	generalized modal displacement in the j^{th} mode of vibration
z^*	normalized vertical distance w.r.t. height of the dam
α_r	wave reflection coefficient
Γ	reservoir boundary surface
γ	unit weight of water
ζ_j	critical damping ratio in the j^{th} mode of vibration
κ	separation constant
Λ	diagonal matrix of the eigenvalues of the infinite domain of the reservoir
λ_m	eigenvalues of the infinite domain of the reservoir
Λ_d	direction cosine matrix.
ρ_w	density of water
ϕ_j^f	vector of j^{th} natural mode modes of the dam along the dam-reservoir interface
ϕ_j	vector of the j^{th} natural mode shapes of the dam structure
φ_d	shape function of the elements in the dam structure
φ_f	shape function of the boundary element of the reservoir
Ψ_m	the m^{th} eigenvector of the infinite domain of the reservoir
Ω	excitation frequency normalized with respect to the natural frequency of infinite domain
ω	excitation frequency

- ω_j natural vibration frequency of the dam structure
- ω_1 first natural frequency of the infinite domain of the reservoir

1. INTRODUCTION

The ever increasing demand for energy and the need to better manage our limited water resources necessitates the design and construction of dams. Often, dams have to be constructed in regions of considerable seismic activity. The catastrophic consequences of a dam failure make it especially important that such structures be designed to withstand seismic activity. The evaluation of the safety of existing dams subjected to earthquakes is also of vital importance. Thus, there exists a strong motivation for research leading to better analysis and design methods to study the earthquake response of dam systems. The present study will concentrate on the earthquake response of arch dam systems.

An arch dam system consists of the arch dam itself, the foundation and the reservoir. The study of the earthquake response of an arch dam system is complicated by the dynamical interactions between these components. Improved understanding of the complex interactions between these aspects is necessary to the development of more reliable analysis procedures and mathematical models. As a result, extensive research has been carried out on the complete dam-reservoir-foundation system in an attempt to achieve better understanding of the dynamic behavior of the sub-systems and their interactions. In spite of the great volume of work on dam-reservoir systems, the inherently complex system still remains a difficult problem. The rapid progress in modern computing technology, together with significant developments in numerical methods has paved the way to the development of more effective and accurate procedures to study the dynamic interactions among the structural, hydrodynamical and geotechnical aspects and the behavior of the total system.

1.1. Problem Definition

The arch dam-reservoir-foundation system includes domains with different properties and behaviors. These domains are the concrete arch dam, the foundation rock, the impounded water in the reservoir and the bottom sediments. During earthquakes these domains interact, therefore it is essential to carry out the analysis of the complete system. The development of a technique to study the earthquake response of arch dams is complicated by several geometrical and interactive factors. The deformations of the dam interactively influence water

motion in the reservoir and the deformation of the bed rock. Numerical methods are the only solution means able to overcome such complexities

The application of numerical methods to model the complete response of the dam-fluid-foundation system was greatly improved with the introduction of the substructure concept. In addition to its efficiency in reducing computational effort and storage, it permits the application of different mathematical methods to model each of the substructures. Based on the method, the foundation and reservoir domains are first solved separately as substructures. Subsequently, these solutions are used to modify the equations of the dam structure and of the other substructures.

A survey of past studies indicates that the finite element method is the preferred method for modeling the arch dam structure. The reservoir, in most cases, extends to a very large distance in the upstream direction. To include a sufficient part of the reservoir into the analysis, it is customary to idealize it as a finite region of irregular geometry adjacent to an infinite domain with uniform cross section. The inclusion of a realistic representation of the reservoir geometry in the finite region requires considerable computational effort. The compatibility and equilibrium conditions of pressure and pressure gradients are applied at the so-called far boundary or scattering boundary along the interface of the finite and infinite regions.

As the interaction problem is defined on the interface of the dam and the reservoir, the boundary element method seems to be a logical choice in modeling the reservoir domain. The major difficulty encountered in applying the classical boundary elements formulation to the dynamic analysis of the arch dam-reservoir system is due to the fact that the system matrices implicitly contain the frequency parameter embedded in the fundamental solution. A recent development in the boundary element method is the adopting of a frequency independent fundamental solution which results in the dual reciprocity method. The method was applied successfully to model a two-dimensional dam-reservoir interaction in the frequency domain by Tsai et al (1988). One of the objectives of the present study, is to extend the formulation based on the dual reciprocity method to include the bottom absorption effects and to apply the method to model the three-dimensional finite region of the reservoir.

To account for the energy loss due to the radiation damping in the infinite domain, an effective model was proposed by Hall and Chopra(1980). The model utilized the separation of variables technique to combine a two-dimensional finite element discretization over the uniform cross section of the domain with a continuum expression in the upstream direction. The problem ultimately reduced to the solution of a standard eigenvalue problem. An alternative model, due to Rashed and Kandasamy (1990), based on the boundary element method had the major drawback that the system matrices were implicitly dependent on the eigenvalues of the system which meant that the problem could not be cast in the form of a standard eigenvalue problem.

Recent developments in the dual reciprocity method have proven the method to be an effective tool in the application to free vibration elasticity problems (Nardini and Brebbia,1982, Ahmad and Banerjee,1986) and acoustic eigenvalues analysis (Banerjee, et al,1988, Ali, et al,1991). Another objective of this study is to use the dual reciprocity method together with the separation of variables technique to model the radiation condition at the far end of the reservoir.

In summary, the objectives of the present study are:

- (a) to model the arch dam-reservoir system, using the finite element method for the dam structure and the dual reciprocity method for the reservoir domain;
- (b) to develop a formulation based on the dual reciprocity method to account for the radiation condition at the reservoir far end;
- (c) to study the interaction effects of the arch dam-reservoir system on the hydrodynamic pressure in the reservoir; and
- (d) to study the seismic response of the Karakaya dam-reservoir system.

1.2. Literature Survey

Over the last two decades, great progress in analyzing and testing the earthquake behavior of concrete dams has been made. Early studies were mainly concerned with the analytical solution of the hydrodynamic pressure distribution on rigid dams. The introduction of numerical techniques into the analysis has facilitated comprehensive studies of the dynamic behavior of the complete reservoir-dam-foundation system. Special attention was given to the interactions among the different domains (the dam structure, the reservoir and the foundation rock). A survey of the literature in this area reveals the development of various analytical and numerical models to study the problem. In this section, a review of the existing analytical, numerical and experimental studies is presented.

1.2.1. Concrete Gravity Dam

In general, the length of a concrete gravity dam is large in comparison to its thickness and its cross-section usually remains constant throughout its length. In practice, for a majority of the cases, a concrete gravity dam may be considered as a two-dimensional system. The literature contains numerous studies of the seismic response of gravity dam-reservoir-foundation systems.

The first analytical study of the earthquake induced hydrodynamic pressure on rigid dams was carried out by Westergaard (1933). In his study, he solved the hydrodynamic pressure on a rigid vertical dam due to the horizontal harmonic motion for a compressible reservoir. He suggested the “added mass” concept which influenced designers for a long time.

The importance of reservoir-dam interaction in determining the dynamic behavior of the system was demonstrated by Chopra (1967a, 1967 b, 1968, 1970). In his studies, he represented the deformations of the dam by considering the first fundamental mode shape of the dam. He treated the reservoir as a continuum whose motion was governed by a two-dimensional wave equation. He determined complex frequency responses for the coupled reservoir-dam system subjected to both arbitrary ground motions and to stationary white noise excitation. He found that neglecting the water compressibility may lead to results with significant error. He

demonstrated that simple analyses which ignore dam-reservoir interaction may not be satisfactory in predicting the behavior of the dam. Chakrabarti and Chopra (1974) found the contribution of the vertical component of ground motion to be of special importance in the dam-reservoir seismic response.

The analysis of the complete response of the dam-fluid-foundation system was greatly enhanced with the introduction of the substructure concept. Applications of the substructure technique to the dam-water-foundation interaction system were carried out by Chakrabarti and Chopra (1973a,1973b,1974) to model the dam-reservoir interaction, by Vanish and Chopra (1974) to model the dam-foundation system and by Chopra and Chakrabarti (1981) to model the dam-water-foundation system. Chakrabarti and Chopra (1973b,1974) applied the finite element method to model the dam structure, and a continuum solution to model the reservoir. The structural displacements of the dam, including effects of the water, were expressed as a linear combination of undamped free vibration modes of the dam structure. They found the procedure to be very effective and to give excellent results even though only the first few modes were used.

The finite element method was used to model the reservoir by Hall and Chopra (1980). In their study, treating the dam structure and fluid domain as substructures, they developed two- and three-dimensional finite and infinite reservoir models. In the infinite reservoir model, they coupled the finite element model with the continuum solution to model the radiation waves at the far end of the reservoir. To account for the effects of foundation flexibility on the hydrodynamic pressure response, they proposed a simplified one-dimensional fluid-foundation interaction model which allowed energy dissipation along the fluid-foundation boundary. Chandrasher and Humar (1993) verified the simplified model by comparing it with a hybrid finite elements- boundary elements model. They concluded that the difference between the model and the simplified approach was minor in the case of the displacement response functions.

Different approaches to study the radiation and scattering of water waves in two-dimensional reservoirs were proposed by Humar and Roufail (1983), Sharan and Gladwell (1985) and Sharan (1987). They used finite elements to model the reservoir and proposed

different analytical formulations to model the radiation boundary condition in the frequency domain.

The effects of energy absorption due to the interaction between the reservoir water and the underlying sediments and the flexible soil, were studied extensively by Fenves and Chopra (1983,1984a,1984b,1985). In their studies, they demonstrated the importance of reservoir bottom absorption in reservoir and dam responses. In the models, considering the foundation to be rigid, these responses can be affected primarily in the case where the excitation frequency is smaller than the fundamental frequency of the reservoir. Lotfi et al (1987) proposed fluid-solid hyper-elements and Cheng(1986) proposed the use of poro-elastic sediments to model the reservoir bottom sediment effects.

Rapid developments in boundary elements methods in the last decade have facilitated the application of the method to model the dam-reservoir-foundation system. Humar and Jablonski (1988) applied the method to analyze the hydrodynamic forces on a rigid dam. Medina and Dominguez (1989) applied the method to account for the dynamic interaction of dam-water-foundation systems in the seismic response of concrete gravity dams. Tsai, et al (1988,1992) proposed a hybrid scheme based on finite elements to model the dam structure and boundary elements with particular integrals to model the near reservoir domain. In his analysis, he demonstrated the efficiency of the frequency independent fundamental solution in the boundary-elements formulation of the fluid domain.

1.2.2. Arch-Dam

The behavior of arch dam-reservoir-foundation system is a complex phenomenon. The geometrical and interactive complexities make the prediction of the system response by analytical means difficult, and suggest numerical methods as the only solution strategy for the analysis of the complete system. Due to these complexities, studies on the seismic analysis of arch dams have not been as detailed as those of concrete gravity dams.

Earlier studies have treated the arch dam as a rigid body in order to obtain the analytical formulations of the hydrodynamic pressures on the upstream face of the arch dam.

Kotsubo(1961) idealized the arch dam to have a central arch angle of 90° , a constant upstream radius and radially extended vertical banks. In his study, he solved the three-dimensional wave equation analytically for harmonic excitations. Extending the analytical formulations to permit arbitrary ground excitations, Perumalswami and Kar(1973a) demonstrated the importance of compressibility in the seismic hydrodynamic response on the arch dams. Neglecting water compressibility, Zienkiewicz and Nath(1963) computed the hydrodynamic pressure distribution on arbitrary three-dimensional reservoir and dam geometry using the electrical analogue. To account for the arch dam-reservoir interaction, one-mode analysis of the idealized arch dam subjected to the upstream-downstream ground motion was developed by Perumalswami and Kar(1973b). Utilizing the substructure technique, Porter and Chopra (1980,1981,1982) presented a generalization of the work so as to include any number of vibration modes. The arch dam was idealized with finite elements while the hydrodynamic pressure distribution in the reservoir was determined analytically. They showed the importance of two factors on the arch dam response: the arch dam-reservoir interaction and the additional hydrodynamic force resulting from the motion of the banks.

The finite-elements method has been successfully applied to model the arch dam-reservoir system. In their model, Hall and Chopra (1980,1982a,1982b) have treated the dam structure and the reservoir as substructures. Taking the fluid-foundation interaction into consideration, they applied the method for both finite and infinite reservoir domains. In modeling the infinite reservoir domain, they assumed the reservoir to be of a constant cross section beyond some upstream point. For such an infinite, uniform region, the finite element discretization over the cross section was combined with a continuum representation. Nath(1981) focused on modeling the coupled natural frequencies and mode shapes of realistic circular cylindrical arch dams using novel mapping finite elements.

The complete arch dam-reservoir-foundation was modeled using the finite elements by Fok and Chopra (1985,1986a,1986b,1986c). In their studies, they extended the works of Hall and Chopra (1980,1982). They considered the bottom absorption coefficient in the water-foundation model to account for sedimentary material on the reservoir boundary. Using finite elements, they developed a homogeneous, massless foundation rock model to incorporate the foundation flexibility into the structure-foundation system. As an alternative to this model, two-

dimensional boundary elements with Fourier expansion formulation was developed to model the foundation impedance matrix by Zhang and Chopra (1991). Further developments to include the material and radiation damping of the foundation were done by Tan and Chopra (1995) utilizing the boundary element method.

Although the solution of continuum domain vibration problems by boundary element techniques offers many advantages, there are only a few studies in the application of the method to solve the dam-reservoir-foundation system. In the literature, most of the studies have applied the method to model the foundation domain in the dam structure-foundation rock problem. The works of Nowak and Hall (1990) and Tan and Chopra (1995) are examples to these studies. Boundary elements were applied to solve the fluid domain in the arch dam-reservoir system by Tsai and Lee (1987). Neglecting water compressibility, they applied a hybrid finite elements/boundary elements scheme. Considering the compressibility of the water, Humar and Jablonski and Humar (1986) applied the method in solving the three-dimensional wave equation to evaluate the hydrodynamic pressure on a rigid arch dam. The Boundary elements method was applied to the complete dam-reservoir-foundation system by Maeso and Dominguez (1993). They utilized the classical boundary elements formulation to model all three domains, taking into consideration the arch dam- foundation rock interaction, the arch dam-reservoir interaction, the reservoir-foundation rock interaction and traveling waves.

1.3. Scope of the Study

In the present study, the substructure technique in the frequency domain is adopted to treat the arch dam-reservoir interaction system assuming the foundation rock at the dam base and canyon banks to be infinitely rigid. The finite element method is utilized to model dam structure and the dual reciprocity method is used to model the reservoir domain. In the model, the behaviors of the arch dam and the reservoir are assumed to be linear and the free-field ground motion is assumed to be uniform across the arch dam-reservoir system.

In Chapter 2, the material and geometrical properties and the assumptions of each of the domains in the arch dam-reservoir system are stated and the input ground motion is defined.

In Chapter 3, the frequency domain equations of motion and the boundary conditions of the dam structure and the reservoir are presented together with the substructure procedure. In Chapters 4 and 5, the three-dimensional dual reciprocity formulations for the finite domain of the reservoir and the two-dimensional dual reciprocity with the continuum expression for the infinite domain are presented. The model results are verified by comparing them with the analytical solution of the hydrodynamic response of the three-dimensional rectangular reservoir in Chapter 6. The hydrodynamic and structural response of the Karakaya dam-reservoir system are studied in Chapter 7. In Chapter 8, the conclusions and recommendations for future research are presented.

2. ARCH DAM-RESERVOIR SYSTEMS AND GROUND MOTION

The arch dam-reservoir-foundation system includes domains with different properties and behaviors. These domains are the concrete arch dam, the foundation rock, the impounded water in the reservoir and the bottom sediments. During earthquakes these domains interact, therefore it is essential to carry out the analysis of the complete system. In this study, the substructure technique in the frequency domain is adopted to treat the fluid-structure interaction system assuming the foundation rock at the dam base and canyon banks to be infinitely rigid. Based on the method, the foundation and reservoir domains are first solved separately as substructures. Subsequently, these solutions are used to modify the equations of the dam structure and of the other substructures. In the dynamic analysis of the system, the behaviors of the arch dam and the reservoir are assumed to be linear. Therefore, there is no possibility of water cavitation, concrete cracking or opening of the construction joints during the earthquake. The free-field ground motion is assumed to be uniform across the arch dam-reservoir system.

2.1. The Arch Dam

An Arch dam is a type of concrete dam that is curved upstream in the plan. Arch dams are designed to transmit a major part of the imposed loads to the canyon walls by horizontal thrust. In this study, finite elements are used to discretize the dam. Two types of elements are used in the analysis, three-dimensional solid elements and three-dimensional thick shell elements. The dam material is considered to be linearly elastic and the deformations of the dam small, resulting in linear force-deformation relations for the arch dam. The properties of each finite element are characterized by its Young's modulus, Poisson's ratio, the unit weight of the concrete and the damping factor. The vibrational energy dissipation properties of the dam are characterized by the constant hysteretic damping factor.

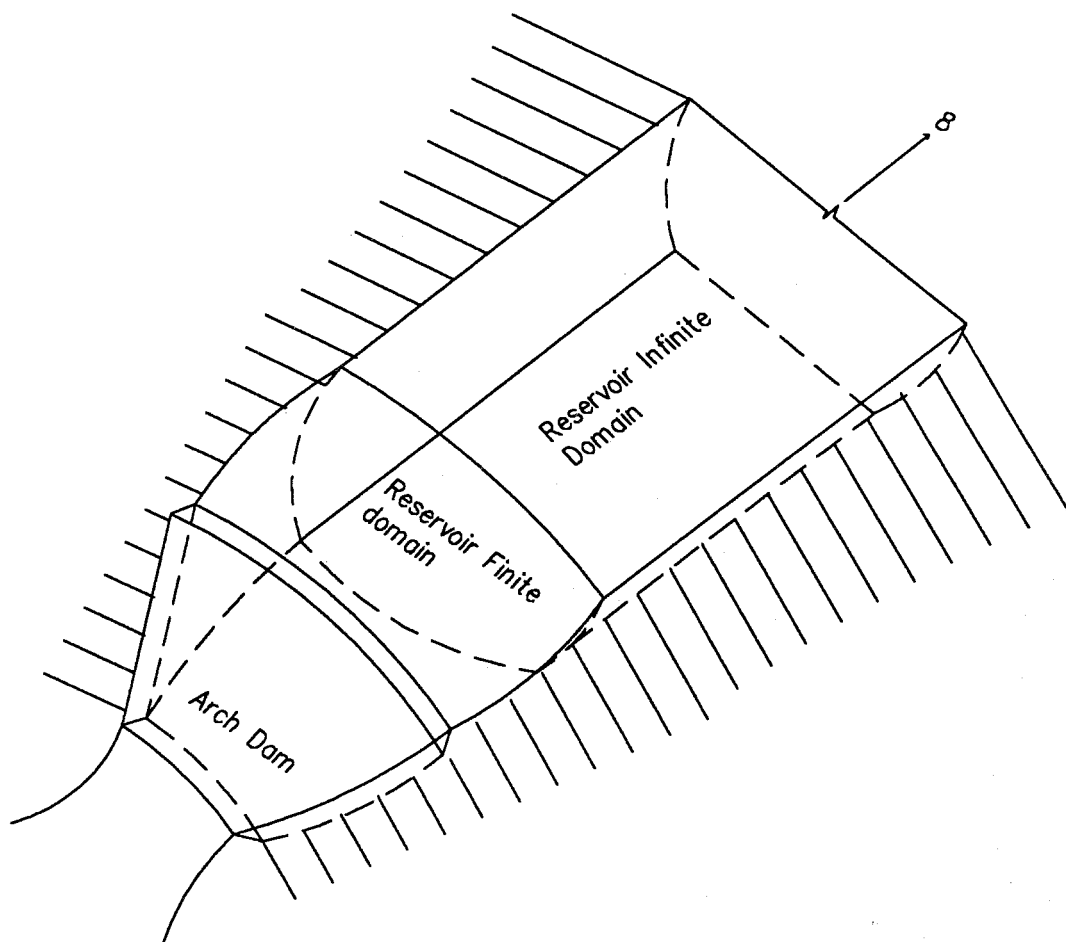


FIGURE 2.1. Arch dam-reservoir system

2.2. The Reservoir

The reservoir of an arch dam is usually of complicated shape. In some cases, the reservoir geometry may be such that the entire fluid domain can be incorporated in the model, while in other cases, only part of an extensive reservoir may be included in the analysis. As the bottom topography in the immediate vicinity of the dam affects the hydrostatic pressure distribution, an efficient analysis needs to include a realistic part of the reservoir geometry. The bottom of a reservoir upstream from a dam may consist of highly variable layers of exposed bedrock, alluvium, silt and other sedimentary material. The absorptive reservoir bottom provides an important energy radiation mechanism through refraction of pressure waves into the foundation medium deposited to a significant depth.

The reservoir is considered to extend to a very large distance in the upstream direction. Therefore, to model wave radiation, it is appropriate to idealize it as a finite region of irregular geometry adjacent to an infinitely long channel with uniform cross section. The compatibility and equilibrium conditions of pressure and pressure gradients are applied at the so-called far boundary or scattering boundary along the interface of the finite and infinite regions. In the arch dam-reservoir system, the interaction problem is defined on the interface of the dam and the reservoir, therefore the boundary element method seems to be a logical choice in modeling the reservoir domain.

In this study, the dual reciprocity boundary element method is applied to model the three-dimensional finite domain of the reservoir. For the infinite domain, a two-dimensional eigenvalue analysis based on the dual reciprocity formulations over the cross section, together with a continuum expression in the upstream direction, is utilized to model the variation of pressure and pressure gradient across the interface of the finite and infinite regions. In modeling the reservoir, the boundary of the reservoir domain is discretized using four-node linear and eight -node quadrilateral surface elements, therefore, linear and quadratic representations of the geometry, pressure and normal acceleration are possible. The absorption of hydrodynamic waves at the reservoir boundary is approximately represented by a one-dimensional model proposed by (Hall and Chopra, 1980). The fundamental parameter characterizing the effects of absorption of hydrodynamic pressure waves at the reservoir boundary is the wave reflection coefficient which may vary in the range from 0 to 1 to cover

the wide range of materials encountered at the bottom of actual reservoirs.

The properties of the reservoir domain model are characterized by the pressure wave velocity, the unit weight of the water and the wave reflection coefficient at the bottom of the reservoir.

2.3. Ground Motion

The earthquake ground motion is defined by the three transnational components: Upstream, cross stream and vertical. In this study, the free-field ground motion was assumed to be uniform across the arch dam-reservoir system. For arch dam sites this free-field ground motion is expected to vary over the interface. To include these variations appropriately into the analysis, a complete dam-foundation-reservoir interaction system required to be modeled, which is beyond the scope of this study. Therefore, these spatial variations in the ground motion are not included in this study.

3. ANALYSIS OF THE ARCH DAM-RESERVOIR SYSTEM RESPONSE

The seismic response analysis of the arch dam-reservoir system is complicated by the geometrical and interactive aspects existing in the system. Numerical methods are the only solution means able to overcome such complexities. In this study, the substructure concept is utilized to treat the arch dam and reservoir domain as separate substructures. The substructures are analyzed separately, then coupled through a general analysis procedure. This procedure permits the application of different mathematical methods to model the substructures. The finite-elements method is utilized to model the arch dam structure while the boundary element method is applied to model the reservoir. The foundation domain is considered to be infinitely rigid.

3.1. Equations of Motion for the Dam Structure

The equation of motion of the arch dam substructure, idealized as a three-dimensional thick shell finite elements system and subjected to ground motion acceleration, $\ddot{\mathbf{u}}_g(t)$, is

$$\mathbf{M}\ddot{\mathbf{u}} + \mathbf{C}\dot{\mathbf{u}} + \mathbf{K}\mathbf{u} = -\mathbf{M}\mathbf{E}\ddot{\mathbf{u}}_g(t) + \mathbf{Q}(t) \quad (3.1)$$

where \mathbf{M} , \mathbf{C} , \mathbf{K} , are respectively the mass, damping and stiffness matrices for the finite element system. \mathbf{u} is the vector for the three translational components of nodal displacements above the base, relative to the free ground motion. The related nodal velocity and acceleration are denoted by the vectors $\dot{\mathbf{u}}$ and $\ddot{\mathbf{u}}$. \mathbf{E} is the influence matrix which contains the pseudo-static influence vectors associated with the three translational components of ground motion acceleration, $\ddot{\mathbf{u}}_g(t)$. $\mathbf{Q}(t)$ is the vector of the nodal static equivalent of the hydrodynamic forces on the upstream face of the arch dam.

The consistent mass and stiffness matrices of the arch dam elements are evaluated by applying isoparametric three dimensional solid elements or isoparametric three dimensional thick shell elements and following standard finite element method procedures (Zeinkiewicz, 1977). The damping properties are expressed in terms of the damping ratios eliminating the need to evaluate the damping matrix.

Following the substructure technique, nodal displacements of the arch dam system, including the hydrodynamic interaction effects, are approximately expressed as a linear combination of undamped, free-vibration modes of the arch dam. The natural vibration mode shapes, ϕ_j , and corresponding natural frequencies, ω_j , of the arch dam are the solutions of the free vibration eigenvalue problem of the system

$$\mathbf{K}\phi_j = \omega_j^2 \mathbf{M}\phi_j \quad (3.2)$$

The nodal displacements of the arch dam system are expressed as

$$\mathbf{u}(t) = \sum_{j=1}^J Y_j(t) \phi_j \quad (3.3)$$

in which, Y_j are the generalized modal displacements in the j^{th} mode of vibration. All modes contributing significantly to the response should be included in Eq.(3.3). Generally, the number of modes necessary is a small fraction of the total number of the degree of freedom of the system. The nodal velocities and accelerations are expressed respectively, as

$$\dot{\mathbf{u}}(t) = \sum_{j=1}^J \dot{Y}_j(t) \phi_j \quad (3.4)$$

and

$$\ddot{\mathbf{u}}(t) = \sum_{j=1}^J \ddot{Y}_j(t) \phi_j \quad (3.5)$$

in which, $\dot{Y}_j(t)$ and $\ddot{Y}_j(t)$ are the generalized modal velocities and accelerations in the j^{th} mode of vibration.

Applying the above transformations to Eq.(3.1) and considering the orthogonality properties of the mode shapes, results in a set of equations in terms of the generalized modal displacement, Y_j , as

$$M_j \ddot{Y}_j(t) + C_j \dot{Y}_j(t) + K_j Y_j(t) = P_j(t) \quad (3.6)$$

where

$$M_j = \phi_j^T \mathbf{M} \phi_j$$

$$C_j = \phi_j^T \mathbf{C} \phi_j = 2\zeta_j \omega_j M_j$$

$$K_j = \phi_j^T \mathbf{K} \phi_j = \omega_j^2 M_j$$

$$P_j(t) = -\phi_j^T \mathbf{M} \mathbf{E} \ddot{\mathbf{u}}_g(t) + \phi_j^{fT} \mathbf{Q}^f(t)$$

In the expressions above, M_j , C_j and K_j are the generalized mass, damping and stiffness for the j^{th} vibration mode. ζ_j is the critical damping ratio and $P_j(t)$ is the generalized load. The nodal force vector, $\mathbf{Q}^f(t)$, is the static equivalent of the hydrodynamic pressure on the arch dam-reservoir interface, computed by applying the principle of virtual work. The vector ϕ_j^f is a sub-vector of the j^{th} vibration mode shape, ϕ_j , including the components associated with the nodes along the arch dam-reservoir interface.

The response of a linear system to steady state harmonic excitation of frequency ω can be conveniently described by its complex frequency response function which is also harmonic at the same frequency. In analyzing the arch dam-reservoir system for harmonic ground accelerations, $\ddot{\mathbf{u}}_g(t) = e^{i\omega t}$, the generalized modal displacements, velocities and accelerations can be expressed in terms of their complex frequency response functions as

$$Y_j(t) = Y_j(\omega) e^{i\omega t} \quad (3.7)$$

$$\dot{Y}_j(t) = i\omega \dot{Y}_j(\omega) e^{i\omega t} \quad (3.8)$$

$$\ddot{Y}_j(t) = -\omega^2 \ddot{Y}_j(\omega) e^{i\omega t} \quad (3.9)$$

The nodal hydrodynamic forces vector can be expressed in terms of its complex frequency response functions as

$$\mathbf{Q}(t) = \mathbf{Q}(\omega) e^{i\omega t} \quad (3.10)$$

Substituting the corresponding terms into Eq.(3.6), the equation can be expressed in the frequency domain as

$$\left\{ -\omega^2 M_j + i\omega C_j + K_j \right\} Y_j(\omega) = P_j(\omega) \quad (3.11)$$

where, $P_j(\omega)$ is the generalized load in the frequency domain, and can be expressed as

$$P_j(\omega) = -\phi_j^T \mathbf{M} \mathbf{E} + \phi_j^f{}^T \mathbf{Q}(\omega) \quad (3.12)$$

In order to solve the system of equations, there is a need to know the hydrodynamic force response on the arch dam-reservoir interface. The hydrodynamic forces will be expressed in terms of the accelerations at the upstream face of the dam, as a result of the analysis of the reservoir domain in the following section.

3.2. Equations of Motion and Boundary Conditions for the Fluid Domain:

The motion of the water in the three-dimensional reservoir is governed by the Navier-Stokes equations. However, under the assumption of small amplitude motion for irrotational compressible water and neglecting surface waves and viscous effects, the hydrodynamic pressure distribution in excess of the hydrostatic pressure can be expressed in terms of the three dimensional pressure wave equation, as

$$\frac{\partial^2 p}{\partial x^2} + \frac{\partial^2 p}{\partial y^2} + \frac{\partial^2 p}{\partial z^2} = \frac{1}{c^2} \frac{\partial^2 p}{\partial t^2} \quad (3.13)$$

where x, y, z are the Cartesian coordinates, $p(x,y,z,t)$ is the hydrodynamic pressure in excess of the hydrostatic pressure and c is the velocity of sound waves in water.

For harmonic ground motion, $\ddot{\mathbf{u}}_g(t) = \mathbf{E} e^{i\omega t}$, the hydrodynamic pressure, $p(x,y,z,t)$, can be expressed in terms of the complex frequency response function, $p(x,y,z,\omega)$, as

$$p(x, y, z, t) = p(x, y, z, \omega) e^{i\omega t} \quad (3.14)$$

The wave equation thus reduces to the well known three dimensional Helmholtz equation,

$$\frac{\partial^2 p}{\partial x^2} + \frac{\partial^2 p}{\partial y^2} + \frac{\partial^2 p}{\partial z^2} = -\frac{\omega^2}{c^2} p \quad (3.15)$$

which governs the hydrodynamic pressure responses, subject to the boundary conditions given in the following sections.

3.2.1. Reservoir Free Surface Boundary Condition

The hydrodynamic pressure vanishes at the free surface, and the pressure is set equal to the gage pressure.

$$p(x, y, z, \omega) = 0 \quad (3.16)$$

3.2.2. Arch Dam-fluid Interface Boundary Condition

The hydrodynamic pressure, $p(x,y,z,t)$, and the acceleration $a_n(t)$ of any particle of water along the dam interface should satisfy,

$$q(x, y, z, t) = -\frac{w}{g} a_n(t) \quad (3.17)$$

where, $q = \partial p / \partial n$, is the normal derivative of the hydrodynamic pressure, n is the outward normal to the interface, w is the specific weight of water and g is the gravitational acceleration., $a_n(t)$, is the arch dam acceleration along the interface. For steady state response cases, the frequency response function of the outward normal component of arch dam acceleration along the interface, can be expressed as

$$a_n(\omega) = a_g(\omega) - \omega^2 \sum_{j=1}^J Y_j(\omega) \phi_j^f \quad (3.18)$$

in which, the first term of the right hand side represents the accelerations of the rigid arch dam, while the second term arises from the arch dam deformations. Using Eq. (3.18), Eq.(3.17) can be written as

$$q(x, y, z, \omega) = -\frac{w}{g} \left(a_g(\omega) - \omega^2 \sum_{j=1}^J Y_j(\omega) \phi_j^f \right) \quad (3.19)$$

3.2.3. Reservoir Bottom and Banks Boundary Condition

The absorptive reservoir bottom and banks provide an important energy radiation mechanism through the refraction of pressure waves into the foundation medium. This absorption mechanism through the reservoir-foundation interface can be represented approximately by a one-dimensional model assuming the seismic pressure to propagate in a direction normal to the boundary. This model leads to the partial absorption of the hydrodynamic pressure waves at the reservoir bottom into the foundation medium. As presented by Hall and Chopra(1980), for the steady state response case, this model leads to the expression

$$q(x, y, z, \omega) = -\frac{w}{g} a_n(\omega) + i\omega \gamma p(x, y, z, \omega) \quad (3.20)$$

in which, a_n is the outward normal acceleration component at the reservoir bottom and banks, γ is the foundation damping coefficient given by

$$\gamma = \frac{1}{c} \left(\frac{1 - \alpha_r}{1 + \alpha_r} \right)$$

In the expression above, α_r is the wave reflection coefficient which is unity for the rigid foundation case and vanishes for the full absorption case.

3.2.4. The Radiation Boundary Conditions

To model the wave radiation for the infinite domain, the reservoir may be idealized as a finite region of irregular geometry adjacent to an infinitely-long channel with uniform cross-section. Compatibility of hydrodynamic pressures and pressure gradients are forced along the scattering boundary which is located at the interface of the finite and infinite domains of the reservoir. The energy loss due to radiation damping in the reservoir is considered by applying a special radiation condition at the interface. This radiation condition is derived by applying a two-dimensional dual reciprocity formulation to model the infinite region. The details of this model are discussed in the following chapters.

3.2.5. Hydrodynamic Pressure and Force Responses on the Upstream of the Dam

For the steady state response case, the governing equation of the fluid domain together with the specified boundary conditions could be solved using the three dimensional dual reciprocity method as explained in the next chapter. The resulting hydrodynamic pressure in the reservoir domain, $p(x,y,z,\omega)$, can be expressed as

$$\mathbf{p}(x, y, z, \omega) = \mathbf{p}_0(x, y, z, \omega) - \omega^2 \sum_{j=1}^J \mathbf{p}_j(x, y, z, \omega) Y_j(\omega) \quad (3.21)$$

where, $\mathbf{p}_0(x,y,z,\omega)$ is the complex frequency hydrodynamic pressure vector due to the ground motion acceleration considering arch dam to be rigid, $\mathbf{p}_j(x,y,z,\omega)$ is the corresponding vector due to the arch dam acceleration in its j^{th} vibration mode without motion of the boundary.

By applying the virtual work principal, the complex frequency response functions for the hydrodynamic forces on the upstream face of the arch dam can be expressed as

$$\mathbf{Q}(\omega) = \mathbf{Q}_0(\omega) - \omega^2 \sum_{j=1}^J \mathbf{Q}_j(\omega) Y_j(\omega) \quad (3.22)$$

where, $\mathbf{Q}(\omega)$ and $\mathbf{Q}_j(\omega)$ are the static equivalents of the corresponding pressure functions $\mathbf{p}_0(x,y,z,\omega)$ and $\mathbf{p}_j(x,y,z,\omega)$ respectively.

3.3. Equations of the Arch Dam-reservoir System

In the previous sections, the substructure technique was applied to solve the coupled arch dam-reservoir system. Initially, the arch dam substructure was modeled separately using the finite element method. The modal displacements and accelerations of the arch dam were expressed in terms of the generalized displacement associated with free vibration modes of the arch dam. Then, the reservoir was modeled utilizing the dual reciprocity method. At the arch dam-reservoir interface boundary, the hydrodynamic pressure of the reservoir is frequency dependent and can be expressed in terms of the generalized displacements.

Substitution of the expression for the hydrodynamic force, Eq.(3.22), into the

expression of the generalized load vector, Eq.(3.12), results in

$$P_j(\omega) = -\phi_j^T \mathbf{M} \mathbf{E} + \phi_j^T \left\{ \mathbf{Q}_0(\omega) - \omega^2 \sum_{j=1}^J \mathbf{Q}_j(\omega) Y_j(\omega) \right\} \quad (3.23)$$

Thus, Eq.(3.11) which expresses the equations of motion in terms of generalized displacements can be expressed in matrix form as

$$\mathbf{S}(\omega) \mathbf{Y}(\omega) = \mathbf{L}(\omega) \quad (3.24)$$

where the frequency dependent matrix $\mathbf{S}(\omega)$ relates the generalized displacement vector $\mathbf{Y}(\omega)$ to the corresponding generalized loads $\mathbf{L}(\omega)$, as follows

$$S_{ij}(\omega) = -\omega^2 \phi_j^T \mathbf{Q}(\omega) \quad (3.25)$$

$$S_{jj}(\omega) = -\omega^2 M_j + i\omega C_j + K_j - \omega^2 \phi_j^T \mathbf{Q}(\omega) \quad (3.26)$$

$$L_j(\omega) = -\phi_j^T \mathbf{M} \mathbf{E} - \phi_j^T \mathbf{Q}_0(\omega) \quad (3.27)$$

The hydrodynamic terms modify both $\mathbf{L}(\omega)$ and $\mathbf{S}(\omega)$ in terms of added masses and added loads respectively. The added load is the hydrodynamic force on the rigid arch dam face due to the ground motion excitation while the added mass terms are due to hydrodynamic forces resulting from the arch dam deformations with respect to the ground motion.

For a steady state response, the system of equations represented by Eq.(3.24) can be solved for the generalized displacements. Substituting the resulting generalized displacements into Eqs.(3.4) and (3.5), the modal displacements and accelerations of the dam can be computed. The hydrodynamic pressure in the frequency domain may now be computed from Eq.(3.21).

3.4. Responses to Arbitrary Ground Motion

The responses of the arch dam-reservoir system to arbitrary excitation, such as earthquakes, can be conveniently obtained from the complex frequency response functions by using Fourier synthesis. Once the complex frequency responses, $Y(\omega)$, are obtained for a range of excitation frequencies, ω , the responses to an arbitrary ground acceleration $a_g(t)$, can be obtained from the individual harmonic components. That is,

$$Y_j(t) = \frac{1}{2\pi} \int_{-\infty}^{\infty} Y_j(\omega) a_g(\omega) e^{i\omega t} d\omega \quad (3.28)$$

where, $a_g(\omega)$, is the Fourier transform of $a_g(t)$ given by

$$a_g(\omega) = \int_0^{t_d} a_g(t) e^{-i\omega t} dt \quad (3.29)$$

In the equation above, t_d is the duration of the ground motion. Similarly, the hydrodynamic pressure response in the reservoir due to an arbitrary ground acceleration can be obtained from its harmonic components as,

$$p(t) = \frac{1}{2\pi} \int_{-\infty}^{\infty} p(\omega) a_g(\omega) e^{i\omega t} d\omega \quad (3.30)$$

The transforms of Eqs. (3.28), (3.29) and (3.30) can readily be obtained using the Fast Fourier Transform (FFT) algorithm. Once the generalized displacements are known, the response of the nodal displacements of the dam can be obtained from Eq.(3.3)

4. THREE-DIMENSIONAL DUAL RECIPROCITY METHOD FOR THE RESERVOIR DOMAIN

In the present study, the reservoir is considered to extend to a very large distance in the upstream direction. Therefore, to model wave radiation, it is appropriate to idealize it as a finite region of irregular geometry adjacent to an infinitely long channel with uniform cross section. In the arch dam-reservoir system, the interaction problem is defined on the interface of the dam and the reservoir, therefore the boundary element method seems to be a logical choice in modeling the reservoir domain. The method requires only the boundaries of the domain to be discretized, thus there is a considerable reduction in data preparation efforts. Over the last decade, there have been numerous studies to apply the method to the dynamic analysis of dam-reservoir-foundation systems (Beskos, 1997). The major difficulty encountered in applying the classical boundary elements formulation to the dynamic analysis in the frequency domain response is due to the fact that the system matrices implicitly contain the frequency parameter embedded in the fundamental solution. A recent development in the boundary element method is the adopting of a frequency independent fundamental solution which results in the dual reciprocity method. The method was applied successfully to model a two-dimensional dam-reservoir interaction problem by Tsai et al (1988). In their model, within a general solution procedure to model the dam-reservoir system, a formulation based on the particular integral approach was utilized to model the two-dimensional reservoir. In the model, the bottom absorbing effects were ignored and an analytical formulation was utilized to account for the infinite domain. In this chapter, the formulation based on the dual reciprocity approach is extended to include the bottom absorption effects and is applied to model the three-dimensional finite domain of the reservoir.

4.1. Formulations for the Finite Domain of the Reservoir

The hydrodynamic pressure response in the reservoir domain, as shown in Figure 4.1, is governed by the three-dimensional Helmholtz equation

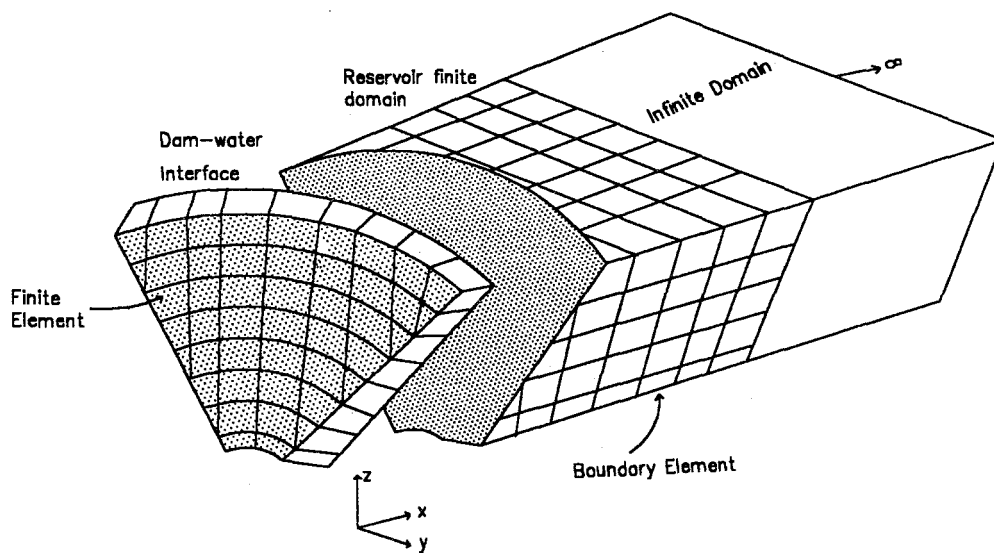


FIGURE 4.1 Idealization of arch dam-reservoir system

$$\nabla^2 p = -\frac{\omega^2}{c^2} p \quad (4.1)$$

where, ∇^2 is the Laplacian operator given by

$$\nabla^2 = \frac{\partial^2}{\partial x^2} + \frac{\partial^2}{\partial y^2} + \frac{\partial^2}{\partial z^2}$$

The governing equation is subjected to the following boundary conditions:

$$p_1 = 0 \quad \text{on } \Gamma_1 \quad (4.2)$$

$$q_2 = -\frac{w}{g} \left(a_g(\omega) - \omega^2 \sum_{j=1}^J Y_j(\omega) \phi_j^f \right) \quad \text{on } \Gamma_2 \quad (4.3)$$

$$q_3 = -\frac{w}{g} a_n(\omega) + i\omega \gamma p_3 \quad \text{on } \Gamma_3 \quad (4.4)$$

$$\mathbf{q}_4 = \mathbf{R} \mathbf{p}_4 \quad \text{on } \Gamma_4 \quad (4.5)$$

where Γ_1 is the free surface of the reservoir, Γ_2 is the arch dam-reservoir interface, Γ_3 is the surface of the reservoir bottom and banks and Γ_4 is the radiation boundary which is the interface between the finite and infinite reservoir domains. \mathbf{R} is the radiation matrix which relates the hydrodynamic pressure vector to the corresponding pressure gradient vector at the boundary. The radiation matrix is a result of applying the dual reciprocity method to model the infinite domain as explained in the next chapter.

4.2. Dual Reciprocity Method for the Helmholtz Equation

In this section, the dual reciprocity method is applied to solve the Helmholtz Equation. Eq.(4.1) is multiplied by frequency independent fundamental solution of the Laplace equation, g , and integrated over the reservoir domain, Ω , to yield

$$\int_{\Omega} g \nabla^2 p d\Omega = -\frac{\omega^2}{c^2} \int_{\Omega} g p d\Omega \quad (4.6)$$

While the left hand side of Eq.(4.6) readily converts to a boundary integral by the application of Green's second identity, the dual reciprocity method is applied to the right hand side to convert the domain integral into a boundary integral.

Following the dual reciprocity formulations proposed by Partridge et al (1992), the total hydrodynamic pressure response can be expressed as

$$p = \tilde{p} + \hat{p} \quad (4.7)$$

where, \tilde{p} is the homogeneous solution satisfying

$$\nabla^2 \tilde{p} = 0 \quad (4.8)$$

and \hat{p} is the particular solution, such that

$$\nabla^2 \hat{p} = -\frac{\omega^2}{c^2} p \quad (4.9)$$

The method proposes a series of particular solutions of the form

$$\hat{p} = \sum_{j=1}^{N+L} \alpha_j \hat{p}_j \quad (4.10)$$

where α_j are initially unknown coefficients. N is the number of boundary nodes and L represents the number of internal nodes that are used in approximating the particular solution. Substituting the proposed particular solutions into Eq.(4.9) results in

$$\sum_{j=1}^{N+L} \alpha_j \nabla^2 \hat{p}_j \cong -\frac{\omega^2}{c^2} p \quad (4.11)$$

The above expression may be substituted into the domain integral on the right hand side of Eq.(4.6), to obtain

$$\int_{\Omega} \nabla^2 p g d\Omega = \sum_{j=1}^{N+L} \alpha_j \int_{\Omega} \nabla^2 \hat{p}_j g d\Omega \quad (4.12)$$

As it can be noticed from the above expression, the domain integral on the right-hand

side becomes similar to that on the left-hand side, therefore, it also can be expressed in the form of boundary integrals. Applying Green's second identity to both sides, results in

$$-c_i p_i + \int_{\Gamma} (g_n p - g q) d\Gamma = \sum_{j=1}^{N+L} \alpha_j \left[-c_i p_{ij} + \int_{\Gamma} (g_n \hat{p} - g \hat{q}) d\Gamma \right] \quad (4.13)$$

where c_i is geometric coefficient which depends on the location of the source point (Brebbia et al, 1984) and c is the boundary of the domain. $g_n = \partial g / \partial n$ is the normal derivative of the fundamental solution on the boundary. Defining r to represent the distance from the source point to the field point, the fundamental solution of the three-dimensional Laplace equation is given in standard boundary elements texts (Banerjee, 1994 and Brebbia et al, 1984) as

$$g(x, \xi) = \frac{1}{4\pi r} \quad (4.14)$$

Discretizing the domain boundary, Γ , into a series of three-dimensional surface elements, $\Delta\Gamma_k$, Eq.(4.13) becomes

$$-c_i p_i + \sum_{k=1}^N \int_{\Delta\Gamma_k} (g_n p - g q) d\Gamma = \sum_{j=1}^{N+L} \alpha_j \left[-c_i p_{ij} + \sum_{k=1}^N \int_{\Delta\Gamma_k} (g_n \hat{p} - g \hat{q}) d\Gamma \right] \quad (4.15)$$

Evaluation of the integrals in Eq.(4.15) using appropriate shape functions, ϕ_k , yields

$$-c_i p_i + \sum_{k=1}^N (h_{ik} p_k - g_{ik} q_k) = \sum_{j=1}^{N+L} \alpha_j \left[-c_i p_{ij} + \sum_{k=1}^N (h_{ik} \hat{p}_{kj} - g_{ik} \hat{q}_{kj}) \right] \quad (4.16)$$

where the coefficients h_{ik} and g_{ik} are to be computed from,

$$h_{ik} = \int_{\Delta\Gamma_k} g_n N_k d\Gamma \quad g_{ik} = \int_{\Delta\Gamma_k} g N_k d\Gamma$$

Expressing Eq.(4.16) in matrix form and incorporating the $-c_i$ terms into the diagonal terms of \mathbf{H} , the following matrix equation is obtained

$$\mathbf{Gq} - \mathbf{Hp} = \sum_{j=1}^{N+L} \alpha_j (\mathbf{H}\hat{\mathbf{q}}_j - \mathbf{G}\hat{\mathbf{p}}_j) \quad (4.17)$$

The matrices \mathbf{G} and \mathbf{H} are computed on the boundary elements by integrating the Laplace fundamental solution multiplied by an appropriate interpolation function. The vectors $\hat{\mathbf{p}}_j$ and $\hat{\mathbf{q}}_j$ are developed utilizing the dual reciprocity approximation function, as it will be

described in the following sections. Defining $\hat{\mathbf{Q}}$ and $\hat{\mathbf{P}}$ such that each of their columns is, respectively, one of the vectors $\hat{\mathbf{q}}_j$ and $\hat{\mathbf{p}}_j$, gives the following matrix expression

$$\mathbf{G}\mathbf{q} - \mathbf{H}\mathbf{p} = (\mathbf{H}\hat{\mathbf{Q}} - \mathbf{G}\hat{\mathbf{P}})\boldsymbol{\alpha} \quad (4.18)$$

The approximation functions proposed to compute the vector $\boldsymbol{\alpha}$ are discussed in the following section.

4.3. Dual Reciprocity Approximation Functions

Following Partridge et al (1992), a global shape function, f_j , can be introduced in order to define the particular solution, such that

$$f_j = \nabla^2 \hat{\mathbf{p}}_j \quad (4.19)$$

Substituting into Eq.(4.11), results in

$$\sum_{j=1}^{N+L} \alpha_j f_j \cong -\frac{\omega^2}{c^2} \mathbf{p} \quad (4.20)$$

Several proposals for f_j may be found in the literature. The simplest, yet the one that has been found to yield the best results is to use the distance function r from the fundamental solution in a series of the form

$$f(r) = a_0 + a_1 r + a_2 r^2 + \dots + a_m r^m \quad (4.21)$$

where, the constants a_i are to be selected to suit the problem. Using the above expression, the particular solution of Eq.(4.15) for three dimensional problems can be written as

$$\hat{\mathbf{p}}(r) = \frac{a_0 r^2}{6} + \frac{a_1 r^3}{12} + \frac{a_2 r^4}{20} + \dots + \frac{a_m r^{m+2}}{(m+2)(m+3)} \quad (4.22)$$

The normal derivatives $\hat{\mathbf{q}}(r)$ can be obtained from $\hat{\mathbf{p}}(r)$ as

$$\hat{\mathbf{q}}(r) = \left(\frac{a_0 r}{3} + \frac{a_1 r^2}{4} + \frac{a_2 r^3}{5} + \dots + \frac{a_m r^{m+1}}{(m+3)} \right) \frac{\partial r}{\partial \mathbf{n}} \quad (4.23)$$

Using Eq.(4.20), the particular solutions can be evaluated at boundary and internal points to obtain a set of equations, which can be written in a matrix form as

$$\mathbf{F} \boldsymbol{\alpha} = -\frac{\omega^2}{c^2} \mathbf{p} \quad (4.24)$$

\mathbf{F} represents geometric relationships between the collocation points in the system and is generated using Eq.(4.21). Pre-multiplying both sides of Eq.(4.24) by \mathbf{F}^{-1} , provided it exists, results in

$$\boldsymbol{\alpha} = -\frac{\omega^2}{c^2} \mathbf{F}^{-1} \mathbf{p} \quad (4.25)$$

Substituting the above expression for vector $\boldsymbol{\alpha}$ into Eq.(4.20) leads to

$$\mathbf{Gq} - \mathbf{Hp} = -\frac{\omega^2}{c^2} (\mathbf{H}\hat{\mathbf{Q}} - \mathbf{G}\hat{\mathbf{P}}) \mathbf{F}^{-1} \mathbf{p} \quad (4.26)$$

Defining matrix $\tilde{\mathbf{M}}$ as

$$\tilde{\mathbf{M}} = (\mathbf{H}\hat{\mathbf{Q}} - \mathbf{G}\hat{\mathbf{P}}) \mathbf{F}^{-1} \quad (4.27)$$

Eq.(4.25) can be written as

$$\mathbf{Gq} - \mathbf{Hp} = -\frac{\omega^2}{c^2} \tilde{\mathbf{M}} \mathbf{p} \quad (4.28)$$

The dual reciprocity formulations of the \mathbf{H} , \mathbf{G} and $\tilde{\mathbf{M}}$ matrices are observed to be independent of the frequency parameter. Having this advantage, the dual reciprocity method is very effective in determining the frequency response of the arch dam-reservoir system.

4.4 Dual Reciprocity Formulations for the Reservoir Domain

In this study, the dual reciprocity formulation of the Helmholtz equation expressed in Eq.(4.28) is used to solve Eqs. (4.1-4.5) which governs the hydrodynamic pressure response distribution in the reservoir. For a specified excitation frequency, ω , the system may be rearranged and assembled in the following form

$$\begin{bmatrix} \mathbf{H}_{11} & \mathbf{H}_{12} & \mathbf{H}_{13} & \mathbf{H}_{14} \\ \mathbf{H}_{21} & \mathbf{H}_{22} & \mathbf{H}_{23} & \mathbf{H}_{24} \\ \mathbf{H}_{31} & \mathbf{H}_{32} & \mathbf{H}_{33} & \mathbf{H}_{34} \\ \mathbf{H}_{41} & \mathbf{H}_{42} & \mathbf{H}_{43} & \mathbf{H}_{44} \end{bmatrix} \begin{Bmatrix} \mathbf{p}_1 \\ \mathbf{p}_2 \\ \mathbf{p}_3 \\ \mathbf{p}_4 \end{Bmatrix} - \begin{bmatrix} \mathbf{G}_{11} & \mathbf{G}_{12} & \mathbf{G}_{13} & \mathbf{G}_{14} \\ \mathbf{G}_{21} & \mathbf{G}_{22} & \mathbf{G}_{23} & \mathbf{G}_{24} \\ \mathbf{G}_{31} & \mathbf{G}_{32} & \mathbf{G}_{33} & \mathbf{G}_{34} \\ \mathbf{G}_{41} & \mathbf{G}_{42} & \mathbf{G}_{43} & \mathbf{G}_{44} \end{bmatrix} \begin{Bmatrix} \mathbf{q}_1 \\ \mathbf{q}_2 \\ \mathbf{q}_3 \\ \mathbf{q}_4 \end{Bmatrix} = \quad (4.29)$$

$$-\frac{\omega^2}{c^2} \begin{bmatrix} \tilde{\mathbf{M}}_{11} & \tilde{\mathbf{M}}_{12} & \tilde{\mathbf{M}}_{13} & \tilde{\mathbf{M}}_{14} \\ \tilde{\mathbf{M}}_{21} & \tilde{\mathbf{M}}_{22} & \tilde{\mathbf{M}}_{23} & \tilde{\mathbf{M}}_{24} \\ \tilde{\mathbf{M}}_{31} & \tilde{\mathbf{M}}_{32} & \tilde{\mathbf{M}}_{33} & \tilde{\mathbf{M}}_{34} \\ \tilde{\mathbf{M}}_{41} & \tilde{\mathbf{M}}_{42} & \tilde{\mathbf{M}}_{43} & \tilde{\mathbf{M}}_{44} \end{bmatrix} \begin{Bmatrix} \mathbf{p}_1 \\ \mathbf{p}_2 \\ \mathbf{p}_3 \\ \mathbf{p}_4 \end{Bmatrix}$$

where \mathbf{H}_{ij} , \mathbf{G}_{ij} and $\tilde{\mathbf{M}}_{ij}$ are the respective sub-matrices of \mathbf{H} , \mathbf{G} and $\tilde{\mathbf{M}}$. The indices i and j refer to the boundary condition types: free surface of the reservoir on Γ_1 , arch dam-reservoir interface on Γ_2 , absorbing boundary of the reservoir bottom and banks on Γ_3 and radiation boundary on Γ_4 . The corresponding specified boundary conditions of Eqs.(4.2-4.5) are introduced into Eq.(4.29), and the system is rearranged such that all the coefficients of the specified boundary conditions are collected on the left hand side. Defining $\tilde{\mathbf{H}} = \mathbf{H} + \omega^2 / c^2 \tilde{\mathbf{M}}$, the system takes the form

$$\begin{bmatrix} -\mathbf{G}_{11} & \tilde{\mathbf{H}}_{12} - i\omega\gamma\mathbf{G}_{12} & \tilde{\mathbf{H}}_{13} - i\omega\gamma\mathbf{G}_{13} & \tilde{\mathbf{H}}_{14} - \mathbf{G}_{14}\mathbf{R} \\ -\mathbf{G}_{21} & \tilde{\mathbf{H}}_{22} - i\omega\gamma\mathbf{G}_{22} & \tilde{\mathbf{H}}_{23} - i\omega\gamma\mathbf{G}_{23} & \tilde{\mathbf{H}}_{24} - \mathbf{G}_{24}\mathbf{R} \\ -\mathbf{G}_{31} & \tilde{\mathbf{H}}_{32} - i\omega\gamma\mathbf{G}_{32} & \tilde{\mathbf{H}}_{33} - i\omega\gamma\mathbf{G}_{33} & \tilde{\mathbf{H}}_{34} - \mathbf{G}_{34}\mathbf{R} \\ -\mathbf{G}_{41} & \tilde{\mathbf{H}}_{42} - i\omega\gamma\mathbf{G}_{42} & \tilde{\mathbf{H}}_{43} - i\omega\gamma\mathbf{G}_{43} & \tilde{\mathbf{H}}_{44} - \mathbf{G}_{44}\mathbf{R} \end{bmatrix} \begin{Bmatrix} \mathbf{q}_1 \\ \mathbf{p}_2 \\ \mathbf{p}_3 \\ \mathbf{p}_4 \end{Bmatrix} = \quad (4.30)$$

$$-\frac{\omega}{g} \left\{ \begin{bmatrix} \mathbf{G}_{12} & \mathbf{G}_{13} \\ \mathbf{G}_{22} & \mathbf{G}_{23} \\ \mathbf{G}_{32} & \mathbf{G}_{33} \\ \mathbf{G}_{42} & \mathbf{G}_{43} \end{bmatrix} \begin{Bmatrix} \mathbf{a}_{n2} \\ \mathbf{a}_{n3} \end{Bmatrix} - \omega^2 \sum_{j=1}^J \mathbf{Y}_j \begin{bmatrix} \mathbf{G}_{12} \\ \mathbf{G}_{22} \\ \mathbf{G}_{32} \\ \mathbf{G}_{42} \end{bmatrix} \begin{bmatrix} \phi_j \end{bmatrix} \right\}$$

where \mathbf{a}_{n2} and \mathbf{a}_{n3} are the ground motion acceleration component normal to the arch dam-reservoir interface Γ_2 and the reservoir bottom Γ_3 , respectively.

Introducing the notation $\hat{\mathbf{H}}$ for the elements of the left hand side matrix, the system becomes

$$\begin{Bmatrix} \hat{\mathbf{H}}_{11} & \hat{\mathbf{H}}_{12} & \hat{\mathbf{H}}_{13} & \hat{\mathbf{H}}_{14} \\ \hat{\mathbf{H}}_{21} & \hat{\mathbf{H}}_{22} & \hat{\mathbf{H}}_{23} & \hat{\mathbf{H}}_{24} \\ \hat{\mathbf{H}}_{31} & \hat{\mathbf{H}}_{32} & \hat{\mathbf{H}}_{33} & \hat{\mathbf{H}}_{34} \\ \hat{\mathbf{H}}_{41} & \hat{\mathbf{H}}_{42} & \hat{\mathbf{H}}_{43} & \hat{\mathbf{H}}_{44} \end{Bmatrix} \begin{Bmatrix} \mathbf{q}_1 \\ \mathbf{p}_2 \\ \mathbf{p}_3 \\ \mathbf{p}_{14} \end{Bmatrix} = -\frac{w}{g} \begin{Bmatrix} \mathbf{G}_{12} & \mathbf{G}_{13} \\ \mathbf{G}_{22} & \mathbf{G}_{23} \\ \mathbf{G}_{32} & \mathbf{G}_{33} \\ \mathbf{G}_{42} & \mathbf{G}_{43} \end{Bmatrix} \begin{Bmatrix} \mathbf{a}_{n2} \\ \mathbf{a}_{n3} \end{Bmatrix} - \omega^2 \sum_{j=1}^J Y_j \begin{Bmatrix} \mathbf{G}_{12} \\ \mathbf{G}_{22} \\ \mathbf{G}_{32} \\ \mathbf{G}_{42} \end{Bmatrix} \begin{Bmatrix} \phi_j \end{Bmatrix} \quad (4.31)$$

Multiplying both sides of the equation above by $\bar{\mathbf{H}} = \hat{\mathbf{H}}^{-1}$ yields

$$\begin{Bmatrix} \mathbf{q}_1 \\ \mathbf{p}_2 \\ \mathbf{p}_3 \\ \mathbf{p}_{14} \end{Bmatrix} = -\frac{w}{g} \begin{Bmatrix} \bar{\mathbf{H}}_{11} & \bar{\mathbf{H}}_{12} & \bar{\mathbf{H}}_{13} & \bar{\mathbf{H}}_{14} \\ \bar{\mathbf{H}}_{21} & \bar{\mathbf{H}}_{22} & \bar{\mathbf{H}}_{23} & \bar{\mathbf{H}}_{24} \\ \bar{\mathbf{H}}_{31} & \bar{\mathbf{H}}_{32} & \bar{\mathbf{H}}_{33} & \bar{\mathbf{H}}_{34} \\ \bar{\mathbf{H}}_{41} & \bar{\mathbf{H}}_{42} & \bar{\mathbf{H}}_{43} & \bar{\mathbf{H}}_{44} \end{Bmatrix} \begin{Bmatrix} \mathbf{G}_{12} & \mathbf{G}_{13} \\ \mathbf{G}_{22} & \mathbf{G}_{23} \\ \mathbf{G}_{32} & \mathbf{G}_{33} \\ \mathbf{G}_{42} & \mathbf{G}_{43} \end{Bmatrix} \begin{Bmatrix} \mathbf{a}_{n2} \\ \mathbf{a}_{n3} \end{Bmatrix} - \omega^2 \sum_{j=1}^J Y_j \begin{Bmatrix} \mathbf{G}_{12} \\ \mathbf{G}_{22} \\ \mathbf{G}_{32} \\ \mathbf{G}_{42} \end{Bmatrix} \begin{Bmatrix} \phi_j \end{Bmatrix} \quad (4.32)$$

The equations related to the vector \mathbf{p}_2 , the hydrodynamic pressure vector acting on the upstream face of the arch dam, can be extracted from the system as

$$\mathbf{p}_2 = -\frac{w}{g} \begin{Bmatrix} \bar{\mathbf{H}}_{11} & \bar{\mathbf{H}}_{12} & \bar{\mathbf{H}}_{13} & \bar{\mathbf{H}}_{14} \end{Bmatrix} \begin{Bmatrix} \mathbf{G}_{12} & \mathbf{G}_{13} \\ \mathbf{G}_{22} & \mathbf{G}_{23} \\ \mathbf{G}_{32} & \mathbf{G}_{33} \\ \mathbf{G}_{42} & \mathbf{G}_{43} \end{Bmatrix} \begin{Bmatrix} \mathbf{a}_{n2} \\ \mathbf{a}_{n3} \end{Bmatrix} - \omega^2 \sum_{j=1}^J Y_j \begin{Bmatrix} \mathbf{G}_{12} \\ \mathbf{G}_{22} \\ \mathbf{G}_{32} \\ \mathbf{G}_{42} \end{Bmatrix} \begin{Bmatrix} \phi_j \end{Bmatrix} \quad (4.33)$$

\mathbf{p}_2 , can now be rewritten as

$$\mathbf{p}_2 = \mathbf{p}_0(\omega) - \omega^2 \sum_{j=1}^J \mathbf{p}_j(\omega) Y_j(\omega) \quad (4.34)$$

where \mathbf{p}_0 , given by

$$\mathbf{p}_0 = -\frac{w}{g} \begin{Bmatrix} \bar{\mathbf{H}}_{11} & \bar{\mathbf{H}}_{12} & \bar{\mathbf{H}}_{13} & \bar{\mathbf{H}}_{14} \end{Bmatrix} \begin{Bmatrix} \mathbf{G}_{12} & \mathbf{G}_{13} \\ \mathbf{G}_{22} & \mathbf{G}_{23} \\ \mathbf{G}_{32} & \mathbf{G}_{33} \\ \mathbf{G}_{42} & \mathbf{G}_{43} \end{Bmatrix} \begin{Bmatrix} \mathbf{a}_{n2} \\ \mathbf{a}_{n3} \end{Bmatrix} \quad (4.35)$$

is the complex hydrodynamic pressure response vector due to the ground motion acceleration considering the arch dam to be rigid, and \mathbf{p}_j given by,

$$\mathbf{p}_j = \frac{w}{g} \begin{bmatrix} \bar{\mathbf{H}}_{11} & \bar{\mathbf{H}}_{12} & \bar{\mathbf{H}}_{13} & \bar{\mathbf{H}}_{14} \end{bmatrix} \begin{bmatrix} \mathbf{G}_{12} \\ \mathbf{G}_{22} \\ \mathbf{G}_{32} \\ \mathbf{G}_{42} \end{bmatrix} [\phi_j] \quad (4.36)$$

is the corresponding vector due to the arch dam acceleration in its j^{th} vibration mode with no ground motion.

Applying the virtual work principal (Tsai et al,1988), the equivalent nodal forces on the upstream face of the arch dam due to harmonic pressure induced by earthquake ground motion are given by

$$\mathbf{Q}_2 = - \int_{\Gamma_2} \phi_d^T \Lambda_d \phi_f d\Gamma_2 \mathbf{p}_2 \quad (4.37)$$

where, ϕ_d , is the shape function related the finite elements of the dam structure, ϕ_f is the shape function of the boundary elements of the reservoir and Λ_d is the direction cosine matrix of the interface boundary.

Utilizing Eqs. (4.34) and (4.37), the nodal hydrodynamic forces associated with the hydrodynamic pressure on the upstream face of the dam can be expressed as

$$\mathbf{Q}_2 = \mathbf{Q}_0(\omega) - \omega^2 \sum_{j=1}^J \mathbf{Q}_j(\omega) Y_j(\omega) \quad (4.38)$$

where the hydrodynamic force vector \mathbf{Q}_0 and \mathbf{Q}_j are static equivalents of the corresponding pressure functions \mathbf{p}_0 and \mathbf{p}_j , respectively.

5. TWO-DIMENSIONAL DUAL RECIPROCITY METHOD TO MODEL THE INFINITE DOMAIN

The reservoir domain is idealized as a finite region of irregular geometry adjacent to an infinite domain of uniform cross section. The compatibility and equilibrium conditions of pressure and pressure gradients are applied at the so-called far boundary or radiation boundary along the interface of the finite and infinite regions. Hall and Chopra (1980) have applied the finite element method to model both the finite and the infinite domains of the reservoir. In the infinite domain model, they applied the separation of variables technique to combine a two-dimensional finite element discretization over the uniform cross section of the domain with a continuum expression in the upstream direction. The problem ultimately reduced to the solution of a standard eigenvalue problem. As an alternative, Rashed and Kandasamy (1990) applied a two dimensional boundary element discretization together with the continuum expression to model the infinite reservoir system of uniform cross section. The major drawback of their method is the frequency dependent fundamental solution, which means that, the system could not be cast in the form of a standard eigenvalue problem. To obtain a standard eigenvalue problem, the dual reciprocity method with a frequency independent fundamental solution may be used. This method has proven to be an effective tool in the solution of free vibration elasticity problems (Nardini and Brebbia, 1982 and Ahmad and Banerjee, 1986) and acoustic eigenvalues analysis (Banerjee, et al, 1988 and Ali, et al, 1991).

In this study, the dual reciprocity method along with the separation of variables technique is adopted to model a three-dimensional infinite domain of uniform cross section. The variation of the pressure response in the upstream direction is represented by a continuum expression. A two-dimensional eigenvalue analysis based on the dual reciprocity formulations is utilized over the cross section of the domain.

5.1. The Boundary Value Problem for the Infinite Region of the Reservoir

The infinite reservoir domain is assumed to have a uniform cross section with absorptive bottom and sides as it is shown in Figure 5.1. The governing equation for the hydrodynamic pressure response is the Helmholtz equation given as,

$$\nabla^2 p = -\frac{\omega^2}{c^2} p \quad (5.1)$$

The solution sought is to be subject to the following boundary conditions:

(A) The free surface boundary condition, the pressure is set equal to the gage pressure

$$p = 0 \quad (5.2)$$

(B) Absorbing boundary conditions at the bottom and sides of the reservoir as suggested by (Hall and Chopra, 1980)

$$q = -\frac{w}{g} a_n (\omega) + i\omega \gamma p \quad (5.3)$$

in which, a_n is the outward normal acceleration component at the reservoir bottom and sides, γ is the bottom absorption damping coefficient given by Eq.(3.20)

(C) Matching boundary conditions at the interface of the finite and infinite regions

$$p_{\text{finite}} = p_{\text{infinite}} \quad q_{\text{finite}} = -q_{\text{infinite}} \quad (5.4)$$

(D) Radiation boundary conditions at the far end of reservoir in the upstream direction

$$p_{\infty} = 0 \quad (5.5)$$

which means that pressure waves leaving the reservoir domain are not reflected at infinity.

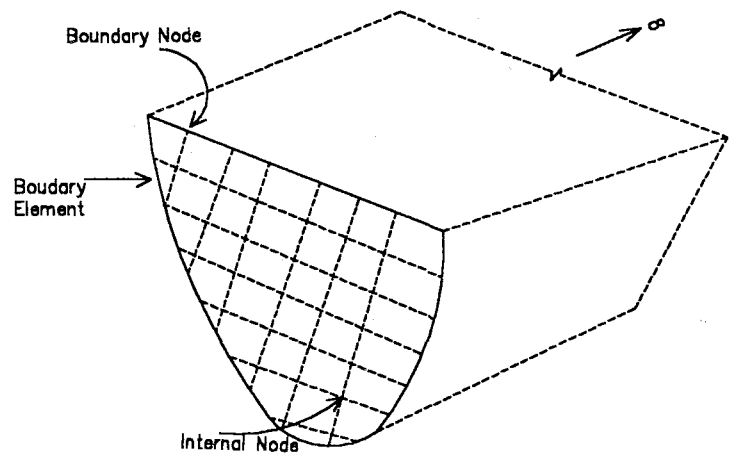
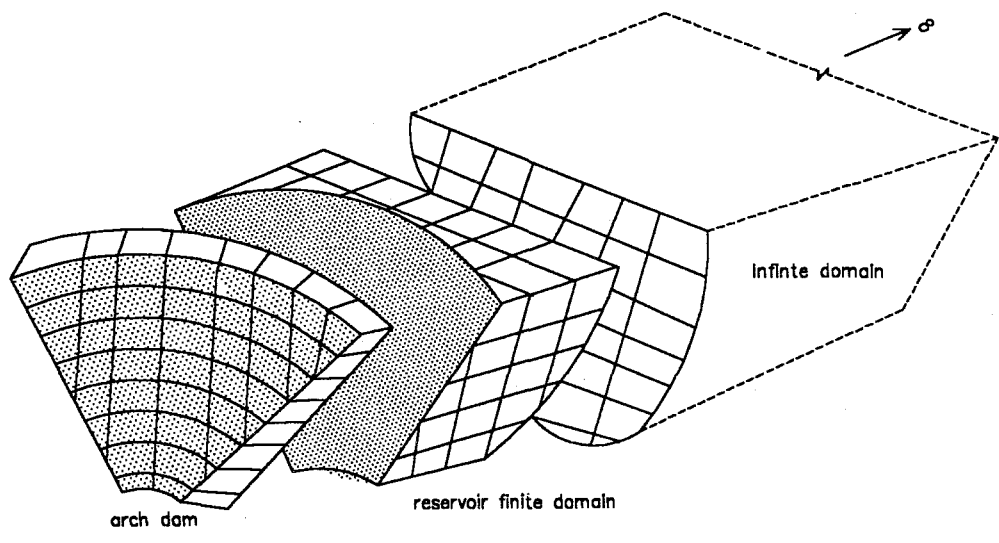


FIGURE 5.1. Infinite domain radiation model

With the assumption of uniform ground motion along the upstream direction, x , the hydrodynamic pressure response in this direction, can be separated from the pressure distribution over the uniform cross section y - z plane. The hydrodynamic pressure response can be written as

$$p = p_x p_{yz} \quad (5.6)$$

thus enabling Eq.(5.1) to be recast in the form

$$\frac{\partial^2 p_x}{\partial x^2} + \frac{\partial^2 p_{yz}}{\partial y^2} + \frac{\partial^2 p_{yz}}{\partial z^2} = -\frac{\omega^2}{c^2} p_x p_{yz} \quad (5.7)$$

The application of the separation of variables technique yields two boundary value problems for the hydrodynamic pressure response. One for the upstream direction, x , and the other for the uniform cross section y - z plane. The governing equations for these are,

$$\frac{\partial^2 p_x}{\partial x^2} - \kappa^2 p_x = 0 \quad (5.8)$$

and

$$\frac{\partial^2 p_{yz}}{\partial y^2} + \frac{\partial^2 p_{yz}}{\partial z^2} + \lambda^2 p_{yz} = 0 \quad (5.9)$$

where $\lambda^2 = \omega^2 / c^2 + \kappa^2$ and κ is the separation constant.

5.2. Continuum Expression for the Pressure Along the Upstream Direction

The hydrodynamic pressure response in the upstream direction is governed by Eq.(5.8), and satisfies the radiation boundary condition at the far end of domain. The pressure waves propagate away to infinity or decay with increasing distance, thus, the pressure can be cast in the form of a continuum expression in the x -direction as

$$p_x = e^{-\kappa_m x} \quad m = 1, 2, 3, \dots \quad (5.10)$$

where

$$\kappa_m = \sqrt{\lambda_m^2 - \frac{\omega^2}{c^2}}$$

In the above expression, λ_m 's are the eigenvalues obtained from the solution of Eq.(5.9), the governing equation for the pressure response distribution in the y-z plane.

5.3. Dual Reciprocity Formulation for the Pressure Over the Uniform Cross Section

The hydrodynamic pressure response distribution over the y-z plane is governed by the two-dimensional Helmholtz equation expressed in Eq.(5.9) and satisfies the free surface and the bottom absorption boundary conditions expressed by Eqs.(5.2) and (5.3), respectively. The dual reciprocity formulation for the Helmholtz equation, as derived in the previous chapter, is given by

$$\mathbf{Gq} - \mathbf{Hp} = -\lambda^2 \tilde{\mathbf{M}}p \quad (5.11)$$

where, the matrices \mathbf{G} and \mathbf{H} are computed on the boundary elements by integrating the Laplace fundamental solution multiplied by an appropriate interpolation function, the matrix $\tilde{\mathbf{M}}$ is computed using the dual reciprocity approximation functions.

For the two-dimensional case, the fundamental solution of the Laplace equation (Brebbia et al, 1984) is given by

$$g(x, \xi) = \frac{1}{2\pi} \ln(r) \quad (5.12)$$

The radial basis approximation functions utilized in the analysis are of the form

$$f(r) = a_0 + a_1 r + a_2 r^2 + \dots + a_m r^m \quad (5.13)$$

The particular solution for the two-dimensional case can be derived (Partridge, et al 1992) as

$$\hat{p}(r) = \frac{a_0 r^2}{4} + \frac{a_1 r^3}{9} + \frac{a_2 r^4}{16} + \dots + \frac{a_m r^{m+2}}{(m+2)^2} \quad (5.14)$$

The normal derivatives $\hat{q}(r)$ can be obtained from $\hat{p}(r)$ as

$$\hat{q}(r) = \left(\frac{a_0 r}{2} + \frac{a_1 r^2}{3} + \frac{a_2 r^3}{4} + \dots + \frac{a_m r^{m+1}}{(m+2)} \right) \frac{\partial r}{\partial n} \quad (5.15)$$

For a specified excitation frequency, ω , Eq.(5.11) may be rearranged and assembled in the following discretized form

$$\begin{bmatrix} \mathbf{H}_{11} & \mathbf{H}_{12} & \mathbf{0} \\ \mathbf{H}_{21} & \mathbf{H}_{22} & \mathbf{0} \\ \mathbf{H}_{31} & \mathbf{H}_{32} & \mathbf{I} \end{bmatrix} \begin{Bmatrix} \mathbf{p}_1 \\ \mathbf{p}_2 \\ \mathbf{p}_3 \end{Bmatrix} - \begin{bmatrix} \mathbf{G}_{11} & \mathbf{G}_{12} & \mathbf{0} \\ \mathbf{G}_{21} & \mathbf{G}_{22} & \mathbf{0} \\ \mathbf{G}_{31} & \mathbf{G}_{32} & \mathbf{0} \end{bmatrix} \begin{Bmatrix} \mathbf{q}_1 \\ \mathbf{q}_2 \\ \mathbf{q}_3 \end{Bmatrix} = -\lambda^2 \begin{bmatrix} \tilde{\mathbf{M}}_{11} & \tilde{\mathbf{M}}_{12} & \tilde{\mathbf{M}}_{13} \\ \tilde{\mathbf{M}}_{21} & \tilde{\mathbf{M}}_{22} & \tilde{\mathbf{M}}_{23} \\ \tilde{\mathbf{M}}_{31} & \tilde{\mathbf{M}}_{32} & \tilde{\mathbf{M}}_{33} \end{bmatrix} \begin{Bmatrix} \mathbf{p}_1 \\ \mathbf{p}_2 \\ \mathbf{p}_3 \end{Bmatrix} \quad (5.16)$$

where \mathbf{I} is a unitary matrix and \mathbf{H}_{ij} , \mathbf{G}_{ij} and $\tilde{\mathbf{M}}_{ij}$ are the respective sub-matrices of \mathbf{H} , \mathbf{G} and $\tilde{\mathbf{M}}$. The indices i and j refer to the boundary condition types: free surface of the reservoir on Γ_1 , absorbing boundary of the reservoir bottom and banks on Γ_2 and the internal nodes in the domain $\Omega_3 \dots$

Introducing the specified boundary conditions of Eqs.(5.2-5.3) into Eq.(5.16), results in

$$\begin{bmatrix} \mathbf{H}_{11} & \mathbf{H}_{12} & -i\omega\gamma\mathbf{G}_{12} & \mathbf{0} \\ \mathbf{H}_{21} & \mathbf{H}_{22} & -i\omega\gamma\mathbf{G}_{22} & \mathbf{0} \\ \mathbf{H}_{31} & \mathbf{H}_{32} & -i\omega\gamma\mathbf{G}_{32} & \mathbf{I} \end{bmatrix} \begin{Bmatrix} \mathbf{0} \\ \mathbf{p}_2 \\ \mathbf{p}_3 \end{Bmatrix} - \begin{bmatrix} \mathbf{G}_{11} & \mathbf{G}_{12} & \mathbf{0} \\ \mathbf{G}_{21} & \mathbf{G}_{22} & \mathbf{0} \\ \mathbf{G}_{31} & \mathbf{G}_{32} & \mathbf{0} \end{bmatrix} \begin{Bmatrix} \mathbf{q}_1 \\ -\frac{w}{g}\mathbf{a}_{n2} \\ \mathbf{0} \end{Bmatrix} = -\lambda^2 \begin{bmatrix} \tilde{\mathbf{M}}_{11} & \tilde{\mathbf{M}}_{12} & \tilde{\mathbf{M}}_{13} \\ \tilde{\mathbf{M}}_{21} & \tilde{\mathbf{M}}_{22} & \tilde{\mathbf{M}}_{23} \\ \tilde{\mathbf{M}}_{31} & \tilde{\mathbf{M}}_{32} & \tilde{\mathbf{M}}_{33} \end{bmatrix} \begin{Bmatrix} \mathbf{0} \\ \mathbf{p}_2 \\ \mathbf{p}_3 \end{Bmatrix} \quad (5.17)$$

The above system of equations can be partitioned as follows

$$\begin{bmatrix} \mathbf{H}_{12} & -i\omega\gamma\mathbf{G}_{12} & \mathbf{0} \end{bmatrix} \begin{Bmatrix} \mathbf{p}_2 \\ \mathbf{p}_3 \end{Bmatrix} - [\mathbf{G}_{11}]\{\mathbf{q}_1\} + \frac{w}{g}[\mathbf{G}_{12}]\{\mathbf{a}_{n2}\} = -\lambda^2 [\tilde{\mathbf{M}}_{12} \quad \tilde{\mathbf{M}}_{13}] \begin{Bmatrix} \mathbf{p}_2 \\ \mathbf{p}_3 \end{Bmatrix} \quad (5.18)$$

$$\begin{bmatrix} \mathbf{H}_{22} - i\omega\gamma\mathbf{G}_{22} & \mathbf{0} \\ \mathbf{H}_{32} - i\omega\gamma\mathbf{G}_{32} & \mathbf{I} \end{bmatrix} \begin{Bmatrix} \mathbf{p}_2 \\ \mathbf{p}_3 \end{Bmatrix} - \begin{bmatrix} \mathbf{G}_{21} \\ \mathbf{G}_{31} \end{bmatrix} \{\mathbf{q}_1\} + \frac{w}{g} \begin{bmatrix} \mathbf{G}_{22} \\ \mathbf{G}_{32} \end{bmatrix} \{\mathbf{a}_{n2}\} = -\lambda^2 \begin{bmatrix} \tilde{\mathbf{M}}_{22} & \tilde{\mathbf{M}}_{23} \\ \tilde{\mathbf{M}}_{32} & \tilde{\mathbf{M}}_{33} \end{bmatrix} \begin{Bmatrix} \mathbf{p}_2 \\ \mathbf{p}_3 \end{Bmatrix} \quad (5.19)$$

In order to set the system of the equation as eigenvalue problem in terms of the unknown pressure $\mathbf{p}_{x,y}$, \mathbf{q}_1 can be eliminated from the above two system of equations and the vector \mathbf{q}_1 can be solved for the system of Eq.(5.18) as

$$\{\mathbf{q}_1\} = [\mathbf{G}_{11}]^{-1} \left\{ \begin{bmatrix} \mathbf{H}_{12} - i\omega\gamma\mathbf{G}_{12} & \mathbf{0} \end{bmatrix} \begin{Bmatrix} \mathbf{p}_2 \\ \mathbf{p}_3 \end{Bmatrix} + \frac{w}{g} [\mathbf{G}_{12}] \{\mathbf{a}_{n2}\} + \lambda^2 \begin{bmatrix} \tilde{\mathbf{M}}_{12} & \tilde{\mathbf{M}}_{13} \end{bmatrix} \begin{Bmatrix} \mathbf{p}_2 \\ \mathbf{p}_3 \end{Bmatrix} \right\} \quad (5.20)$$

Substituting Eq.(5.20) into Eq.(5.19) results in the following eigenvalue problem

$$\left[\tilde{\mathbf{H}} + i\omega\gamma\tilde{\mathbf{G}} - \lambda^2\tilde{\mathbf{M}} \right] \{\mathbf{p}_{yz}\} = -\frac{w}{g}\tilde{\mathbf{d}} \quad (5.21)$$

where

$$\{\mathbf{p}_{yz}\} = \begin{Bmatrix} \mathbf{p}_1 \\ \mathbf{p}_2 \end{Bmatrix}$$

$$\tilde{\mathbf{H}} = \begin{bmatrix} \mathbf{H}_{22} & \mathbf{0} \\ \mathbf{H}_{32} & \mathbf{I} \end{bmatrix} - \begin{bmatrix} \mathbf{G}_{21} \\ \mathbf{G}_{31} \end{bmatrix} [\mathbf{G}_{11}]^{-1} \begin{bmatrix} \mathbf{H}_{12} & \mathbf{0} \end{bmatrix}$$

$$\tilde{\mathbf{G}} = -\begin{bmatrix} \mathbf{G}_{22} & \mathbf{0} \\ \mathbf{G}_{32} & \mathbf{0} \end{bmatrix} + \begin{bmatrix} \mathbf{G}_{21} \\ \mathbf{G}_{31} \end{bmatrix} [\mathbf{G}_{11}]^{-1} \begin{bmatrix} \mathbf{G}_{12} & \mathbf{0} \end{bmatrix}$$

$$\tilde{\mathbf{M}} = -\begin{bmatrix} \tilde{\mathbf{M}}_{22} & \tilde{\mathbf{M}}_{23} \\ \tilde{\mathbf{M}}_{32} & \tilde{\mathbf{M}}_{33} \end{bmatrix} + \begin{bmatrix} \mathbf{G}_{21} \\ \mathbf{G}_{31} \end{bmatrix} [\mathbf{G}_{11}]^{-1} \begin{bmatrix} \tilde{\mathbf{M}}_{12} & \tilde{\mathbf{M}}_{13} \end{bmatrix}$$

$$\tilde{\mathbf{d}} = \left\{ \begin{bmatrix} \mathbf{G}_{22} \\ \mathbf{G}_{32} \end{bmatrix} - \begin{bmatrix} \mathbf{G}_{21} \\ \mathbf{G}_{31} \end{bmatrix} [\mathbf{G}_{11}]^{-1} \begin{bmatrix} \mathbf{G}_{12} \end{bmatrix} \right\} \{\mathbf{a}_{n2}\}$$

The matrices, $\tilde{\mathbf{H}}$, $\tilde{\mathbf{G}}$ and $\tilde{\mathbf{M}}$ are non-symmetrical and are independent of the excitation frequency. Only the nodes below the free surface within the cross section are included in the system of Eq.(5.21). It is interesting to observe that the eigenvalue problem of Eq.(5.21) has a similar form to that obtained by Hall and Chopra (1980) using the finite element discretization as shown in Appendix. C.

5.4. Formulation of the Radiation Matrix

In the three-dimensional earthquake response analysis of arch dam-reservoir systems, the boundary motions of the reservoir domain can be classified as due to :

- (a) the deformational motions of the arch dam without any ground motion,
- (b) the upstream-downstream excitation or the x-component of the ground motion,
- (c) the cross stream excitation or the y-component of the ground motion, and
- (d) the vertical excitation or the z-component of the ground motion.

For cases (1) and (2), the boundary motion of the reservoir is normal to the surface boundary of the reservoir. Therefore, the right hand vector $\tilde{\mathbf{d}}$ of Eq.(5.21) vanishes and the equation is simplified to the form

$$\left[\tilde{\mathbf{H}} + i\omega\gamma\tilde{\mathbf{G}} \right] \{ \mathbf{p}_{yz} \} = -\lambda^2 \tilde{\mathbf{M}} \{ \mathbf{p}_{yz} \} \quad (5.22)$$

which represents a generalized eigenvalue problem. For an absorptive reservoir boundary, the eigenvalues λ_m and the eigenvectors, Ψ_m , obtained from the solution of Eq.(5.22) are complex valued and dependent on the excitation frequency. The eigenvectors, Ψ_m , are orthogonal and normalized so that

$$\Psi^T \left[\tilde{\mathbf{M}} \right] \Psi = \mathbf{I} \quad (5.23)$$

and they satisfy the equation

$$\Psi^T \left[\mathbf{H} + i\omega\gamma\tilde{\mathbf{G}} \right] \Psi = \Lambda \quad (5.24)$$

where, Λ is a diagonal matrix of M eigenvalues $\lambda_1^2, \lambda_2^2, \dots, \lambda_M^2$ and Ψ is the matrix of M

eigenvectors, $[\Psi_1, \Psi_2, \dots, \Psi_M]$.

The hydrodynamic pressure response over the cross section of the infinite domain can be expressed approximately as a linear combination of the M eigenvectors. That is,

$$\mathbf{p}_{yz} = \sum_{m=1}^M \eta_m \Psi_m \quad (5.25)$$

where, η_m , are unknown coefficients.

Substituting, Eqs.(5.10) and (5.25) into Eq.(5.6), the hydrodynamic pressure response vector in the infinite domain can be written as

$$\mathbf{p} = \sum_{m=1}^M \eta_m \Psi_m e^{-\kappa_m x} \quad (5.26)$$

Differentiating the hydrodynamic pressure response with respect to the outward normal to the cross section plane (y - z), noting that the normal is parallel to upstream direction, x , results in

$$\mathbf{q} = - \sum_{m=1}^M \kappa_m \eta_m \Psi_m e^{-\kappa_m x} \quad (5.27)$$

Eqs.(5.26) and (5.27) can be rewritten in matrix form as

$$\mathbf{p} = \Psi \mathbf{E} \boldsymbol{\eta} \quad (5.28)$$

$$\mathbf{q} = -\Psi \mathbf{K} \mathbf{E} \boldsymbol{\eta} \quad (5.29)$$

In Eqs.(5.28) and (5.29), $\boldsymbol{\eta}$, is the vector of unknown coefficients, \mathbf{K} is a diagonal matrix with elements, $\kappa_1, \kappa_2, \dots, \kappa_M$ and \mathbf{E} is another diagonal matrix with elements $e^{-\kappa_m x}$.

By eliminating $\mathbf{E} \boldsymbol{\eta}$ between Eqs.(5.28) and (5.29), the relation between \mathbf{p} and \mathbf{q} can be obtained as

$$\mathbf{q} = \mathbf{R} \mathbf{p} \quad (5.30)$$

where,

$$\mathbf{R} = \Psi \mathbf{K} \Psi^{-1} \quad (5.31)$$

The radiation matrix, \mathbf{R} , relates the pressure response vector, \mathbf{p} , and its normal derivative, \mathbf{q} , for the nodes below the free surface on the radiation boundary between the finite and infinite domains of the reservoir. For the absorbing bottom boundary of the reservoir, \mathbf{R} is dependent on the excitation frequency, ω .

Using the same procedure in Eqs.(5.28-5.31), it is also possible to generate a radiation matrix, \mathbf{R} , based on the Hall and Chopra(1980) model for the infinite domain. This formulation is discussed in Appendix C.

For vertical and cross-stream excitations, cases (3) and (4) of Vertical and cross-stream ground motions, no variation in ground motion is assumed along the upstream direction. The solution of the infinite reservoir system with uniform cross section is independent of x . As a result, the normal derivative of the pressure response, q , along the radiation boundary is equal to zero, therefore the radiation matrix, \mathbf{R} , identically zero.

6. VERIFICATION OF THE HYDRODYNAMIC MODEL

In the previous chapters, an effective numerical model based on a hybrid FEM-DRBEM scheme has been developed to study the fluid-structure interaction and earthquake response of arch dam-reservoir systems. Applying the substructure technique, the finite element method is utilized to model dam structure and the dual reciprocity method was used to model the reservoir domain. Considering the bottom absorption effects, the reservoir domain was idealized as a finite region of irregular geometry adjacent to an infinite domain of uniform cross section. Based on the model, a computer code was developed to calculate the seismic response of a three-dimensional dam-reservoir system of arbitrary geometry to upstream-downstream, cross-stream and vertical harmonic ground motion. In this chapter, the model is verified by comparing the hydrodynamic response of a three-dimensional rectangular reservoir with that from the analytical formulation existing in the literature.

6.1. Case Study: Three-Dimensional Rectangular Reservoir

To check the validity of the numerical model, the hydrodynamic pressure distribution in a three-dimensional rectangular reservoir is compared with that given through the analytical expressions derived by Rashed and Iwan (1984). The verification is carried out for all three components of the ground motion. A sketch of the reservoir used in the analysis is given in Figure 6.1. In the computations, the reservoir properties used are as follows: Water depth, $H=100\text{m}$, radiation boundary is placed at a distance $L=100\text{m}$ from the upstream face of the dam, the velocity of the sound in water, $c=1440\text{m/sec}$ and the mass density of water $\rho_w=1000\text{ kg/m}^3$. The first fundamental frequency of the reservoir with the above properties is determined from $\omega_1=\pi c/2H$, and is $22.62\text{ rad/sec}(3.6\text{Hz})$.

Earlier studies [Jablonski,1990] have shown that the numerical results depend strongly on the modeling of the radiation boundary for excitation frequencies greater than ω_1 . Accurate results can be obtained from the numerical model provided the element size in the mesh is not more than one-tenth of the shortest wave length in the reservoir.

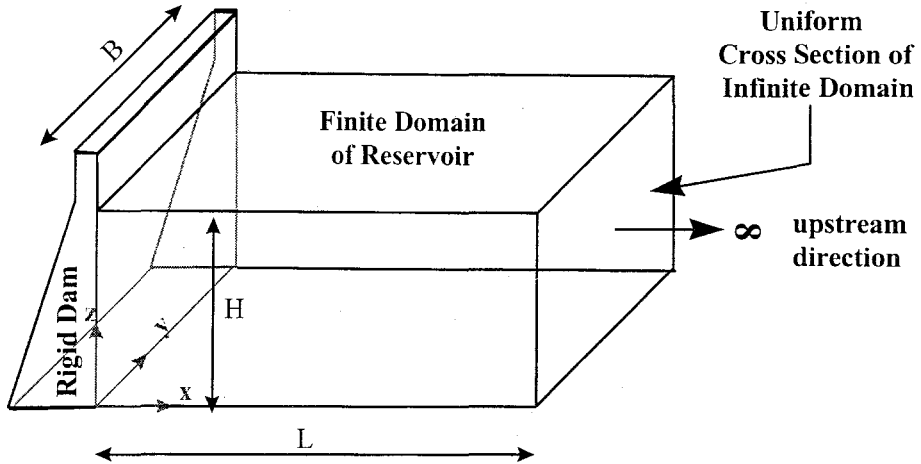


FIGURE 6.1. Three-dimensional rectangular infinite reservoir.

The reservoir boundary is discretized into 600 three-dimensional isoparametric first order quadrilateral elements with 441 internal nodes. To model the radiation condition in the finite and uniform infinite domains a two-dimensional dual reciprocity model is considered. Boundaries of the uniform cross section of the infinite domain are discretized into 40 isoparametric linear elements. The internal nodes existing on the interface are considered as internal nodes for the radiation model. The thin plate spline approximating function is used in the dual reciprocity models. To check the validity of the radiation model, a finite element model based on the formulation given in Appendix C was also developed. In this model, 15 isoparametric four-node linear quadrilateral elements were used.

6.2. Verification of the DRBEM-Radiation Model

The radiation model for the reservoir infinite domain is based on applying the separation technique to combine a two-dimensional eigenvalue problem over the cross section with a continuum expression for the variation of the pressure response in the upstream direction. The model applies the dual reciprocity formulations derived in Chapter 5 to develop an eigenvalue problem for the infinite domain of the reservoir. The procedure results in a generalized eigenvalue problem which can be solved using the QZ algorithm originally developed by Moler and Stewart(1973).

To verify the model results, the eigenvalues of the system are compared with those obtained using the finite element method and with the eigenvalues determined using the analytical formulation of Rashed and Iwan,1984. For a fully reflective reservoir boundary, $\alpha=1.0$, the eigenvalues are independent of the excitation frequency. The first 10 eigenvalues are presented in Table 6.1. Despite the non-symmetric nature of the dual reciprocity matrices, the model is found to yield results which compare extremely well with those obtained from Rashed and Iwan(1984). The maximum relative error for the represented eigenvalues is less than 0.63 %. Some of the complex eigenvalues of the system appear only at higher frequencies where the higher order vibration modes are inevitable in the continuum problem. The finite element model results are presented for the sake of comparison. The maximum relative error for the same eigenvalues range is 3.64%. For fully reflecting reservoir boundaries, the eigenvalues obtained from the finite element method are real valued. When boundary

absorption effects are included the eigenvalues given by both the DRBEM and the FEM are complex valued and dependent on the excitation frequency.

6.3. Verification of the DRBEM-Reservoir Model

The hydrodynamic pressure and hence the hydrodynamic force on the upstream face of rigid dams are determined by the hydrodynamic pressure responses in the reservoir domain which includes a finite irregular domain adjacent to an infinite domain of uniform cross-section.

As indicated in the procedure explained in Chapter 4, the hydrodynamic pressure response can be computed for a given excitation frequency by solving the generalized eigenvalue problem for the infinite domain of the reservoir to form the radiation matrix based on the dual reciprocity formulation. The radiation matrix is used to relate the pressure and the pressure gradients across the radiation boundary of the finite domain of the reservoir model. The finite domain of the reservoir is modeled utilizing the dual reciprocity method.

The hydrodynamic responses of a rigid dam-reservoir system are presented for four values of the reservoir boundary reflection coefficient $\alpha_r = 1.0$ (total reflection), 0.75, 0.50, and 0 (total absorption). The following cases are studied:

- (a) rigid dam subjected to upstream ground motion,
- (b) rigid dam subjected to vertical ground motion,
- (c) rigid dam subjected to cross-stream ground motion.

In the following sections, the results of the model are compared with the analytical solution of Rashed and Iwan, 1984.

6.3.1. The Hydrodynamic Pressure

The frequency response functions of the hydrodynamic pressure distribution on the upstream face of the dam are calculated for an excitation amplitude of 1g and a wide range of the excitation frequency values, ω . The four reflection coefficients given above are used.

The following variables were used in the study:

p^* : the hydrodynamic pressure normalized by the hydrostatic pressure at the bottom of the reservoir, $p^*=p/(\gamma H)$.

x^* : the distance along the upstream direction normalized by the upstream length of the finite reservoir.

z^* : the vertical distance across the height of the dam normalized by the reservoir height, H .

Ω : the excitation frequency normalized by $\omega_1 = \pi c/2H$, the first natural vibration frequency of an infinite reservoir of uniform depth H with a rigid reservoir bottom.

For the upstream-downstream ground excitation, the total normalized hydrodynamic pressure on the upstream face along with its in-phase and out-of-phase components is presented in Figures 6.2-6.5 over a frequency range $\Omega=0.4$ to 4.8. The corresponding hydrodynamic pressure distributions on the reservoir bottom along the upstream direction are shown in Figures 6.6-6.9. The dual reciprocity model results are found to be in a good agreement with the analytical solution of Rashed and Iwan(1984). As expected, for the fully reflecting reservoir boundary case, the hydrodynamic pressures are entirely in-phase with the excitation for values of Ω less than unity. For normalized excitation frequencies, Ω , greater than unity, the pressure associated with the higher frequency modes propagates in the upstream direction of the infinite channel resulting in energy radiation to infinity and hence the out-of-phase pressure component appears over this frequency range. For absorbing reservoir boundaries both the in phase and the out of phase components exist over the entire frequency range due to the energy dissipation at the absorbing boundaries in addition to the radiation boundaries .

For vertical ground excitation, the total, in-phase and out-of-phase components of the normalized hydrodynamic pressure on the upstream face of the dam are presented in Figures 6.10-6.13. The dual reciprocity model results are found to be in a good agreement with the analytical solution. For the fully reflecting reservoir boundary case, the hydrodynamic pressures are entirely in-phase with the excitation for the entire frequency range. With the assumption of no variation of ground motion in the upstream direction, no energy will be radiated out of the system. For absorbing reservoir boundary cases, the absorption on the boundaries is the only energy dissipation mechanism. As mentioned above, boundary energy absorption causes the out-of-phase component of the hydrodynamic pressure to appear over

the total frequency range.

The upstream and vertical ground motion excitations have symmetrical vibration modes, while the cross-stream ground excitation has anti-symmetric modes. For the upstream and vertical ground motion, the hydrodynamic pressure does not vary across the width of the upstream face of the dam. In the cross-stream case, the hydrodynamic pressure distribution varies anti-symmetrically across the width of the dam. The total, in-phase and out-of-phase components of the hydrodynamic pressure on the upstream face at the side boundary of the upstream phase where $y=0.0$, are presented in Figures 6.14-6.17 for a frequency range $\Omega=0.4$ to 4.8 and for four different reflection coefficients. The system has an energy dissipation mechanism which is similar to that of the vertical excitation case.

It should be noted that the phase angle of the hydrodynamic pressure response varies along the height of the dam. This means that the maximum pressures along the height do not occur at the same instance of time.

6.3.2. Hydrodynamic Forces

The frequency response functions for the hydrodynamic force on the upstream face of the dam are computed by integrating the corresponding hydrodynamic pressure response functions obtained from the solution of the Helmholtz equation. The hydrodynamic force F^* is normalized with respect to the hydrostatic force on of the upstream face of the dam, $F_{st} = 0.5\gamma H^2 B$, where γ is the unit weight of the water, H is the water depth and B is the width of the reservoir. As before, the excitation frequency is normalized with respect to w_1 .

The total, in-phase and out-of-phase components of the total hydrodynamic force on the upstream face of a rigid dam are computed for normalized excitation frequencies $\Omega=0.0$ to 5.0 and for an excitation amplitude of $1g$ in the upstream-downstream, vertical and cross-stream ground motion directions. The reservoir boundary reflection coefficients $\alpha = 0.0, 0.5, 0.75$ and 1.0 are used. The model results are compared with the hydrodynamic forces obtained from the analytical formulation of Rashed and Iwan, 1984.

For the upstream-downstream ground motion excitation, the total, in-phase and out-

phase components of the normalized hydrodynamic force on the upstream face, are presented in Figures 6.18-6.20 for the different values of the reflection coefficient. The results for vertical ground motion excitation are represented in Figures 6.21-6.23. As the hydrodynamic pressure response to cross-stream ground motion is anti-symmetrical, the hydrodynamic force on one half of the dam is of opposite phase relative to the force on the other half. For cross-stream ground motion excitation, the hydrodynamic force on one half of the upstream face is normalized with respect to the corresponding hydrostatic force and plotted in Figures 6.24-6.27. The model results compare favorably to the analytical formulation results for all the three ground motion excitations and different reservoir boundaries absorbing factors.

For the fully reflecting reservoir boundary, $\alpha_r=1.0$, the hydrodynamic force response functions are unbounded at the natural frequencies of the infinite uniform domain for all directions of ground motion excitation considered. The hydrodynamic force responses due to upstream ground motion are entirely in-phase with the excitation frequency for Ω less than unity. The out-of-phase component exists at higher excitation frequencies indicating radiation due to propagation of hydrodynamic pressure waves in the upstream direction. With increasing excitation frequency, a larger number of modes are associated with the propagating pressure waves, leading to increased energy radiation and hence smaller hydrodynamic force, except for the local resonance behavior near the natural vibration frequencies of the infinite domain. For vertical and cross-stream ground motions, the out-of-phase component does not exist since, as mentioned above, upstream radiation of energy does not take place.

When reservoir boundary absorption exists, the hydrodynamic force response functions are bounded for all excitation frequencies for all three components of ground motion due to the boundary energy dissipation. The out-of-phase component of the hydrodynamic force response exists for all excitation frequencies. For normalized excitation frequencies less than unity, the out-of-phase component arises from the radiation of energy due to the absorption of pressure waves into the absorptive reservoir boundary, whereas for higher excitation frequencies, the out-of-phase component arises from the radiation of energy due to both the propagation of pressure waves in the upstream direction and the refraction into the adsorptive reservoir boundary.

TABLE 6.1. Comparison of natural frequencies of the infinite domain in a three-dimensional rectangular reservoir.

Natural frequency, ω (rad/sec)	Analytical (Rashed and Iwan, 1984)	FEM (Hall and Chopra, 1981)	DRBEM (Present study)
ω_1	22.604	22.626 (0.10%)	22.635 (0.14%)
ω_2	50.544	50.720 (0.35%)	50.603 (0.12%)
ω_3	67.811	68.440 (0.93%)	67.837 (0.04%)
ω_4	81.499	82.126 (0.77%)	81.600 (0.12%)
ω_5	93.198	94.653 (1.56%)	93.440 (0.26%)
ω_6	113.02	114.59 (1.39%)	112.99 (0.03%)
ω_7	113.02	115.94 (1.39%)	112.99 (0.03%)
ω_8	121.72	124.51 (2.29%)	122.31 (0.48%)
ω_9	137.49	142.49 (3.64%)	138.35 (0.63%)
ω_{10}	144.73	147.95 (2.22%)	145.07 (0.23%)

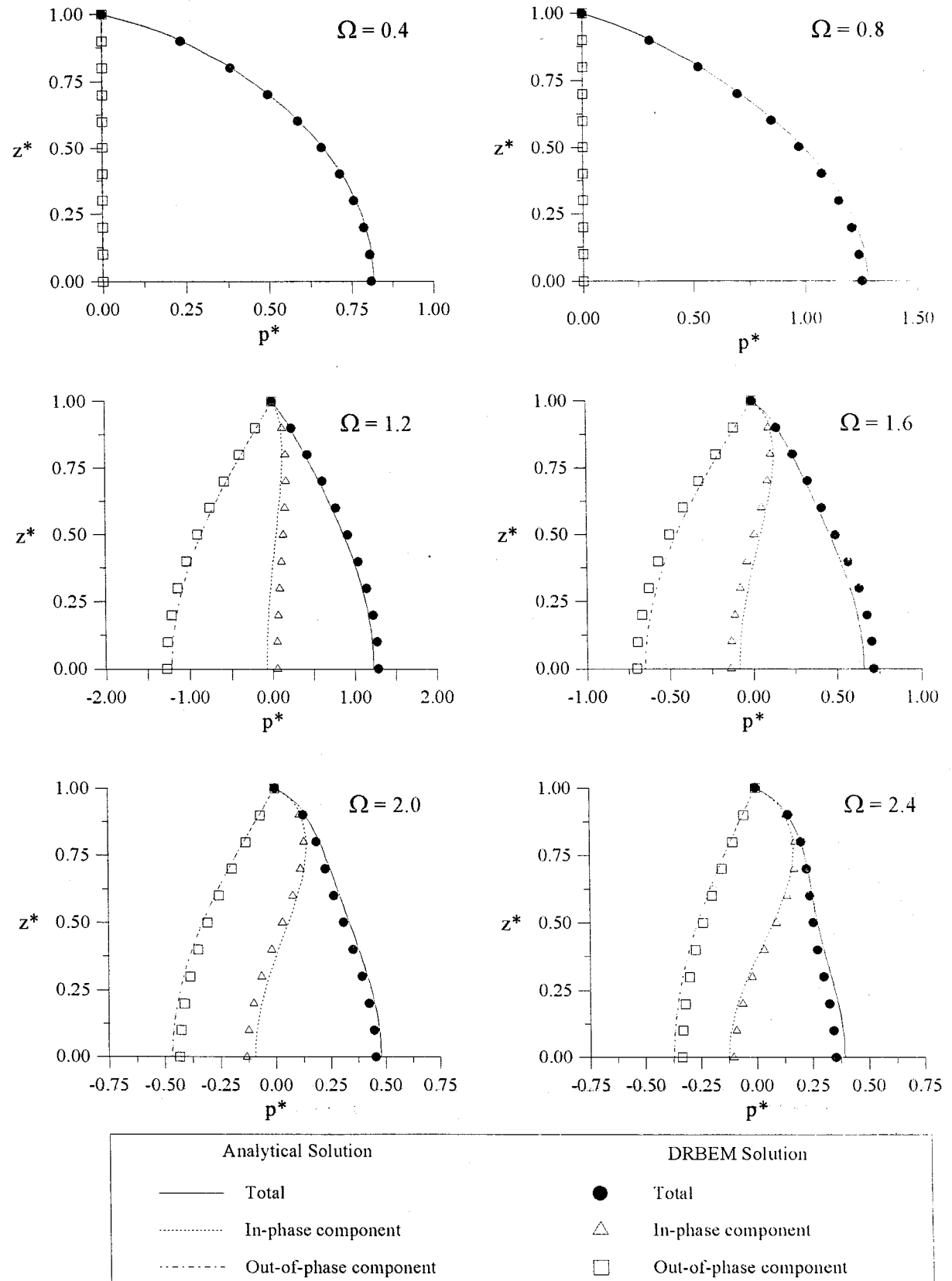


FIGURE 6.2.(a) Hydrodynamic pressure distribution on the upstream face of the rigid dam (harmonic upstream ground motion, reservoir boundary reflection coefficient, $\alpha_r = 1.0$).

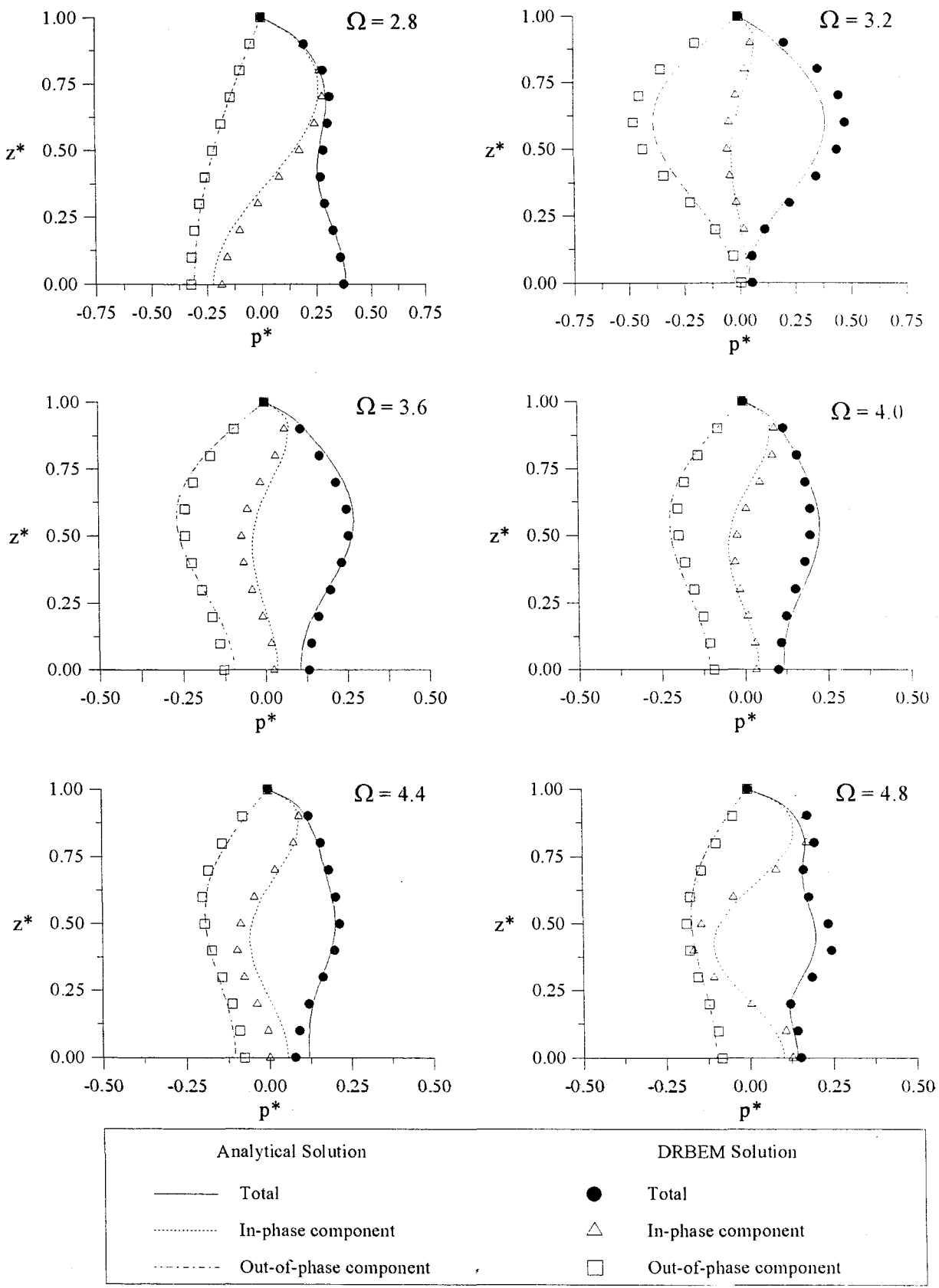


FIGURE 6.2.(b) Hydrodynamic pressure distribution on the upstream face of the rigid dam (harmonic upstream ground motion, reservoir boundary reflection coefficient, $\alpha_r = 1.0$).

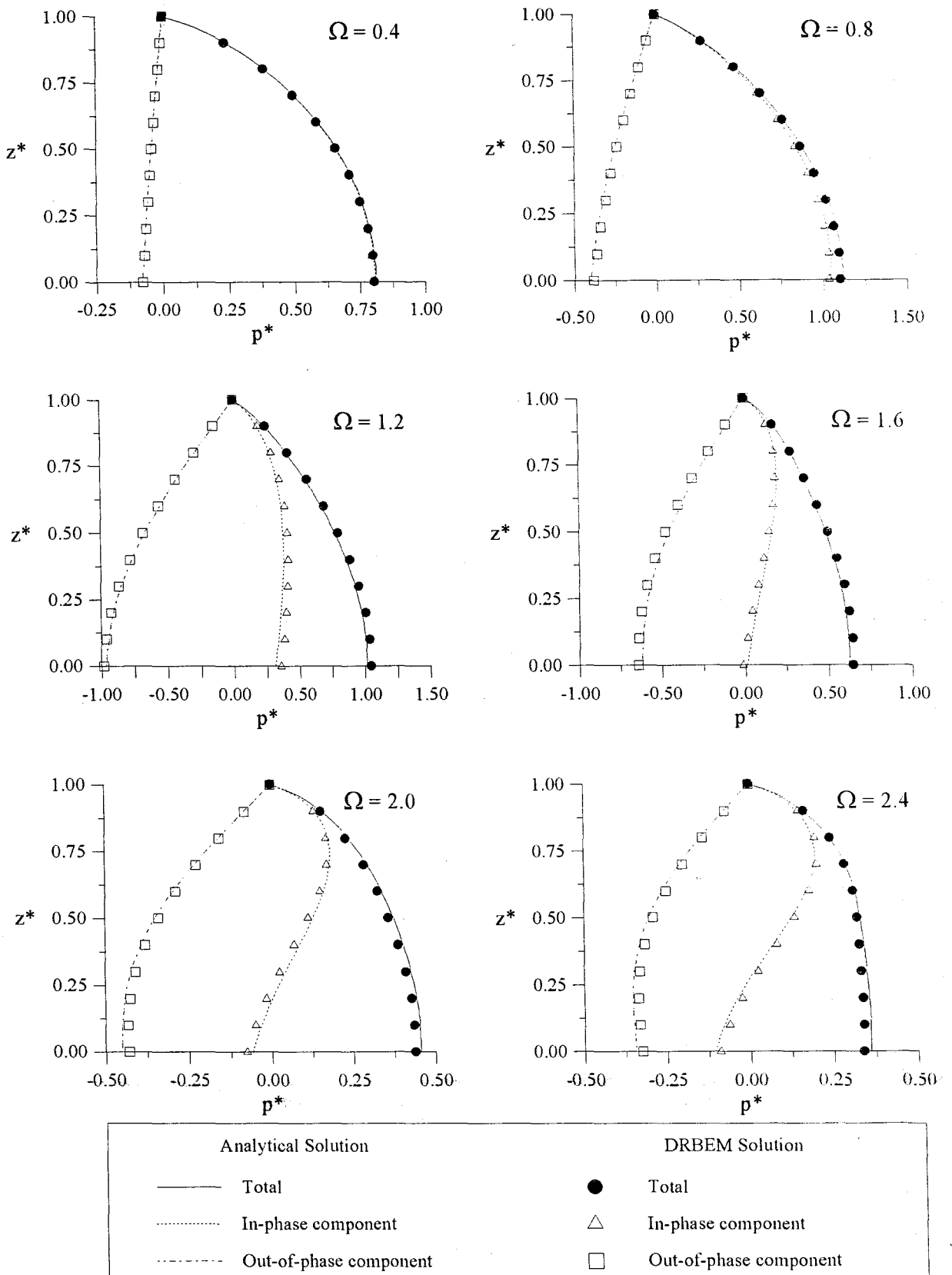


FIGURE 6.3.(a) Hydrodynamic pressure distribution on the upstream face of the rigid dam (harmonic upstream ground motion, reservoir boundary reflection coefficient, $\alpha_r = 0.75$).

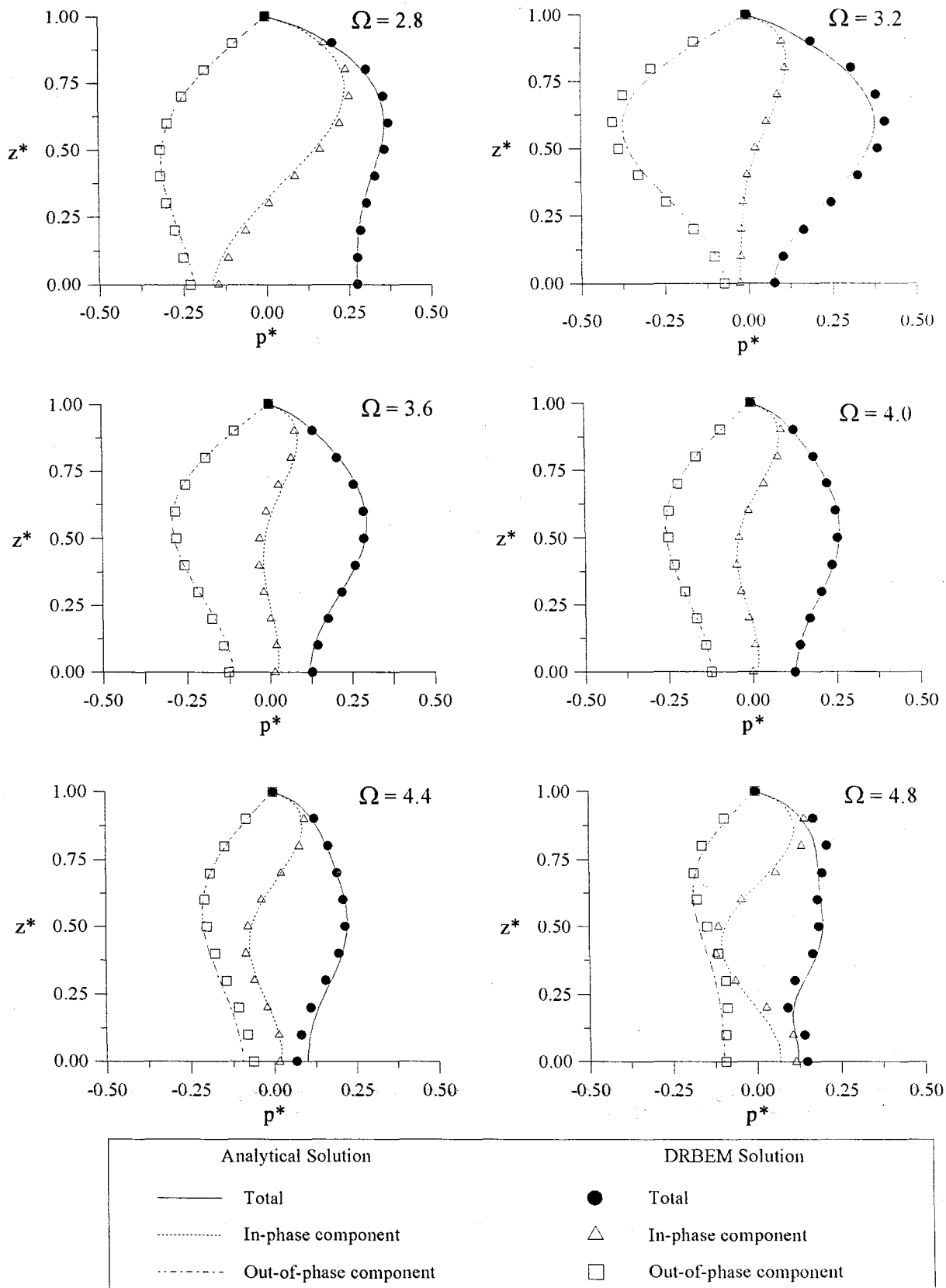


FIGURE 6.3.(b) Hydrodynamic pressure distribution on the upstream face of the rigid dam (harmonic upstream ground motion, reservoir boundary reflection coefficient, $\alpha_r=0.75$).

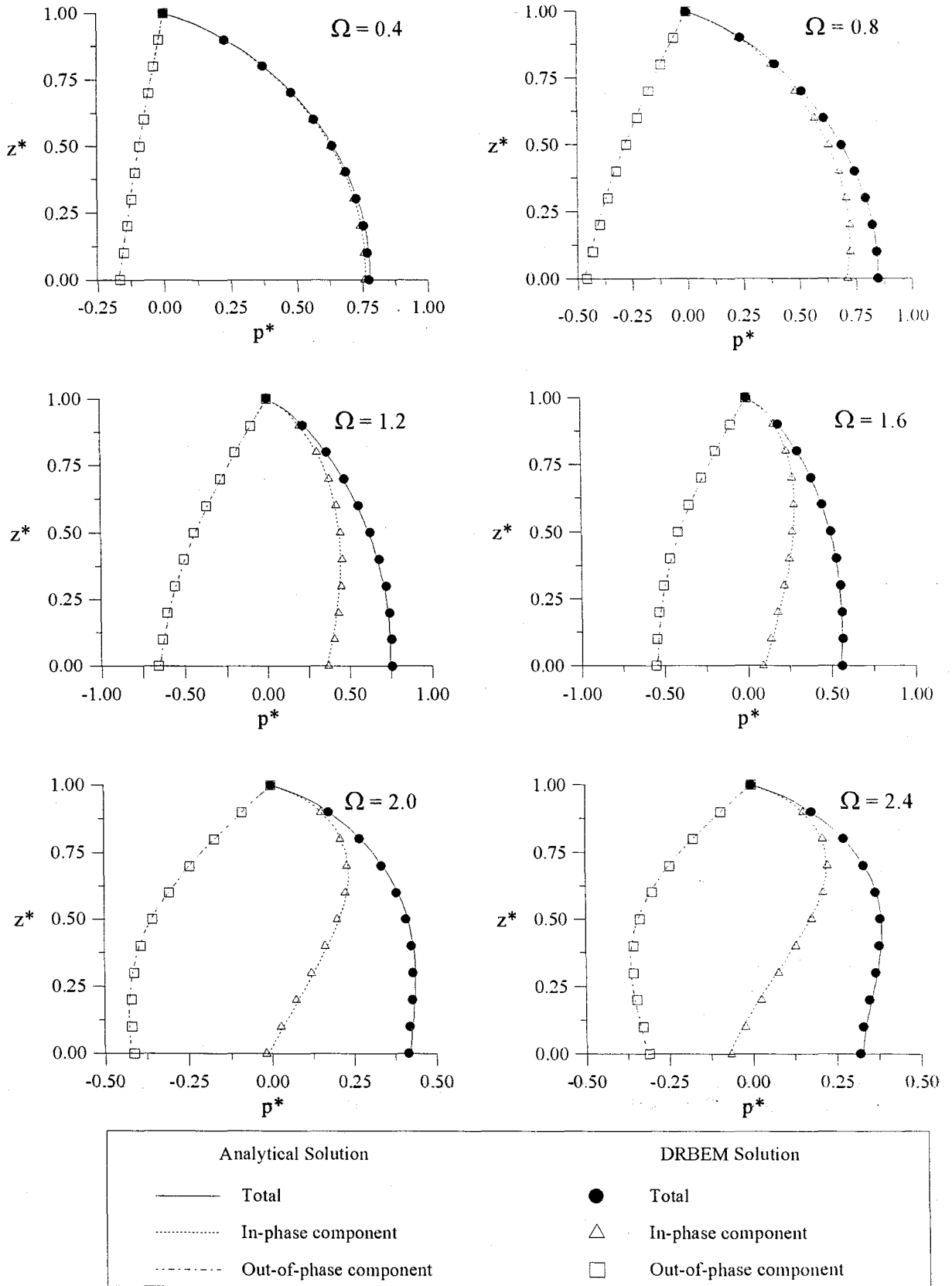


FIGURE 6.4.(a) Hydrodynamic pressure distribution on the upstream face of the rigid dam (harmonic upstream ground motion, reservoir boundary reflection coefficient, $\alpha_r = 0.5$).

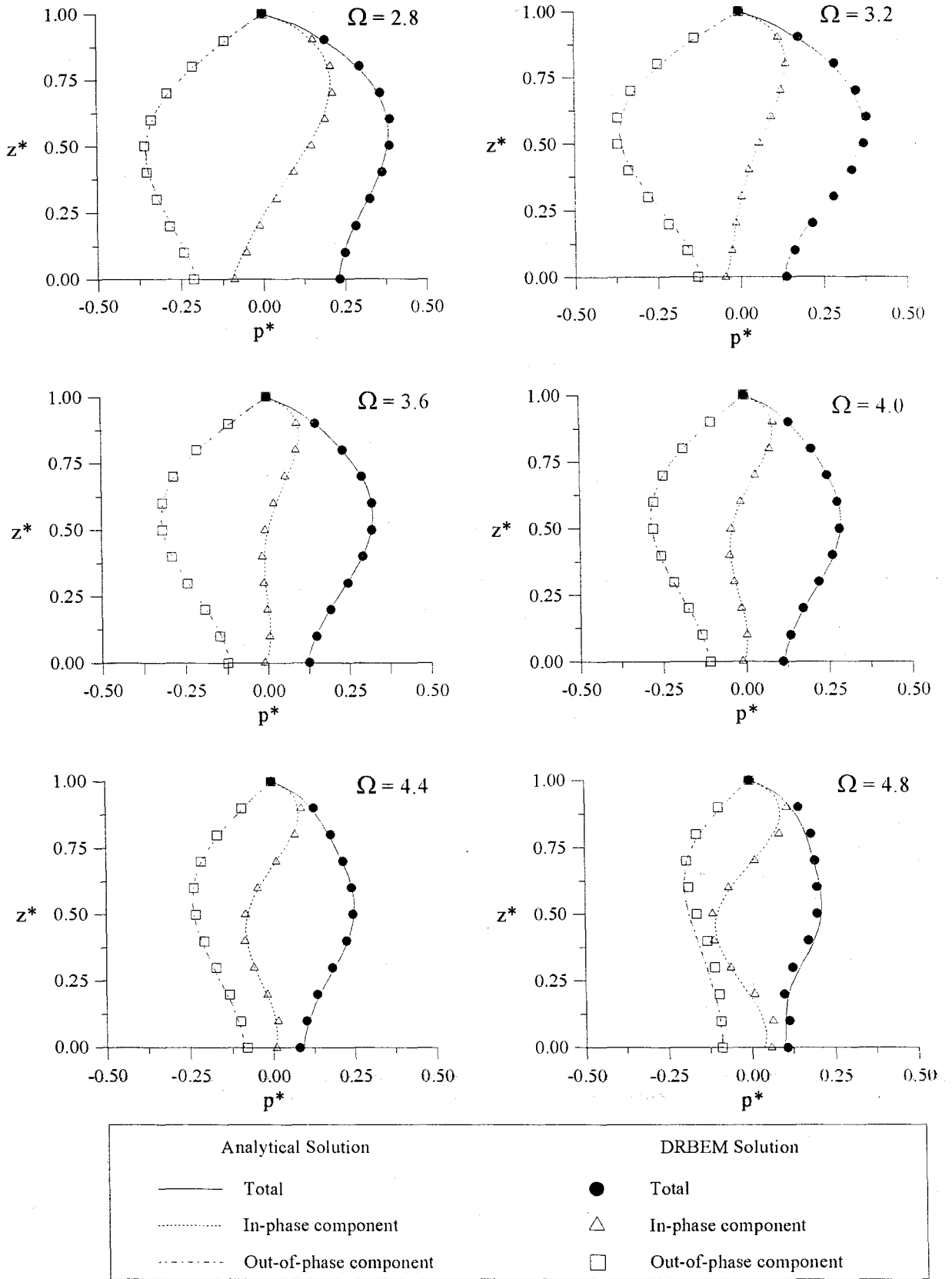


FIGURE 6.4.(b) Hydrodynamic pressure distribution on the upstream face of the rigid dam (harmonic upstream ground motion, reservoir boundary reflection coefficient, $\alpha_r = 0.5$).

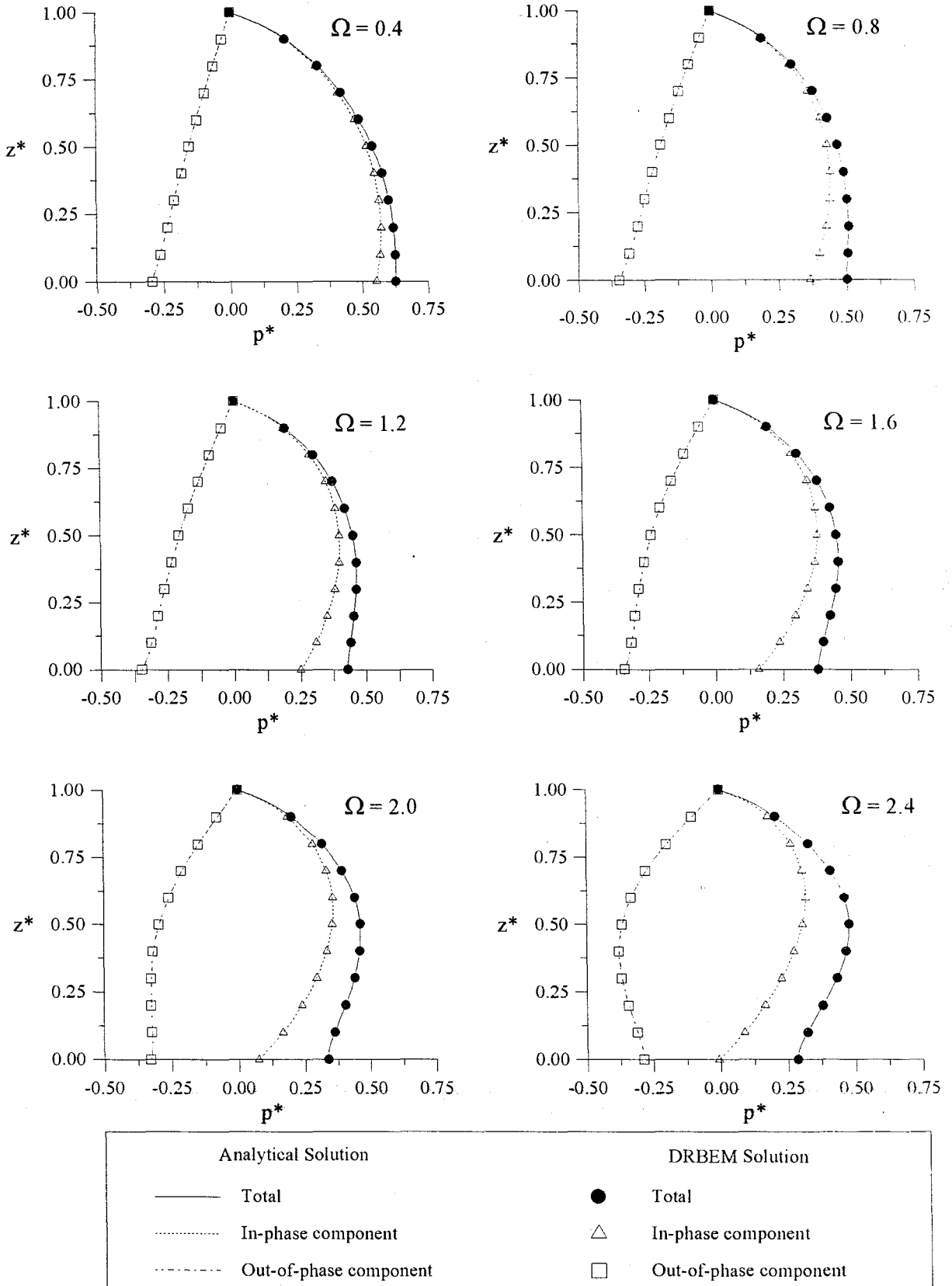


FIGURE 6.5.(a) Hydrodynamic pressure distribution on the upstream face of the rigid dam (harmonic upstream ground motion, reservoir boundary reflection coefficient, $\alpha_r = 0.0$).

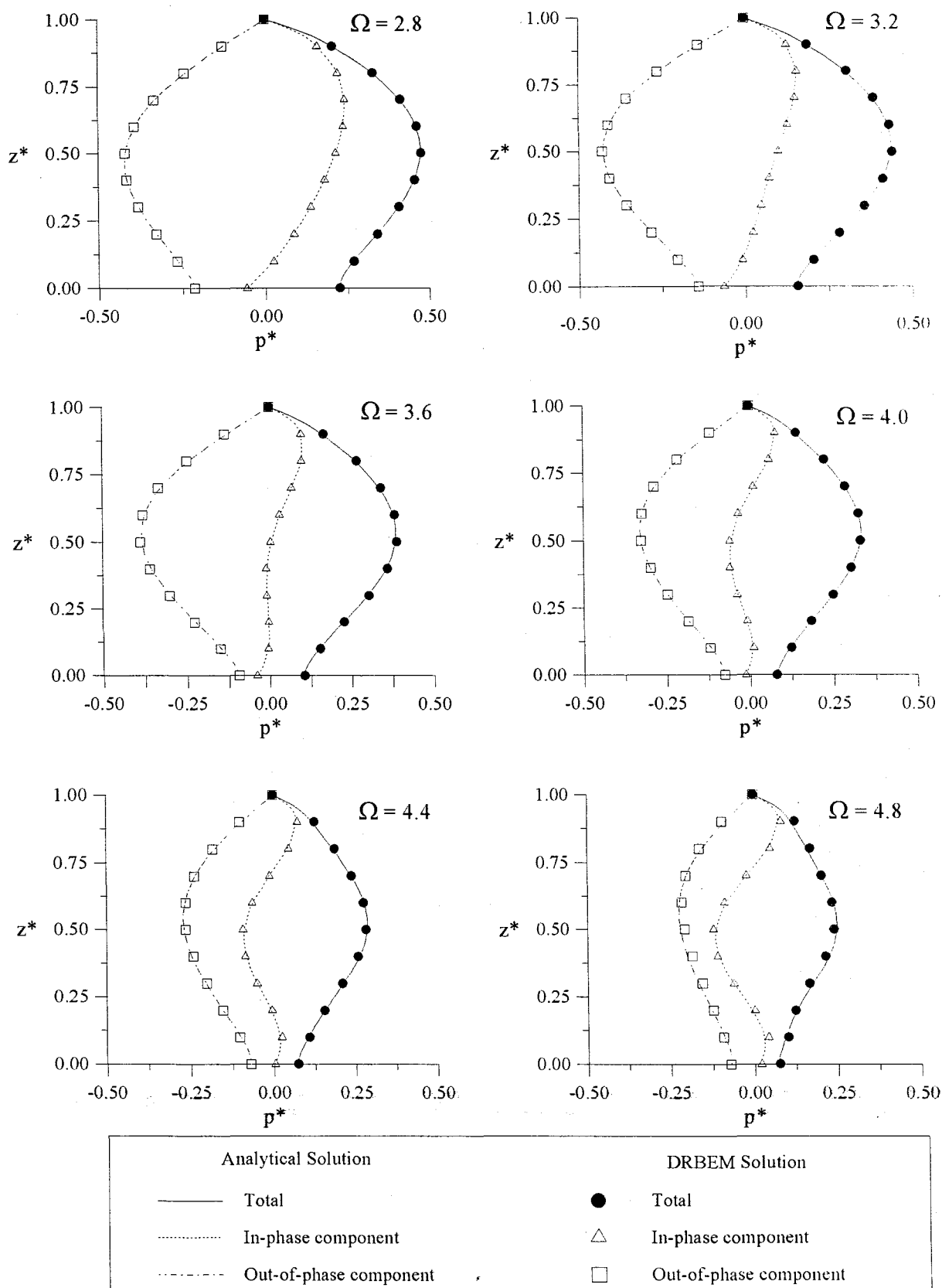


FIGURE 6.5.(b) Hydrodynamic pressure distribution on the upstream face of the rigid dam (harmonic upstream ground motion, reservoir boundary reflection coefficient, $\alpha_r=0$.)

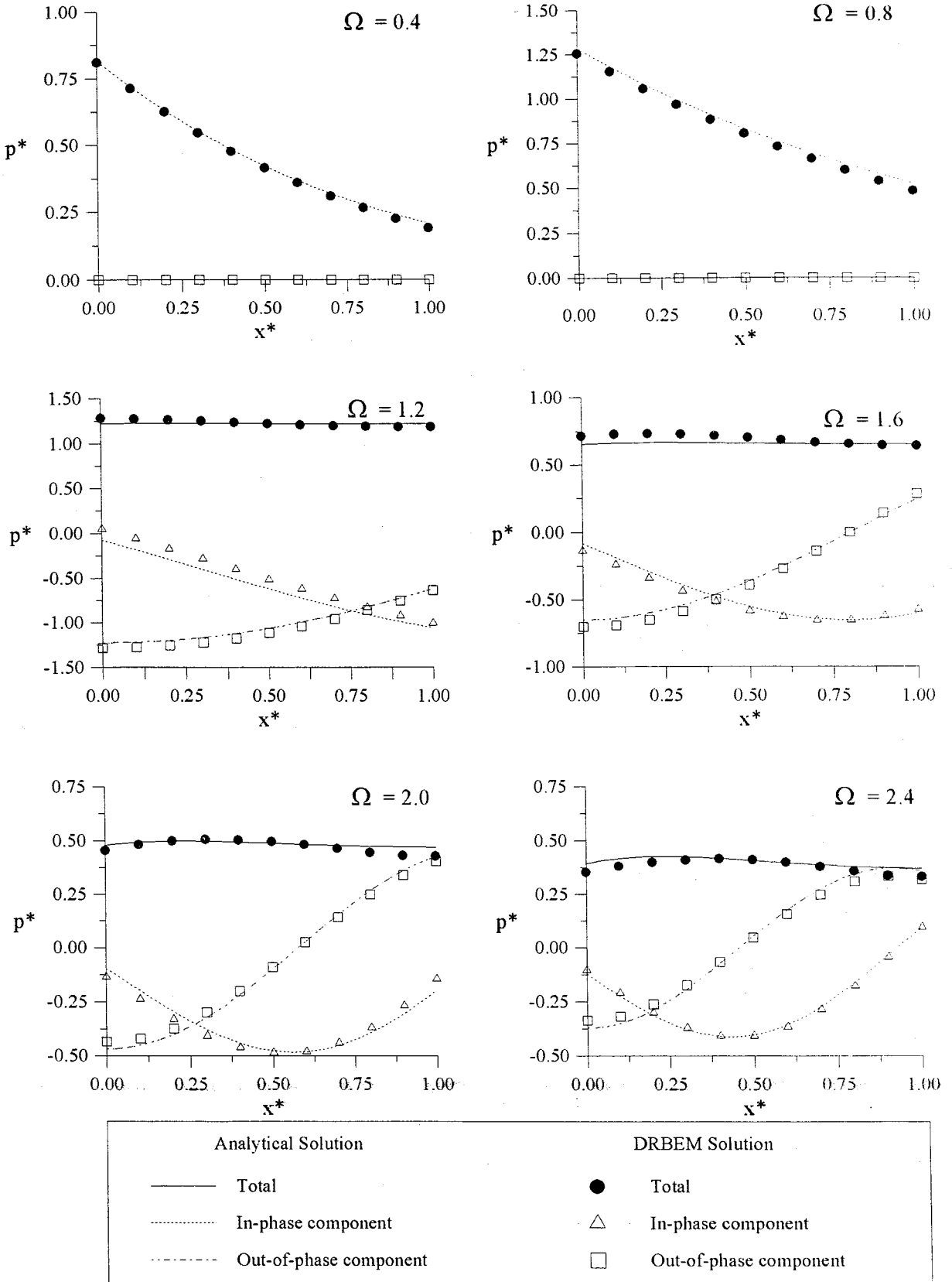


FIGURE 6.6.(a) Hydrodynamic pressure distribution along the reservoir bottom (rigid dam, harmonic upstream ground motion, boundary reflection coefficient, $\alpha_r = 1.0$).

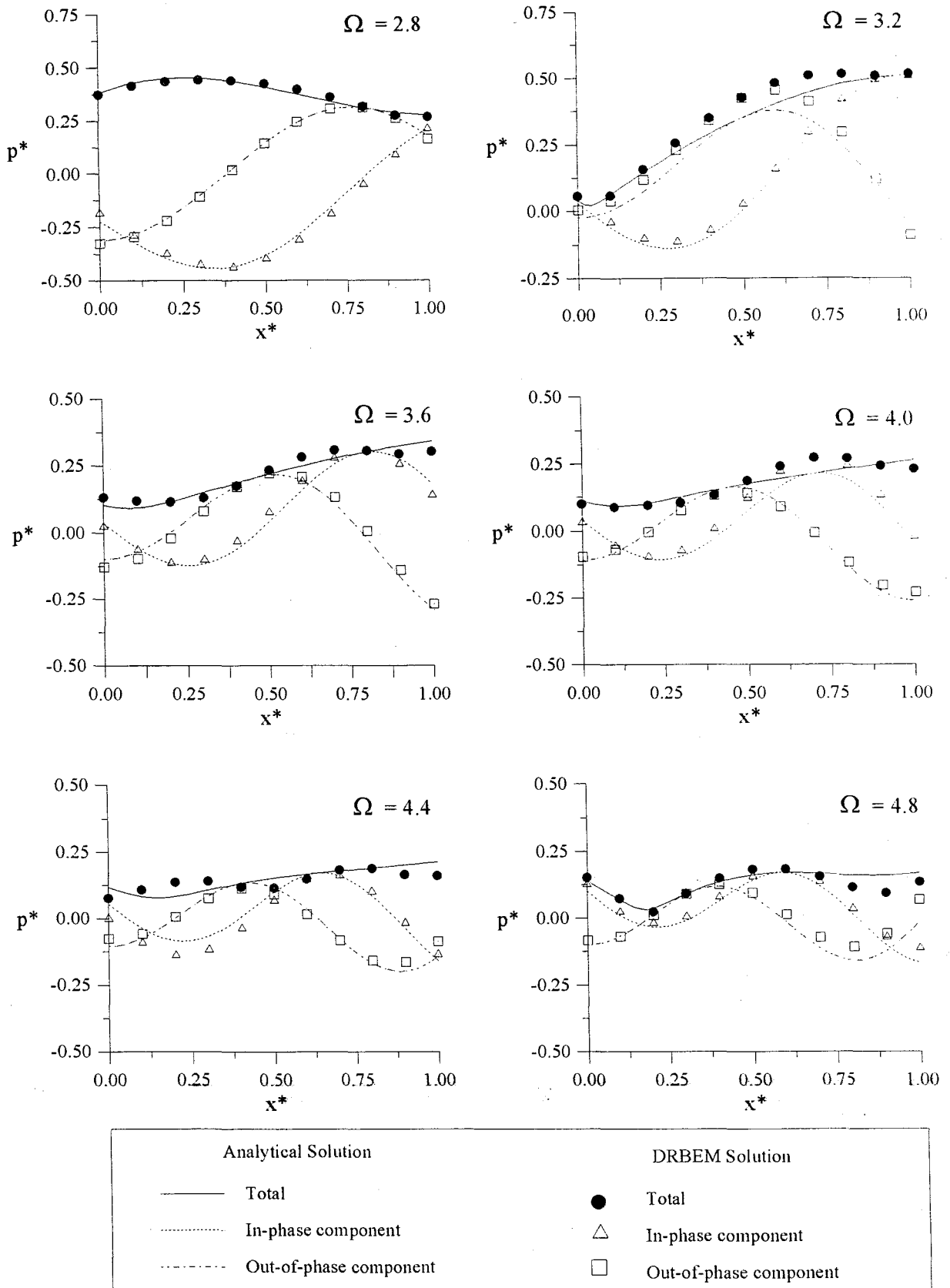


FIGURE 6.6.(b) Hydrodynamic pressure distribution along the reservoir bottom (rigid dam, harmonic upstream ground motion, boundary reflection coefficient, $\alpha_r = 1.0$).

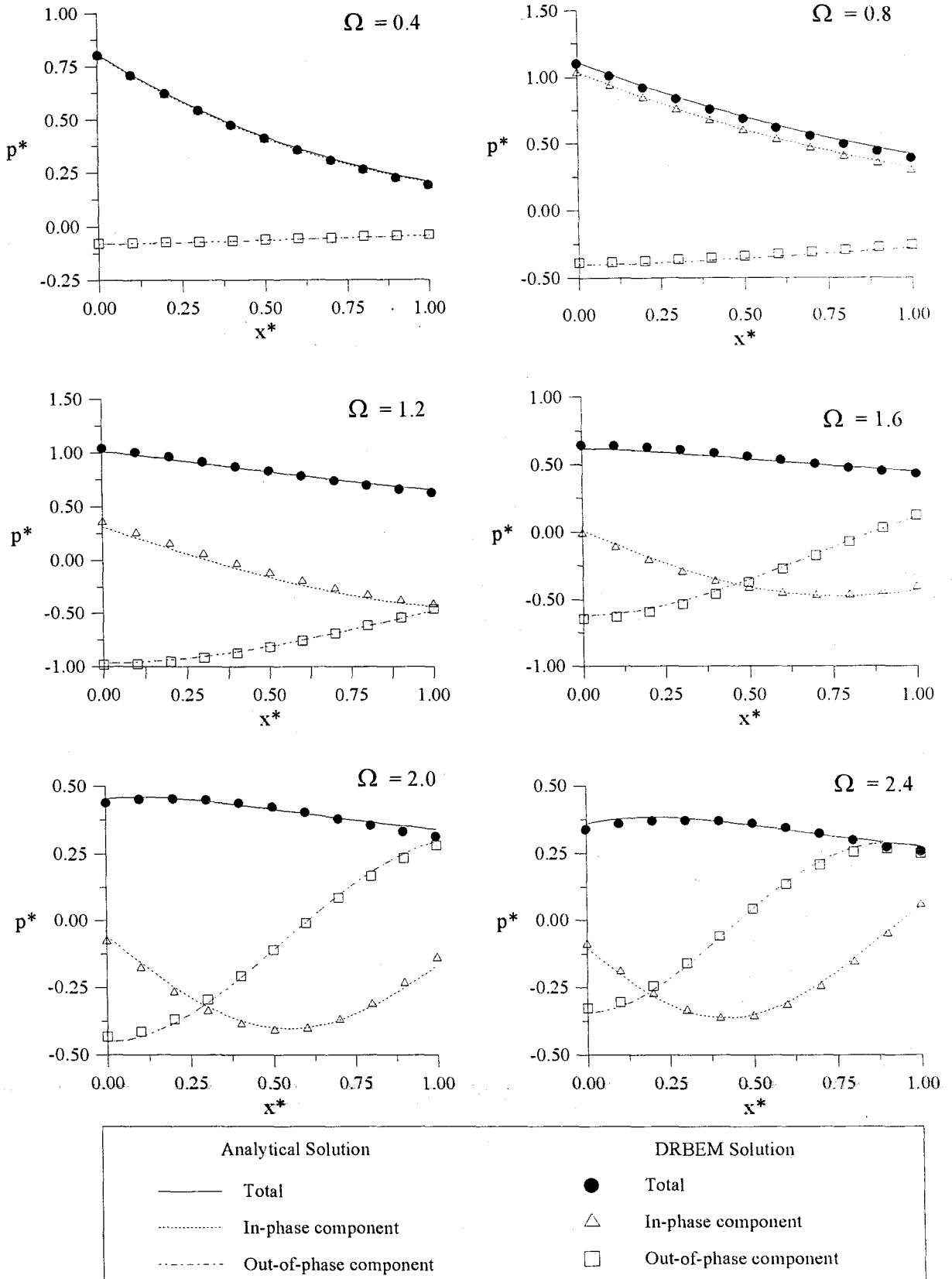


FIGURE 6.7.(a) Hydrodynamic pressure distribution along the reservoir bottom (rigid dam, harmonic upstream ground motion, boundary reflection coefficient, $\alpha_r = 0.75$).

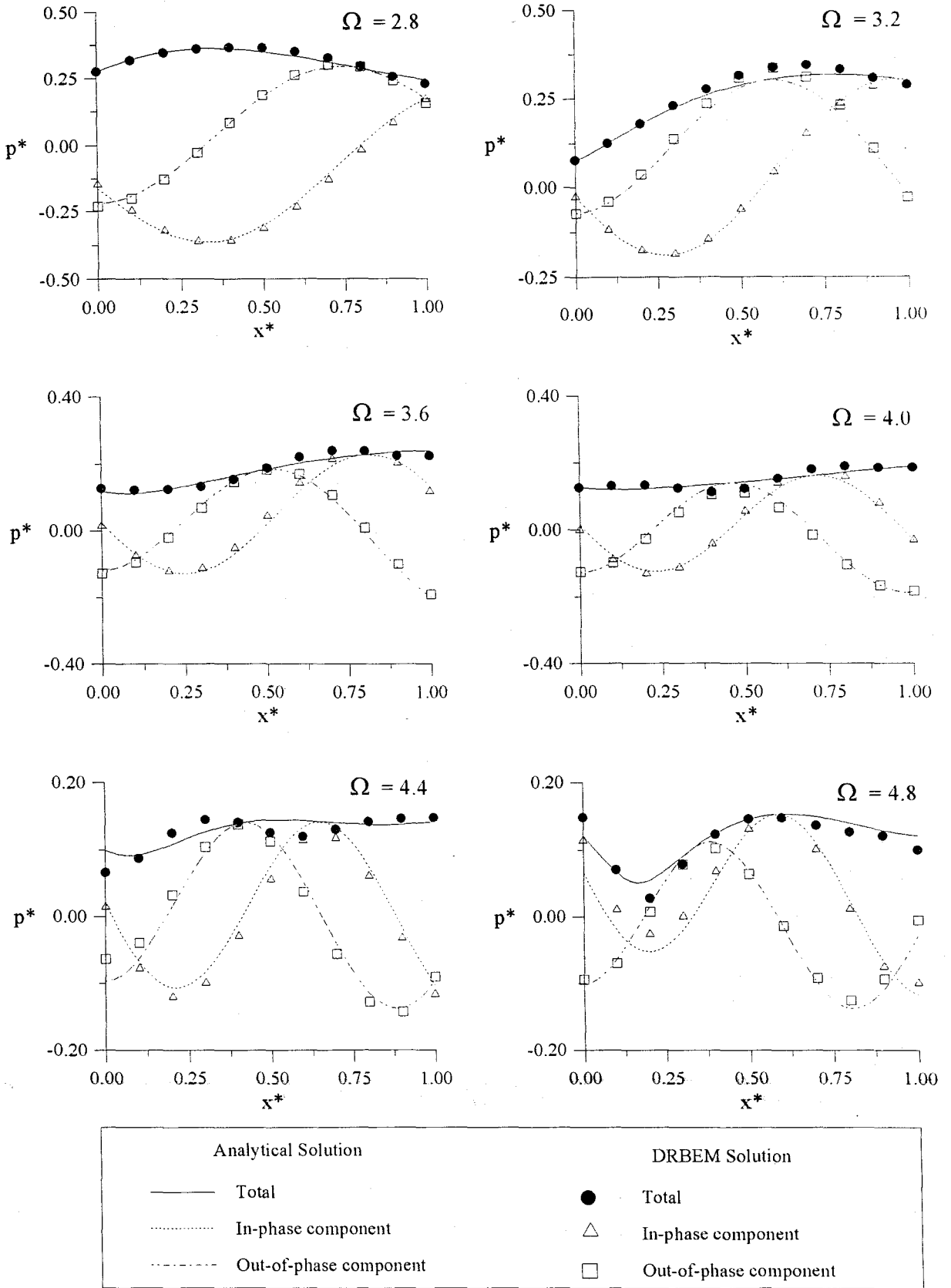


FIGURE 6.7.(b) Hydrodynamic pressure distribution along the reservoir bottom (rigid dam, harmonic upstream ground motion, boundary reflection coefficient, $\alpha_r = 0.75$).

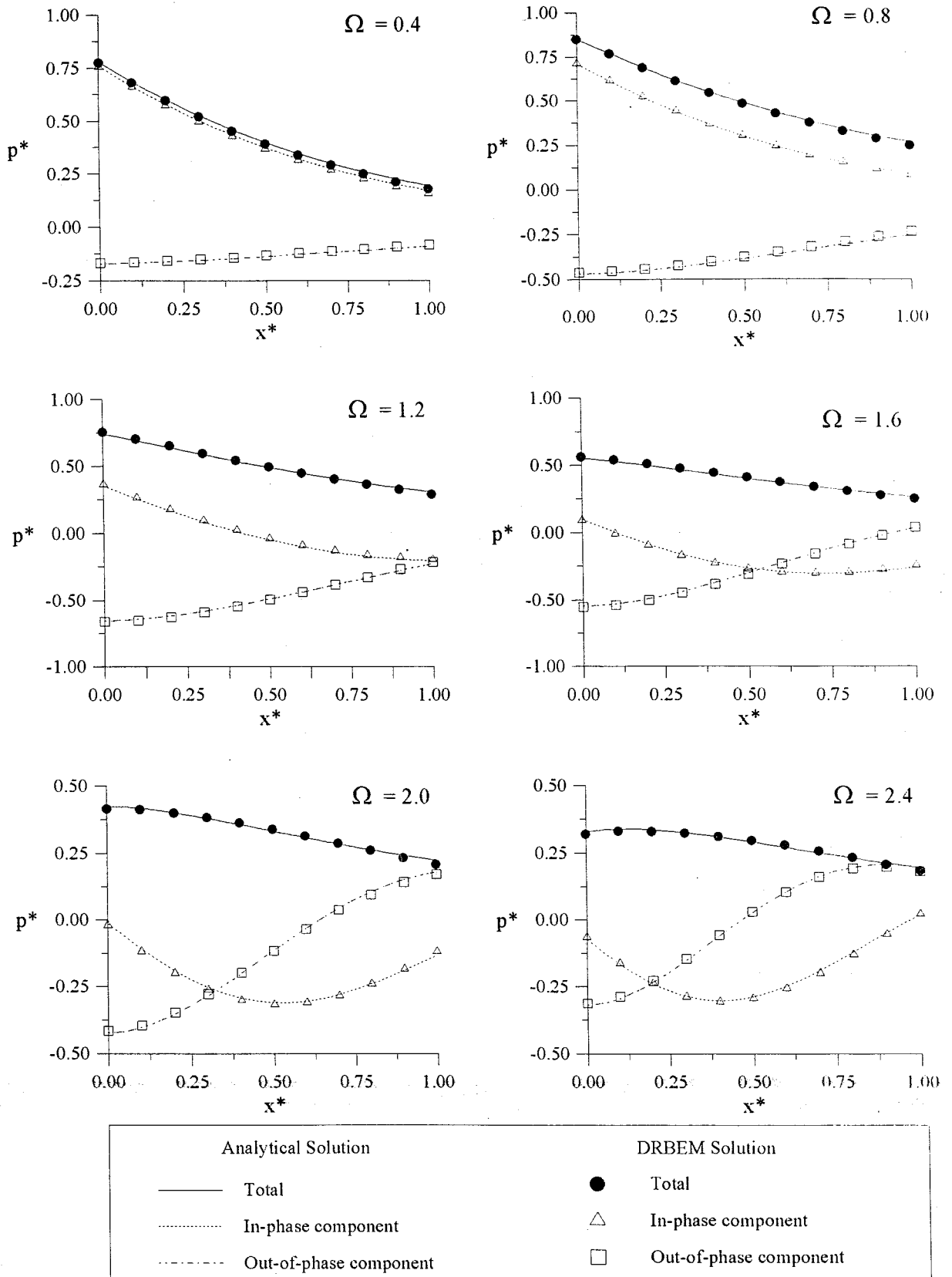


FIGURE 6.8.(a) Hydrodynamic pressure distribution along the reservoir bottom (rigid dam, harmonic upstream ground motion, boundary reflection coefficient $\sigma_r=0.75$).

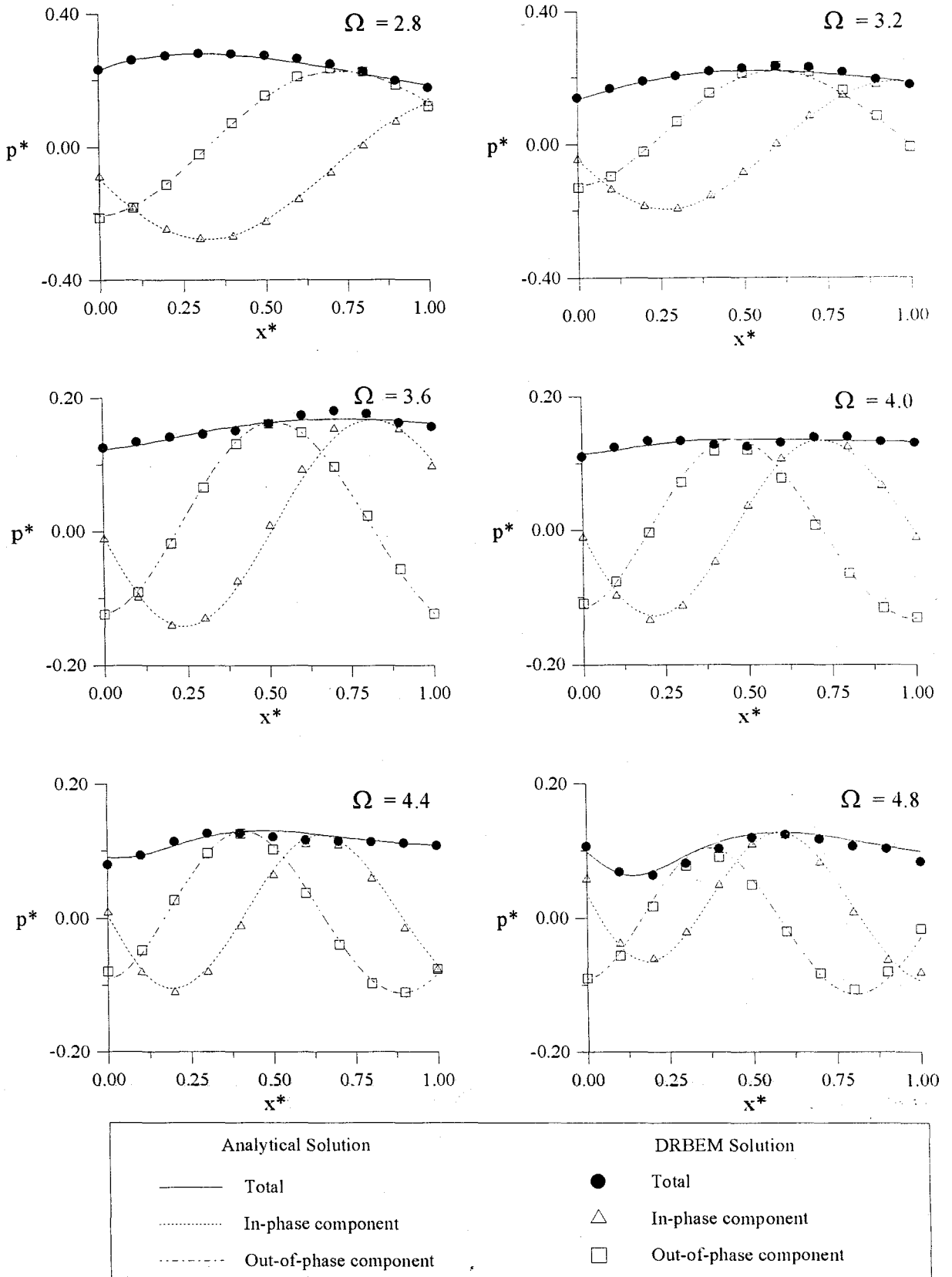


FIGURE 6.8.(b) Hydrodynamic pressure distribution along the reservoir bottom (rigid dam, harmonic upstream ground motion, boundary reflection coefficient, $\alpha_r = 0.5$).

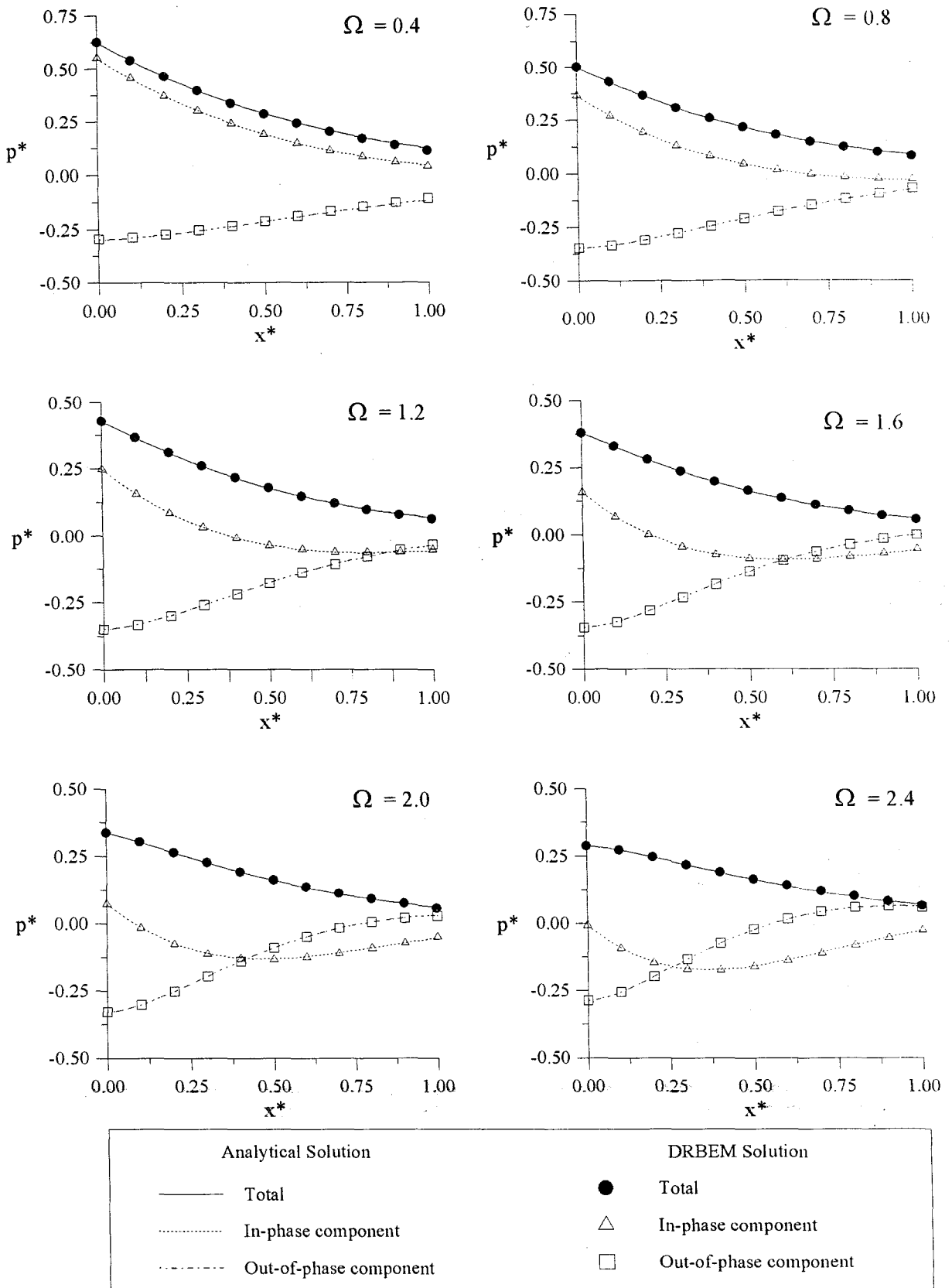


FIGURE 6.9.(a) Hydrodynamic pressure distribution along the reservoir bottom (rigid dam, harmonic upstream ground motion, boundary reflection coefficient, $\alpha_r = 0.0$).

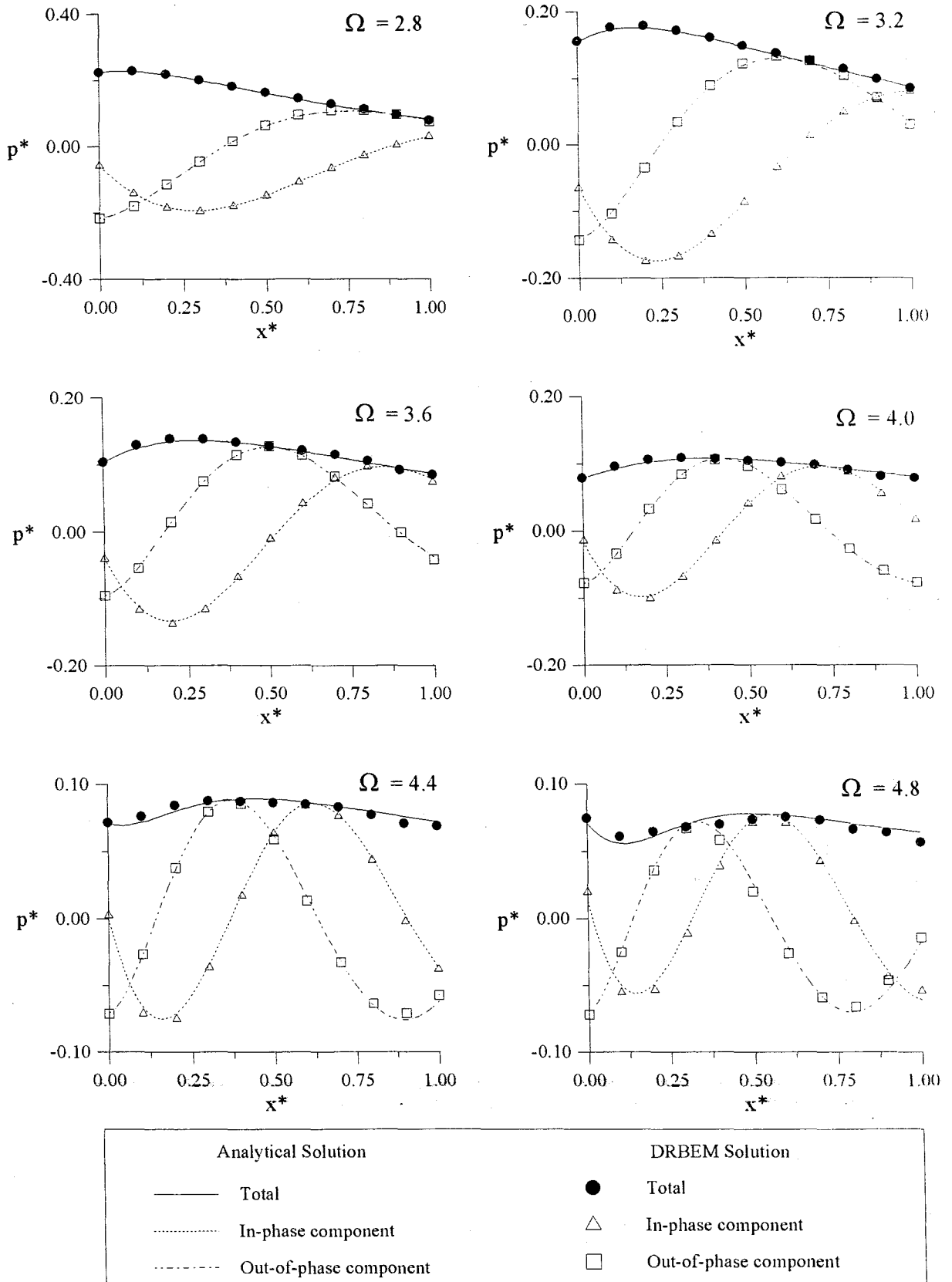


FIGURE 6.9.(b) Hydrodynamic pressure distribution along the reservoir bottom (rigid dam, harmonic upstream ground motion, boundary reflection coefficient, $\alpha_1 = 0.0$).

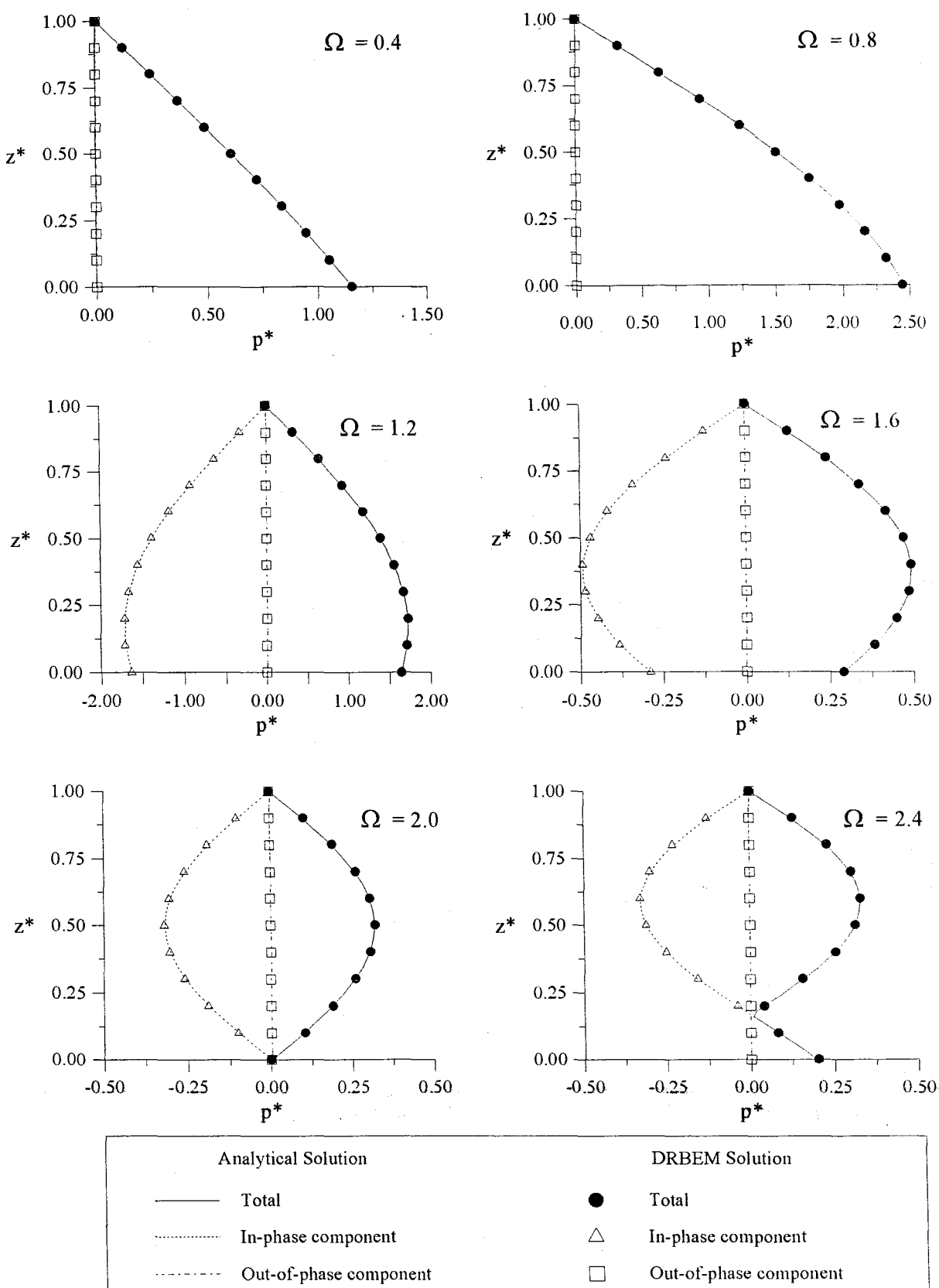


FIGURE 6.10.(a) Hydrodynamic pressures distribution on the upstream face of the rigid dam (harmonic vertical ground motion, reservoir boundary reflection coefficient, $\alpha_r = 1.0$).

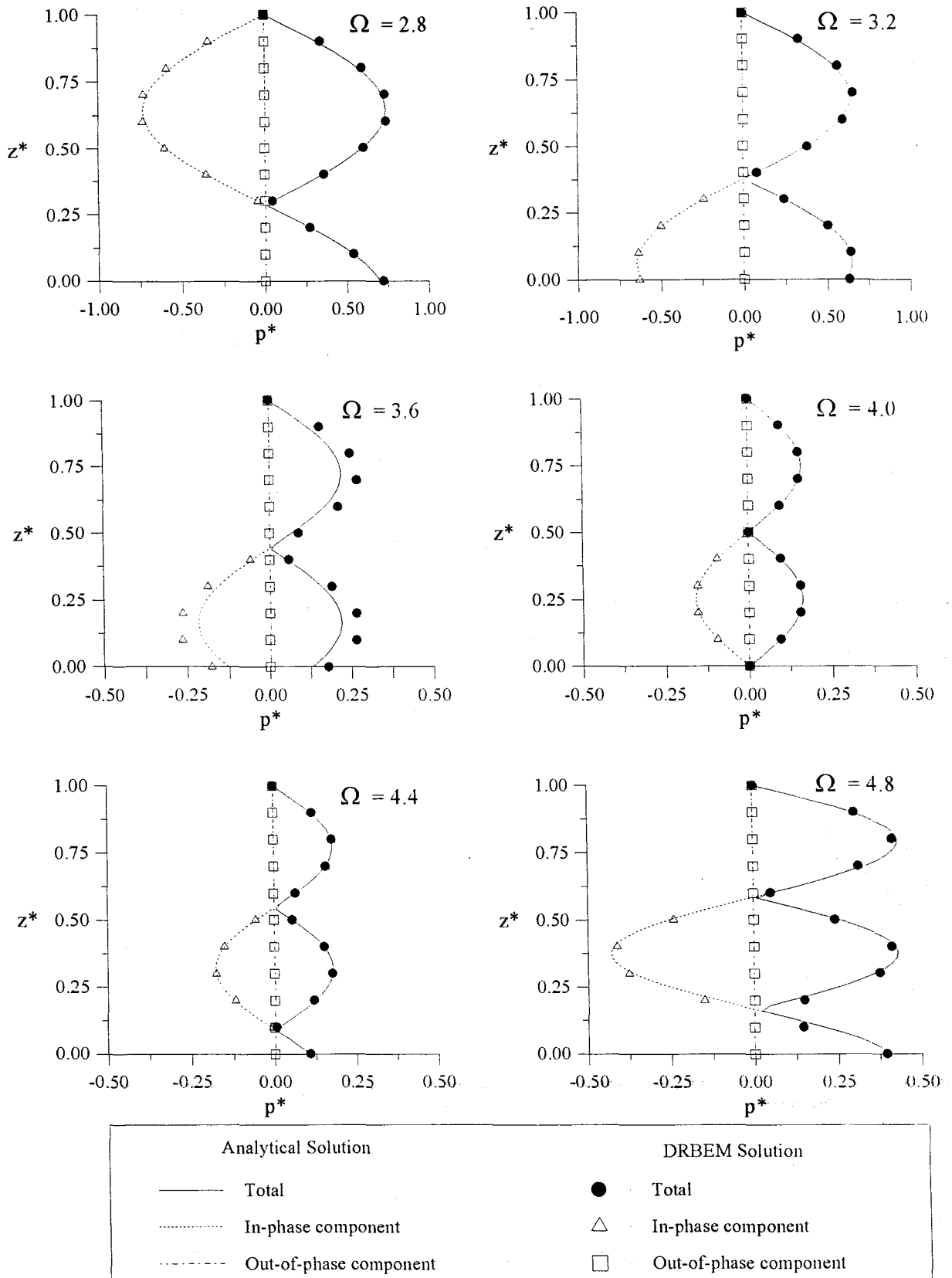


FIGURE 6.10.(b) Hydrodynamic pressures distribution on the upstream face of the rigid dam (harmonic vertical ground motion, reservoir boundary reflection coefficient, $\alpha_r = 1.0$).

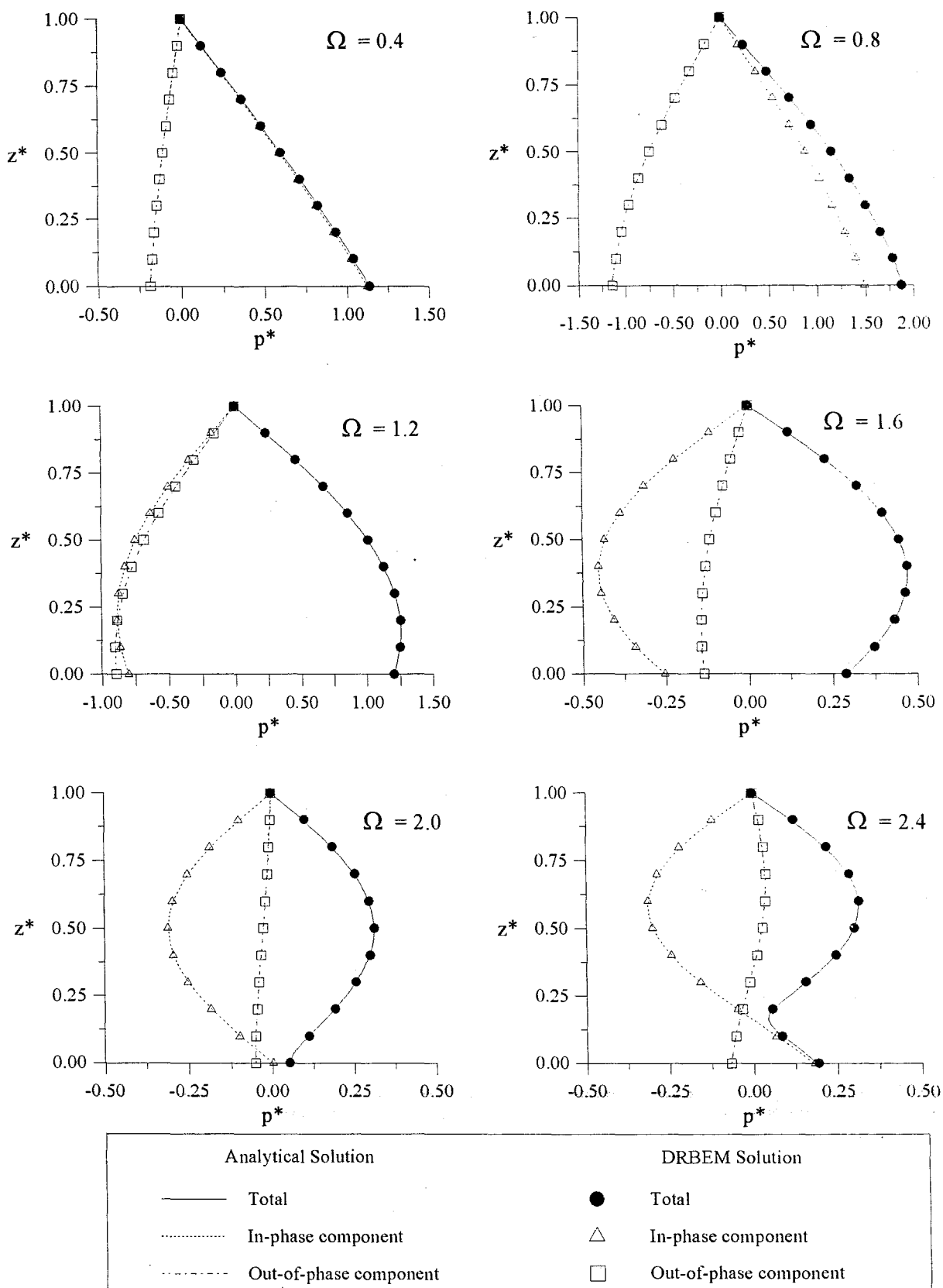


FIGURE 6.11.(a) Hydrodynamic pressures distribution on the upstream face of the rigid dam (harmonic vertical ground motion, reservoir boundary reflection coefficient, $\alpha_r=0.75$).

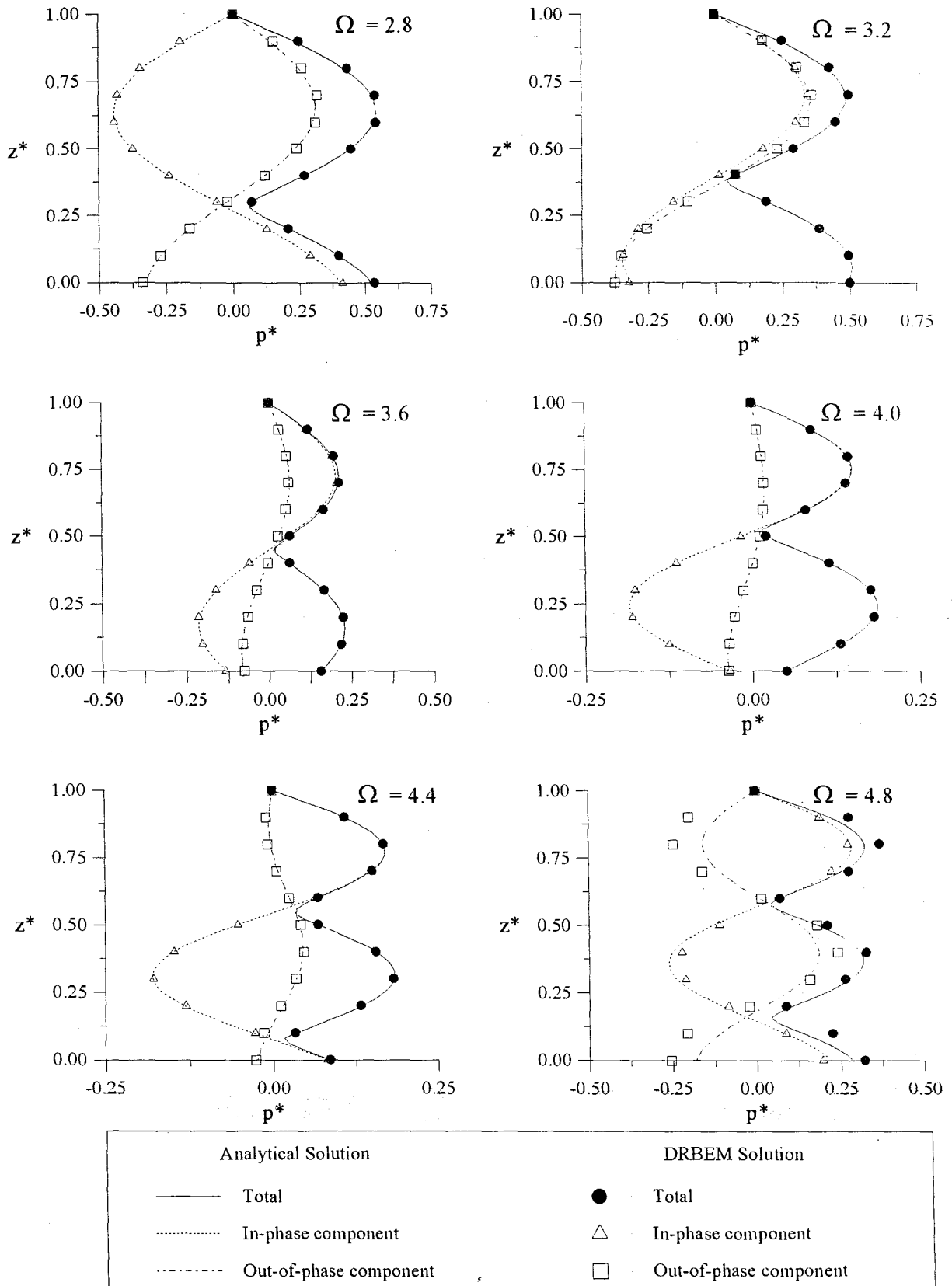


FIGURE 6.11.(b) Hydrodynamic pressures distribution on the upstream face of the rigid dam (harmonic vertical ground motion, reservoir boundary reflection coefficient, $\alpha_r=0.75$).

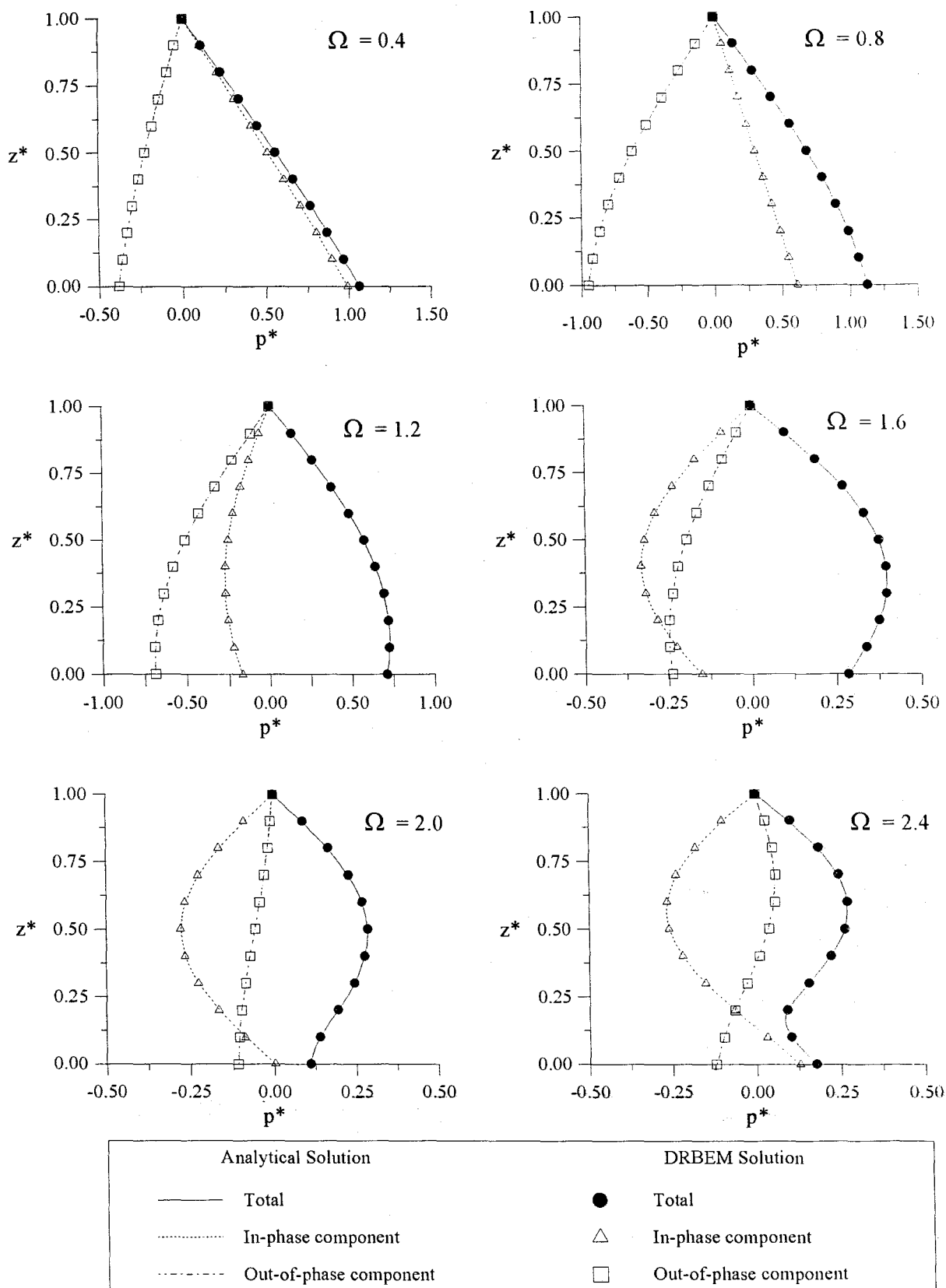


FIGURE 6.12.(a) Hydrodynamic pressures distribution on the upstream face of the rigid dam (harmonic vertical ground motion, reservoir boundary reflection coefficient, $\alpha_r=0.5$).

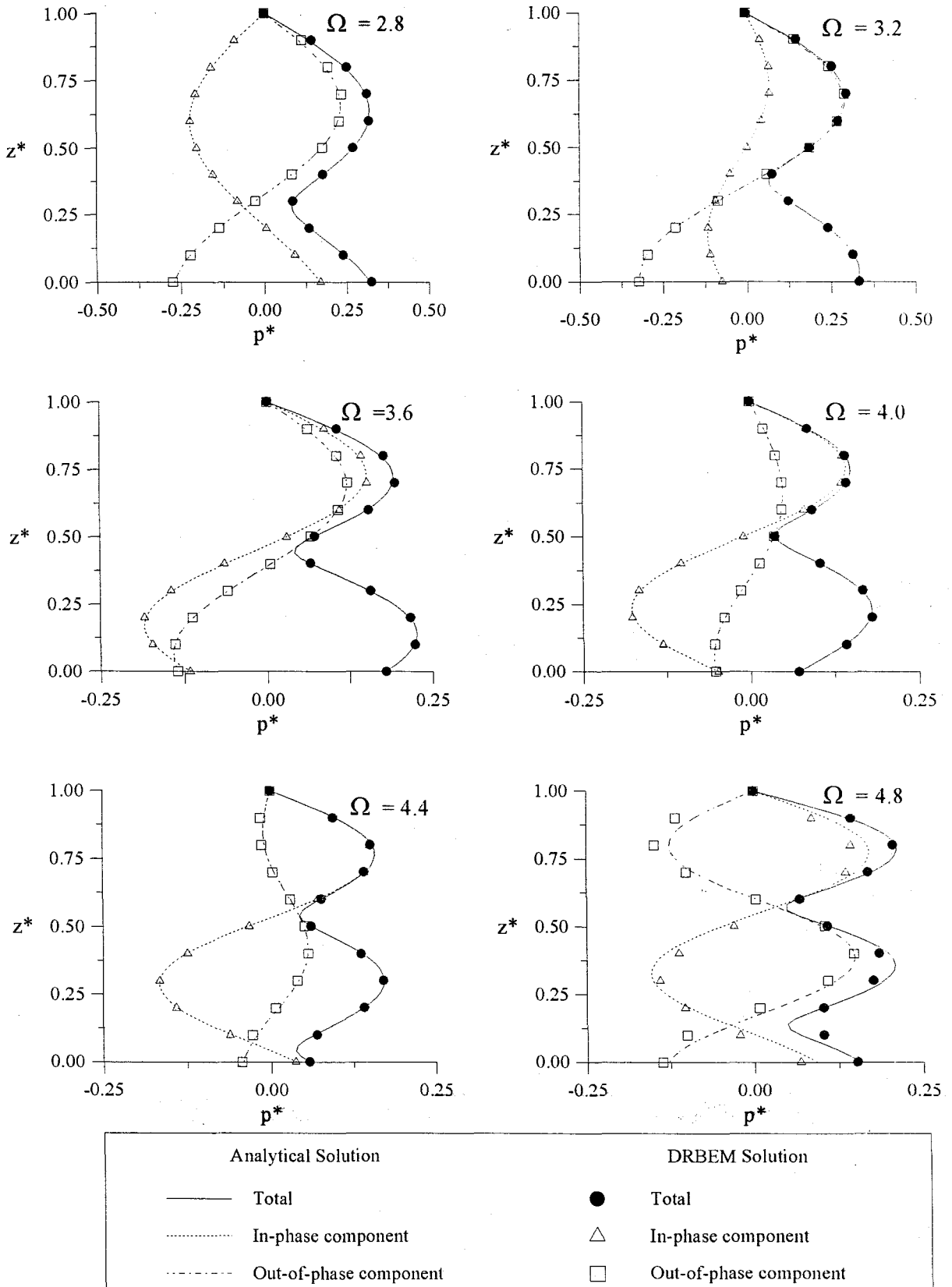


FIGURE 6.12.(b) Hydrodynamic pressures distribution on the upstream face of the rigid dam (harmonic vertical ground motion, reservoir boundary reflection coefficient, $\alpha_r=0.5$).

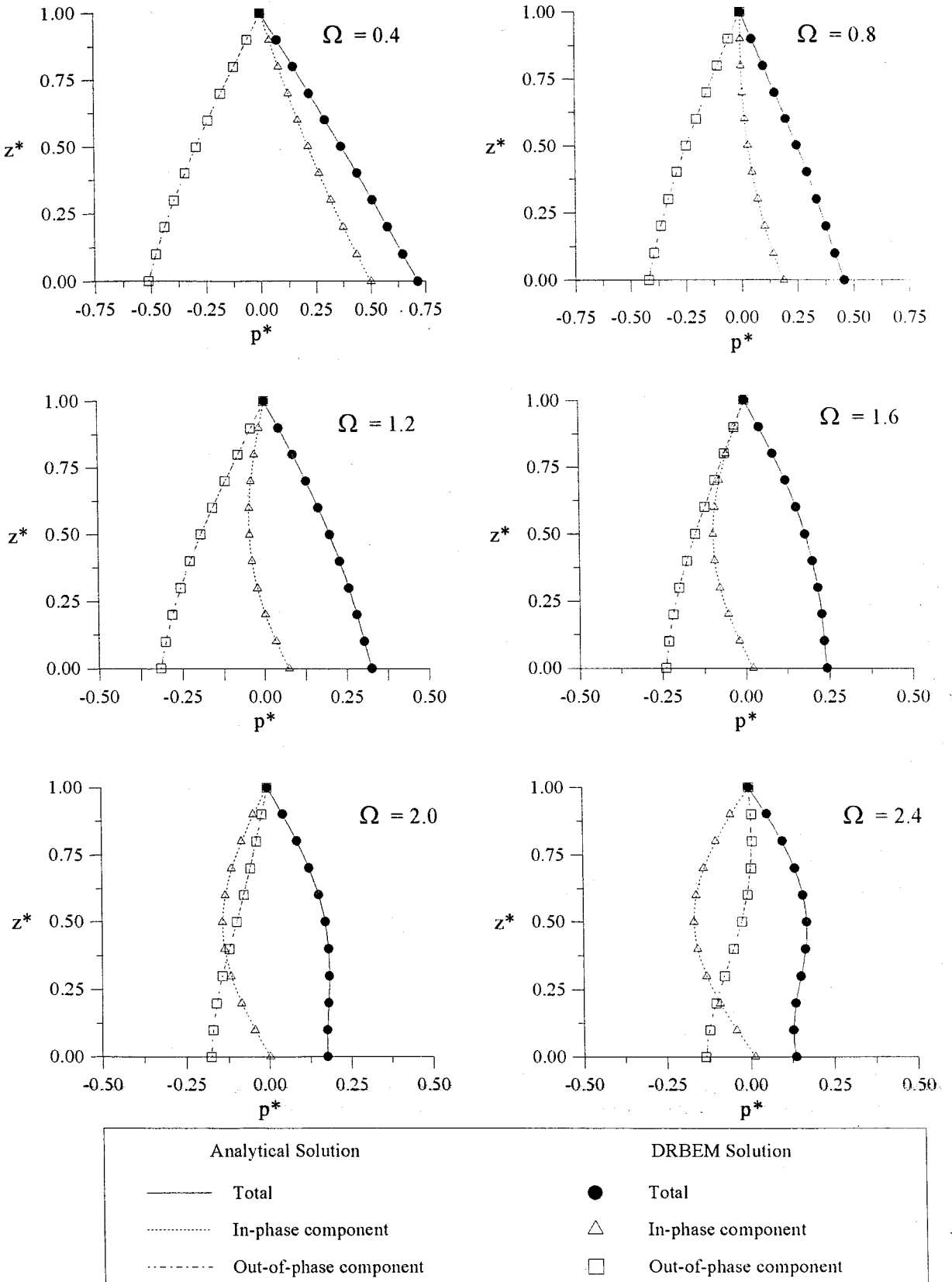


FIGURE 6.13.(a) Hydrodynamic pressures distribution on the upstream face of the rigid dam (harmonic vertical ground motion, reservoir boundary reflection coefficient, $\alpha_r=0.0$).

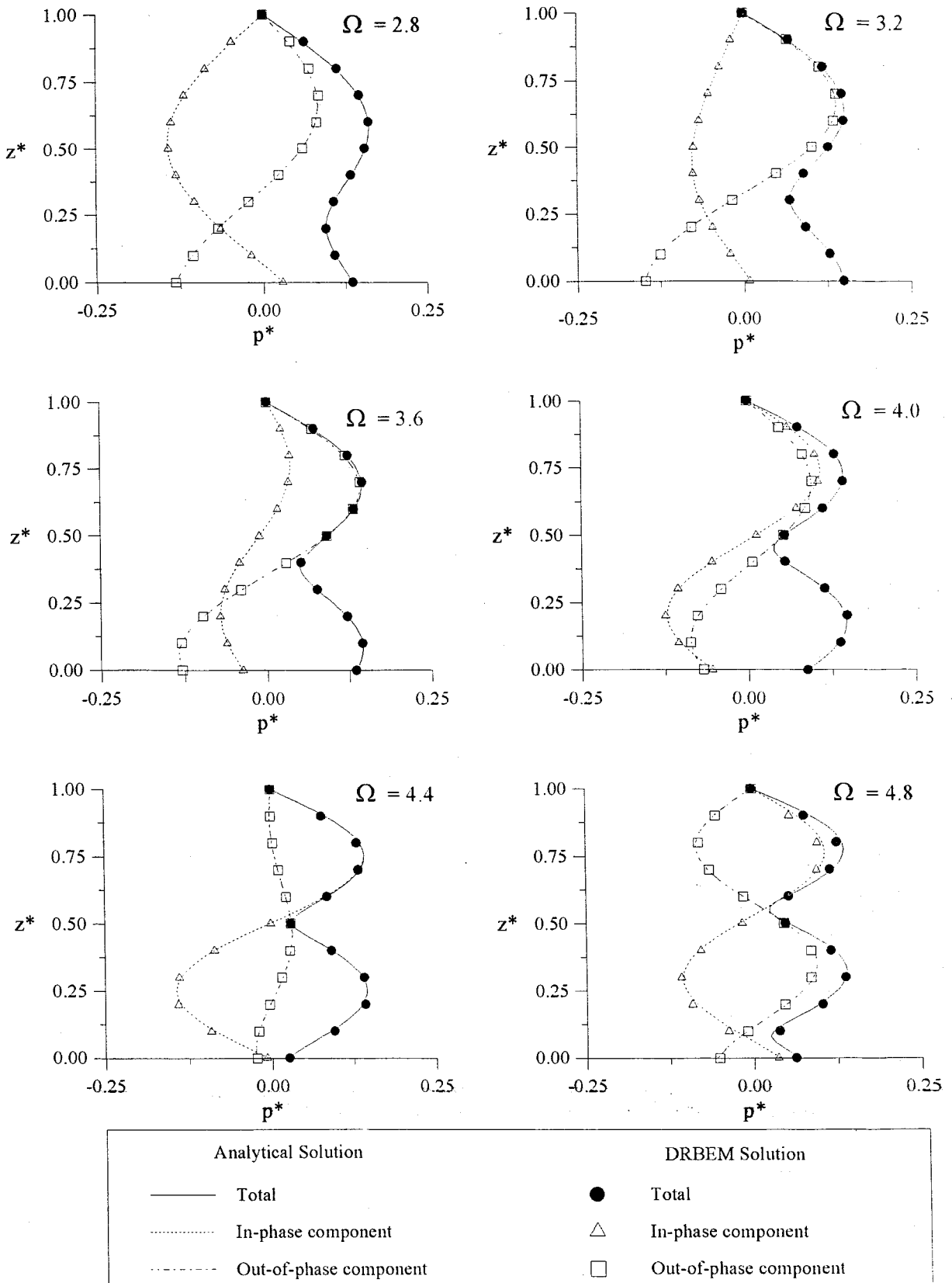


FIGURE 6.13.(b) Hydrodynamic pressures distribution on the upstream face of the rigid dam (harmonic vertical ground motion, reservoir boundary reflection coefficient, $\alpha_r=0.0$).

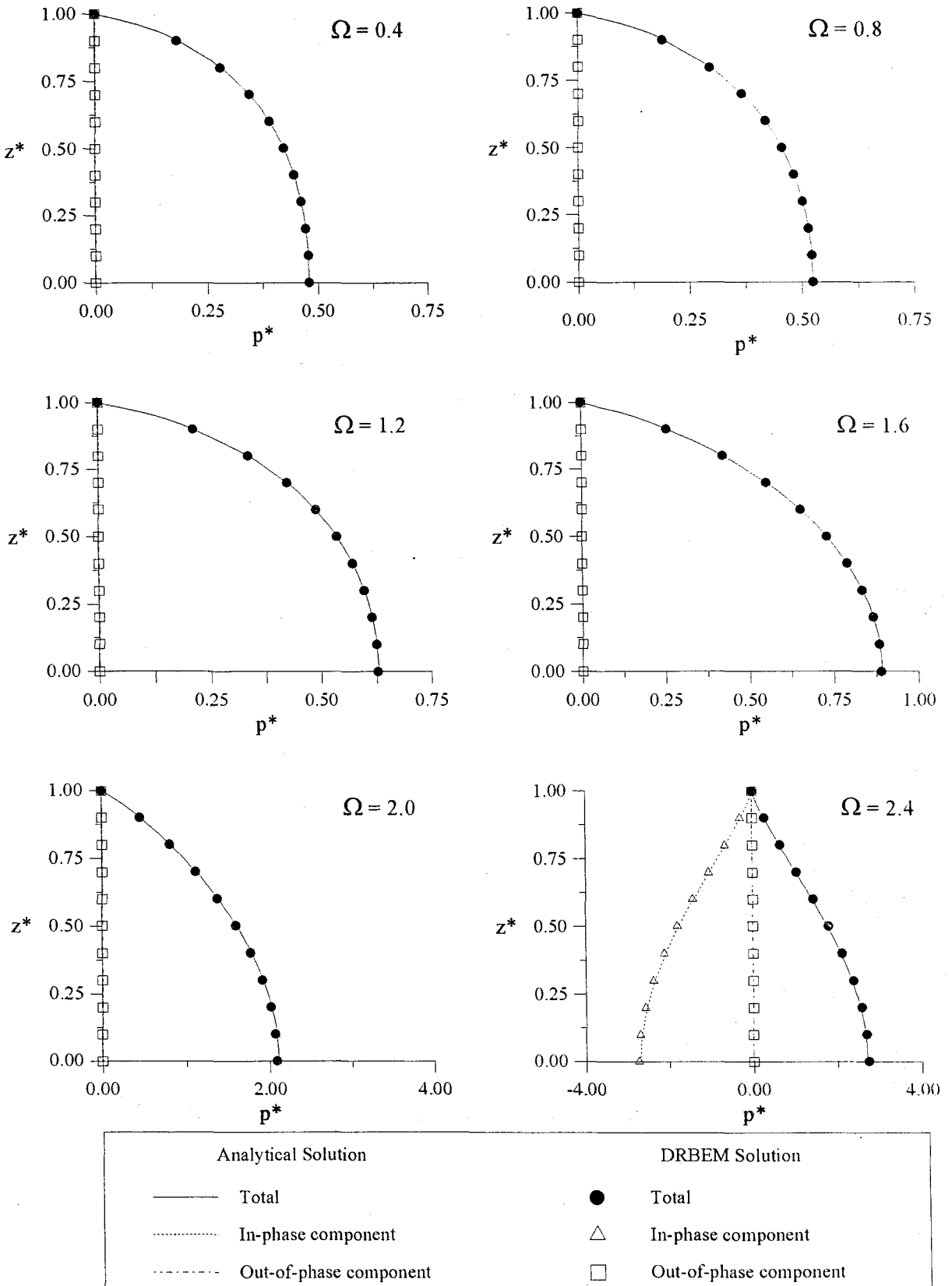


FIGURE 6.14.(a) Hydrodynamic pressures distribution on the upstream face of the rigid dam (harmonic cross-stream ground motion, reservoir boundary reflection coefficient, $\alpha_r = 1.0$).

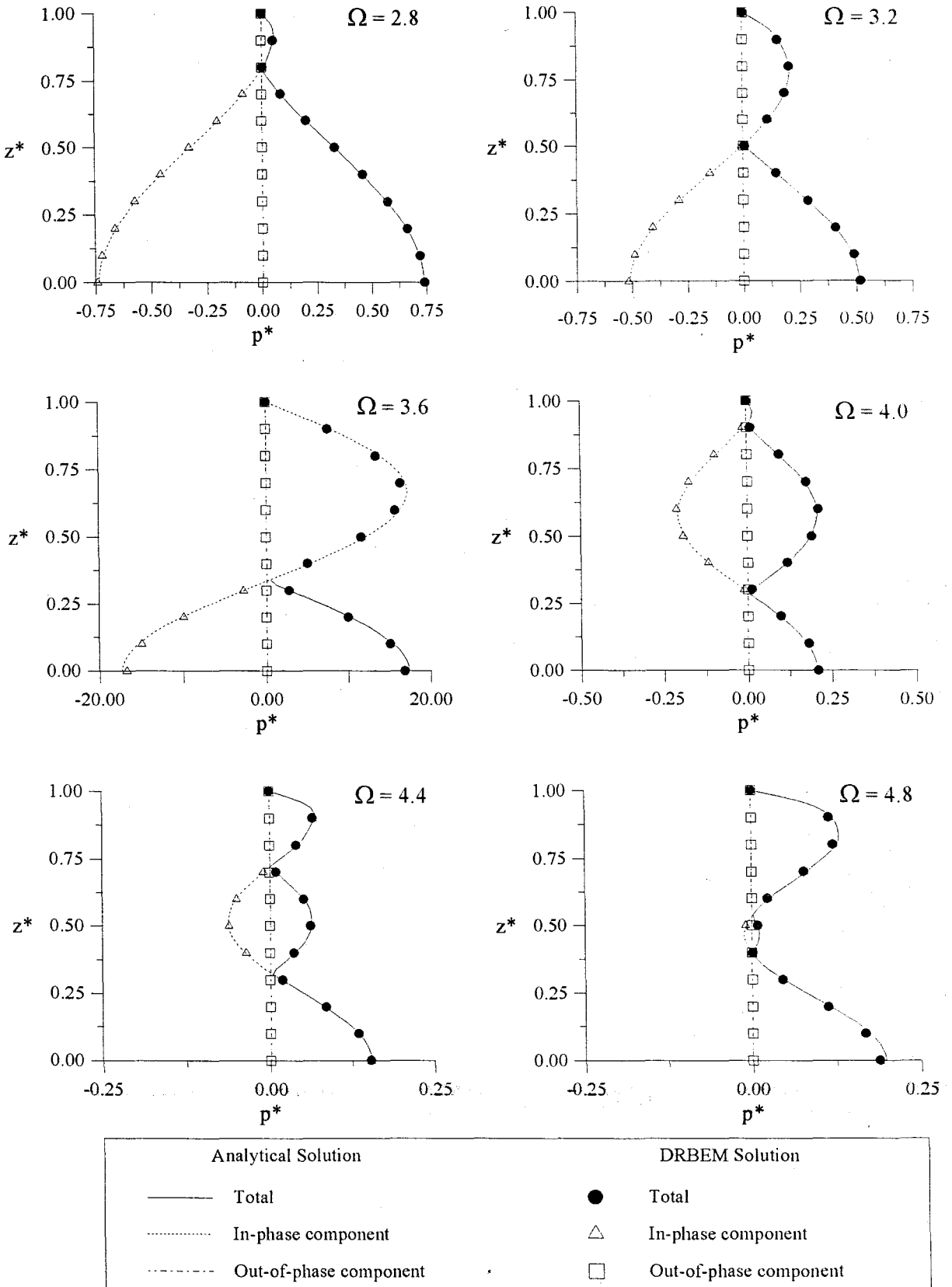


FIGURE 6.14.(b) Hydrodynamic pressures distribution on the upstream face of the rigid dam (harmonic cross-stream ground motion, reservoir boundary reflection coefficient, $\alpha_r = 1.0$).

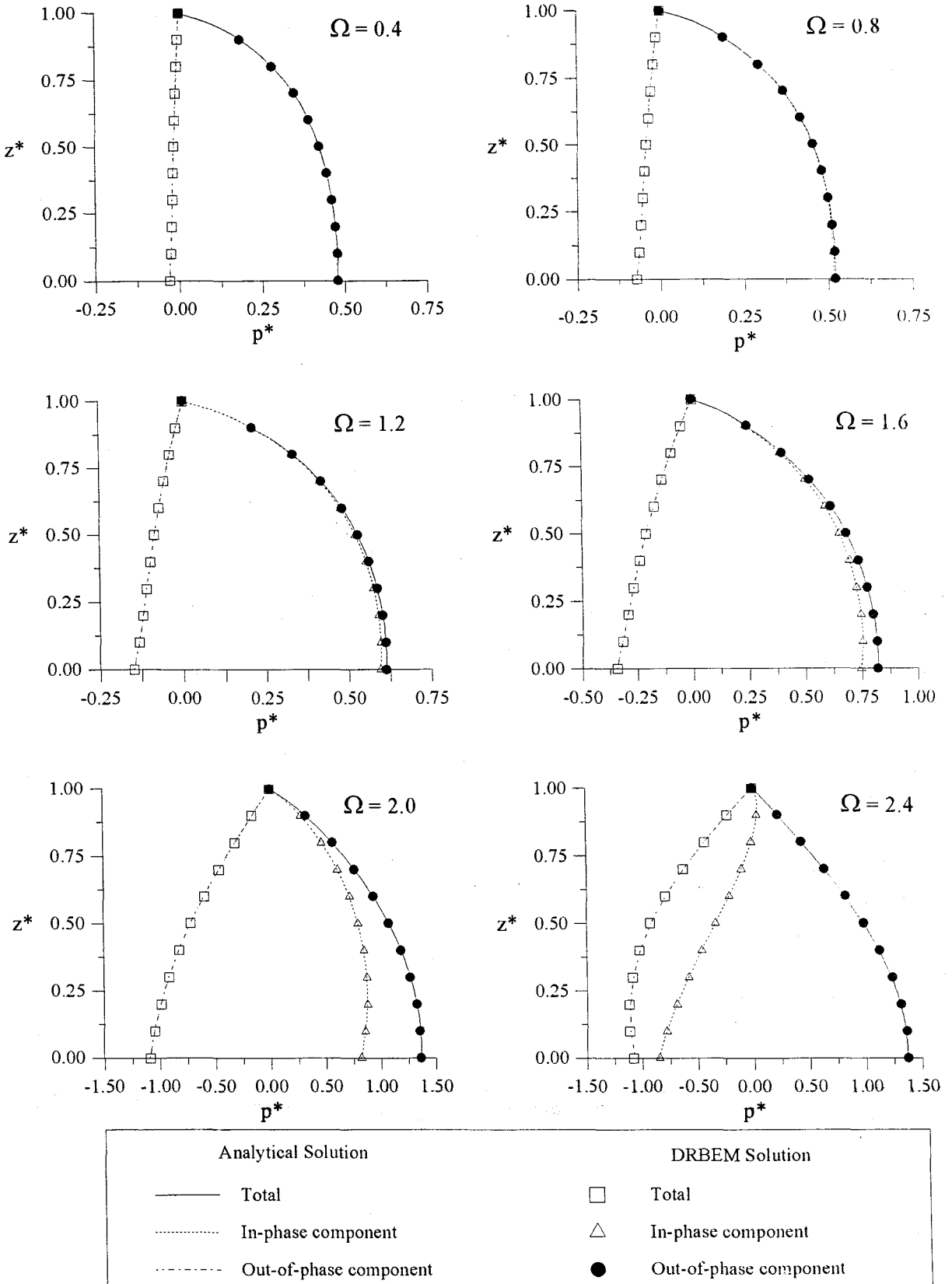


FIGURE 6.15. (a) Hydrodynamic pressures distribution on the upstream face of the rigid dam (harmonic cross-stream ground motion, reservoir boundary reflection coefficient, $\alpha_r = 0.75$).

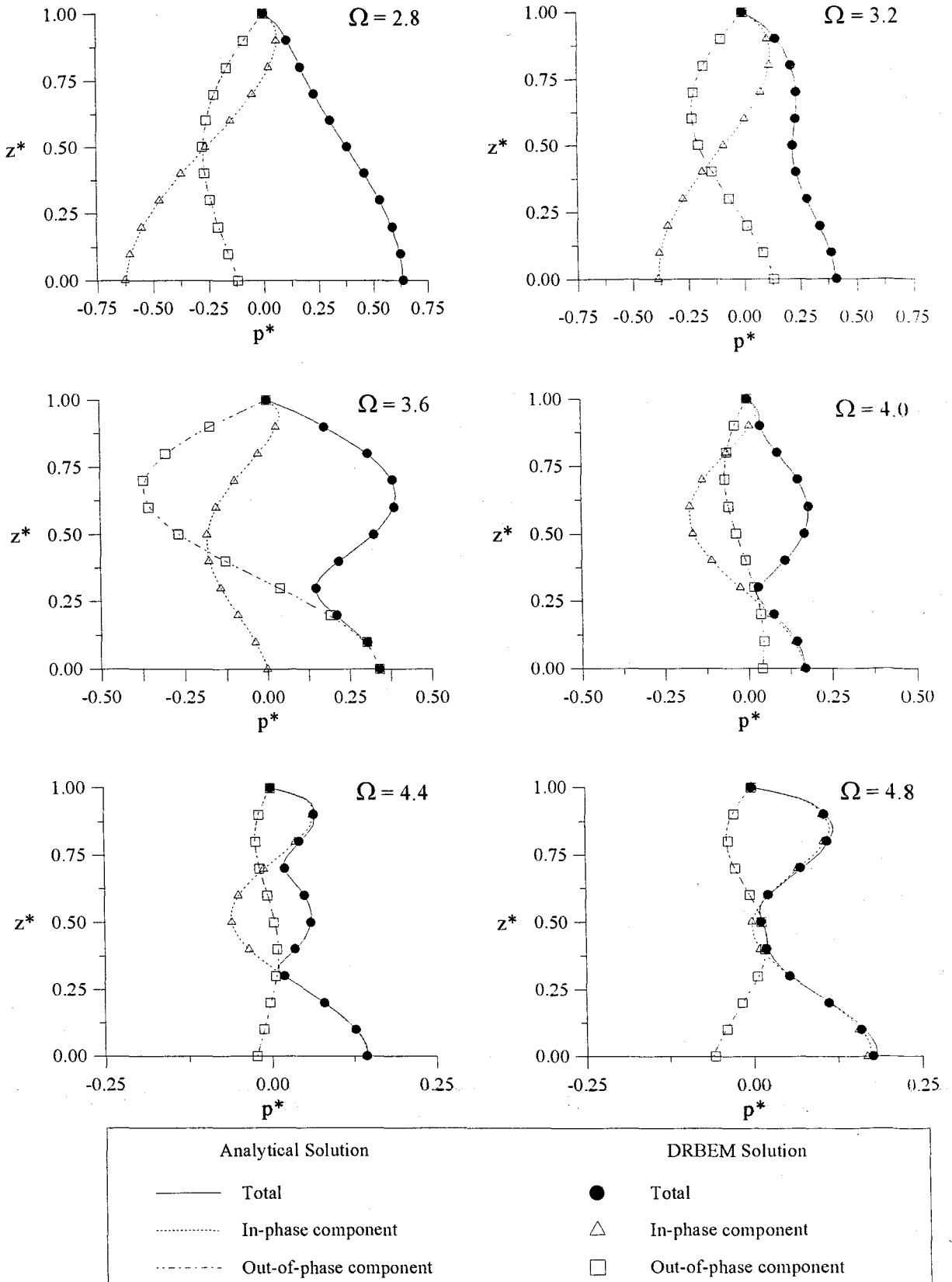


FIGURE 6.15.(b) Hydrodynamic pressures distribution on the upstream face of the rigid dam (harmonic cross-stream ground motion, reservoir boundary reflection coefficient, $\alpha_r = 0.75$).

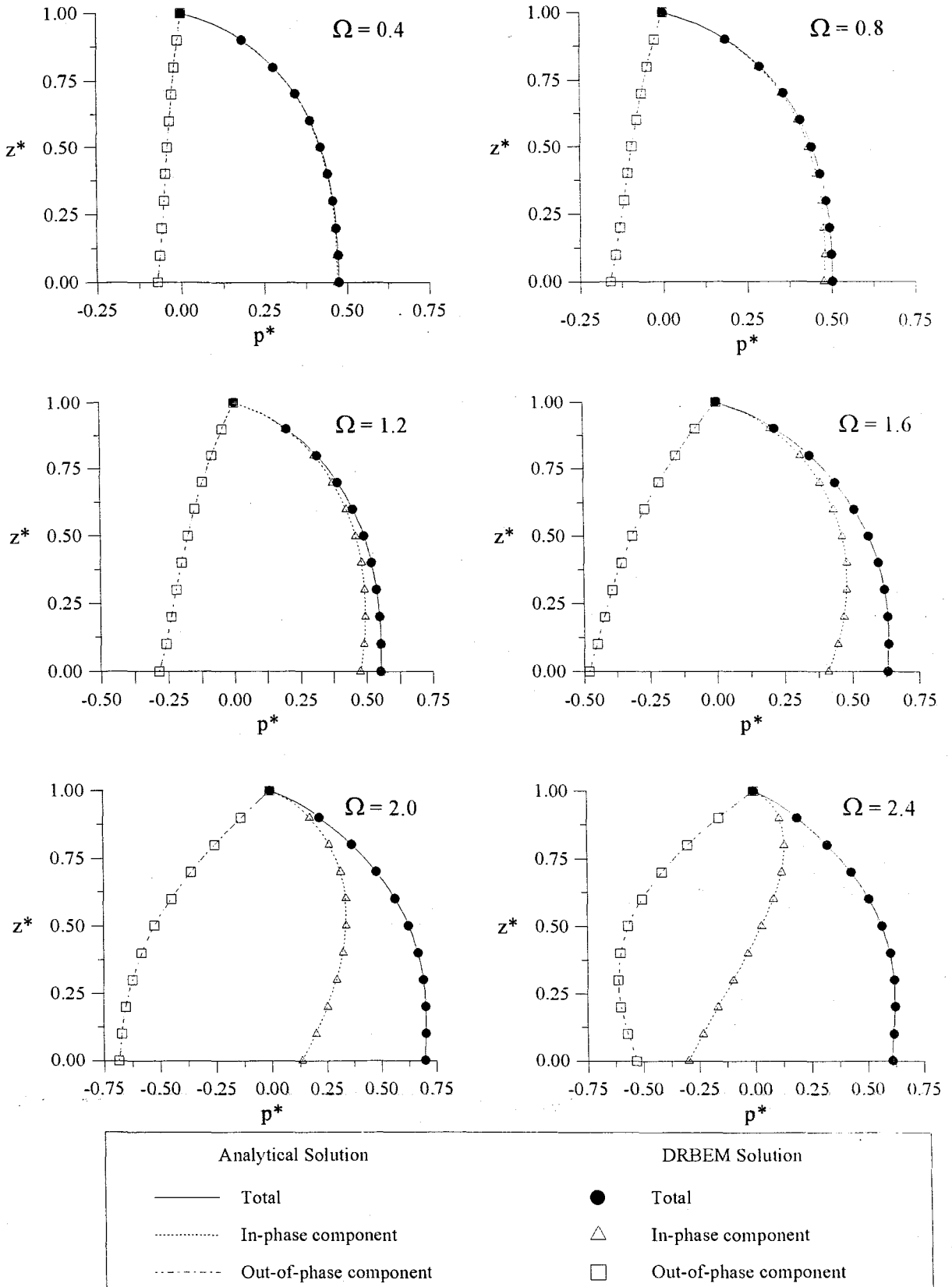


FIGURE 6.16.(a) Hydrodynamic pressures distribution on the upstream face of the rigid dam (harmonic cross-stream ground motion, reservoir boundary reflection coefficient, $\alpha_r = 0.5$).

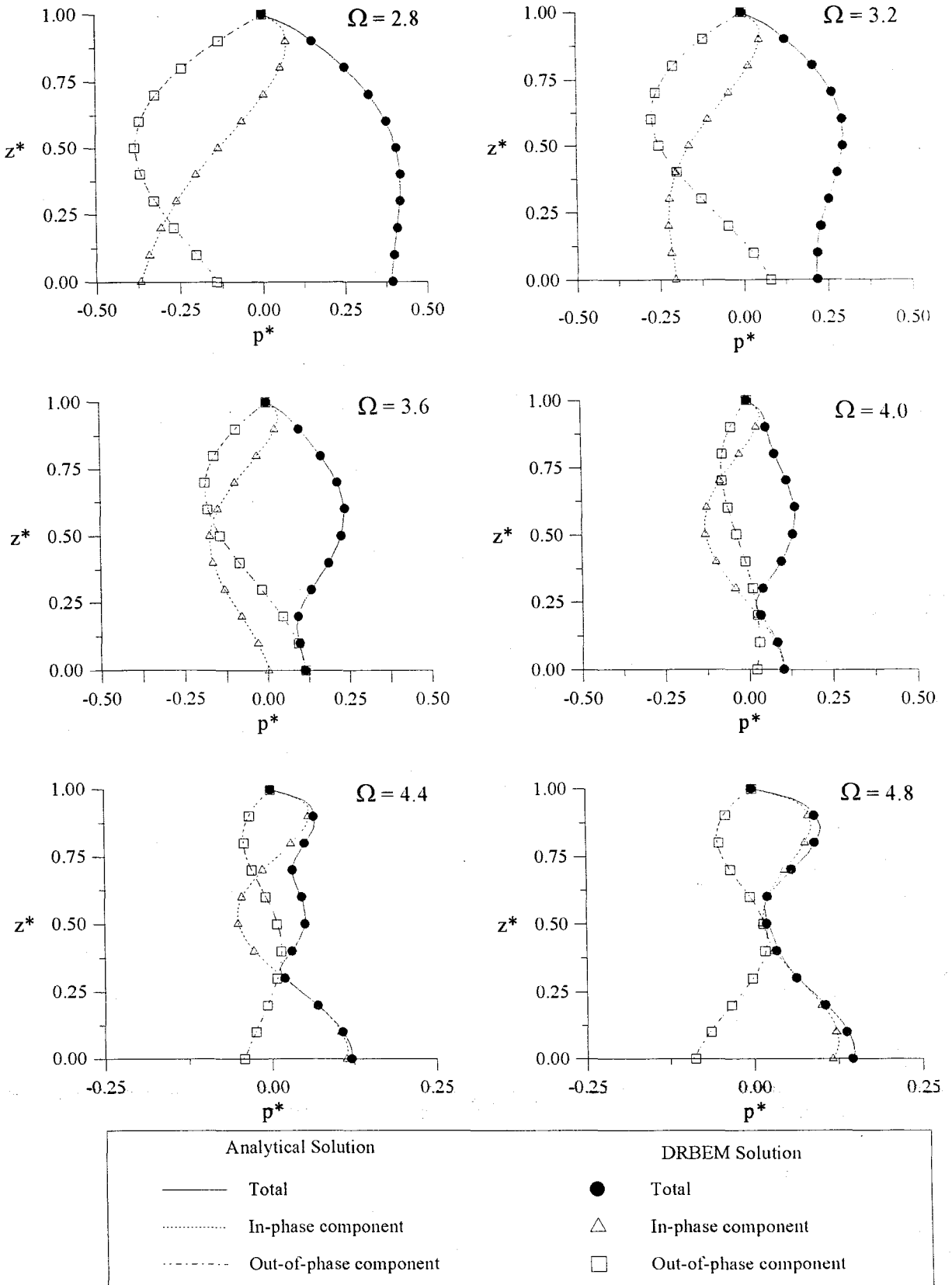


FIGURE 6.16.(b) Hydrodynamic pressures distribution on the upstream face of the rigid dam (harmonic cross-stream ground motion, reservoir boundary reflection coefficient, $\alpha_r = 0.5$).

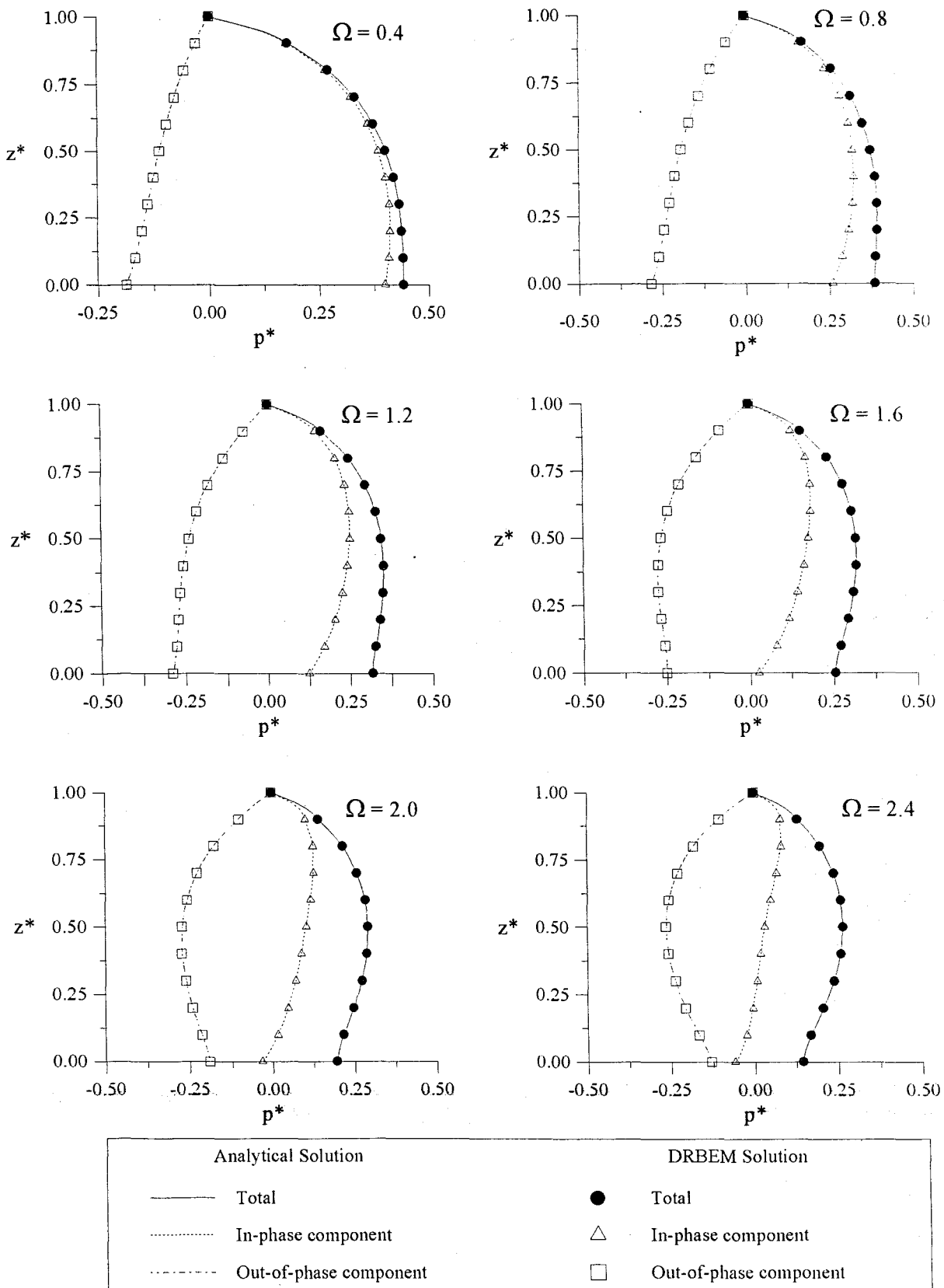


FIGURE 6.17.(a) Hydrodynamic pressures distribution on the upstream face of the rigid dam (harmonic cross-stream ground motion, reservoir boundary reflection coefficient, $\alpha_r = 0.0$).

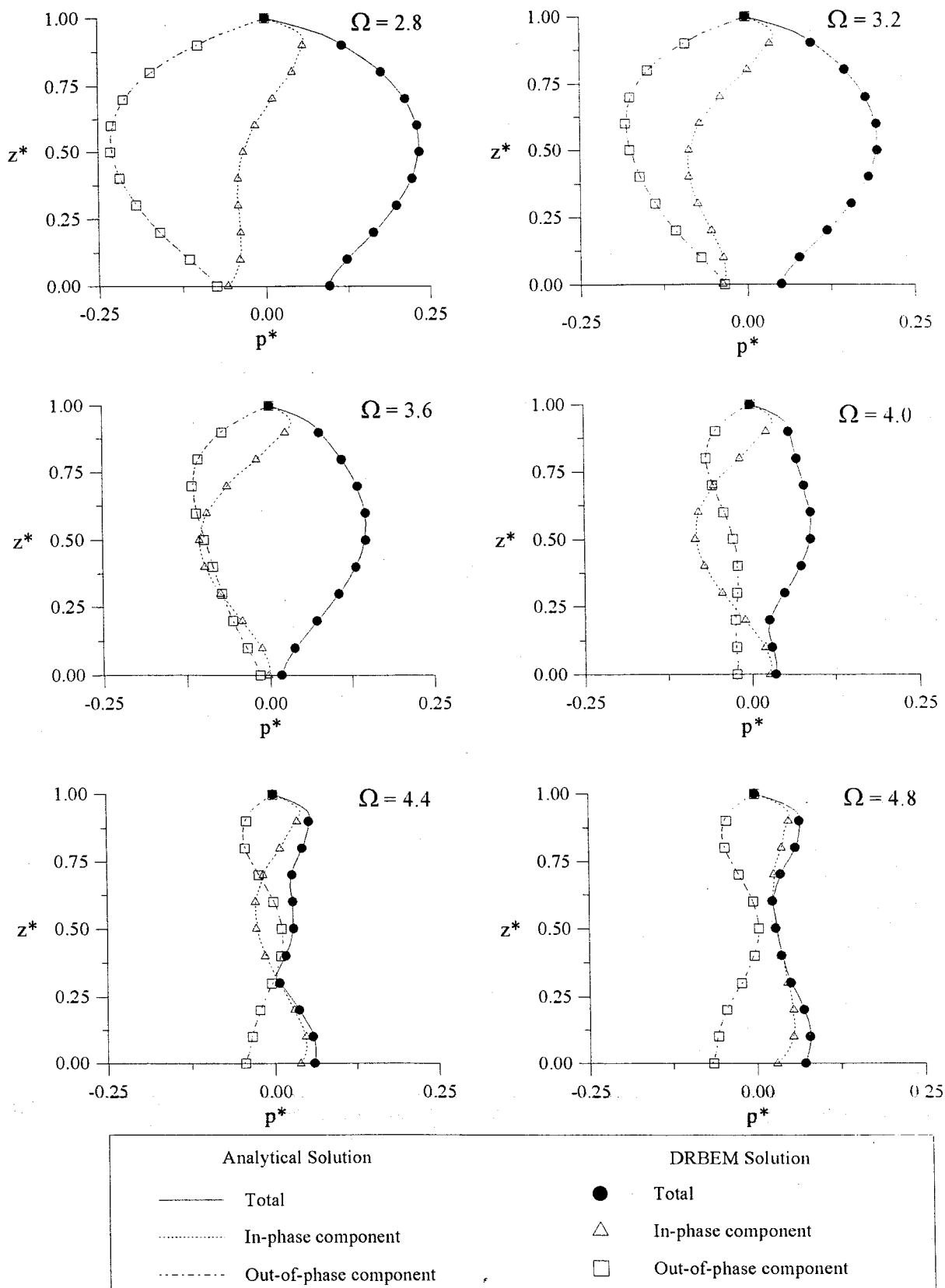


FIGURE 6.17.(b) Hydrodynamic pressures distribution on the upstream face of the rigid dam (harmonic cross-stream ground motion, reservoir boundary reflection coefficient, $\alpha_r = 0.0$).

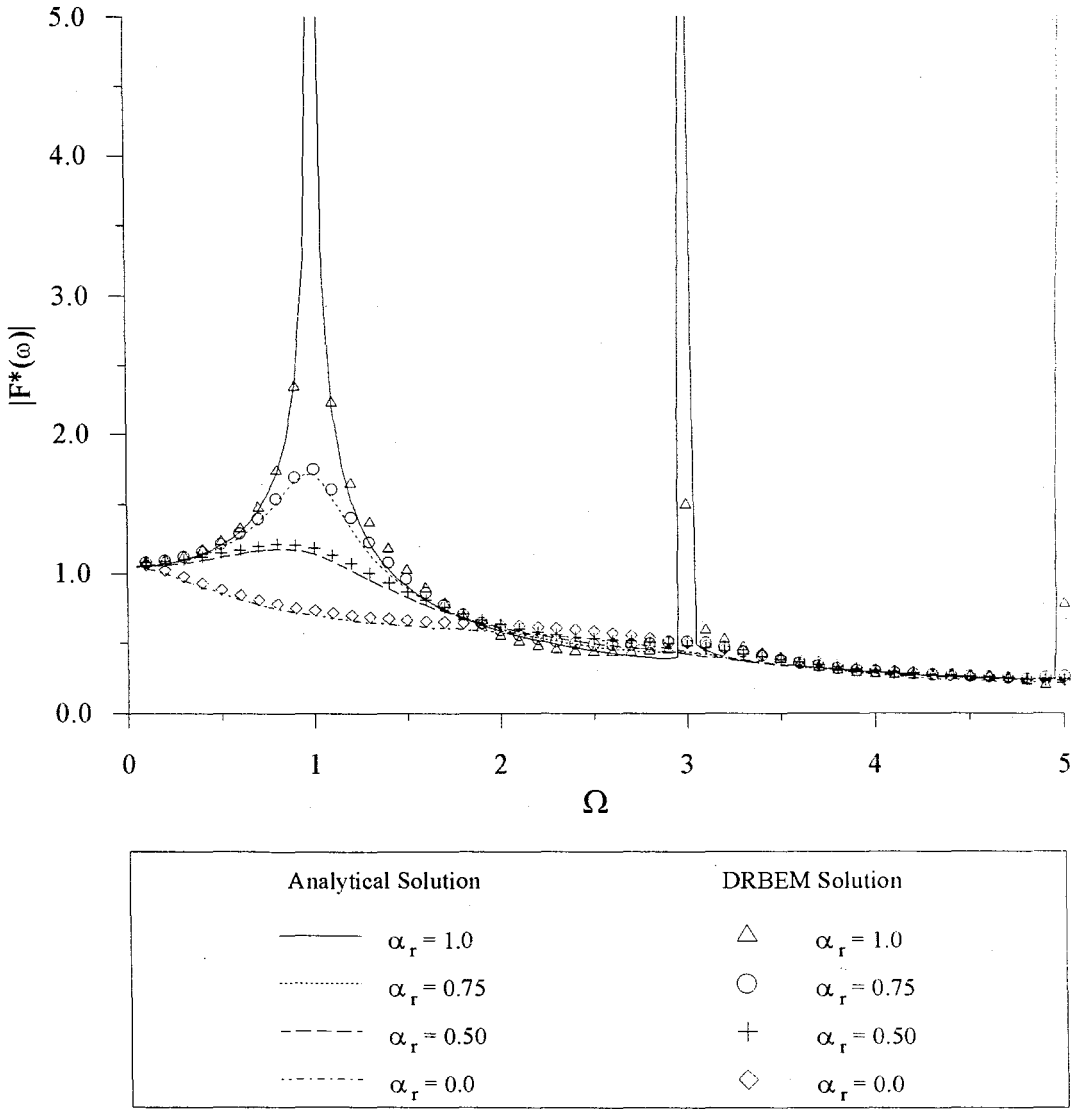
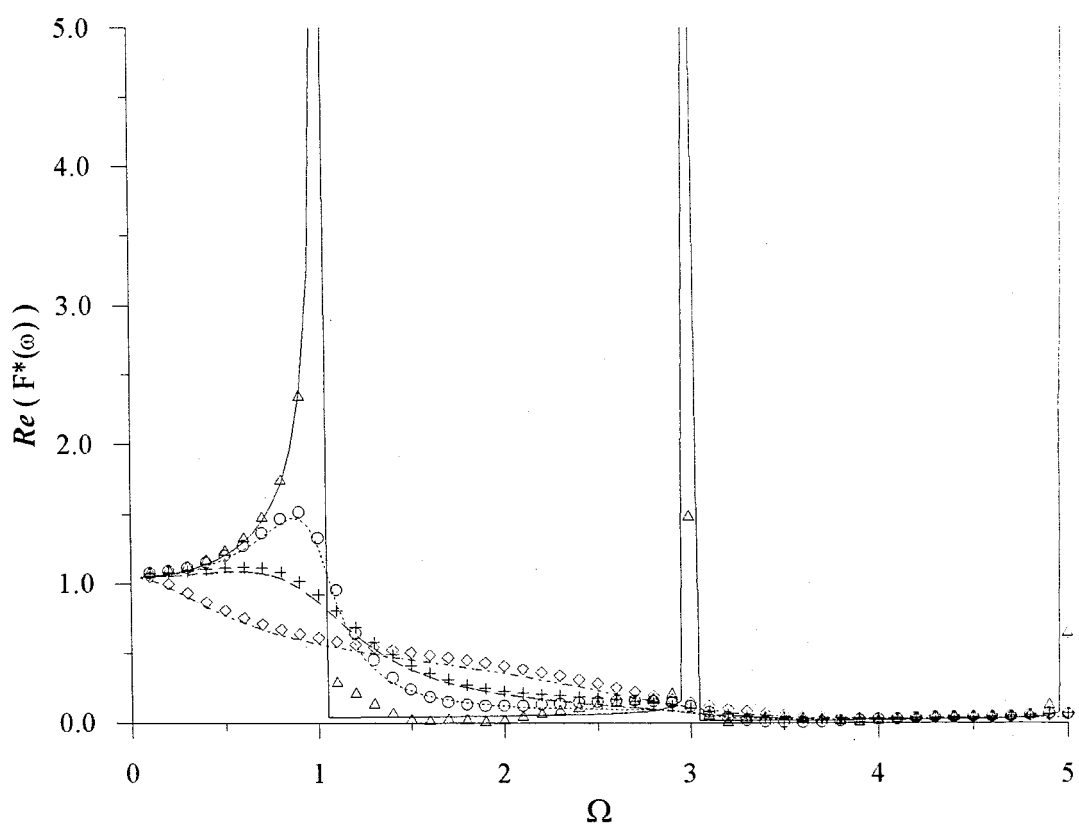
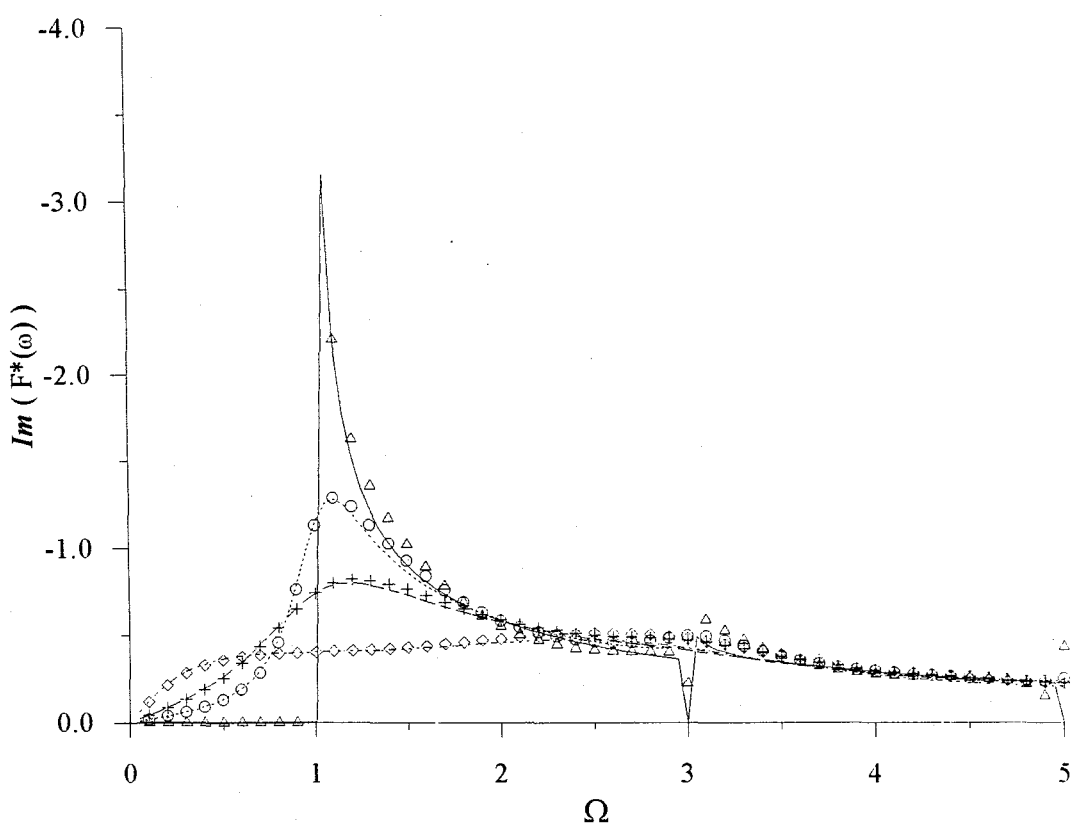


FIGURE 6.18. Total hydrodynamic force on the upstream face of a rigid dam due to harmonic upstream ground motion.



Analytical Solution		DRBEM Solution	
—	$\alpha_r = 1.0$	\triangle	$\alpha_r = 1.0$
⋯	$\alpha_r = 0.75$	\circ	$\alpha_r = 0.75$
- - -	$\alpha_r = 0.50$	+	$\alpha_r = 0.50$
⋯	$\alpha_r = 0.0$	\diamond	$\alpha_r = 0.0$

FIGURE 6.19. In-phase hydrodynamic force on the upstream face of a rigid dam due to harmonic upstream ground motion.



Analytical Solution		DRBEM Solution	
—	$\alpha_r = 1.0$	\triangle	$\alpha_r = 1.0$
.....	$\alpha_r = 0.75$	\circ	$\alpha_r = 0.75$
- - - -	$\alpha_r = 0.50$	+	$\alpha_r = 0.50$
- . - .	$\alpha_r = 0.0$	\diamond	$\alpha_r = 0.0$

FIGURE 6.20. Out-of-phase hydrodynamic force on the upstream face of a rigid dam due to harmonic upstream ground motion.

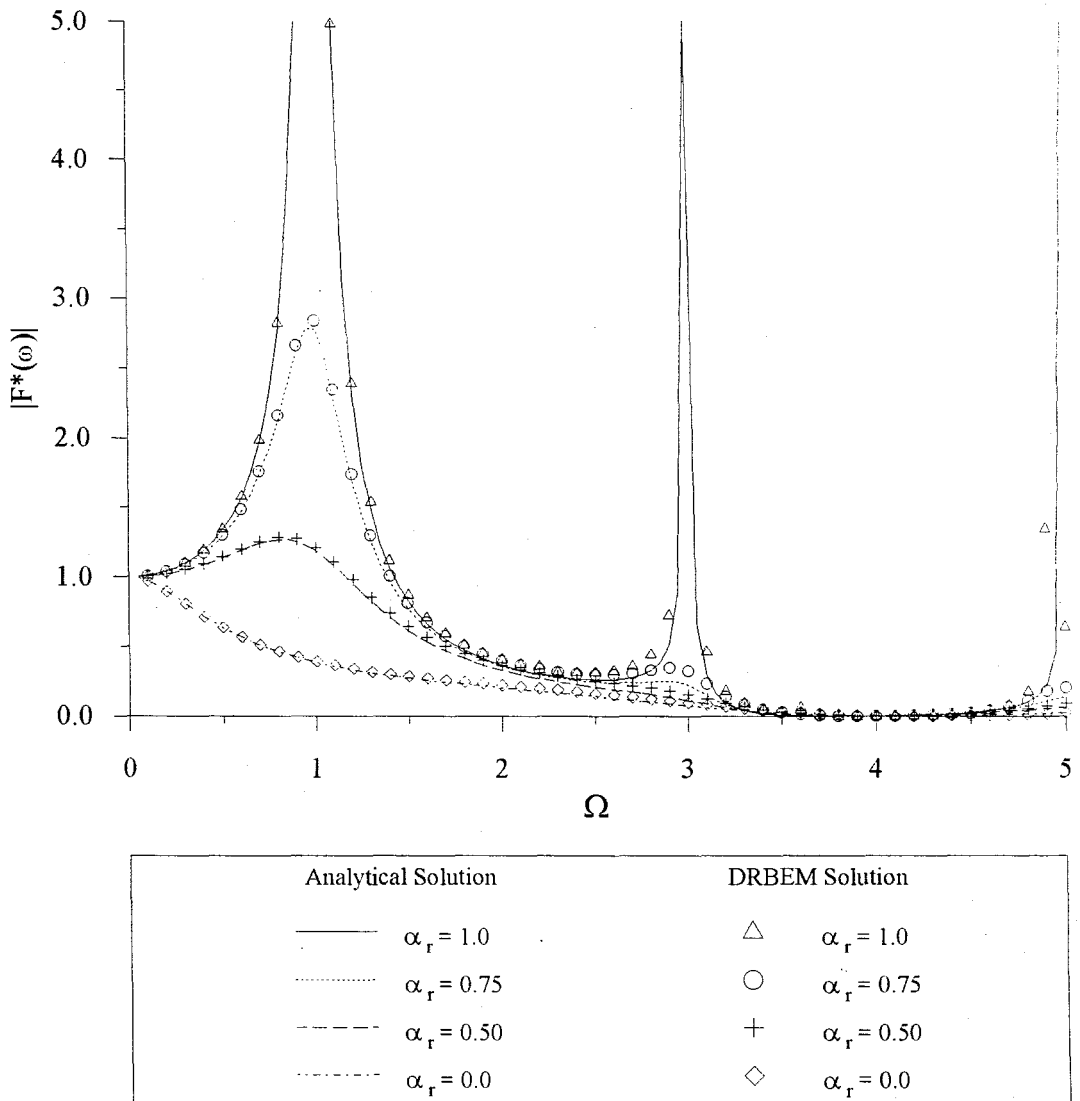
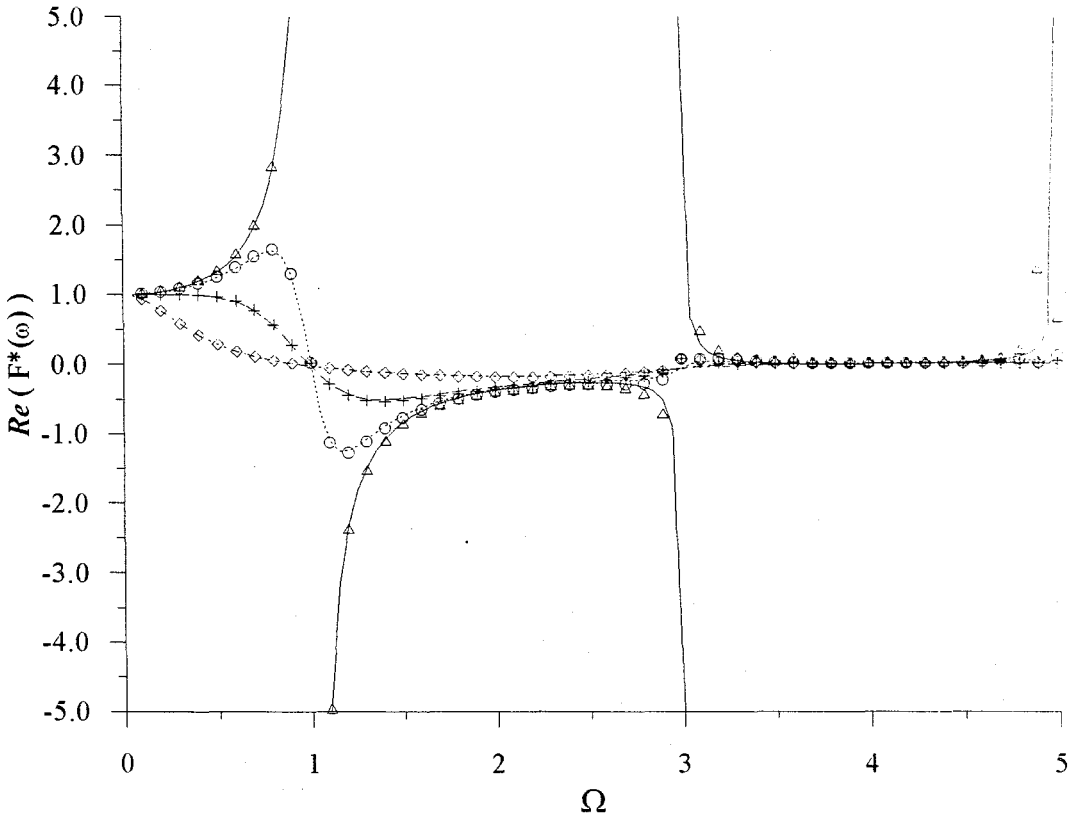


FIGURE 6.21. Total hydrodynamic force on the upstream face of a rigid dam due to harmonic vertical ground motion.



Analytical Solution		DRBEM Solution	
—	$\alpha_r = 1.0$	\triangle	$\alpha_r = 1.0$
⋯	$\alpha_r = 0.75$	\circ	$\alpha_r = 0.75$
- - -	$\alpha_r = 0.50$	+	$\alpha_r = 0.50$
⋯	$\alpha_r = 0.0$	\diamond	$\alpha_r = 0.0$

FIGURE 6.22. In-phase hydrodynamic force on the upstream face of a rigid dam due to harmonic vertical ground motion.

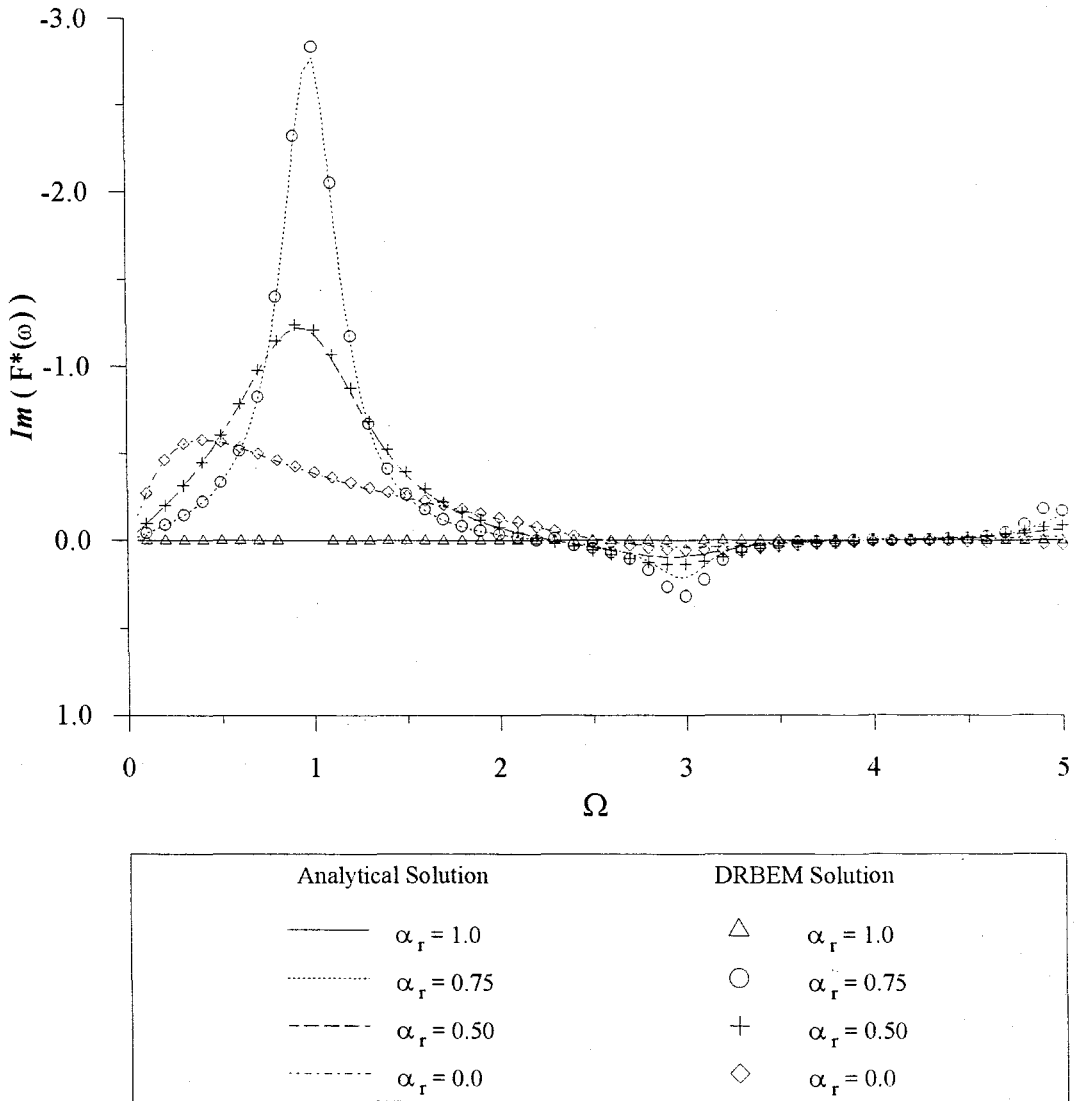


FIGURE 6.23. Out-of-phase hydrodynamic force on the upstream face of a rigid dam due to harmonic vertical ground motion.

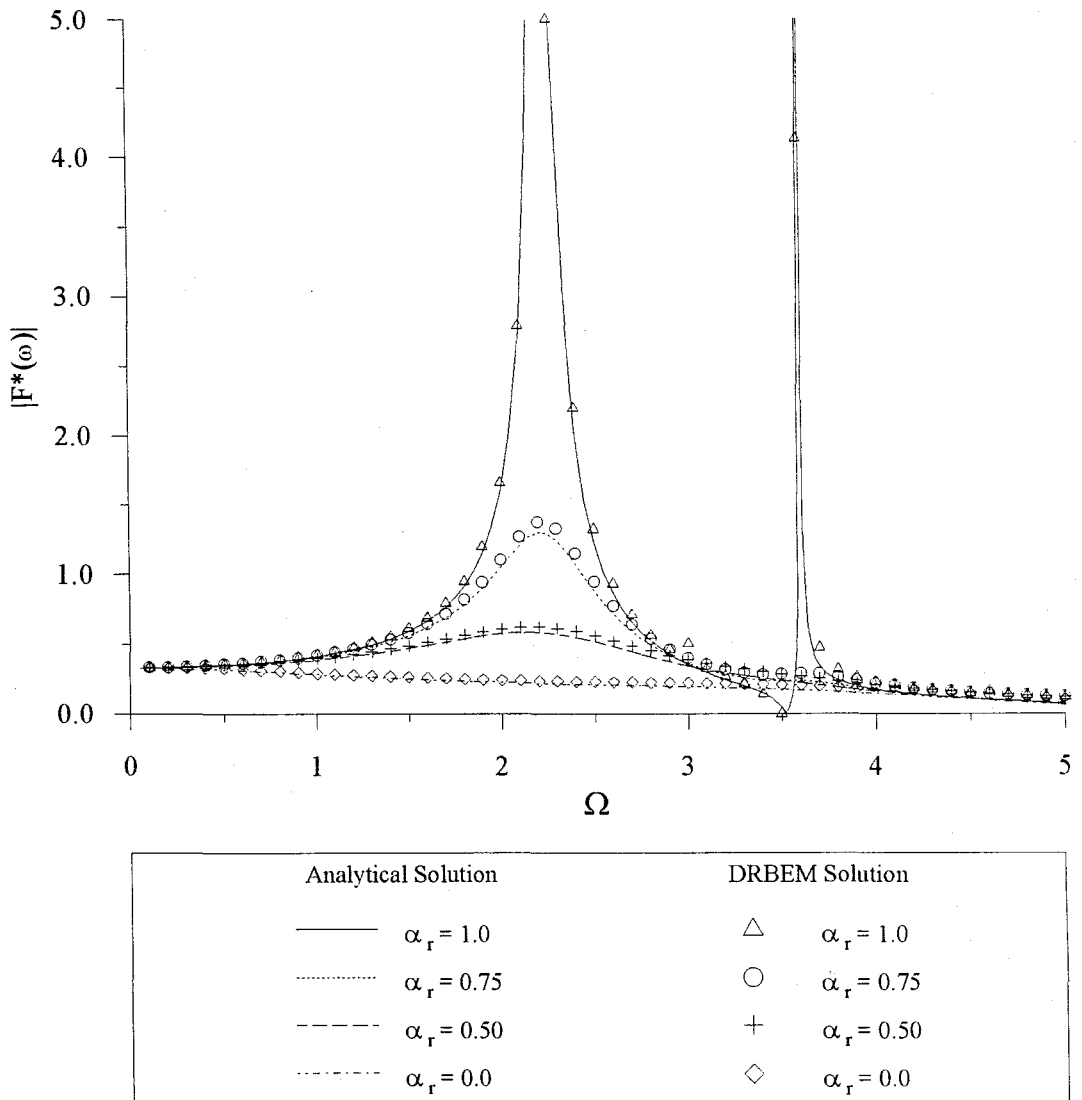


FIGURE 6.24. Total hydrodynamic force on the upstream face of a rigid dam due to harmonic cross-stream ground motion.

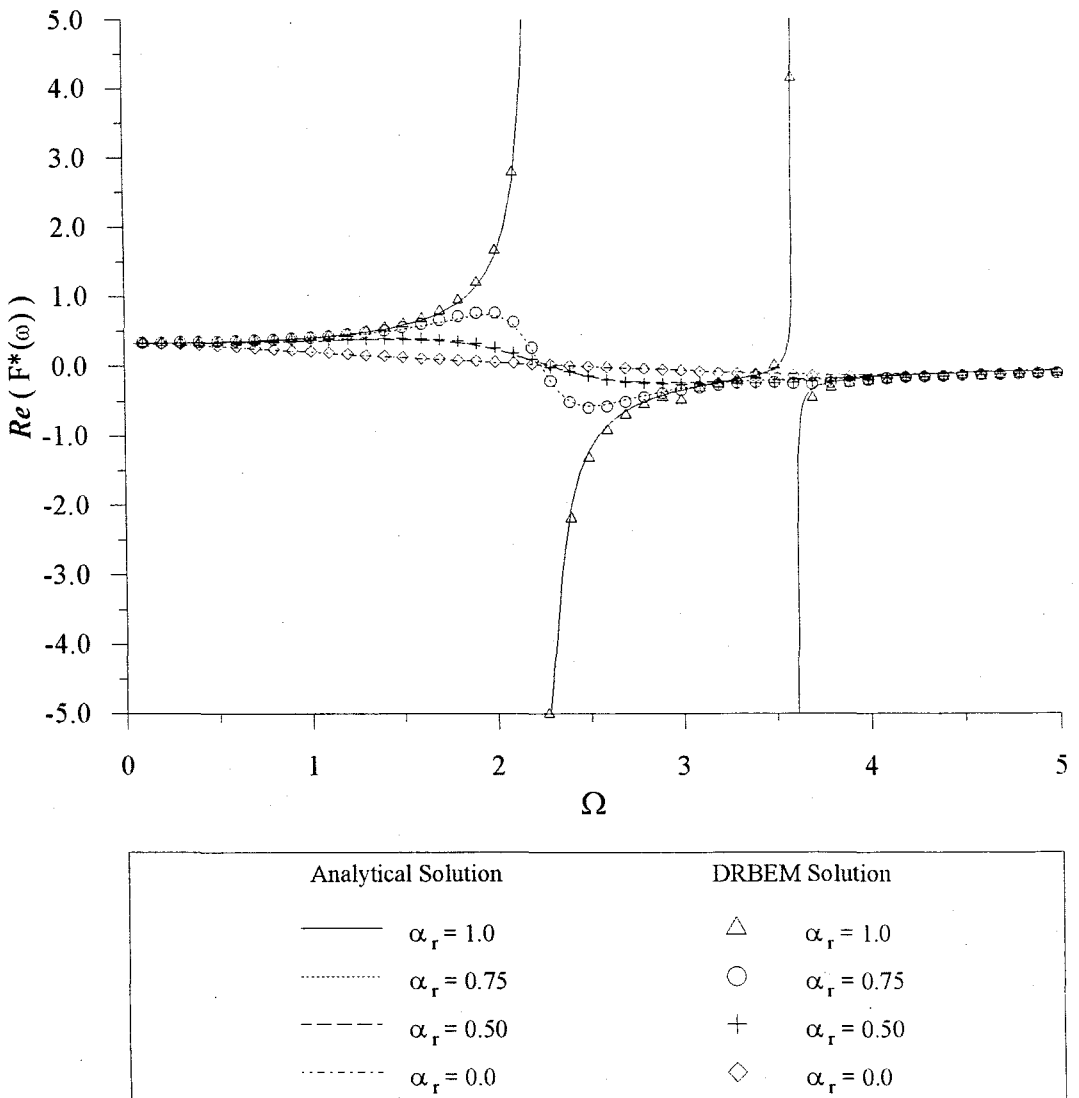


FIGURE 6.25. In-phase hydrodynamic force on the upstream face of a rigid dam due to harmonic cross-stream ground motion.

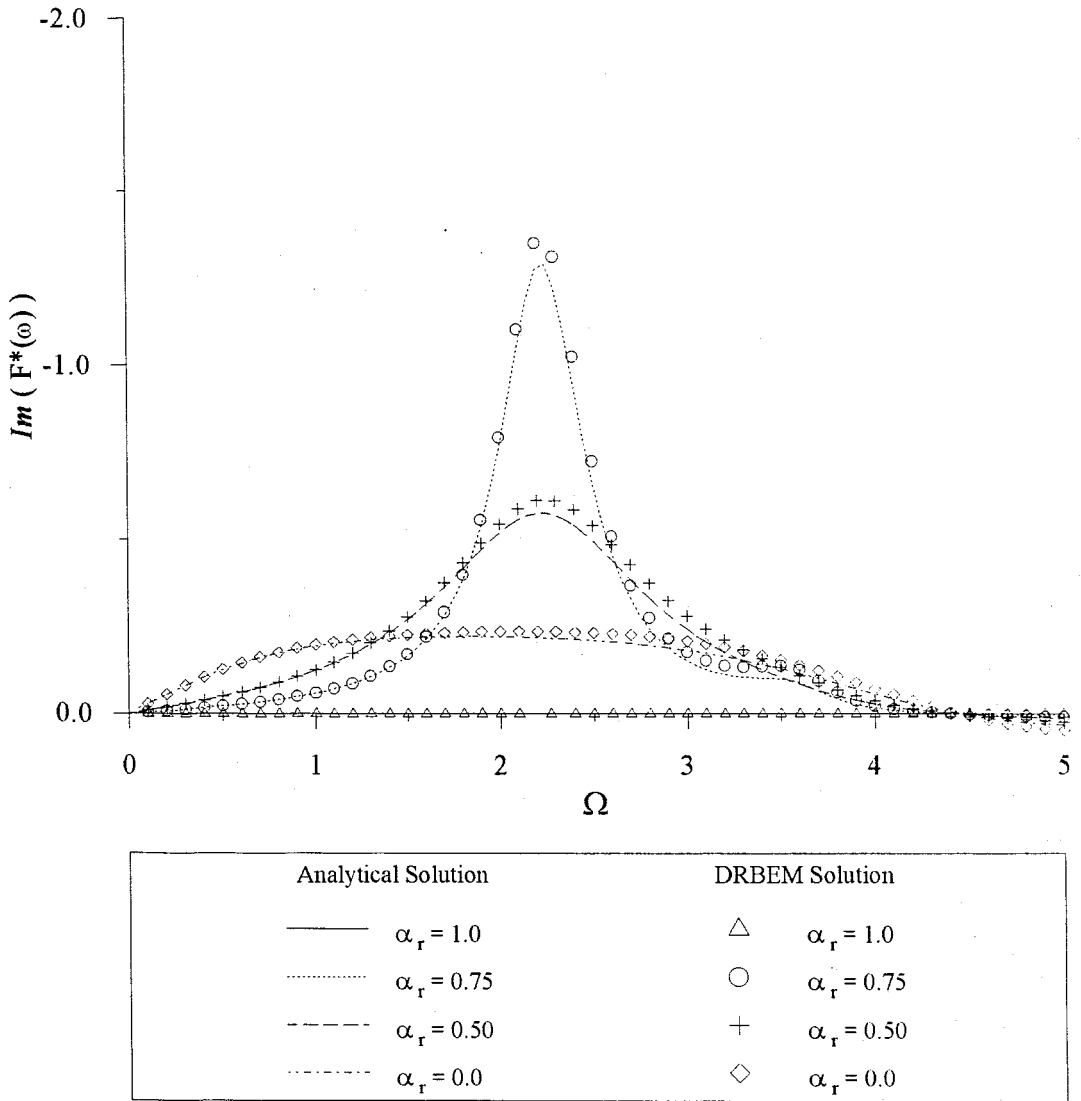


FIGURE 6.26. Out-of-phase hydrodynamic force on the upstream face of a rigid dam due to harmonic cross-stream ground motion.

7. CASE STUDY : DYNAMIC RESPONSES OF KARAKAYA DAM

The responses of the arch dam-reservoir system to harmonic ground motion are presented in this chapter. Responses computed by the model proposed in Chapters 2, 3 and 4 are presented for the upstream-downstream, vertical and cross-stream components of the ground motion, and for the parameters characterizing the geometrical and material properties of the dam structure and reservoir domain. Taking the Karakaya dam-reservoir system as a case study, the effects of the dam-water interaction, reservoir boundary absorption and reservoir geometrical shape on the hydrodynamic pressure response and the dynamic response of the dam are investigated.

7.1. Idealization of the Karakaya Dam-Reservoir System

Karakaya is one of the most important dams in Turkey. Completed in 1987 it is located on the Fırat River in the south east of Turkey. It has 158 m height, 382 m crest length and 9580 hm³ reservoir volume. The dam is a single-centered arch dam with maximum central angle of 118.5° and intrados and extrados radii of 175 m and 225m respectively. Figure 7.1 is an aerial photograph showing the Karakaya dam-reservoir system. A detailed description of the geometry of the dam and reservoir is available in Orhon, et al 1991. In the model, the dam structure and the reservoir are discretized using finite elements and boundary elements respectively. The discretized system is shown in Figure 7.2.

7.1.1. The Dam Structure

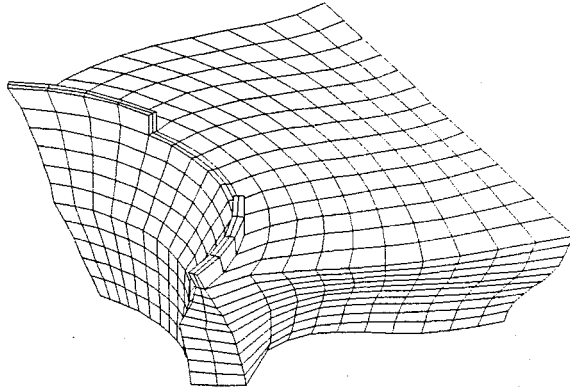
The finite element idealization of the dam, shown in Figure 7.2, consists of 296 eight-node solid elements, with a total of 525 nodes. Taking the foundation rock to be rigid, this idealization has 1242 degrees of freedom. The concrete mass in the dam is assumed to be homogenous, isotropic and linearly elastic with the following properties: Young's modulus, $E_s = 3.5 \times 10^9 \text{ kg/m}^2$, unit weight, $\gamma_s = 2.45 \times 10^3 \text{ kg/m}^3$ and Poisson's ratio $\nu_s = 0.2$. A constant hysteretic damping factor $\eta_s = 0.10$, which corresponds to five percent damping in all vibration modes of the dam with empty reservoir on rigid foundation rock, is selected.



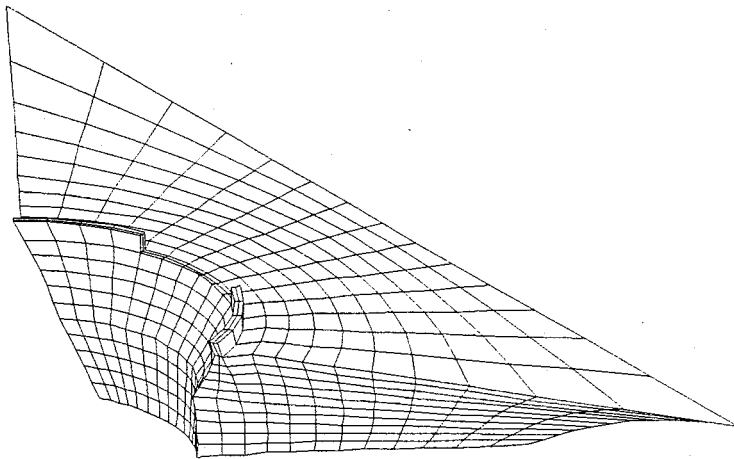
FIGURE 7.1. The Karakaya Dam and reservoir system

(b) Symmetric reservoir

FIGURE 7.2. Localization of the Karakaya dam and reservoir system



(a) Actual geometry reservoir



(b) Symmetric reservoir

FIGURE 7.2. Idealization of the Karakaya dam and reservoir system

7.1.2. The Reservoir Domain

The reservoir is idealized as a finite irregular region combined with an infinite uniform domain. The finite irregular domain boundary is discretized into 760 isoparametric two-dimensional surface quadrilateral elements with a total of 762 boundary nodes and an additional 150 dual reciprocity nodes are placed within the fluid domain. To model the radiation condition on the interface of finite and infinite domains, a two-dimensional dual reciprocity model is considered. Boundaries of the uniform cross section of the infinite domain are discretized into 48 isoparametric linear elements with 48 boundary nodes. The boundary nodes of the finite domain within the interface are considered as internal nodes for the two-dimensional dual reciprocity model. The thin plate spline approximating function is used in the dual reciprocity models. To check the validity of the radiation model, the finite element model based on the formulation in Appendix C is utilized. For this model, 140 isoparametric four-node linear quadrilateral elements with a total of 165 nodes are used.

To investigate the effects of reservoir shape on the hydrodynamic pressure response, the reservoir is discretized in the two different ways shown in Figure 7.2. The first discretization is for the actual reservoir geometry with all its variations. Polynomial interpolating functions are extracted from the contour maps of the dam-reservoir then used to modify the mesh generation routines. The second symmetrical idealization of the geometry is a radially increasing reservoir in the upstream direction which used in analytical solution of the hydrodynamic pressure on the upstream face of the dam (Kotsubo, 1961 and Porter and Chopra, 1980). In the computations, the following properties of the reservoir are used: The water depth, $H=158\text{m}$, the velocity of the sound in water, $c=1439\text{m/s}$ and the mass density of water $\rho_w=1000\text{ kg/m}^3$. The radiation boundary is placed at a distance $L=225\text{m}$ from the upstream face of the dam. To investigate the effects of the reservoir boundary absorption, four different absorbing factors of the reservoir boundary are considered with the following values of coefficient of reflection: $\alpha_r=0.0, 0.5, 0.75$ and 1.0 . The model can handle any water level provided the finite element mesh for the dam is defined to match the nodal points at the water level. In this study, the reservoir is assumed to be full, unless stated otherwise.

7.1.3. The Ground Motion

The excitation for the arch dam-reservoir is defined by three components of the free-field ground motion: The upstream-downstream (x) component, the vertical (z) component and the cross-stream (y) component. Each component of ground acceleration is assumed to be harmonic with the excitation frequency ω which is varied over a wide range. No spatial variations in the ground motion are considered, therefore the ground motion excitations are assumed to be uniform across the arch dam-reservoir system.

7.2. Hydrodynamic Responses on the Rigid Arch Dam

Before studying the response of the complete arch dam-reservoir system, it is useful to investigate the hydrodynamic responses on the upstream face of a rigid arch dam. These responses are determined for both the actual and the idealized reservoir geometries. The analyses have been carried for the three components of the ground motion excitations with an excitation amplitude of 1g and a wide range of the excitation frequency values ω . The coefficient of reflection is taken as: $\alpha_r = 0.0, 0.5, 0.75$ and 1.0. The frequency response functions of the hydrodynamic pressure distribution on the upstream face of the dam are computed using the procedure described in Chapter 4, for no interaction between the arch dam and the reservoir system. The hydrodynamic pressure, force and the excitation frequency are normalized as in Section 6.3.

7.2.1. Free Vibrations of The Infinite Domain

To model the radiation condition along the finite and infinite domains of the reservoir, a radiation model based on the dual reciprocity method was formulated in Chapter 5. The cross section of the finite domain of the reservoir at the scattering surface extends uniformly to infinity to form the infinite domain of the reservoir. The radiation model results in a generalized eigenvalue problem for the infinite domain of the reservoir. The resulting system matrices are real and non-symmetrical. The eigenvalue problem is solved using the QZ algorithm of Moler and Stewart, 1973. To verify the model results, the eigenvalues of the infinite domain of the actual reservoir idealization, are compared with the results obtained from

the finite element model given in Appendix C. For a fully reflecting reservoir boundary ($\alpha=1.0$) the eigenvalues are independent of the excitation frequency. The first 10 eigenvalues resulting from the two models are presented in Table 7.1. The maximum relative difference between the two models, ranges from 0.27% in the first eigenvalue to 10.55% in the ninth eigenvalue. When boundary absorption effects are included the eigenvalues given by both the DRBEM and the FEM are complex valued and dependent on the excitation frequency.

7.2.2. Effects of Reservoir Geometry Shape

To study the effects of the reservoir geometry variations in the vicinity of the arch dam, hydrodynamic responses were investigated for both the symmetrical and the actual geometry reservoir idealizations. The normalized hydrodynamic pressure distributions on the upstream face of the arch dam are presented in Figures 7.6-7.8 for the symmetrical reservoir case and in Figures 7.9-7.11 for the actual geometry reservoir case. The total hydrodynamic pressure response amplitude on the upstream face for the three components of the ground motion excitation are presented over the frequency range, $\Omega=0.4$ to 2.4 and for a reservoir boundary reflection coefficient $\alpha_r=0.75$. As can be seen from the figures and as expected, the presence of the geometrical variations of the reservoir affects the hydrodynamic pressure distributions on the upstream face of the dam. The hydrodynamic pressure distribution is no longer symmetrical and the maximum pressure regions are different from the symmetrical reservoir case. The x-components of the normalized total hydrodynamic force responses acting on the upstream face of the arch dam due to upstream, vertical and cross-stream ground motions are given as frequency response functions in Figures 7.18, 7.19 and 7.20, respectively. For the three components of the ground motions excitations, the geometrical variations of the actual reservoir affect the hydrodynamic response in different manners. It can be clearly noticed that, for the upstream-downstream ground motion excitation case, the geometrical variations reduce the hydrodynamic response for the normalized frequency, Ω , less than unity, and increase the response Ω greater than 3.0.

7.2.3. Effects of Reservoir Boundary Absorption

To study the reservoir boundary absorption effects on the hydrodynamic force responses on the arch dam, the x-component of the total hydrodynamic force responses acting on the upstream face of the dam due to upstream, vertical and cross-stream ground motion, are shown as frequency response functions in Figures 7.6-7.8 for the symmetrical reservoir and in Figures 7.9- 7.11 for the actual geometry reservoir. The hydrodynamic force responses are presented for four values of reservoir boundary reflection coefficients: 1.0, 0.75, 0.50, and 0.0.

For a fully reflecting reservoir boundary, $\alpha_r=1.0$, the hydrodynamic force responses are unbounded at the natural frequencies of the reservoir for all the three components of the ground motion excitation. It can be observed that, the hydrodynamic force responses are extremely sensitive to the excitation frequency and additional bounded peaks appear in the high frequency range $\Omega>2$. The fully reflecting reservoir assumption is not realistic because of the existence of the sediments and the foundation damping at the bottom of the reservoir. Introducing absorption damping into the system, smoothens these additional peaks. For the symmetrical reservoir case, there are double peaks in the vicinity of the natural frequency of the infinite reservoir. This can be interpreted as the effects of the resonance of both the finite and infinite domain of the reservoir. Only one peak exists for the case of the actual geometry reservoir case.

When reservoir boundary absorption is considered, the hydrodynamic forces are bounded for all excitation frequencies for all three components of the ground motion. The hydrodynamic pressure and force responses due to upstream ground motion are complex-valued for all excitation frequencies. With increasing excitation frequency, a larger number of modes are associated with the propagating pressure waves leading to increased energy radiation. For the symmetrical reservoir, the hydrodynamic force responses decrease with increasing excitation frequency for Ω greater than unity. For the real geometry case, the radiation damping has less effect on the hydrodynamic force response due to the boundary reflection effects in the vicinity of the dam.

7.3. Dam-Water Interaction Effects

As discussed in Chapter 3, the substructure concept is utilized to treat the arch dam and reservoir domain as separate substructures. The finite elements method is utilized to model the arch dam structure while the boundary element method is applied to model the reservoir. Based on this procedure, the dam and reservoir domains are first solved separately as substructures. Subsequently, these solutions are used to modify the equations of the dam structure and of the reservoir. Utilizing the analysis procedures developed in Chapters 3-5, the interactions of the arch dam and reservoir system are investigated. The effects of the dam-water interaction on the hydrodynamic and structural responses of the Karakaya dam-reservoir system are presented.

7.3.1. Free Vibration of Karakaya Dam

Based on the substructure procedure discussed in Chapter 3, the free vibration eigenvalue system described in Eq.3.2 is employed to find the natural vibration mode shapes, ϕ_j , and the corresponding natural frequencies, ω_j , of the Karakaya dam. The resulting system matrices are symmetrical. Therefore, Cholesky factorization is utilized to compute the eigenvalues of the system. The routine EVLSF from the IMSL library is used. Discussions of this routine and some timing results are given by Hanson et al. (1990).

The first ten natural frequencies of the Karakaya dam, are presented in Table 7.2. The present finite element model results based on lumped and consistent mass assumptions are compared with SAPIV results. In comparison to SAPIV results, the maximum relative error for the lumped mass approach is less than 0.38 per cent. The first six natural modes of vibration of the Karakaya Dam are presented in Figures 7.3-7.5. Odd natural modes of vibration correspond to the symmetrical mode shapes while the even ones correspond to the anti-symmetrical modes.

7.3.2. Hydrodynamic Forces on the Flexible Dam

Considering the arch dam-reservoir interaction, the hydrodynamic pressure response on the upstream face of the arch dam consists of two components: The hydrodynamic pressure response due to the ground motion acceleration taking the arch dam to be rigid, and the

pressure response due to the arch dam deformational motions without boundary motion. The frequency response functions for the hydrodynamic force are computed by integrating the corresponding hydrodynamic pressure response functions over the upstream face of the arch dam.

Considering the dam-water interaction, the normalized hydrodynamic pressure distributions on upstream face of the arch dam are presented in Figures 7.12-7.14 for the symmetrical reservoir case and in Figures 7.15-7.17 for the actual geometry reservoir case. The total hydrodynamic pressure responses are presented for the three components of the ground motion excitation and over the frequency range $\Omega=0.4$ to 2.4 and for a reservoir boundary reflection coefficient $\alpha_r=0.75$. The dam-water interaction affects both the magnitudes and the distributions of the hydrodynamic pressure responses. For the symmetrical reservoir case, the hydrodynamic responses resulting from the deformational motion of the arch dam act to reinforce the hydrodynamic responses resulting from the ground motion acceleration. In the cases of upstream and vertical ground motions, the symmetric properties of the pressure distribution are preserved because both pressure responses have the same phase over the upstream face of the arch dam. In the cross-stream ground motion case, both of the pressure responses have different phases. The symmetry of the distribution no longer exists. This is especially more pronounced for $\Omega>1$.

Considering the dam-reservoir interaction, the x-components of the normalized total hydrodynamic force responses acting on the upstream face of the arch dam due to upstream, vertical and cross-stream ground motions are given as frequency response functions in Figures 7.27- 7.29 for the symmetrical reservoir case, and in Figures 7.30- 7.32 for actual geometry reservoir. The dam-reservoir interaction has an amplifying effect on the hydrodynamic force responses especially when the normalized frequency is greater than unity. For Ω greater than unity, the hydrodynamic force responses exhibit complex behavior and have additional peaks resulting from the interaction. As it can be seen from both the symmetrical and the actual geometry reservoir cases, the system is strongly coupled in the normalized frequency range, $\Omega=2$ to 4.

7.3.3. Structural Responses

The response of the arch dam with an empty reservoir is the characteristic of a multi-degree of freedom system with frequency-independent mass, stiffness, and damping properties. Considering the water compressibility, the response of the dam with a full reservoir is affected by frequency dependent hydrodynamic terms. As described in Chapter 3, the hydrodynamic terms modify the equations of motion of the arch dam in terms of added masses and added loads. The added load is the hydrodynamic force on the rigid arch dam face due to the ground motion excitation, while the added mass terms are due to hydrodynamic forces resulting from the arch dam deformations with respect to the ground motion.

The dynamic response of Karakaya Dam to harmonic ground accelerations in the upstream-down stream, vertical and cross-stream excitation were investigated. The radial acceleration responses of the dam at different locations on the dam mesh($\theta = 0.0^\circ$, 15.27° and 31.51°) on upstream face of the dam at the spillway level are studied. The center of the dam corresponds to $\theta = 0.0^\circ$ while $\theta = 15.27^\circ$ and 31.51° are two points in-between the center and the right abutment of the dam. Considering both empty and full reservoir cases, these responses are presented in Figures 7.33-7.35 for the symmetrical reservoir and in Figures 7.36-7.38 for the actual geometry reservoir. The reservoir boundary absorption coefficient, α_r , is taken as 0.75 for the analysis. Because of the strong frequency dependence of the hydrodynamic terms, the dam response behaviors are complicated with the interaction of the reservoir. It is observed that, the actual geometry reservoir has more influence on the dam responses, especially at the excitation frequencies in the neighborhood of the natural frequencies of the reservoir.

TABLE 7.1. Comparison of natural frequencies of the infinite reservoir domain of Karakaya Dam (actual geometry reservoir case).

frequency (cycles/sec)	DRBEM (Present study)	FEM (Hall and Chopra, 1981)	Relative Difference
ω_1	2.77	2.78	0.27%
ω_2	4.66	4.68	0.41%
ω_3	5.58	6.03	7.33%
ω_4	7	7.2	2.75%
ω_5	7.72	7.94	2.71%
ω_6	8	8.81	9.22%
ω_7	9.1	9.83	7.42%
ω_8	10.5	10.72	6.23%
ω_9	10.33	11.55	10.55%
ω_{10}	11.15	12.14	8.19%

TABLE 7.2. Comparison of the free vibration frequencies of Karakaya Dam

frequency (cycles/sec)	Present Study (Lumped Mass)	Present Study (Consistent Mass)	SAPIV (Lumped Mass)
ω_1^s	3.2	3.276	3.208
ω_2^s	3.546	3.678	3.555
ω_3^s	4.257	4.521	4.262
ω_4^s	5.022	5.502	5.018
ω_5^s	6.008	6.848	6.004
ω_6^s	6.407	6.951	6.401
ω_7^s	6.604	7.099	6.629
ω_8^s	7.266	7.958	7.259
ω_9^s	7.457	8.085	7.430
ω_{10}^s	7.922	8.513	7.936

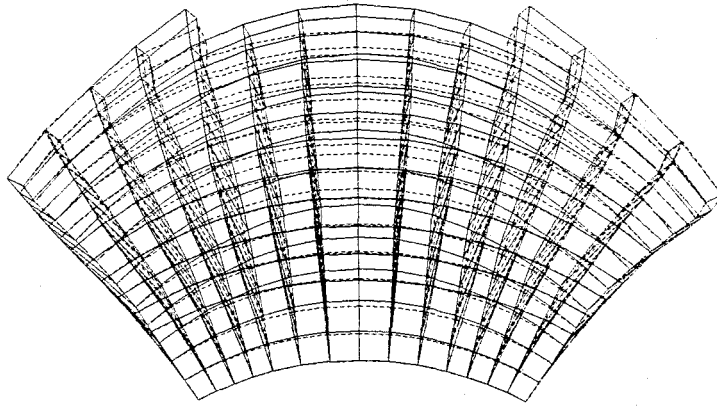
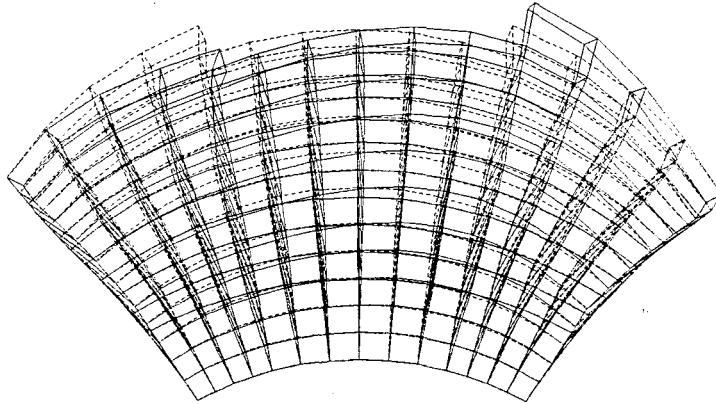
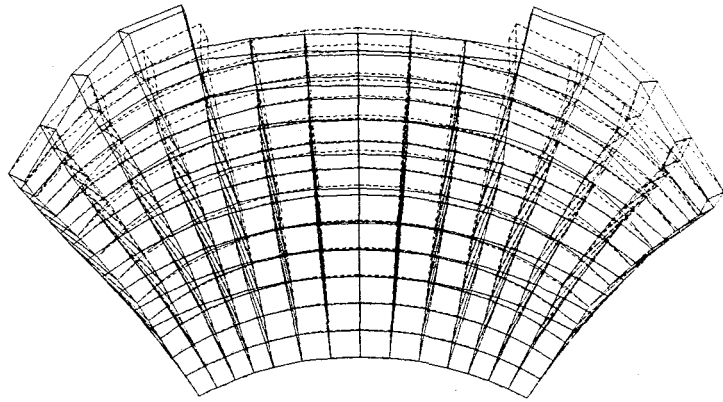
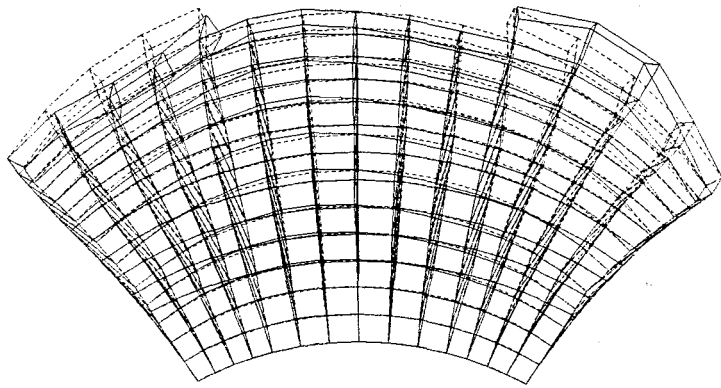
1st mode2nd mode

Figure 7.3. Natural vibration modes of Karakaya Dam



3rd mode



4th mode

Figure 7.4. Natural vibration modes of Karakaya Dam

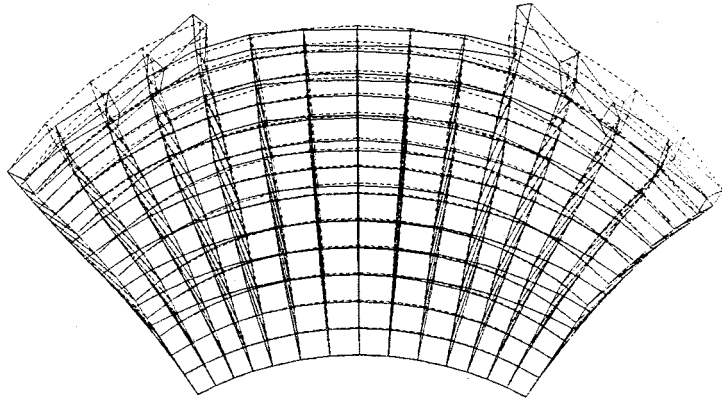
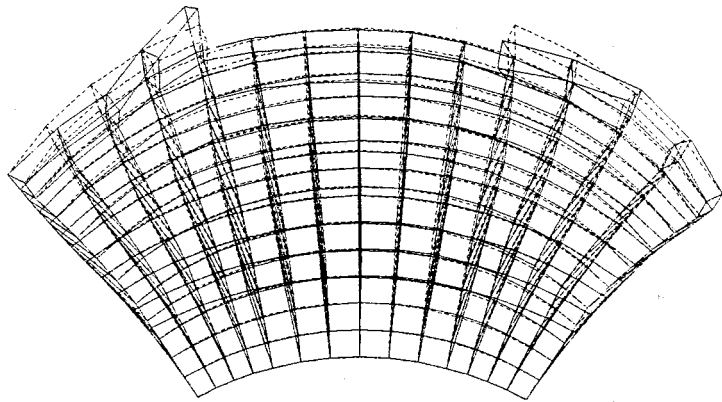
5th mode6th mode

Figure 7.5 Natural vibration modes of Karakaya Dam

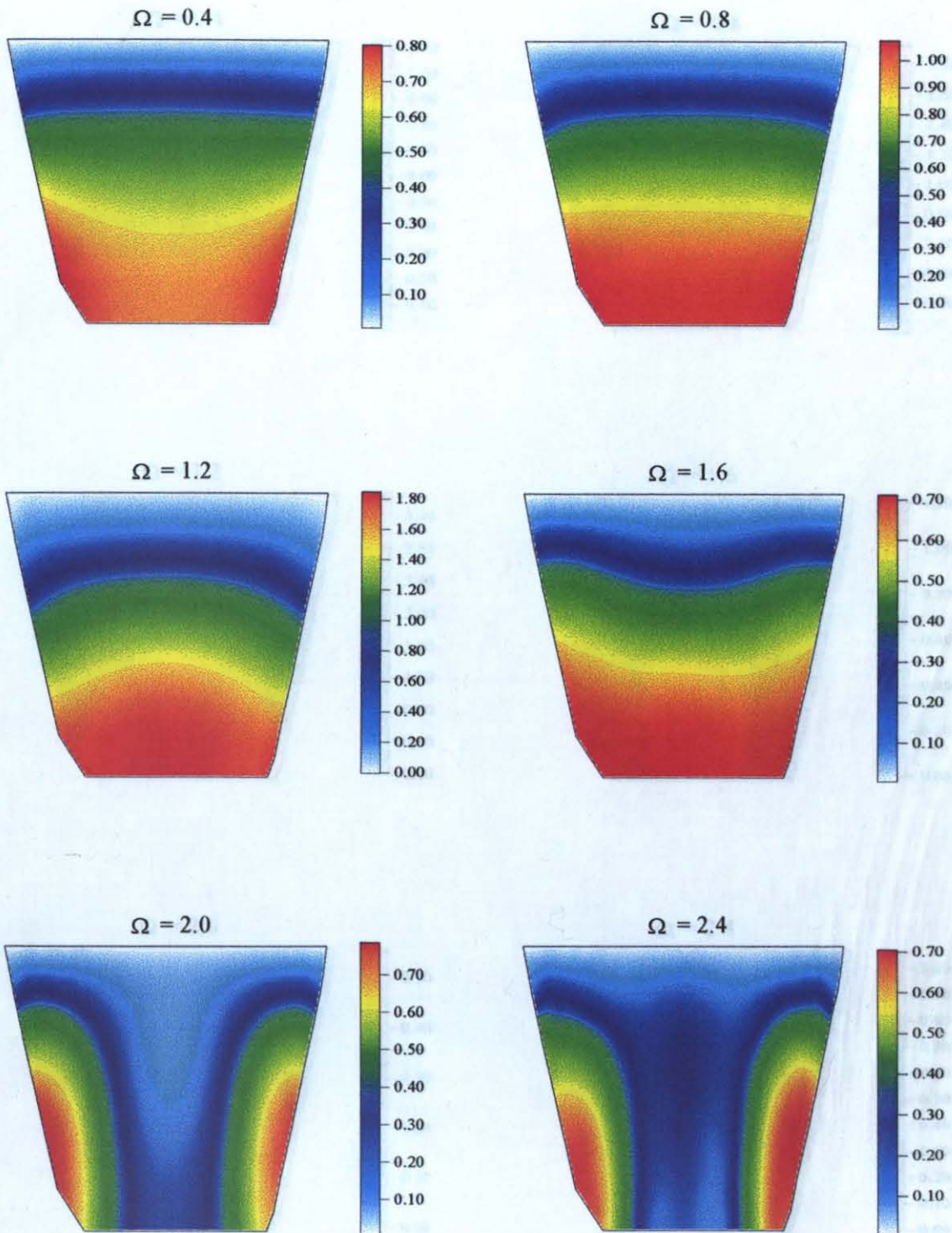


FIGURE 7.7. The hydrodynamic pressure distribution on the upstream face of Karakaya

FIGURE 7.6. The hydrodynamic pressure distribution on the upstream face of Karakaya

Dam : without dam-reservoir interaction, symmetrical reservoir, harmonic upstream-

downstream ground motion, reservoir boundary reflection coefficient, $\alpha_r=0.75$.

($\Omega=0.4,0.8,1.2,1.6,2.0,2.4$ corresponds to $\omega=0.93,1.86,2.78,3.71,4.64,5.57$ cycles/sec)

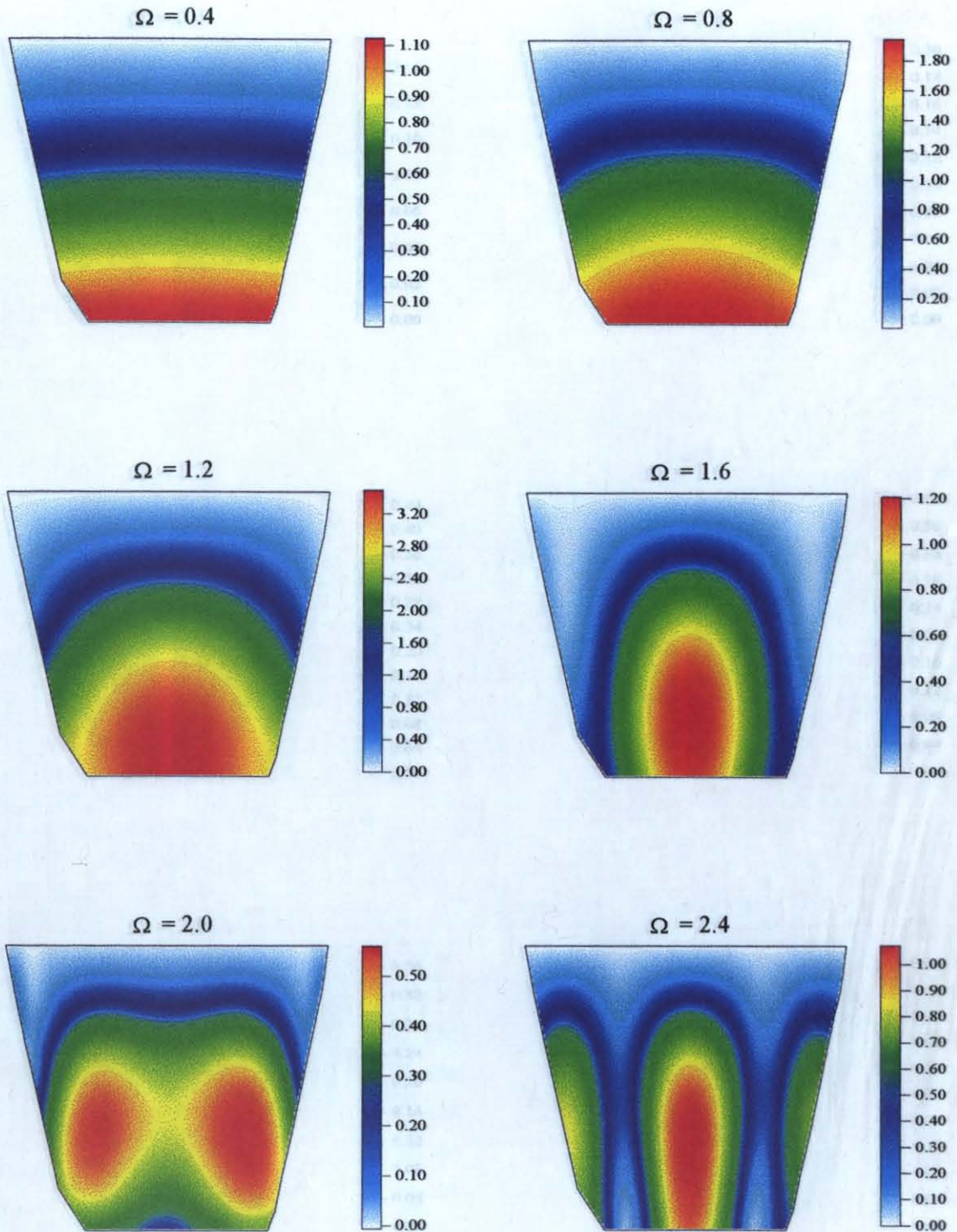


FIGURE 7.7. The hydrodynamic pressure distribution on the upstream face of Karakaya Dam : without dam-reservoir interaction, symmetrical reservoir, harmonic vertical ground motion, reservoir boundary reflection coefficient, $\alpha_r=0.75$.

($\Omega=0.4,0.8,1.2,1.6,2.0,2.4$ corresponds to $\omega=0.93,1.86,2.78,3.71,4.64,5.57$ cycles/sec)

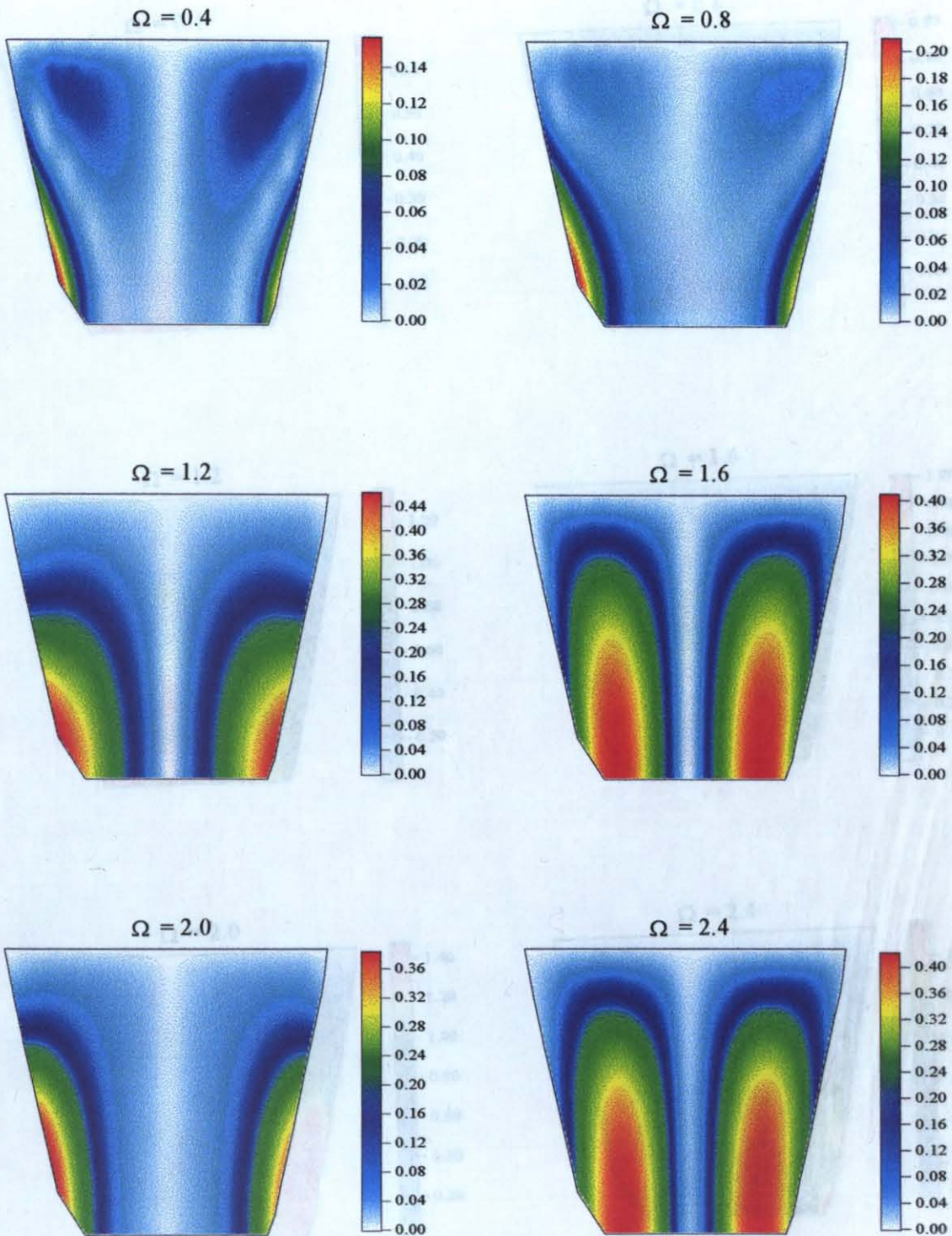


FIGURE 7.8. The hydrodynamic pressure distribution on the upstream face of Karakaya Dam : without dam-reservoir interaction, symmetrical reservoir, harmonic cross-stream ground motion, reservoir boundary reflection coefficient, $\alpha_r=0.75$.

($\Omega=0.4,0.8,1.2,1.6,2.0,2.4$ corresponds to $\omega=0.93,1.86,2.78,3.71,4.64,5.57$ cycles/sec)

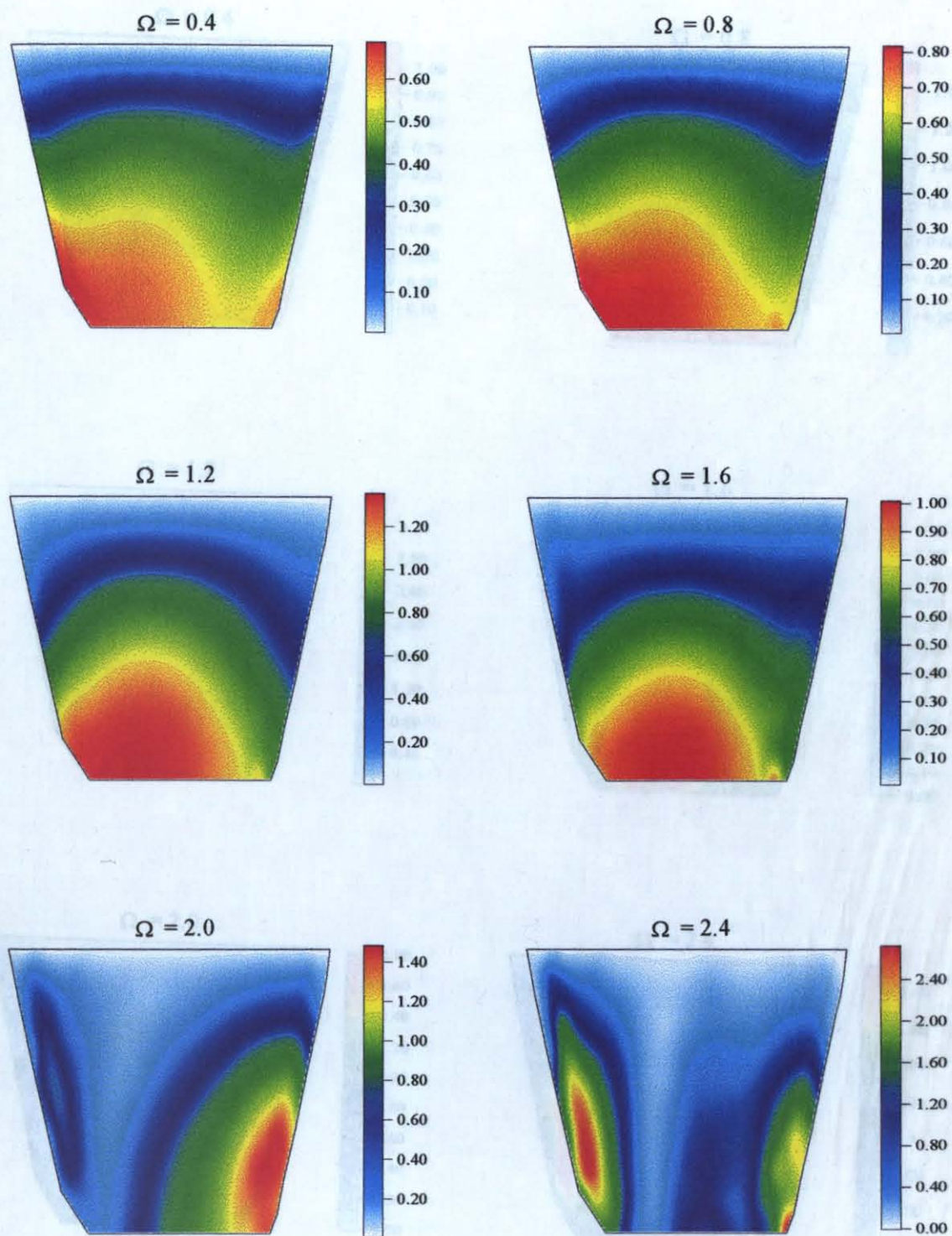


FIGURE 7.9. The hydrodynamic pressure distribution on the upstream face of Karakaya Dam : without dam-reservoir interaction, actual geometry reservoir, harmonic upstream-downstream ground motion, reservoir boundary reflection coefficient, $\alpha_r=0.75$.

($\Omega=0.4,0.8,1.2,1.6,2.0,2.4$ corresponds to $\omega=0.93,1.86,2.78,3.71,4.64,5.57$ cycles/sec)

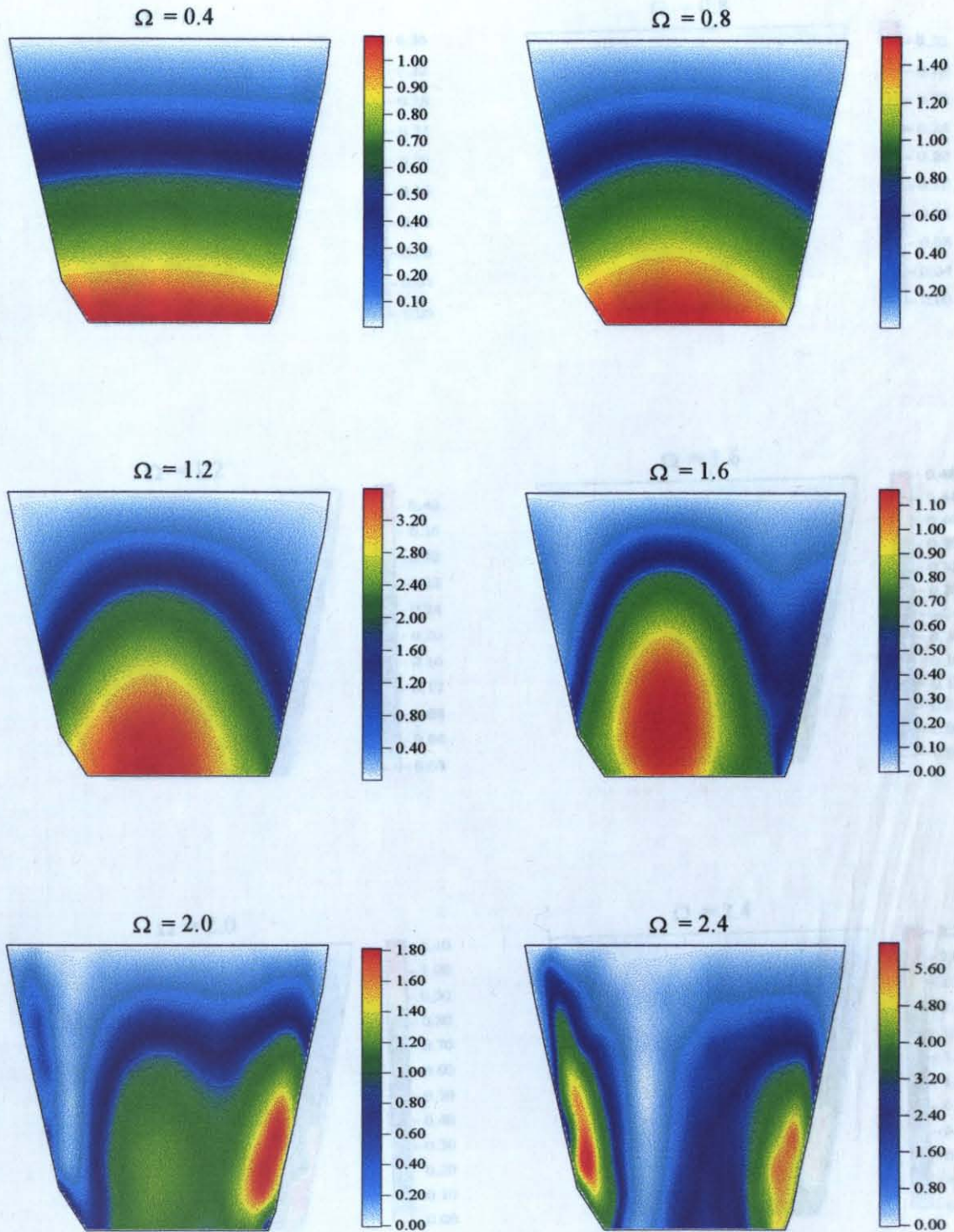


FIGURE 7.10. The hydrodynamic pressure distribution on the upstream face of Karakaya Dam : without dam-reservoir interaction, actual geometry reservoir, harmonic vertical ground motion, reservoir boundary reflection coefficient, $\alpha_r=0.75$.

($\Omega=0.4,0.8,1.2,1.6,2.0,2.4$ corresponds to $\omega= 0.93,1.86,2.78, 3.71,4.64,5.57$ cycles/sec)

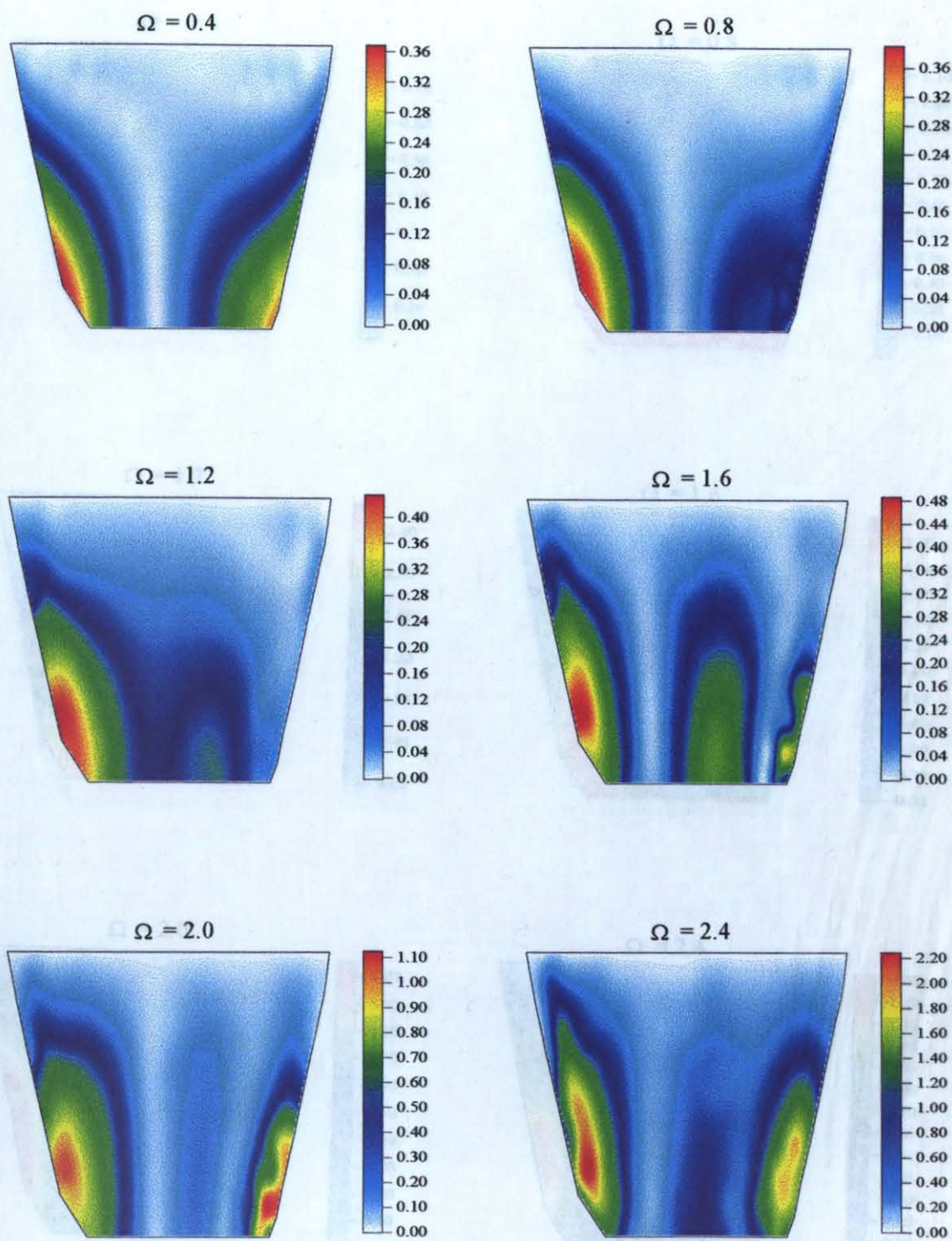


FIGURE 7.11. The hydrodynamic pressure distribution on the upstream face of Karakaya Dam : without dam-reservoir interaction, actual geometry reservoir, harmonic cross-stream ground motion, reservoir boundary reflection coefficient, $\alpha_r=0.75$.

($\Omega=0.4,0.8,1.2,1.6,2.0,2.4$ corresponds to $\omega=0.93,1.86,2.78,3.71,4.64,5.57$ cycles/sec)

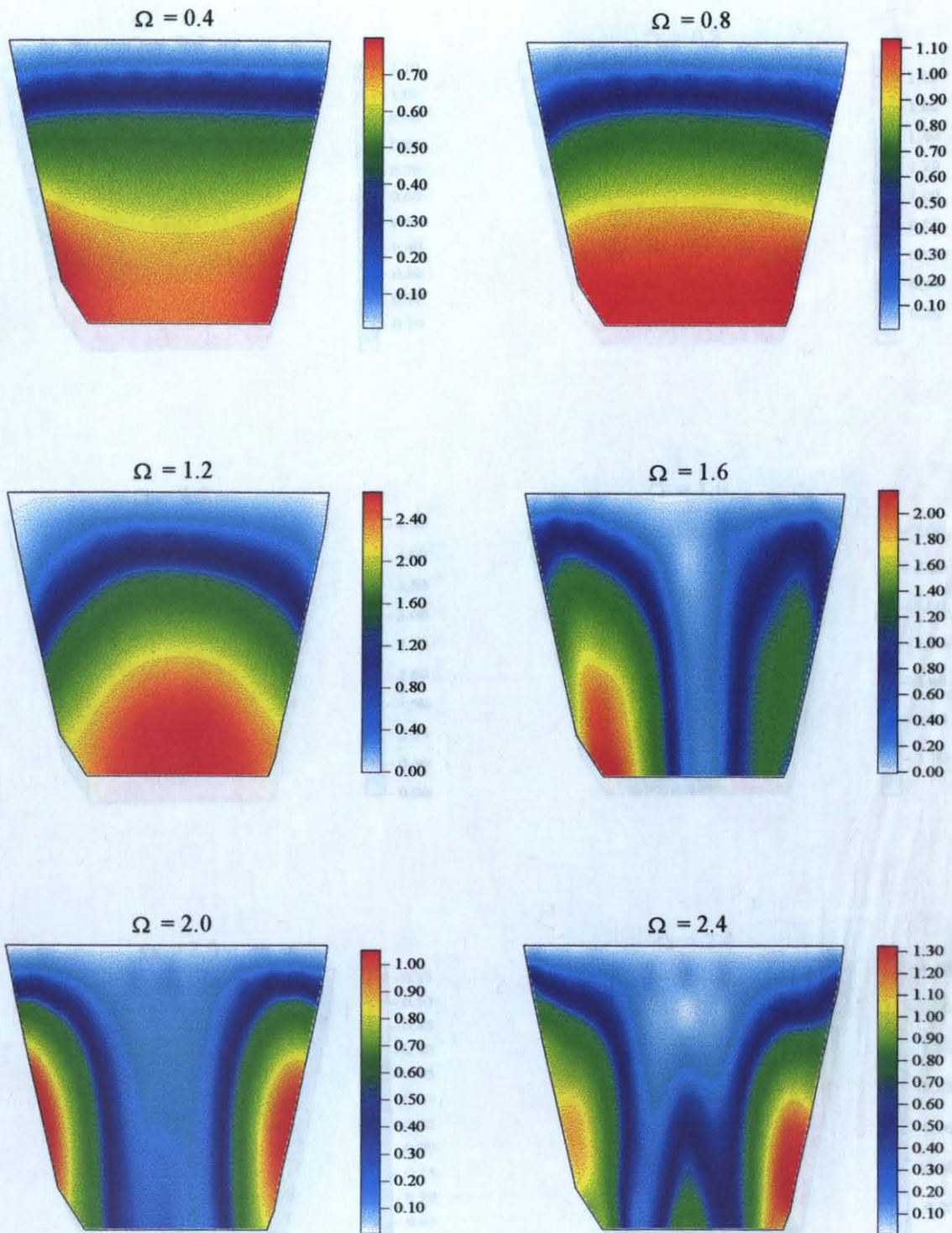


FIGURE 7.12 The hydrodynamic pressure distribution on the upstream face of Karakaya Dam : with dam-reservoir interaction, symmetrical reservoir, harmonic upstream-downstream ground motion, reservoir boundary reflection coefficient, $\alpha_r=0.75$.

($\Omega=0.4,0.8,1.2,1.6,2.0,2.4$ corresponds to $\omega=0.93,1.86,2.78,3.71,4.64,5.57$ cycles/sec)

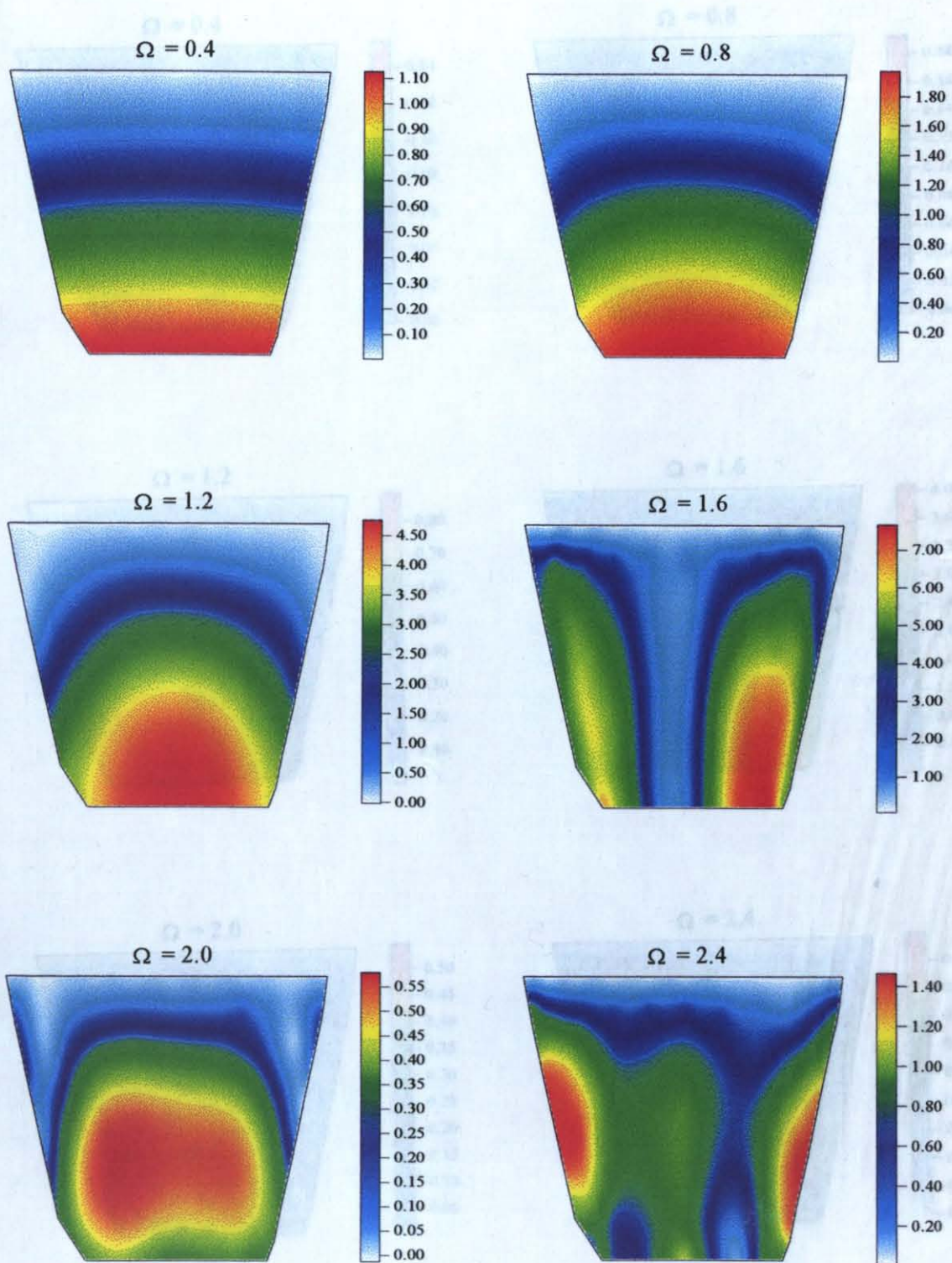


FIGURE 7.13. The hydrodynamic pressure distribution on the upstream face of Karakaya Dam : with dam-reservoir interaction, symmetrical reservoir, harmonic vertical ground motion, reservoir boundary reflection coefficient, $\alpha_r=0.75$.

($\Omega=0.4,0.8,1.2,1.6,2.0,2.4$ corresponds to $\omega= 0.93,1.86,2.78, 3.71,4.64,5.57$ cycles/sec)

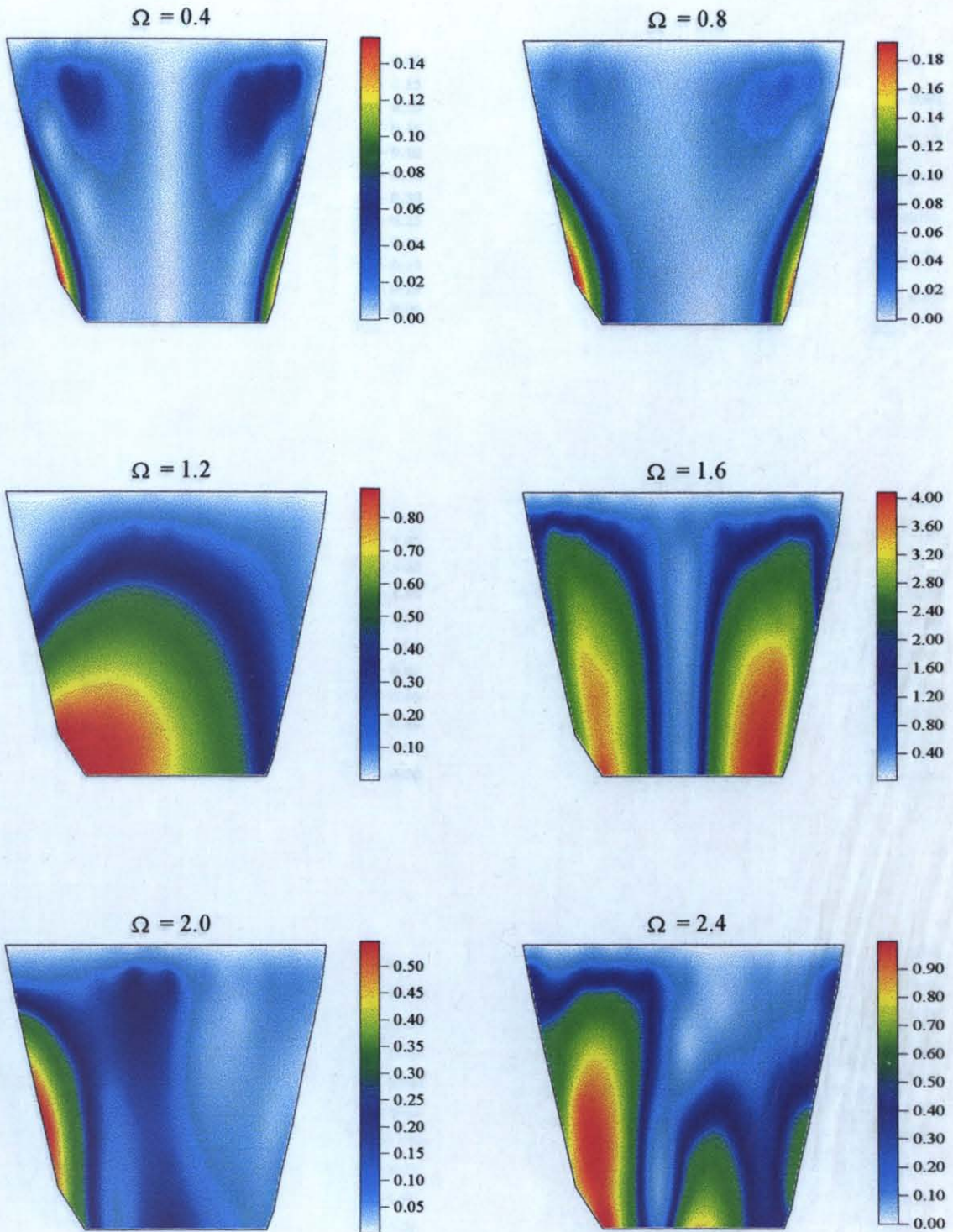


FIGURE 7.14. The hydrodynamic pressure distribution on the upstream face of Karakaya Dam : with dam-reservoir interaction, symmetrical reservoir, harmonic cross-stream ground motion, reservoir boundary reflection coefficient, $\alpha_r=0.75$.

($\Omega=0.4,0.8,1.2,1.6,2.0,2.4$ corresponds to $\omega= 0.93,1.86,2.78, 3.71,4.64,5.57$ cycles/sec)

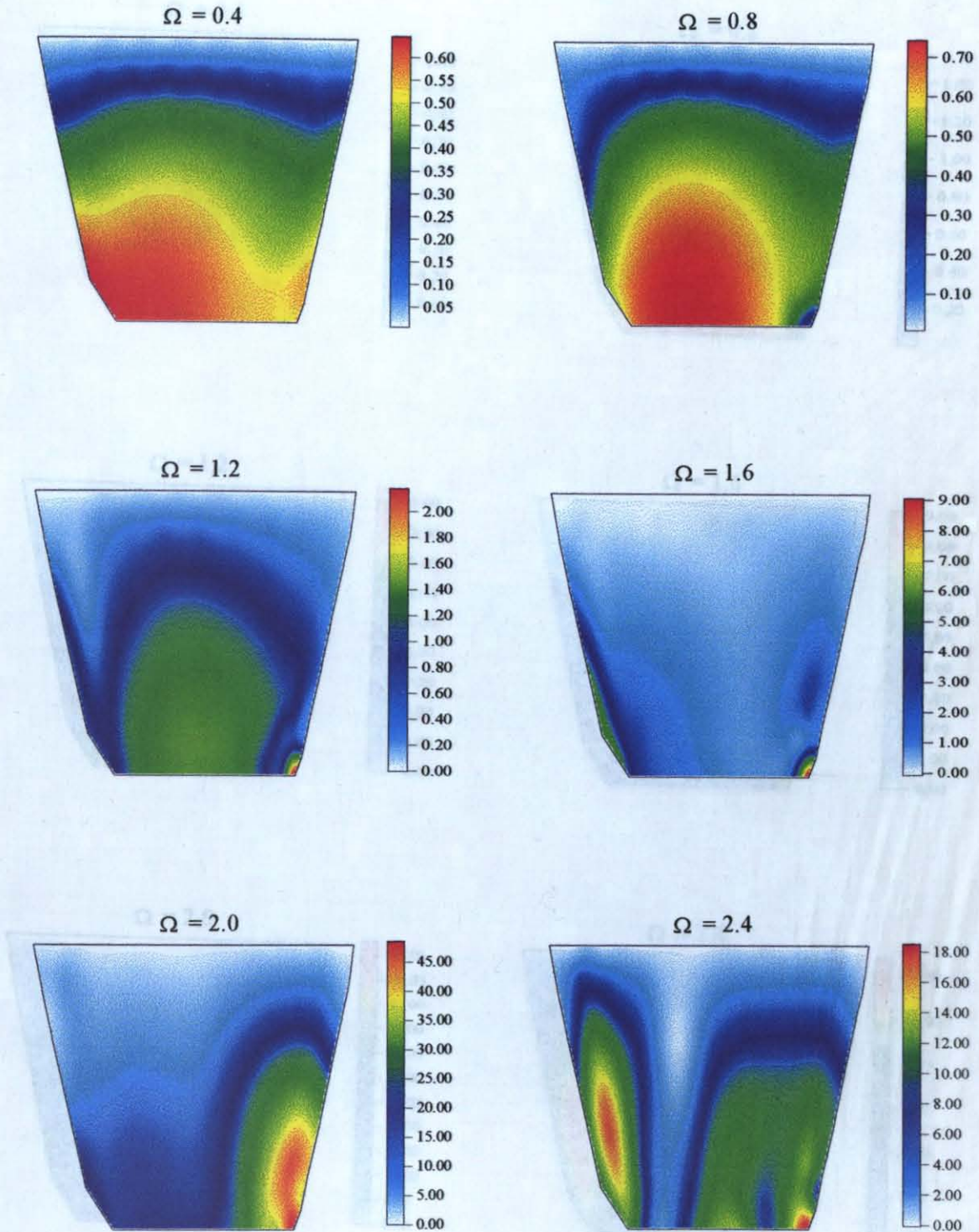


FIGURE 7.15. The hydrodynamic pressure distribution on the upstream face of Karakaya

Dam : with dam-reservoir interaction, actual geometry reservoir, harmonic upstream-downstream ground motion, reservoir boundary reflection coefficient, $\alpha_r=0.75$.

($\Omega=0.4,0.8,1.2,1.6,2.0,2.4$ corresponds to $\omega=0.93,1.86,2.78,3.71,4.64,5.57$ cycles/sec)

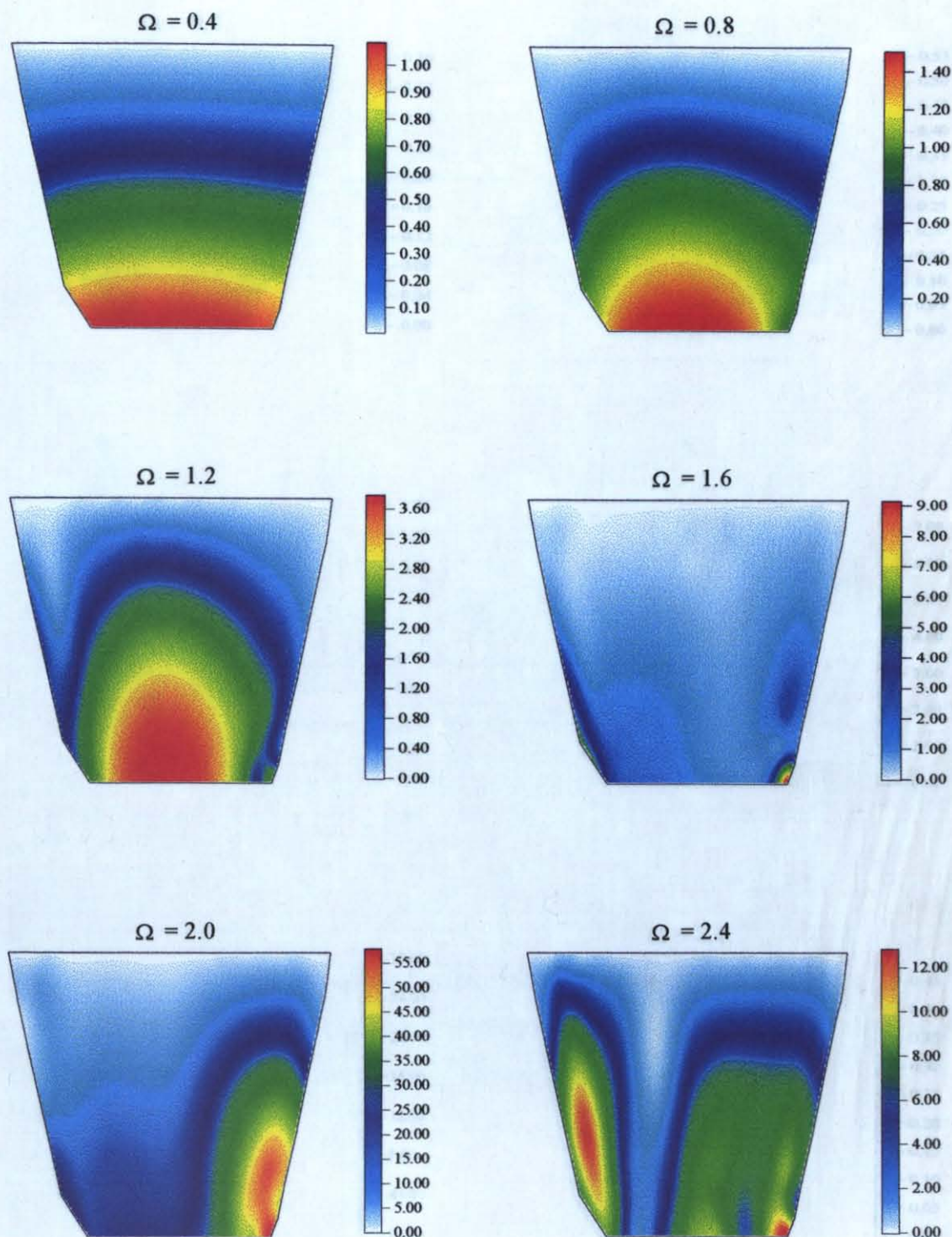


FIGURE 7.16. The hydrodynamic pressure distribution on the upstream face of Karakaya Dam : with dam-reservoir interaction, actual geometry reservoir, harmonic vertical ground motion, reservoir boundary reflection coefficient, $\alpha_r=0.75$.

($\Omega=0.4,0.8,1.2,1.6,2.0,2.4$ corresponds to $\omega=0.93,1.86,2.78,3.71,4.64,5.57$ cycles/sec)

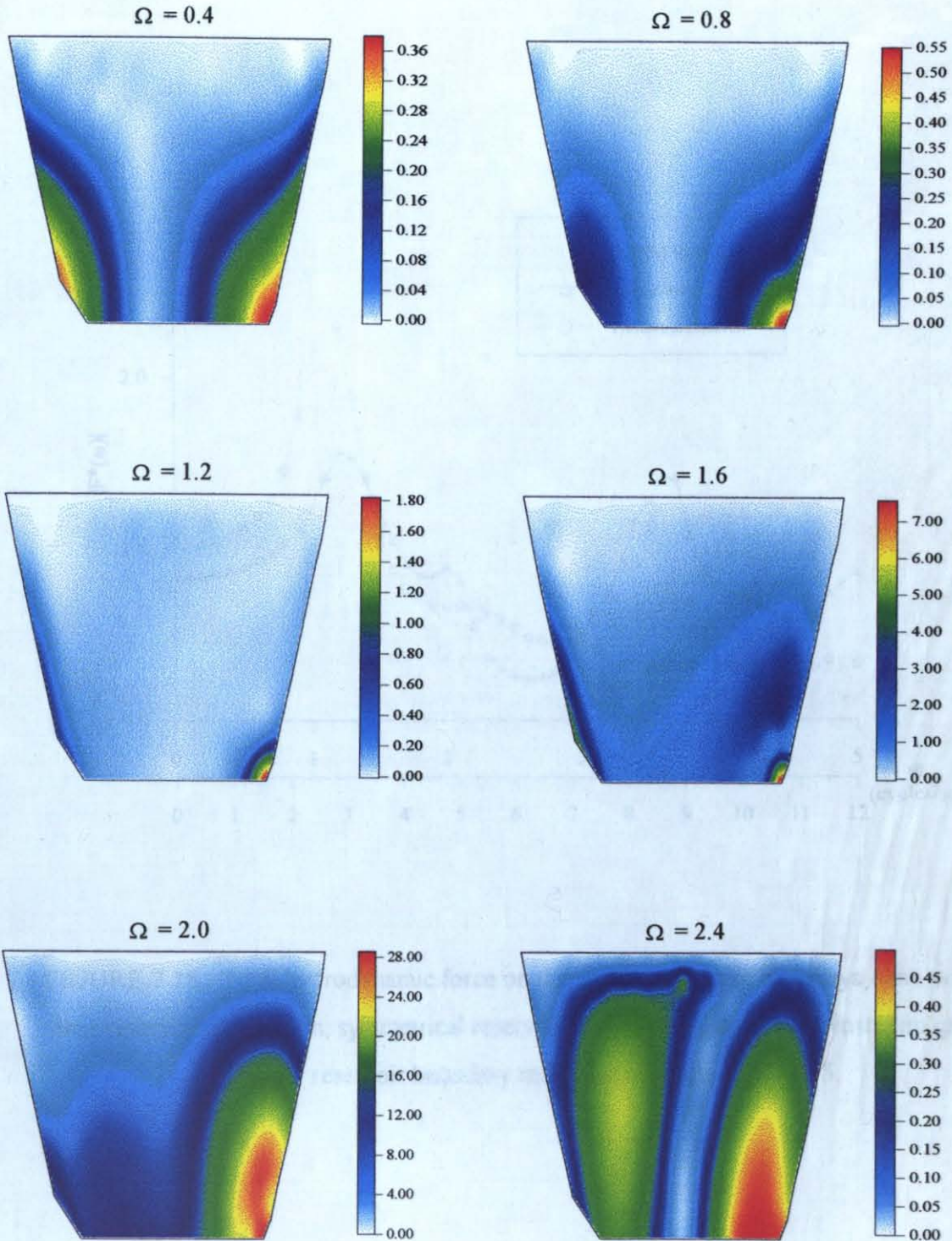


FIGURE 7.17. The hydrodynamic pressure distribution on the upstream face of Karakaya Dam : with dam-reservoir interaction, actual geometry reservoir, harmonic cross-stream ground motion, reservoir boundary reflection coefficient, $\alpha_r=0.75$.

($\Omega=0.4,0.8,1.2,1.6,2.0,2.4$ corresponds to $\omega=0.93,1.86,2.78,3.71,4.64,5.57$ cycles/sec)

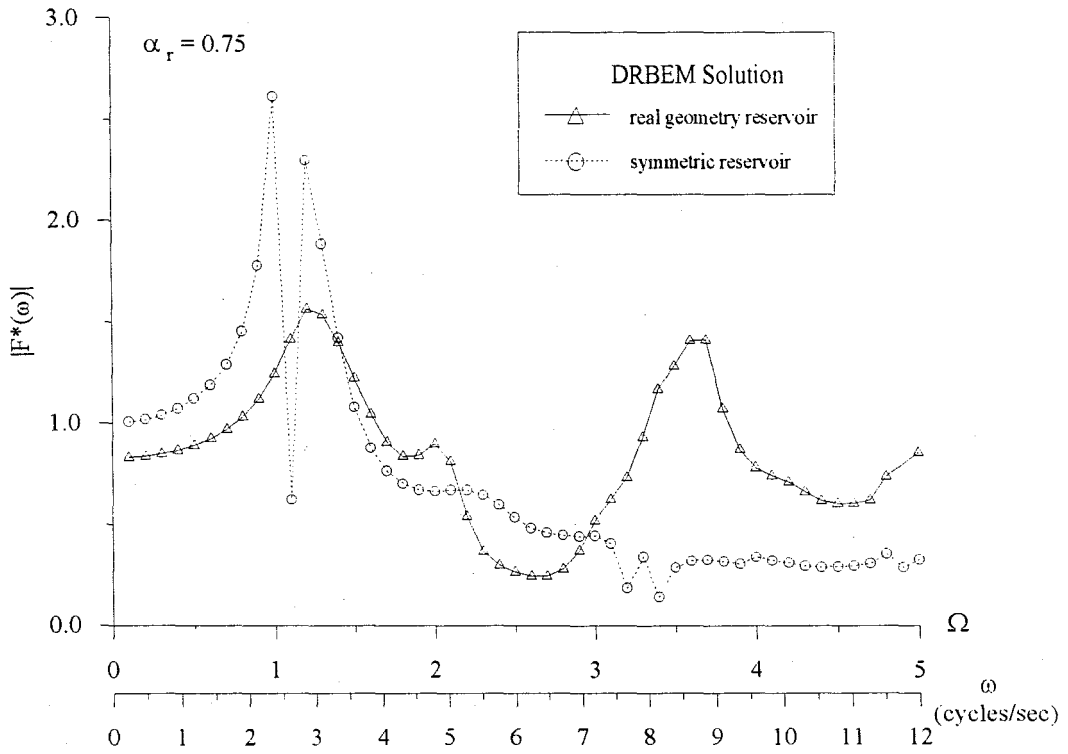


FIGURE 7.18. Total hydrodynamic force on the upstream face of Karakaya dam: without dam-reservoir interaction, symmetrical reservoir, harmonic upstream-downstream ground motion, reservoir boundary reflection coefficient, $\alpha_r=0.75$.

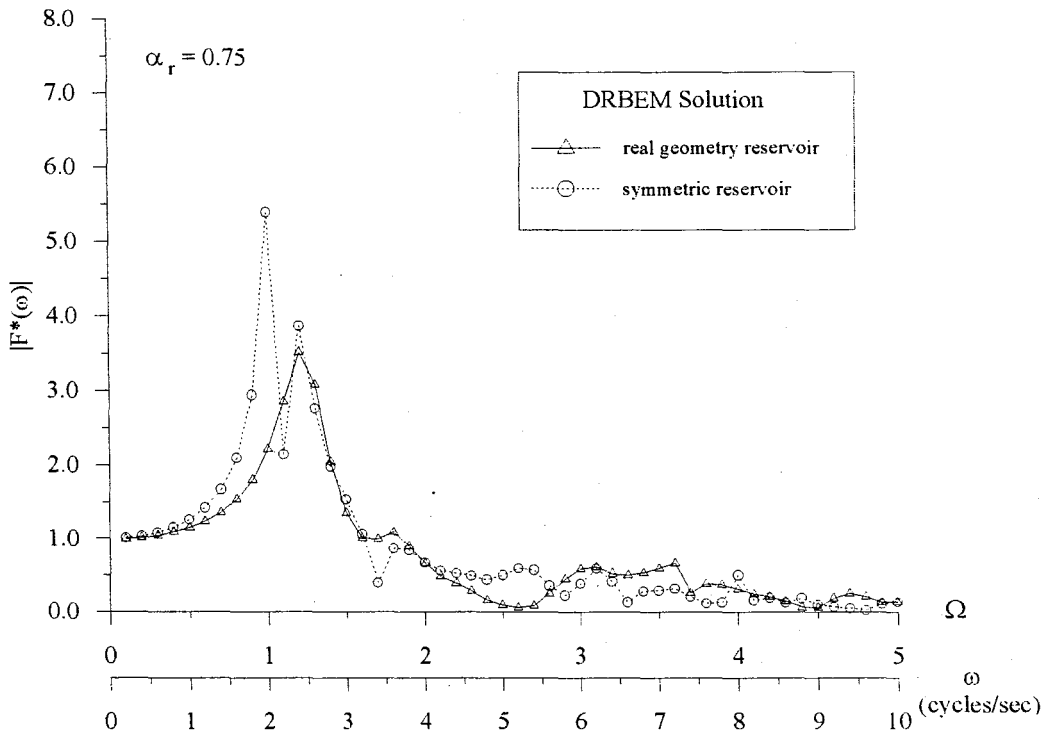


FIGURE 7.19. Total hydrodynamic force on the upstream face of Karakaya dam: without dam-reservoir interaction, symmetrical reservoir, harmonic vertical ground motion, reservoir boundary reflection coefficient, $\alpha_r=0.75$.

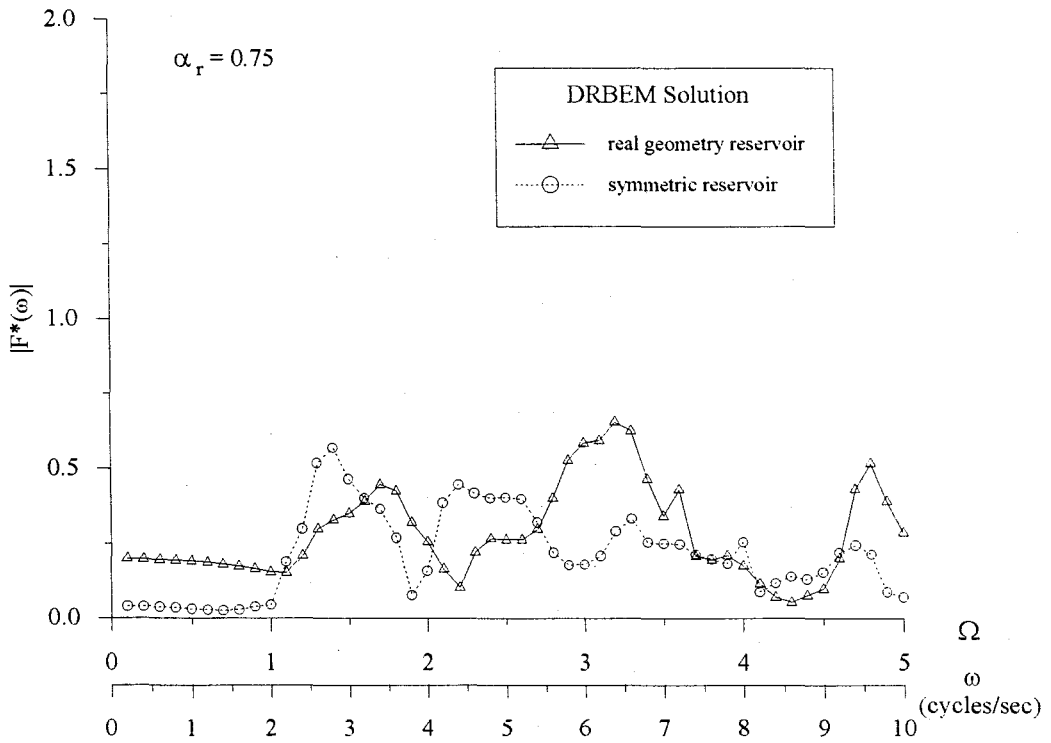


FIGURE 7.20. Total hydrodynamic force on the upstream face of Karakaya dam: without dam-reservoir interaction, symmetrical reservoir, harmonic cross-stream ground motion, reservoir boundary reflection coefficient, $\alpha_r=0.75$.

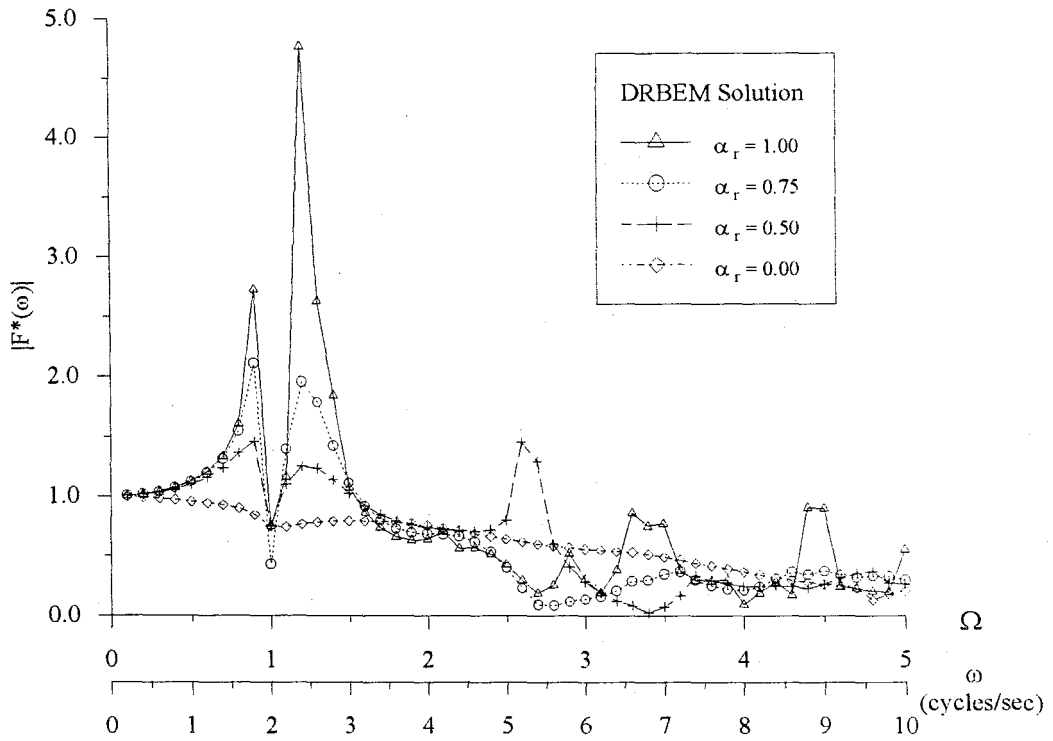


FIGURE 7.21. Total hydrodynamic force on the upstream face of Karakaya dam without dam-reservoir interaction for the symmetrical reservoir case due to harmonic the upstream-downstream ground motion.

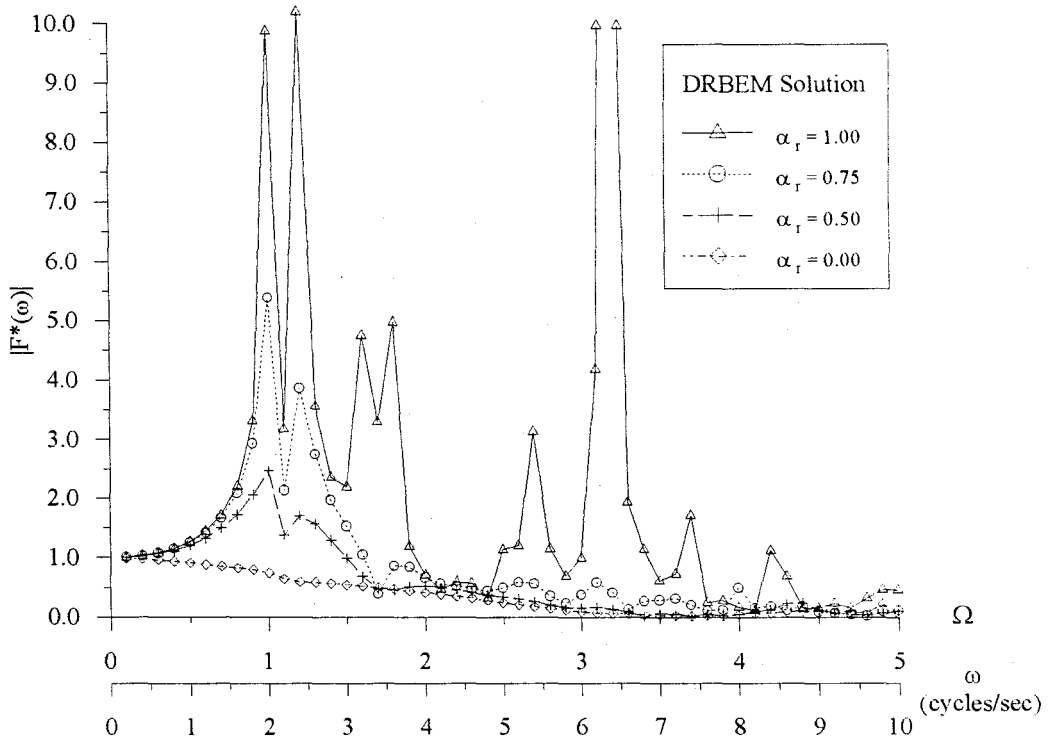


FIGURE 7.22. Total hydrodynamic force on the upstream face of Karakaya dam without dam-reservoir interaction for the symmetrical reservoir case due to harmonic vertical ground motion.

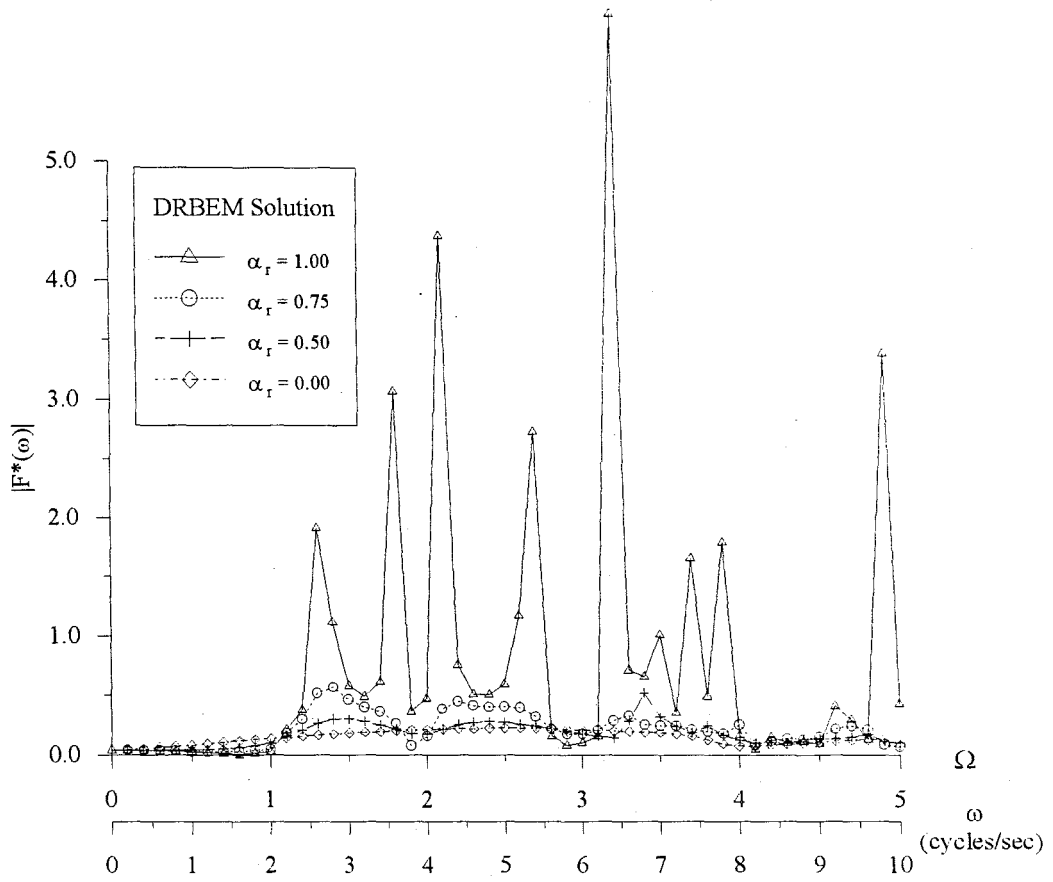


FIGURE 7.23. Total hydrodynamic force on the upstream face of Karakaya dam without dam-reservoir interaction for the symmetrical reservoir case due to harmonic cross-stream ground motion.

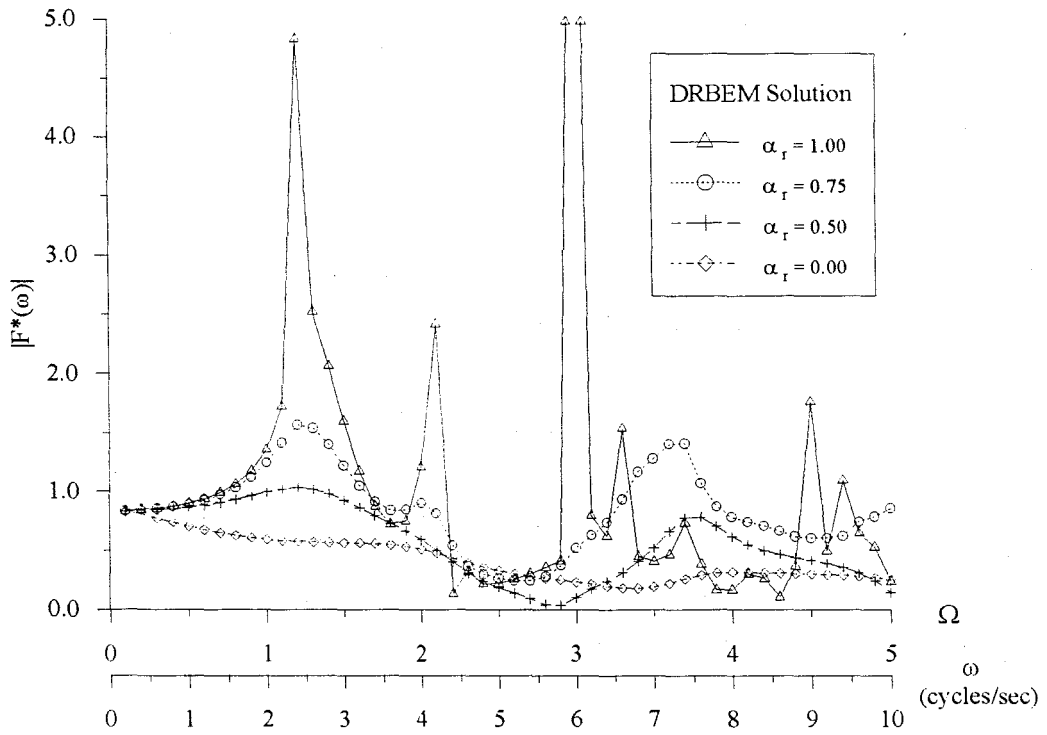


FIGURE 7.24. Total hydrodynamic force on the upstream face of Karakaya dam without dam-reservoir interaction for the actual geometry reservoir case due to harmonic the upstream-downstream ground motion.

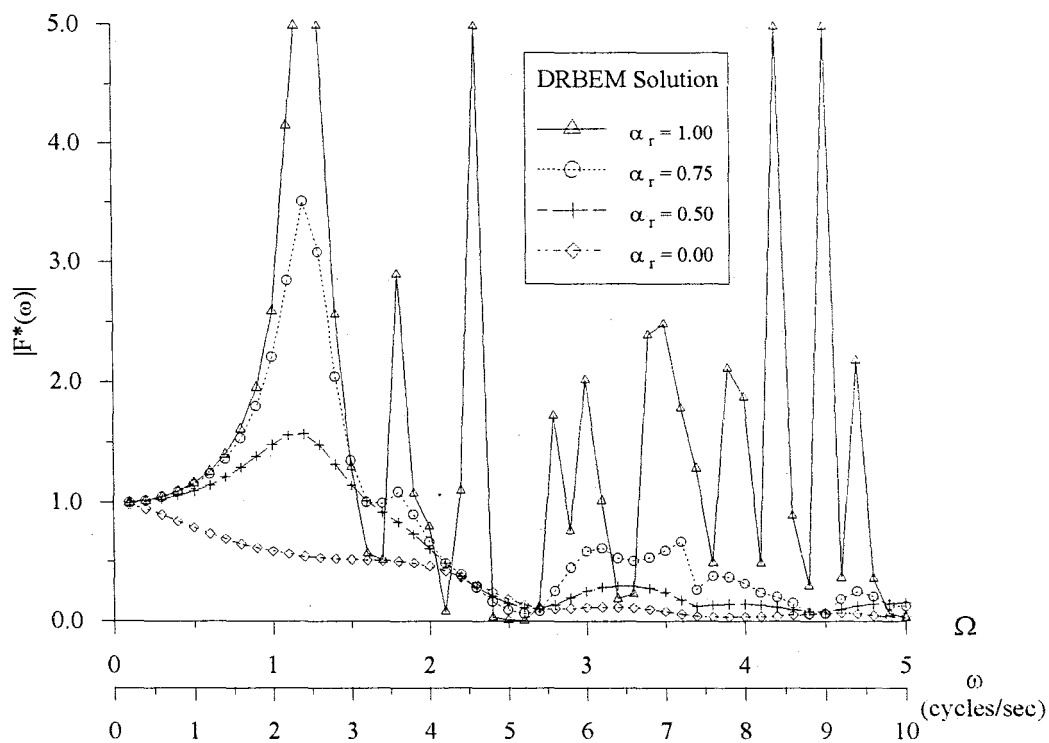


FIGURE 7.25. Total hydrodynamic force on the upstream face of Karakaya dam without dam-reservoir interaction for the actual geometry reservoir case due to harmonic vertical ground motion.

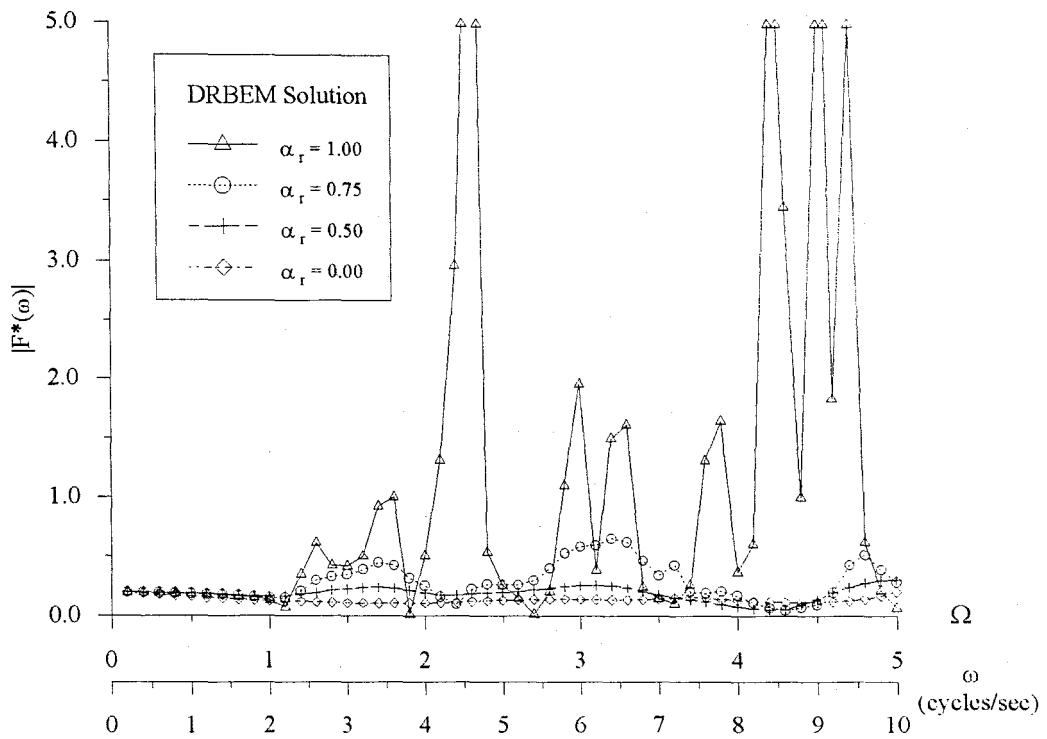


FIGURE 7.26. Total hydrodynamic force on the upstream face of Karakaya dam without dam-reservoir interaction for the actual geometry reservoir case due to harmonic cross-downstream ground motion.

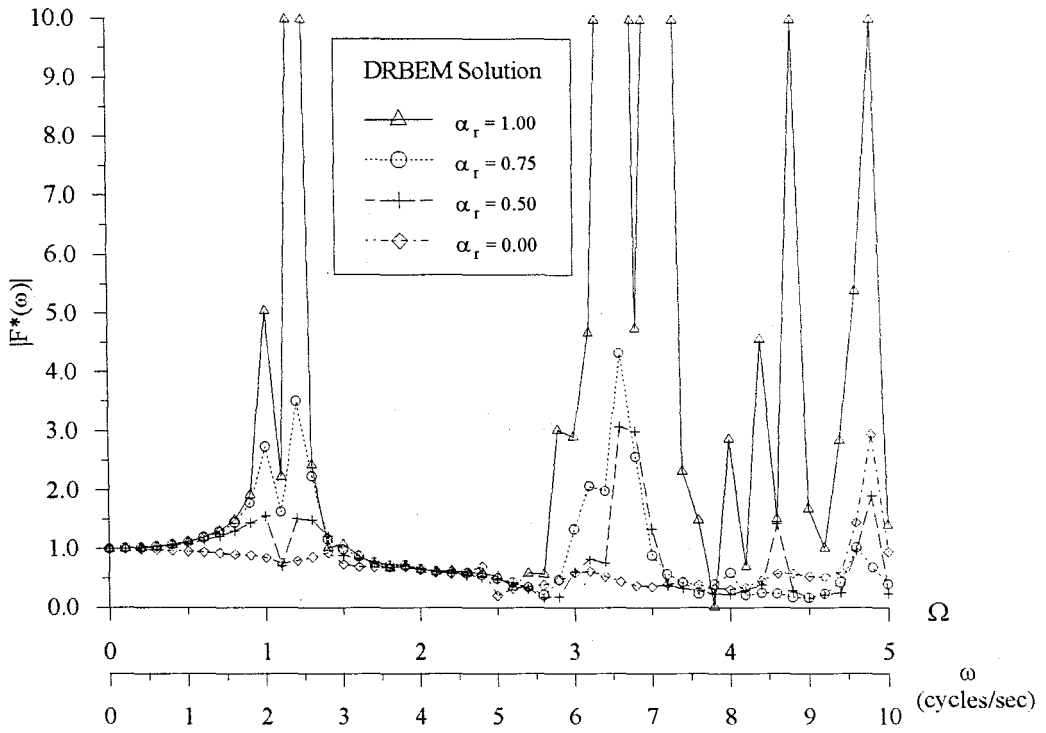


FIGURE 7.27 Total hydrodynamic force on the upstream face of Karakaya dam with dam-reservoir interaction for the symmetrical reservoir case due to harmonic the upstream-downstream ground motion.

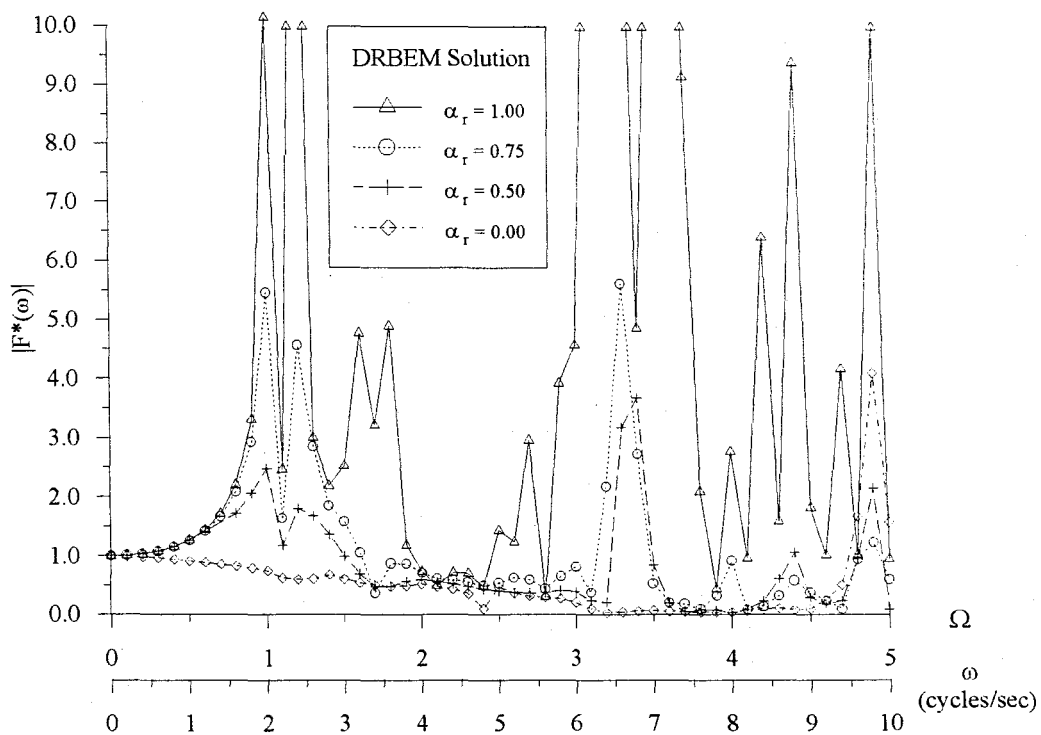


FIGURE 7.28 Total hydrodynamic force on the upstream face of Karakaya dam with dam-reservoir interaction for the symmetrical reservoir case due to harmonic vertical ground motion.

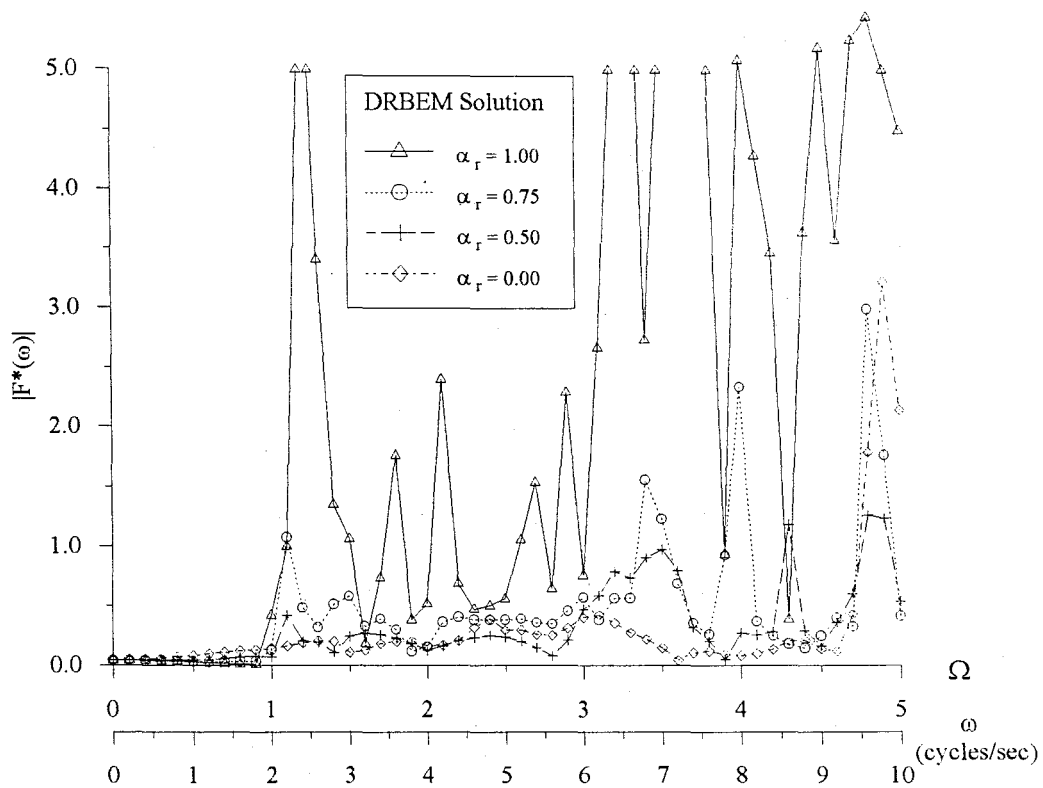


FIGURE 7.29 Total hydrodynamic force on the upstream face of Karakaya dam with dam-reservoir interaction for the symmetrical reservoir case due to harmonic cross-stream ground motion.

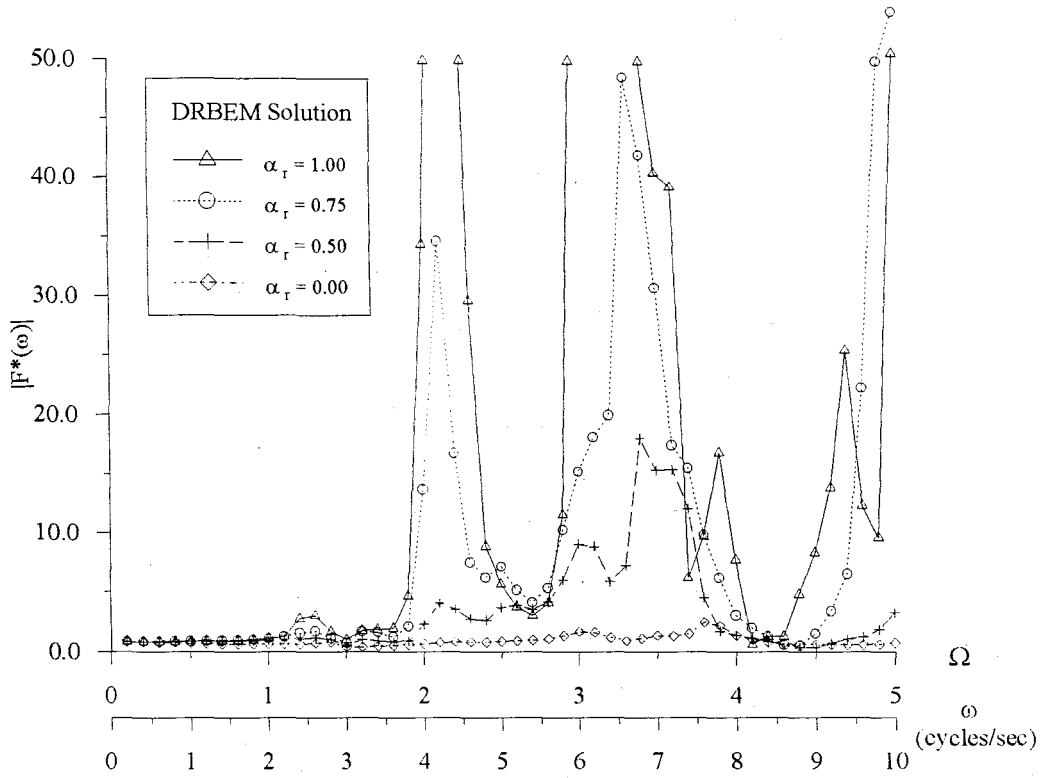


FIGURE 7.30 Total hydrodynamic force on the upstream face of Karakaya dam with dam-reservoir interaction for the actual geometry reservoir case due to harmonic the upstream-downstream ground motion.

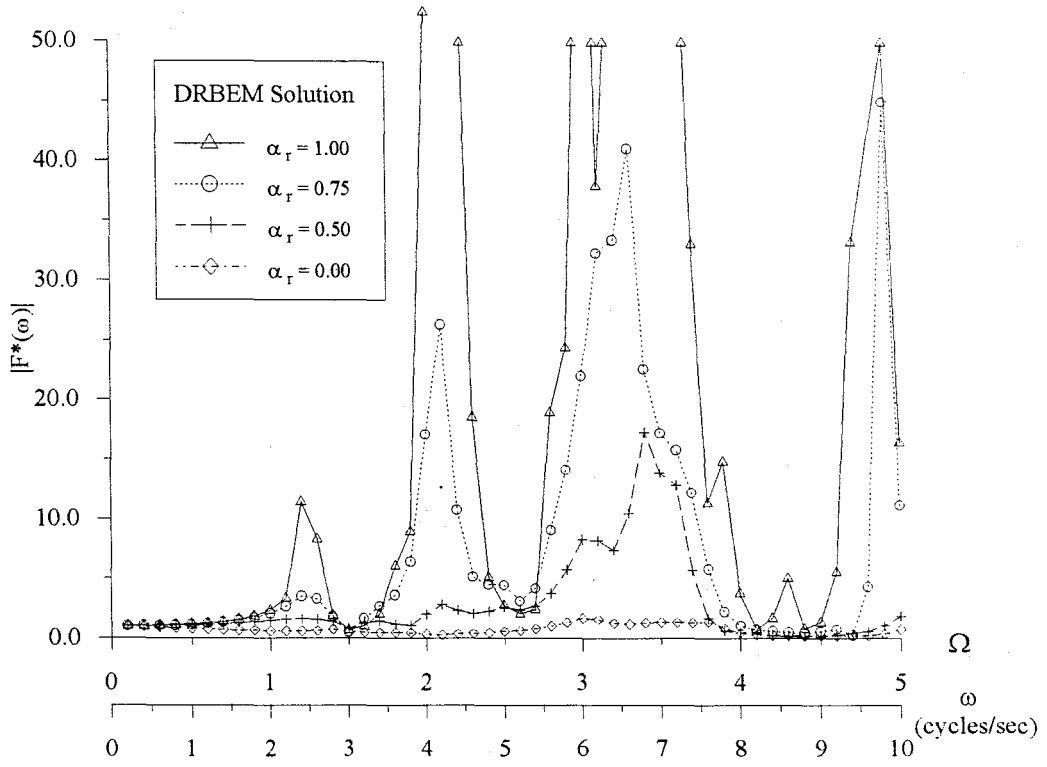


FIGURE 7.31 Total hydrodynamic force on the upstream face of Karakaya dam with dam-reservoir interaction for the actual geometry reservoir case due to harmonic vertical ground motion.

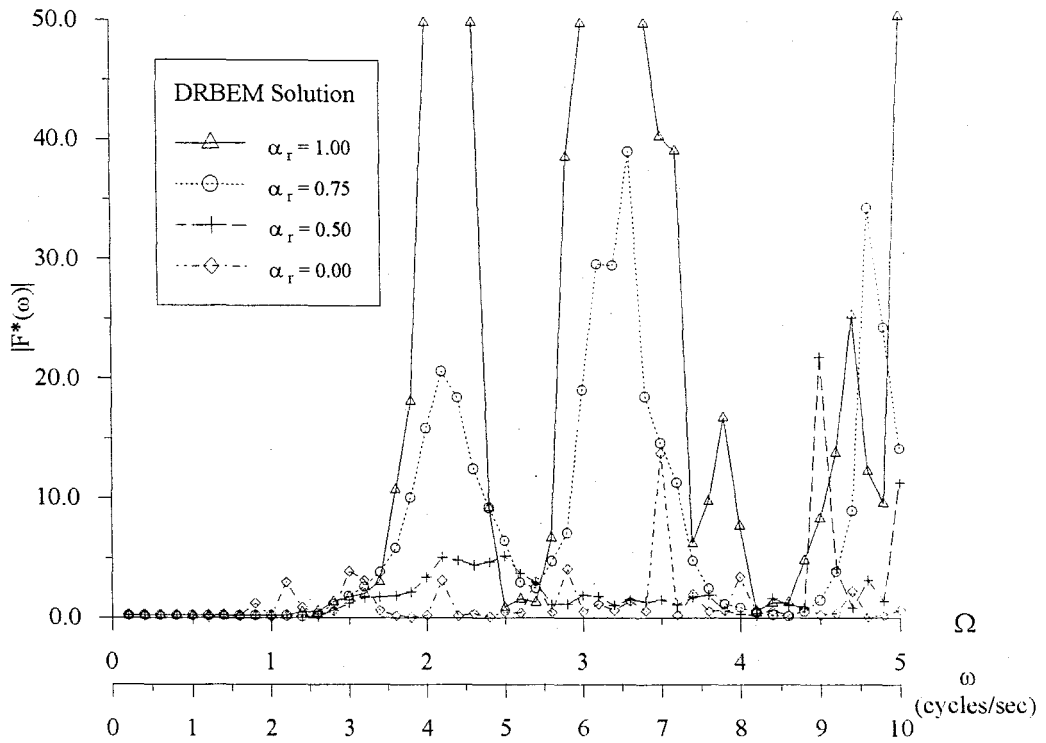


FIGURE 7.32 Total hydrodynamic force on the upstream face of Karakaya dam with dam-reservoir interaction for the actual geometry reservoir case due to harmonic cross-downstream ground motion.

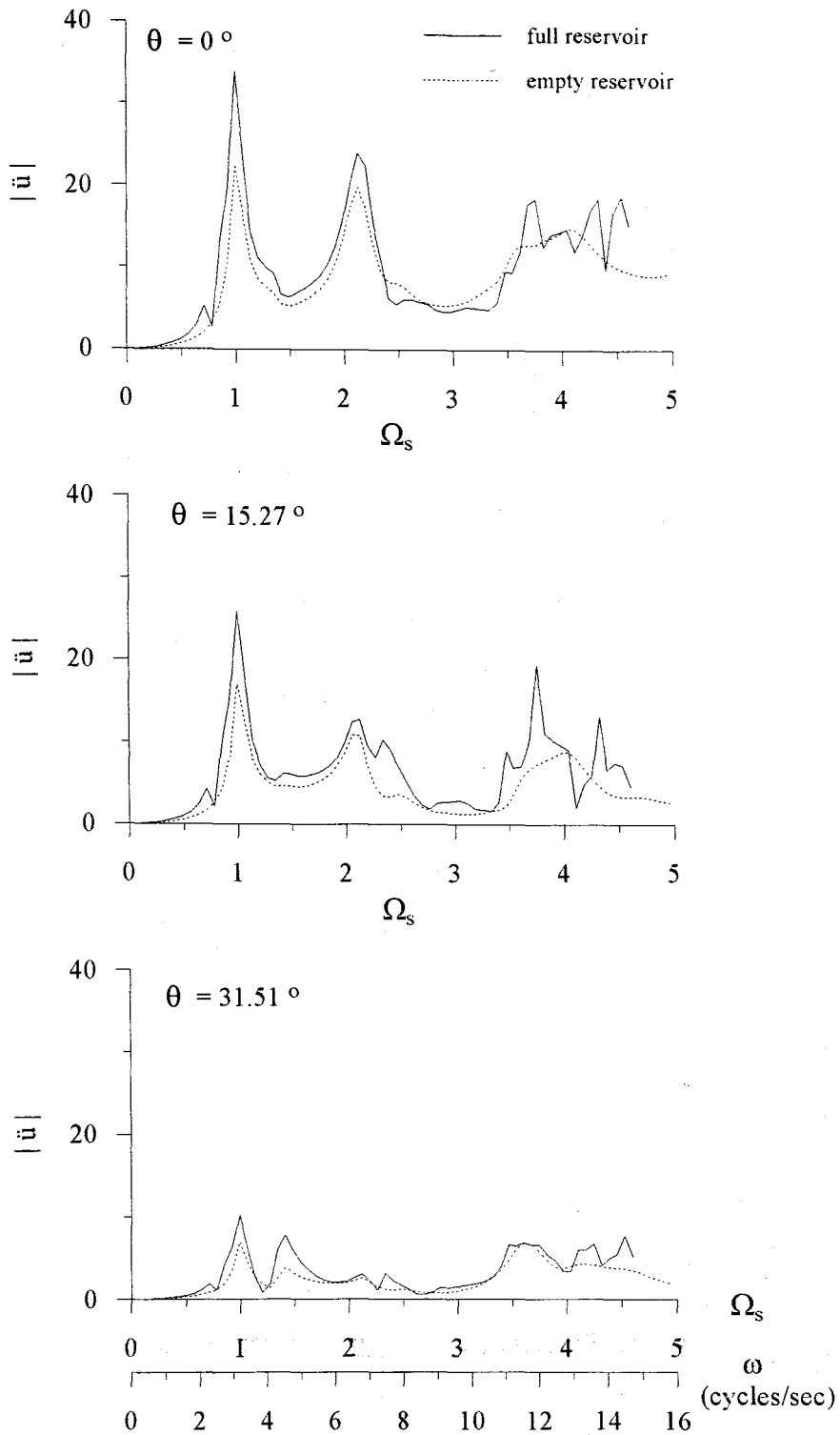


FIGURE 7.33 The radial acceleration response of the Karakaya Dam structure for the symmetrical reservoir case due to harmonic upstream-downstream ground motion with reservoir boundary reflection coefficient, $\alpha_r=0.75$.

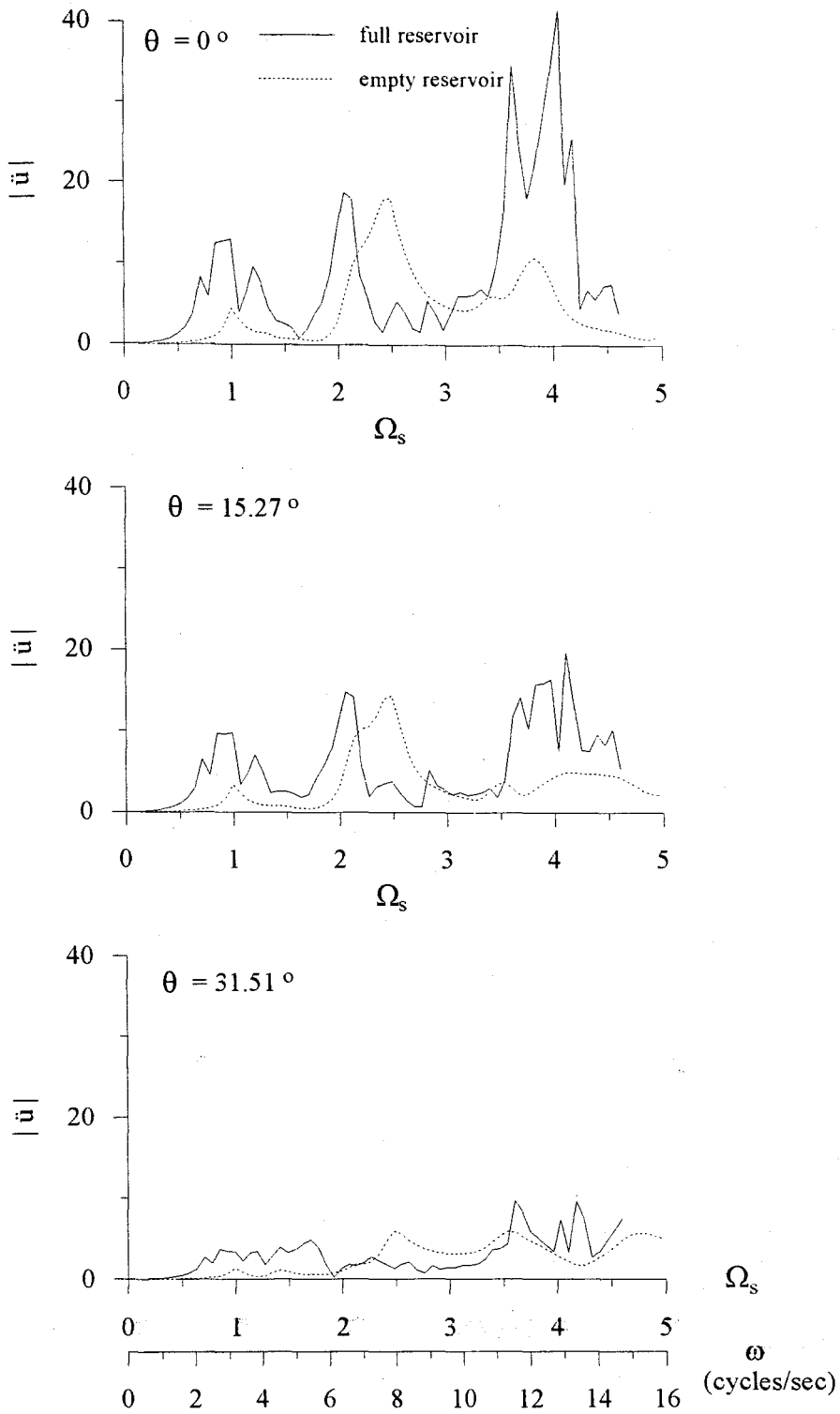


FIGURE 7.34 The radial acceleration response of the Karakaya Dam structure for the symmetrical reservoir case due to harmonic vertical ground motion with reservoir boundary reflection coefficient, $\alpha_r=0.75$

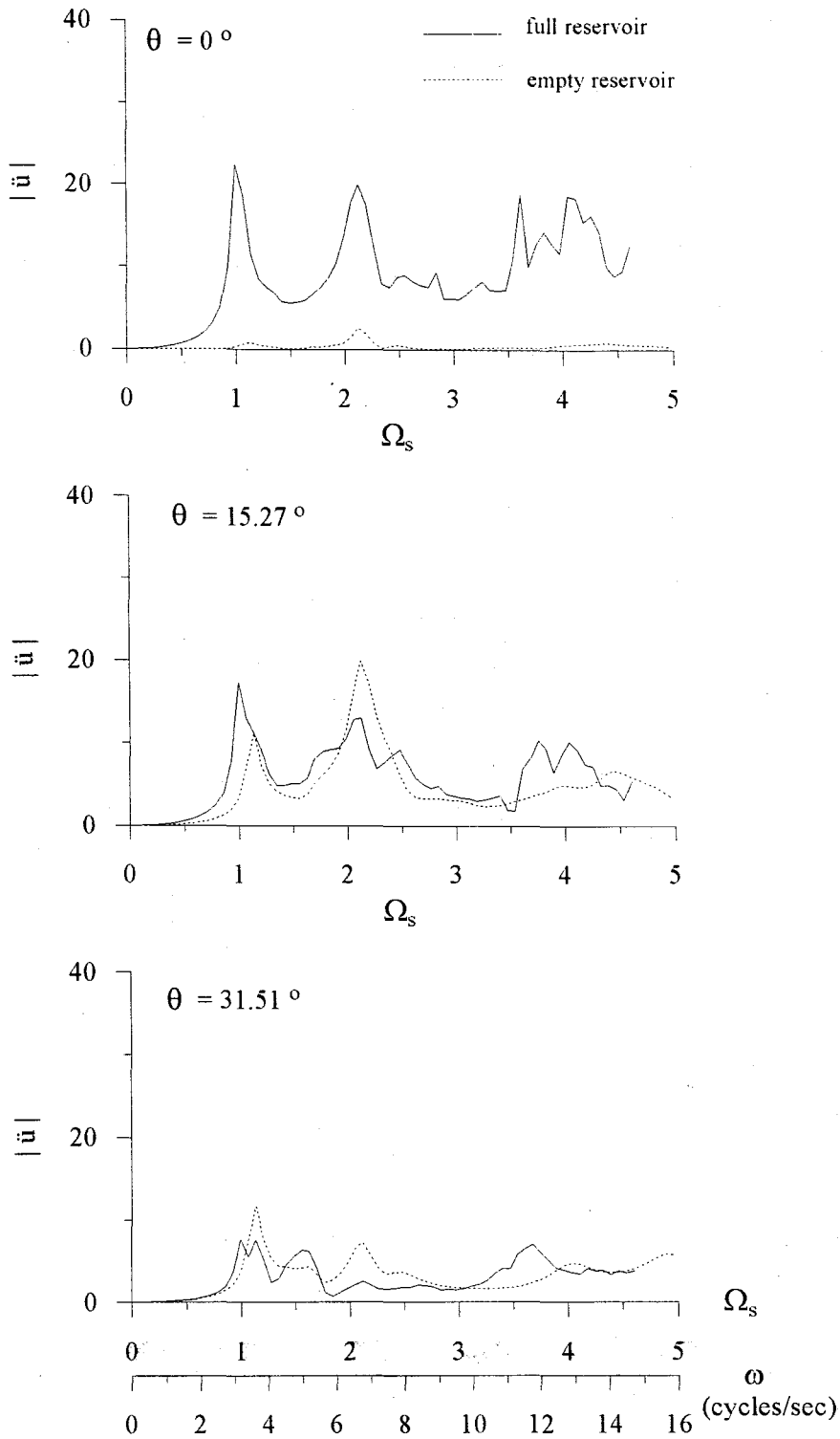


FIGURE 7.35 The radial acceleration response of the Karakaya Dam structure the symmetrical reservoir case due to harmonic cross-stream ground motion with reservoir boundary reflection coefficient, $\alpha_r=0.75$.

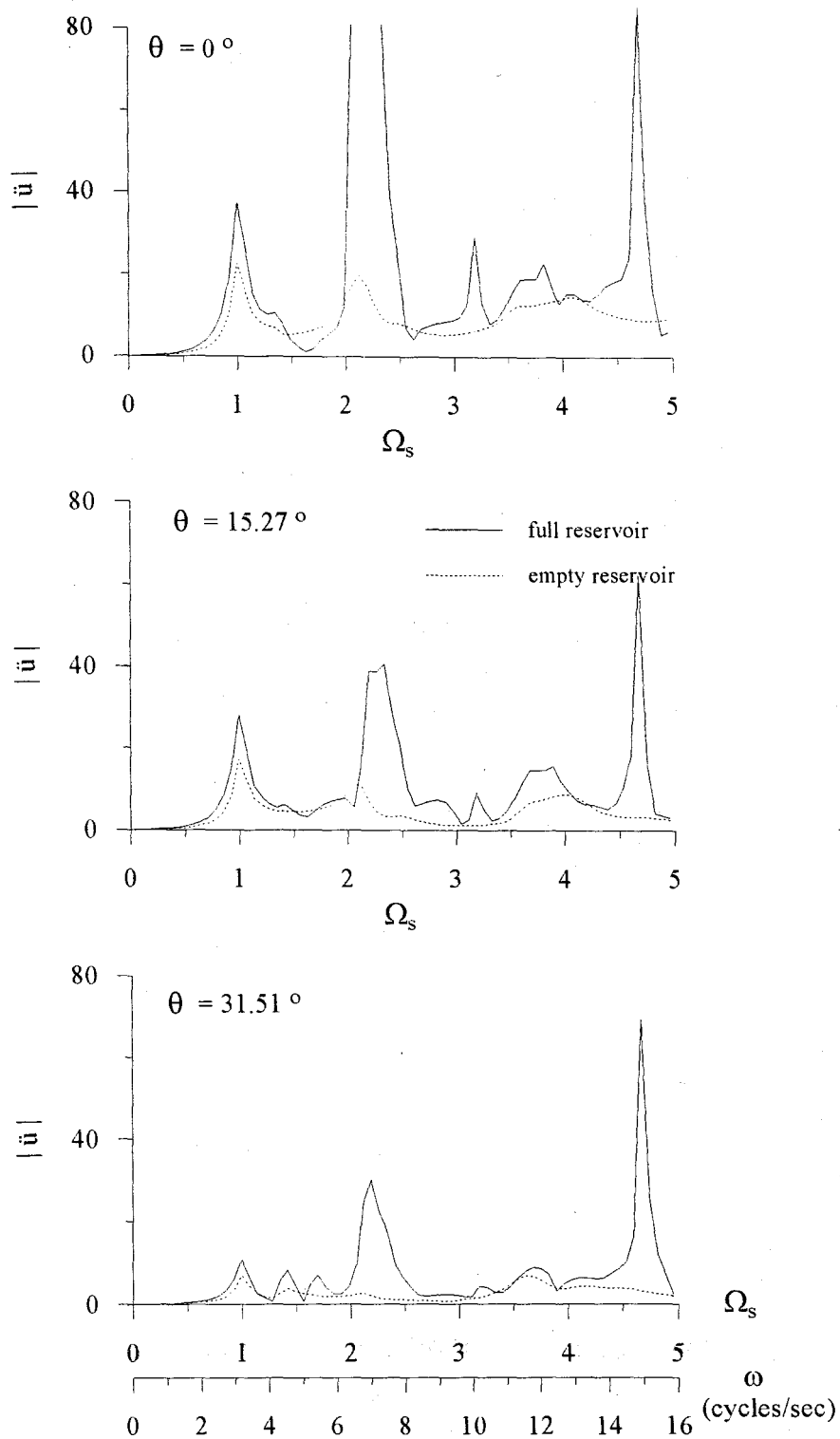


FIGURE 7.36 The radial acceleration response of the Karakaya Dam structure for the actual geometry case due to harmonic upstream-downstream ground motion with reservoir boundary reflection coefficient, $\alpha_r=0.75$

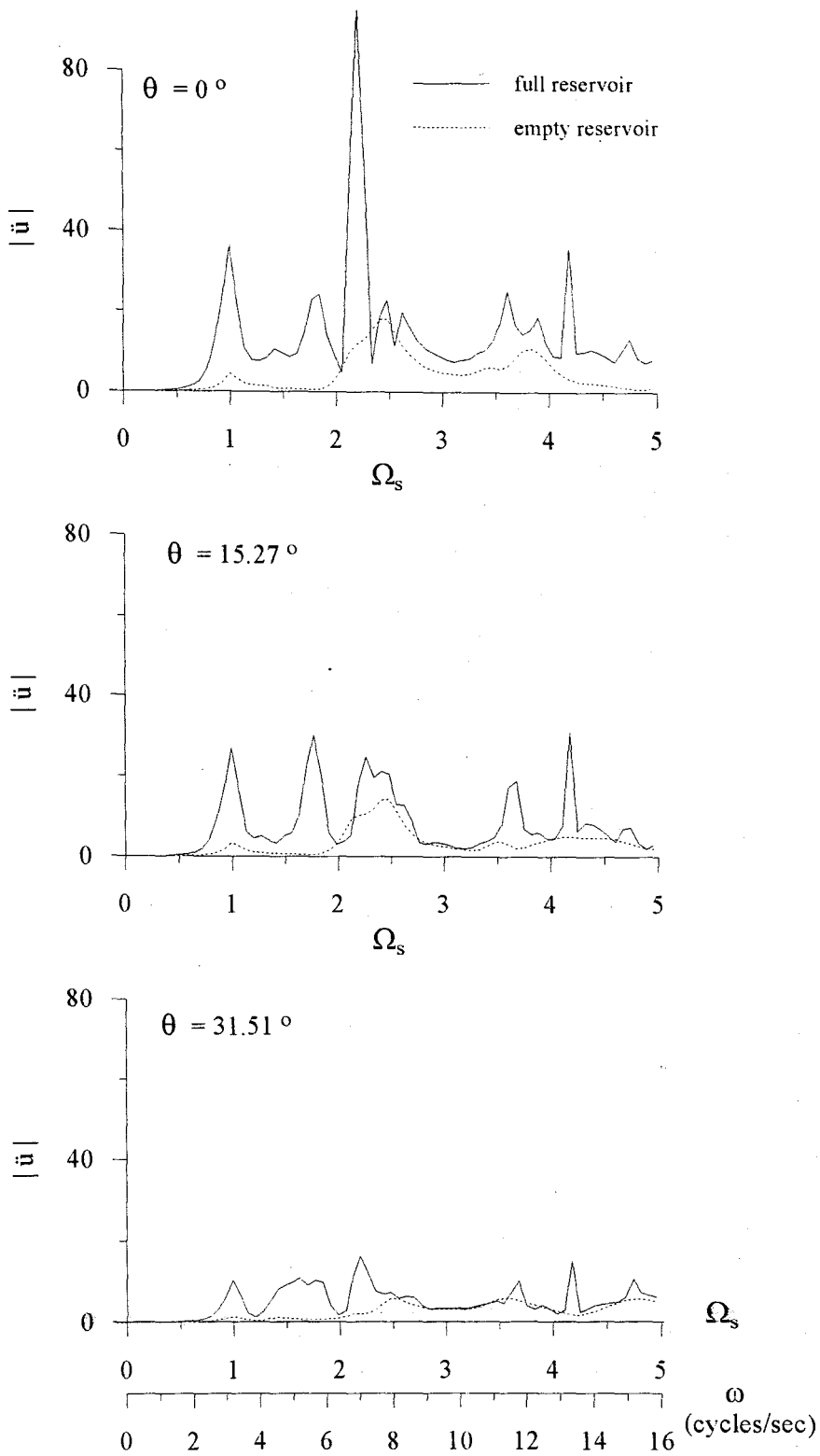


FIGURE 7.37 The radial acceleration response of the Karakaya Dam structure for the actual geometry case due to harmonic vertical ground motion with reservoir boundary reflection coefficient, $\alpha_r=0.75$

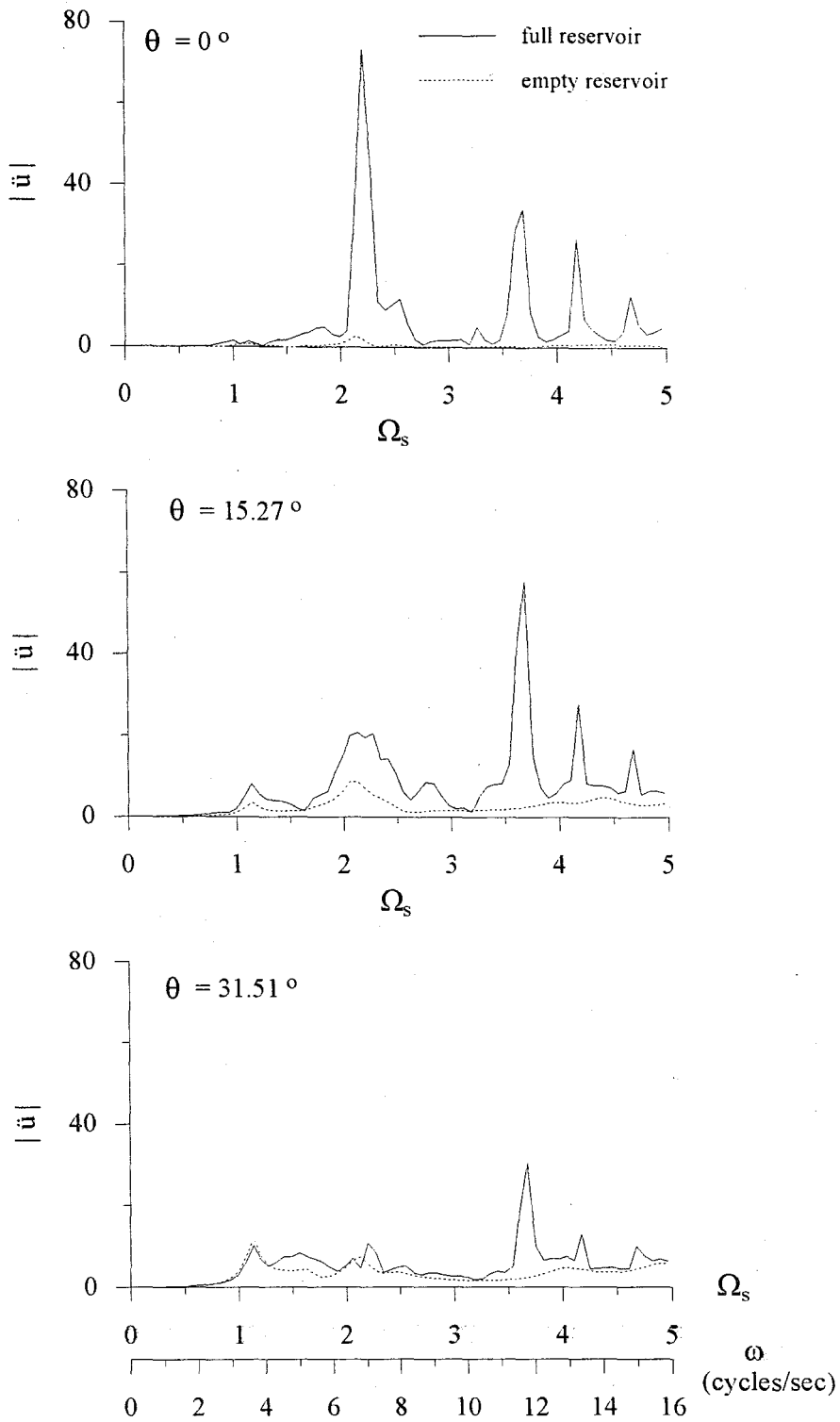


FIGURE 7.38 The radial acceleration response of the Karakaya Dam structure for the actual geometry reservoir case due to harmonic cross-stream ground motion with reservoir boundary reflection coefficient, $\alpha_r=0.75$

8. CONCLUSIONS

Three-dimensional dual reciprocity formulations have been developed to model the reservoir domain in order to study the earthquake response of arch dam-reservoir systems. The substructure technique in the frequency domain has been applied to treat the interaction of the arch dam-reservoir system. Assuming the foundation rock at the dam base and canyon banks to be infinitely rigid, the finite element method is utilized to the model dam structure. Considering the bottom absorption effects, the reservoir domain is idealized as a finite domain of irregular geometry adjacent to an infinite domain of uniform cross section. The three-dimensional dual reciprocity method is applied to model the finite domain of the reservoir. The uniform infinite domain is modeled by applying two-dimensional eigenvalue analysis based on the dual reciprocity formulations over the uniform cross section combined with a continuum expression in the upstream direction.

In the arch dam-reservoir system, the interaction problem is defined on the interface of the dam and the reservoir. By utilizing the dual reciprocity method, there is a considerable reduction in data preparation efforts as the method requires only the boundaries of the domain to be discretized. Dual reciprocity methods overcome the major difficulty encountered in applying the classical boundary elements formulation to the dynamic analysis by utilizing a frequency independent fundamental solution. The system matrices are no longer dependent on the excitation frequency. This results in a great reduction of the computational effort in determining the dynamic response of the arch dam-reservoir system.

The model was applied to investigate the hydrodynamic responses of a three-dimensional rectangular reservoir and the hydrodynamic and structural response of Karakaya dam-reservoir system. The effects of arch dam-reservoir interaction, the reservoir geometry and the reservoir boundary bottom absorption on the hydrodynamic and structural responses are studied.

8.1. Hydrodynamic Response in Three-dimensional Rectangular Reservoir

For upstream-downstream excitation and a fully reflecting reservoir boundary, the hydrodynamic pressures are entirely in-phase with the excitation for values of Ω less than unity. For Ω greater than unity, the pressure associated with the higher frequency modes propagates in the upstream direction of the infinite channel resulting in energy radiation to infinity and hence the out-of-phase pressure component appears over this frequency range. For absorbing reservoir boundaries both the in phase and the out of phase components exist over the entire frequency range due to the energy dissipation at the absorbing boundaries in addition to the radiation boundary.

For vertical and cross-stream ground excitations and a fully reflecting reservoir boundary case, the hydrodynamic pressures are entirely in-phase with the excitation over the entire frequency range. With the assumption of no variation of ground motion in the upstream direction, no energy will be radiated out of the system. For absorbing reservoir boundary cases, the absorption on the boundaries is the only energy dissipation mechanism. The boundary energy absorption causes the out-of-phase component of the hydrodynamic pressure to appear over the total frequency range.

The upstream and vertical ground motion excitations have symmetrical vibration modes and the hydrodynamic pressure does not vary across the width of the upstream face of the dam, while the cross-stream ground excitation has anti-symmetric modes and the hydrodynamic pressure distribution varies anti-symmetrically across the width of the dam.

For a fully reflecting reservoir boundary, the hydrodynamic force response functions are unbounded at the natural frequencies of the infinite uniform domain for all directions of ground motion excitation considered. When reservoir boundary absorption exists, the hydrodynamic force response functions are bounded for all excitation frequencies for all three components of ground motion due to the boundary energy dissipation.

8.2. Hydrodynamic Response on the Upstream Face of Karakaya Dam

The presence of geometrical variations of the reservoir shape affects the hydrodynamic pressure distributions on the upstream face of the dam. The hydrodynamic pressure distribution is no longer symmetrical and the maximum pressure regions are different from the symmetrical reservoir case. For the upstream-downstream ground motion excitation case, the geometrical variations reduce the hydrodynamic response for Ω less than unity, and increase the response in the range $\Omega > 3.0$.

For a fully reflecting reservoir boundary, the hydrodynamic force responses are unbounded at the natural frequencies of the reservoir for all the three components of the ground motion excitation. Additional bounded peaks appear in the high frequency range $\Omega > 2$. Introducing absorption damping into the system smoothens these peaks. For the symmetrical reservoir case, there are double peaks in the vicinity of the natural frequency of the infinite reservoir.

When reservoir boundary absorption is considered, the hydrodynamic forces are bounded for all excitation frequencies for all three components of the ground motion. The hydrodynamic pressure and force responses due to upstream ground motion are complex-valued for all excitation frequencies. With increasing excitation frequency, a larger number of modes are associated with the propagating pressure waves leading to increased energy radiation. For the symmetrical reservoir, the hydrodynamic force responses decrease with increasing excitation frequency for Ω greater than unity. For the actual geometry case, the radiation damping has less effect on the hydrodynamic force response due to the boundary reflection effects in the vicinity of the dam.

8.3. Dam-Water Interaction Effects

For the symmetrical reservoir case, the hydrodynamic responses resulting from the deformational motions of the arch dam act to reinforce the hydrodynamic responses resulting from the ground motion acceleration. In the cases of upstream and vertical ground motions, the symmetric properties of the pressure distribution are preserved because both pressure responses

have the same phase over the upstream face of the arch dam. In the cross-stream ground motion case, both of the pressure responses have different phases. The symmetry of the distribution no longer exists. This is especially more pronounced for $\Omega > 1$.

The dam-reservoir interaction has an amplifying effect on the hydrodynamic force responses especially when the normalized frequency is greater than unity. For Ω , greater than unity, the hydrodynamic force responses exhibit complex behavior and have additional peaks resulting from the interaction. As it can be seen from both the symmetrical and the actual geometry reservoir cases, the system is strongly coupled in the normalized frequency range, $\Omega=2$ to 4.

The actual geometry reservoir has more influence on the resonant amplitudes of acceleration responses of the dam, especially at the excitation frequencies in the neighborhood of the natural frequencies of the reservoir. The responses of the dam to the three components of the ground motion considering the interaction generally exceed those of the dam without water. In the normalized frequency range, $\Omega=2$ to 4, the coupled effects greatly increased the response of the radial acceleration especially for the vertical ground motion.

8.4. Recommendations for Further Research

Further studies could be made on the followings;

- A) Applying DRBEM to model the foundation effects.
- B) Investigation of the relation between the sediment layer properties in the reservoir and the reflection coefficient analytically and experimentally.
- C) Utilizing the model for a comprehensive parametric study for the arch dam-reservoir system for different material and geometrical properties.

APPENDIX A: THIN PLATE SPLINE APPROXIMATION FUNCTIONS IN DRBEM

Several proposals for the approximating function f_j may be found in the literature (Partridge, 1997). Recently, there have been successful implementations of thin plate spline approximation functions to find a particular solution for the Poisson equation (Karur and Ramachandran, 1995) and for elasticity problems (Bridges and Wrobel, 1996). The thin plate spline function is radial basis function and is given by

$$f(r) = r^2 \ln(r) \quad (\text{A.1})$$

The particular solution of Eq.(4-19) can be written in polar coordinates for two and three-dimensional cases, as

$$\nabla^2 \hat{p} = \frac{1}{r} \frac{\partial}{\partial r} \left(r \frac{\partial \hat{p}}{\partial r} \right) = f(r) \quad (2 - D) \quad (\text{A.2})$$

$$\nabla^2 \hat{p} = \frac{1}{r^2} \frac{\partial}{\partial r} \left(r^2 \frac{\partial \hat{p}}{\partial r} \right) = f(r) \quad (3 - D) \quad (\text{A.3})$$

The particular solution, $\hat{p}(r)$, can be obtained by integrating the above expression two times. The integration constants that result are taken to be zero since there is no obvious way of determining what they should be, and also because their inclusion makes the expression exceptionally complicated (Bridges and Wrobel, 1996). Thus, the particular solutions can be obtained as

$$\hat{p}(r) = r^4 \left(\frac{-1}{32} + \frac{\ln(r)}{16} \right) \quad (2 - D) \quad (\text{A.4})$$

$$\hat{p}(r) = r^4 \left(\frac{-9}{400} + \frac{\ln(r)}{20} \right) \quad (3 - D) \quad (\text{A.5})$$

The normal derivatives, $\hat{q}(r)$, can be derived from $\hat{p}(r)$ as

$$\hat{q}(r) = \frac{\partial \hat{p}(r)}{\partial n} = r^3 \left(\frac{-1}{16} + \frac{\ln(r)}{4} \right) \frac{\partial r}{\partial n} \quad (2 - D) \quad (A.6)$$

$$\hat{q}(r) = r^3 \left(\frac{-1}{25} + \frac{\ln(r)}{5} \right) \frac{\partial r}{\partial n} \quad (3 - D) \quad (A.7)$$

APPENDIX B: FINITE ELEMENT FORMULATION OF THE RADIATION MATRIX

The infinite domain of the reservoir is assumed to have a uniform cross section with absorptive bottom and sides. Based on the formulation of Hall and Chopra (1980), the separation of variables technique is applied to combine a two-dimensional finite element discretization over the uniform cross section of the domain with a continuum expression in the upstream direction. The problem ultimately reduces to the solution of a standard eigenvalue problem.

The governing equation and the boundary conditions for the hydrodynamic pressure response in the infinite domain of the reservoir are given in Eqs.(5.2-5.5). Following the procedure given in Chapter(5), the separation of variables technique yields two boundary value problems for the hydrodynamic pressure response. One for the upstream direction, x , and the other for the uniform cross section y - z plane. These are given in Eq.(5.8) and Eq.(5.9), respectively. The solution in the upstream direction is given as a continuum expression in Eq.(5.10).

The hydrodynamic pressure response distribution over the y - z plane is governed by the two-dimensional Helmholtz equation of Eq.(5.9) and satisfies the free surface and the bottom absorption boundary conditions expressed by Eqs.(5.2) and (5.3), respectively. A finite element discretization using a two-dimensional mesh (Fig. B.1) leads to the following matrix equation

$$\left(\mathbf{H}^f + i\omega\gamma\mathbf{B}^f - \lambda^2\mathbf{G}^f \right) \mathbf{p}_{xy} = -\frac{W}{g} \mathbf{d}^f \quad (\text{B.1})$$

where, \mathbf{p}_{xy} is the vector of pressure values at nodes below the free surface. In the above expression, \mathbf{H}^f , \mathbf{B}^f and \mathbf{G}^f are symmetrical matrices analogous to the stiffness, damping and mass matrices arising in the dynamics of solid continua. \mathbf{d}^f , is the vector of nodal accelerations computed from the normal acceleration along the boundary.

For the cases, where boundary motions of the reservoir domain are defined by upstream-downstream excitation or the deformational motions of the arch dam, the right hand vector \mathbf{d}^f of Eq.(B.1) vanishes as described in Section 5.4., and the equation simplifies to the

form

$$\left[\mathbf{H}^f + i\omega\gamma\mathbf{B}^f \right] \{ \mathbf{p}_{yz} \} = -\lambda^2 \mathbf{G}^f \{ \mathbf{p}_{yz} \} \quad (\text{B.2})$$

which represents a generalized eigenvalue problem. For an absorptive reservoir boundary, the eigenvalues, λ_m , and the eigenvectors, Ψ_m , obtained from the solution of Eq.(B.2) are complex valued and depend on the excitation frequency. For the non-absorptive reservoir boundary, where $\gamma = 0$, the eigenvalues and eigenvectors are real valued and frequency independent. The eigenvectors, Ψ_m , are orthogonal and normalized so that

$$\Psi^T \left[\mathbf{G}^f \right] \Psi = \mathbf{I} \quad (\text{B.3})$$

and they satisfy the equation

$$\Psi^T \left[\mathbf{H}^f + i\omega\gamma\mathbf{B}^f \right] \Psi = \Lambda \quad (\text{B.4})$$

where, Λ is a diagonal matrix of N eigenvalues $\lambda_1^2, \lambda_2^2, \dots, \lambda_N^2$ and Ψ is the matrix of N eigenvectors, $[\Psi_1, \Psi_2, \dots, \Psi_N]$.

The hydrodynamic pressure response over the cross section of the infinite domain can be expressed approximately as a linear combination of the N eigenvectors. That is,

$$\mathbf{p}_{yz} = \sum_{m=1}^N \eta_m \Psi_m \quad (\text{B.5})$$

where, η_m , are unknown coefficients.

Substituting, Eqs.(5.10) and (B.5) into Eq.(5.6), the hydrodynamic pressure response vector in the infinite domain can be written as

$$\mathbf{p} = \sum_{m=1}^N \eta_m \Psi_m e^{-\kappa_m x} \quad (\text{B.6})$$

Differentiating the hydrodynamic pressure response with respect to the outward normal to the cross section plane (y - z), noting that the normal is parallel to upstream direction, x ,

results in

$$\mathbf{q} = - \sum_{m=1}^N \kappa_m \eta_m \Psi_m e^{-\kappa_m x} \quad (\text{B.7})$$

Eqs.(B.6) and (B.7) can be rewritten in matrix form as

$$\mathbf{p} = \Psi \mathbf{E} \boldsymbol{\eta} \quad (\text{B.8})$$

$$\mathbf{q} = -\Psi \mathbf{K} \mathbf{E} \boldsymbol{\eta} \quad (\text{B.9})$$

In Eqs.(B.8) and (B.9), $\boldsymbol{\eta}$, is the vector of unknown coefficients, \mathbf{K} is a diagonal matrix with elements, $\kappa_1, \kappa_2, \dots, \kappa_N$ and \mathbf{E} is another diagonal matrix with elements $e^{-\kappa_m x}$.

The results of Eqs.(B.8) and (B.9) will be applied to specify the scattering boundary condition along the interface of the finite and infinite regions. Since the dual reciprocity method is applied to model the finite domain of the reservoir, a relation between the pressure and the pressure gradient vectors along the boundary may be introduced into the formulations.

By eliminating $\mathbf{E} \boldsymbol{\eta}$ between Eqs.(B.8) and (B.9), the relation between \mathbf{p} and \mathbf{q} can be obtained as

$$\mathbf{q} = \mathbf{R} \mathbf{p} \quad (\text{B.10})$$

where,

$$\mathbf{R} = \Psi \mathbf{K} \Psi^{-1} \quad (\text{B.11})$$

The radiation matrix, \mathbf{R} , relates the pressure response vector, \mathbf{p} , and its normal derivative, \mathbf{q} , for those nodes below the free surface on the radiation boundary between the finite and the infinite domains of the reservoir. For the absorbing bottom boundary of the reservoir, \mathbf{R} is dependent on the excitation frequency, ω .

APPENDIX C: DAM3D COMPUTER PROGRAM

The Fortran90 computer program DAM3D was developed for the purpose of investigating the effects of fluid-structure interaction on the hydrodynamic pressure in the reservoir and on the dynamic structural behavior of arch dams. The DAM3D program was developed using Microsoft Fortran Power Station 4.0 and the IMSL Library. The program was compiled and executed using a Pentium Pro/200 system running under Win95. The storage requirements were significantly reduced using the dynamic memory allocation feature supported by Fortran90. The program consists of a main program, seven modules and twenty-two external subroutines. The block diagram of the program is illustrated in Fig.(C.1).

The program is based on the analysis procedures developed in Chapters (2-5). The program calculates the seismic modal response of the arch dam-reservoir system to any of the three components, upstream-downstream, cross-stream and vertical, of the harmonic ground motion. There are no geometrical restrictions for the system, except that the infinite domain of the reservoir be of constant cross section. The arch dam is modeled using finite elements and can be discretized using two type of elements: three-dimensional isoparametric eight node elements and three-dimensional sixteen node thick shell elements. The free vibration eigenvalue analysis is accomplished using the IMSL routine GVCSP. The finite domain of the reservoir is modeled using the dual reciprocity method and can be discretized using three-dimensional isoparametric quadrilateral elements with either four or eight nodes. There are two alternatives in modeling the infinite domain of the reservoir: Either the dual reciprocity method or the finite element method. For dual reciprocity modeling, either two-dimensional two-node linear elements, or 3-node quadratic elements with internal nodes placed within the interface may be used. For the finite element model two-dimensional four node or eight node quadrilateral elements may be used. The resulting eigenvalue problem is solved using the IMSL routine GVCSP.

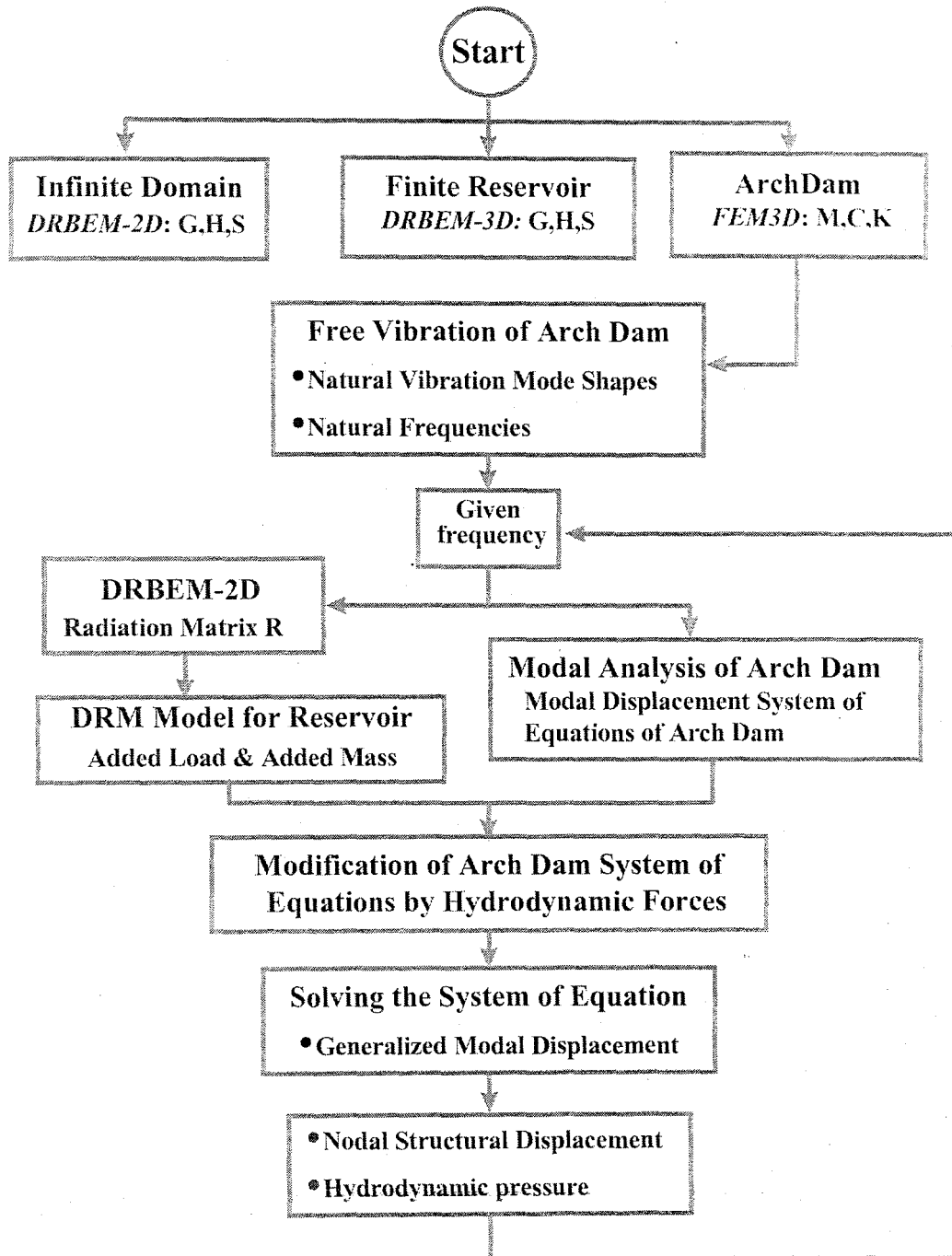


FIGURE C.1. Flowchart of DAM3D computer program

REFERENCES

- Ahmad, S. and P. K. Banerjee, "A New Method for Vibration Analysis by Bem Using Particular Integrals," *Journal of Engineering Mechanics*, ASCE, Vol 113, pp. 682-695, 1986.
- Ali, A., C. Rajakumar and S. M. Yunus, "On the Formulation for Acoustic Boundary Element Eigenvalue Problems," *International Journal for Numerical Methods in Engineering*, Vol. 31, pp. 1271-1282, 1991.
- Banerjee, P. K., S. Ahmad and H. C. Wang, "A New BEM Formulation for the Acoustic Eigenfrequency Analysis," *International Journal for Numerical Methods in Engineering*, Vol. 26, pp. 1299-1309, 1988.
- Banerjee, P. K., *The Boundary Element Methods In Engineering*, McGraw-Hill International (UK) Limited, London, 1994.
- Bathe, K.-J, E.L. Wilson and F.E. Peterson, SAPIV Structure Analysis Program for Static and Dynamic Response of Linear Systems, Earthquake Engineering Research Center, Report No. UCB/EERC-73/11, U.C., Berkeley, California, 1973.
- Beskos, D. E., "Boundary Element Methods in Dynamic Analysis: Part II (1986-1996)," *Applied Mechanics Revision*, ASME, Vol. 50, No. 3, pp. 149-197, 1997.
- Brebbia, C. A., J. C. F. Telles, and L.C. Wrobel, *Boundary Element Techniques: Theory and Application in Engineering*, Springer-Verlag berlin, Heidelberg, 1984.
- Bridges, T. R., and L.C. Wrobel, "A Dual Reciprocity Formulation for Elasticity Problems with Body Forces Using Augmented Thin Plate Splines," *Communications in Numerical Methods in Engineering*, Vol. 12, pp. 209-220, 1996.
- Chakrabarti, P., and A. K. Chopra, "Earthquake Analysis of Gravity Dams Including Hydrodynamic Interaction," *Earthquake Engineering and Structural Dynamics*, Vol. 2, pp.

143-160, 1973a.

Chakrabarti, P., and A. K. Chopra, "Hydrodynamic Pressures and Response on Gravity Dams to Vertical Earthquake Component," *Earthquake Engineering and Structural Dynamics*, Vol. 1, pp. 325-335, 1973b.

Chakrabarti, P., and A. K. Chopra, "Hydrodynamic Effects in Earthquake Response of Gravity dams," *Journal of Structural Division, ASCE*, Vol. 100, No.6, pp. 1211-1224, June 1974.

Chandraseker, R., and J. L. Humar, "Fluid-Foundation Interaction in the Seismic Response of Gravity Dams," *Earthquake Engineering and Structural Dynamics*, Vol. 22, pp. 1067-1084, 1993.

Cheng, A. H.-D., "Effect of Sediment on Earthquake-Induced Reservoir Hydrodynamic Response," *Journal of Engineering Mechanics, ASCE*, Vol.100, No. 7, pp. 654-665, July 1986.

Chopra, A. K., "Reservoir-Dam Interaction During Earthquakes," *Bulletin of the Seismological Society of America*, Vol.57, No. 4, pp. 675-687, August 1967a.

Chopra, A. K., "Hydrodynamic Pressures on Dams During Earthquakes," *Journal of Engineering Mechanics Division, ASCE*, Vol.93, No EM-6, pp. 205-223, December 1967b.

Chopra, A. K., "Earthquake Behavior of Reservoir-Dam Systems," *Journal of Engineering Mechanics Division, ASCE*, Vol. 94, No EM-6, pp. 1475-1500, December 1968.

Chopra, A. K., "Earthquake Response of Concrete Gravity Dam," *Journal of Engineering Mechanics Division, ASCE*, Vol. 96, No EM-4, pp. 443-454, August 1970.

Chopra, A. K., and P. Chakrabarti, "Earthquake Analysis of Gravity Dams Including Dam-Water-Foundation Rock Interaction," *Earthquake Engineering and Structural Dynamics*, Vol. 9, pp. 363- 383, 1981.

Chopra, A. K., and S. Gupta, "Hydrodynamic and Foundation Interaction Effects in Frequency

- Response Functions for Concrete Gravity Dams," *Earthquake Engineering and Structural Dynamics*, Vol. 10, pp. 89-106, 1982
- Dominguez, J., and F. Medina, "Boundary Elements for the Analysis of the Seismic Response of Dams Including Dam-Water-Foundation Interaction Effects. II," *Engineering Analysis with Boundary Elements*, Vol. 6, No. 3, pp. 158- 163, 1989.
- Dominguez, J., and O. Maeso, "Earthquake Analysis of Arch Dams. II: Dam-Water-Foundation Interaction," *Journal of Engineering Mechanics, ASCE*, Vol.119, No.3, pp. 513-530, March 1993.
- Fenves, G., and A. K. Chopra, "Effects of Reservoir Bottom Absorption on Earthquake Response of Concrete Gravity Dams," *Earthquake Engineering and Structural Dynamics*, Vol. 11, pp.809-829, 1983.
- Fenves, G., and A. K. Chopra, "Earthquake Analysis of Concrete Gravity Dams Including Reservoir Bottom Absorption and Dam-Water-Foundation Rock Interaction," *Earthquake Engineering and Structural Dynamics*, Vol. 12, pp.663-680, 1984a.
- Fenves, G., and A. K. Chopra, *Earthquake Analysis and Response of Concrete Gravity Dam*, Earthquake Engineering Research Center, Report No. UCB/EERC- 84/10, U. C., Berkeley, California, 1984b.
- Fenves, G., and A. K. Chopra, "Effects of Reservoir Bottom Absorption and Dam-Water-Foundation Rock Interaction on Frequency Response Functions for Concrete Gravity Dams," *Earthquake Engineering and Structural Dynamics*, Vol. 13, pp.13-31, 1985.
- Fok, K. L., G., and A. K. Chopra, *Earthquake Analysis and Response of Concrete Arch Dam*, Earthquake Engineering Research Center, Report No. UCB/EERC-85/07, U.C., Berkeley, California, 1985.
- Fok, K. L., and A. K. Chopra, "Earthquake Analysis of Arch Dams Including Dam-Water Interaction, Reservoir Boundary Absorption and Foundation Flexibility," *Earthquake Engineering and Structural Dynamics*, Vol. 14, pp.155-184, 1986a.

- Fok, K. L., and A. K. Chopra, "Frequency Response Functions for Arch Dams: Hydrodynamic and Foundation Flexibility Effects," *Earthquake Engineering and Structural Dynamics*, Vol. 14, pp.769-795, 1986b.
- Fok, K. L., and A. K. Chopra, "Water Compressibility in Earthquake response of Arch Dams," *Journal of Structural Engineering, ASCE*, Vol.113, No. 7, pp. 958-975, May 1986c.
- Hall, J. F., and A. K. Chopra, Dynamic Response of Embankment Concrete-Gravity and Arch Dams Including Hydrodynamic Interaction, Earthquake Engineering Research Center, Report No. UCB/EERC-80/39, U. C., Berkeley, California, 1980.
- Hall, J. F., and A. K. Chopra, "Hydrodynamic Effects in the Dynamic Response of Concrete Gravity Dams," *Earthquake Engineering and Structural Dynamics*, Vol. 10, pp. 333-345, 1982a.
- Hall, J. F., and A. K. Chopra, "Two- Dimensional Dynamic Analysis of Concrete Gravity and Embankment Dams Including Hydrodynamic Effects," *Earthquake Engineering and Structural Dynamics*, Vol. 10, pp. 305- 332, 1982b.
- Humar, J., and M. Jablonski, "Boundary Element Reservoir Model for Seismic Analysis of Gravity Dams," *Earthquake Engineering and Structural Dynamics*, Vol. 16, pp. 1129-1156, 1988.
- Humar, J., and M. Roufaiel, "Finite Element Analysis of Reservoir Vibration," *Journal of Engineering Mechanics, ASCE*, Vol. 109, No 1, pp. 215-230, February 1983.
- Jablonski, A. M., J. Humar, "Three Dimensional Boundary Element Reservoir Models for Seismic Analysis of Arch and Gravity Dams," *Earthquake Engineering and Structural Dynamics*, Vol. 19, pp. 359-376, 1990.
- Karur, S. R., G. A. Ramachandran, "Augmented Thin Plate Spline approximation in DRM," *Boundary Elements Communications*, Vol. 6, pp. 55-58, 1995.

- Kotsubo, S., "External Forces on Arch Dams During Earthquakes," *Memoirs Faculty of Engineering, Kyushu University, Japan*, Vol. 20, No. 4, 1961.
- Lotfi, V., Roesset, J. M., and J. L Tassoulas, "A Technique for the Analysis of the Response of Dams to Earthquakes," *Earthquake Engineering and Structural Dynamics*, Vol. 15, pp. 463-490, 1987.
- Maeso, O., and J. Dominguez, "Earthquake Analysis of Arch Dams. I: Dam-Foundation Interaction," *Journal of Engineering Mechanics, ASCE*, Vol.119, No.3, pp. 496-512, March 1993.
- Medina, F., and J. Dominguez, J., "Boundary Elements for the Analysis of Dams Including Dam-water-Foundation Interaction Effects. I," *Engineering. Analysis with Boundary Elements*, Vol. 6, No. 3, pp. 152- 157, 1989.
- Moller, M. and S. Stewart, "An Algorithm for Solving the Generalized Matrix Eigenvalue Problem", *Siam, Journal of Numerical Analysis*, Vol. 10, pp. 241-256, 1973.
- Nardini, D. and Brebbia, C.A., "A new Approach for Free Vibration Analysis using Boundary Elements," *Boundary Element Methods in Engineering*, (Ed C.A. Brebbia), pp 312-326, 1982.
- Nath, B., "Hydrodynamic Pressure on Arch Dams- by a Mapping Finite Element Method," *Earthquake Engineering and Structural Dynamics*, Vol. 9, pp. 117-131, 1981.
- Nowak, P.S., and J.F. Hall, "Arch Dam Response to Nonuniform Seismic Input," *Journal of Engineering Mechanics, ASCE*, Vol. 116, No 1, pp. 125-139, 1990.
- Orhon, M., S. Esendal, and M. A. Kazak, *Dams in Turkey*, Devlet Su İşleri, Ankara, Turkey, 1991.
- Partridge, P. W., "Approximation Functions in the Dual Reciprocity method," *Boundary Elements Communications*, Vol. 8, No. 1, pp. 1-4, 1997.

- Partridge, P. W., C. A. Brebbia, and L. C. Wrobel, *The Dual Reciprocity Boundary Element method*, Computational Mechanics Publications and Elsevier, 1992.
- Permumalswami P. R., and L. Kar, "Earthquake Hydrodynamic Forces on Arch Dams," *Journal of Engineering Mechanics Division, ASCE*, Vol.99, No. EM-5, pp. 965-977, October 1973a.
- Permumalswami, P. R., and L. Kar, "Earthquake Behavior of Arch Dam-Reservoir systems", Proc 5th WCEE, Rome, 1973b.
- Porter, C. S., and A. K. Chopra, Dynamic response of Simple Arch Dams Including Hydrodynamic Interaction, Earthquake Engineering Research Center, Report No. UCB/EERC-80/17, U. C., Berkeley, California, 1980.
- Porter, C. S., and A. K. Chopra, "Dynamic Analysis of Simple Arch Dams Including Hydrodynamic Interaction," *Earthquake Engineering and Structural Dynamics*, Vol. 9, pp. 573-597, 1981.
- Porter, C. S., and A. K. Chopra, "Hydrodynamic Effects in Dynamic Response of Simple Arch Dams," *Earthquake Engineering and Structural Dynamics*, Vol. 10, pp. 417-431, 1982.
- Rashed, A. A., and W. D. Iwan, "Hydrodynamic Pressure of Short-Length Gravity Dams," *Journal of Engineering Mechanics, ASCE*, Vol.110, No. 9, pp. 1264-1283, September 1984.
- Rashed, A., and K. Kandasamy, "A Boundary Element Model of reservoir for the Three-Dimensional Earthquake Analysis of Gravity dams," Proceedings of Fourth U.S. national Conference on Earthquake Engineering, Palm Springs, California, Vol.3, May 20-24, 1990.
- Sharan, S. K., "A Non-Reflecting Boundary in Fluid-Structure Interaction," *Computers and Structures*, Vol. 26, No.5, pp. 821-846, 1987.
- Sharan, S. K., and G. M. L. Gladwell, "A General Method for the Dynamic Response Analysis of Fluid-Structure Systems," *Computers and Structures*, Vol. 21, No. 5, pp. 937-943, 1985.

- Tan, H., and A. K. Chopra, Earthquake Analysis and Response of Concrete Arch Dam, Earthquake Engineering Research Center, Report No. UCB/EERC-95/07, U.C., Berkeley, California, 1995.
- Tsai, C. S., and G. C. Lee, "Arch Dam-Fluid Interactions: by FEM-BEM and Substructure Concept," *International Journal for Numerical Methods in Engineering*, Vol. 24, pp. 2367-2388, 1987.
- Tsai, C. S., G. C. Lee, and R. L. Ketter, "Solution of the Dam-Reservoir Interaction Problem Using a Combination of FEM, BEM with Particular Integrals, Modal analysis, and Substructuring," *Engineering Analysis with Boundary Elements*, Vol.9, pp. 219-232, 1992.
- Tsai, C. S., G. C. Lee, and R. L. Ketter, Solution of the Dam-Reservoir Interaction Problem Using a Combination of FEM, BEM with Particular Integrals, Modal analysis, and Substructuring, National Center for Earthquake Engineering Research, Technical Report NCEER-88-0036, SUNY, Buffalo, 1988.
- Westergaard, H. M., "Water Pressures on Dams During Earthquakes," *Transactions of American Society of Civil Engineers*, Vol. 98, Paper No. 1835, pp. 418-433, 1933.
- Zhang, L., and A. K. Chopra, "Impedance Functions for Three-dimensional Foundations Supported on an Infinitely-Long Canyon of Uniform Cross- Section in a Homogeneous Half-space," *Earthquake Engineering and Structural Dynamics*, Vol. 20, pp. 1011-1027, 1991.
- Zienkiewicz, O. C and B. Nath, "Earthquake Hydrodynamic Pressures on Arch Dam- an Electric Analogue Solution," *Proc. Ins. Civil Engineers, London*, Vol. 25, pp.165-176, 1963.
- Zienkiewicz, O. C. *The Finite Element Method*, McGraw-Hill, New York, NY, USA, 3rd edition, 1977.

REFERENCES NOT CITED

- Antes, H., and O. Von Estorff, "Analysis of Absorption Effects on Dynamic response of Dam-reservoir Systems by Boundary Element Methods," *Earthquake Engineering and Structural Dynamics*, Vol. 15, pp. 1023-1036, 1987.
- Cheng, A. H.-D., O. Lafe and S. Grilli, "Dual-Reciprocity BEM based on Global Interpolation Function", *Engineering Analysis with Boundary Elements*, Vol. 13, pp. 303-311, 1994.
- Chopra, A. K., P. Chakrabarti and S. Gupta, Earthquake response of concrete gravity dams including hydrodynamic and foundation interaction effects, Earthquake Engineering Research Center, Report No. UCB/EERC-80/01, U. C., Berkeley, California, 1980.
- Chwang, A. T., "Hydrodynamic Pressures on Sloping Dams During Earthquakes. Part 2. Exact Theory," *Journal of Fluid Mechanics*, Vol. 87, Part 2, pp. 335-341, 1978
- Chwang, A. T., and G. W. Housner, "Hydrodynamic Pressures on Sloping Dams During Earthquakes. Part 1. Momentum Method," *Journal of Fluid Mechanics*, Vol. 87, Part 2, pp. 335-341, 1978.
- Clough, R.W., J. M. Raphael and S. Mojtahedi, "ADAP: A Computer Program For Static and Dynamic Analysis of Arch Dams," Earthquake Engineering Research Center, Report No. EERC-73/14, U. C., Berkeley, California, 1973.
- Clough, R.W., K.-T. Chang, H.-Q. Chen, and Y. Ghannat, Dynamic Interaction Effects in Arch Dams, Earthquake Engineering Research Center, Report No. UCB/EERC-85/11, U. C., Berkeley, California, 1985.
- Dai, D. N., "An Improved Boundary Element Formulation for Wave Propagation Problems," *Engineering Analysis with Boundary Elements*, Vol. 10, pp. 277-281, 1992.

- Fok, K-L., J. F. Hall and A. K. Chopra, EACD-3D: A Computer Program For Three-Dimensional Earthquake Analysis of Concrete Dams, Earthquake Engineering Research Center, Report No. UCB/EERC-86/09, U. C., Berkeley, California, 1980.
- Ghanaat, Y., and R. W. Clough, EADAP: Enhanced Arch Dam Analysis Program User's Manual, Earthquake Engineering Research Center, Report No. UCB/EERC- 89/07, U.C. Berkeley, California, 1989.
- Hall, J. F., and A. K. Chopra, "Dynamic Analysis of Arch Dams Including Hydrodynamic Effects," *Journal of Engineering Mechanics, ASCE*, Vol.109, No. 1, pp. 149-167, February 1983.
- Hall, J. F.," Study of the Earthquake Response of Pine Flat Dam", *Earthquake Engineering and Structural Dynamics*, Vol.14(2), pp. 281-295, 1986.
- Hanna, Y. G. and Humar, J.L, " Boundary Element Analysis of Fluid Domain," *Journal of Engineering Mechanics Div., ASCE*, Vol.108, No EM2, pp. 436-450, 1982.
- Liu, P. L.-F., and A. H.-D. Cheng, " Boundary Solutions for Fluid-Structure Interaction," *Journal of Hydraulic Engineering*, Vol. 110, No. 1, January 1984.
- Medina, F., J. Dominguez J. and Tassoulas J.L., "Response of Dams to Earthquakes Including effects of Sediments", *Journal of Structural Engineering Div. ASCE 116*, pp.3108--3121, 1990.
- Nath, B., "Natural Frequencies of Arch Dam Reservoir Systems- by a Mapping Finite Element Method," *Earthquake Engineering and Structural Dynamics*, Vol. 10, pp. 719-734, 1982.
- Partridge, P. W., "Technical Note, Dual Reciprocity BEM: Local versus Global Approximation Functions for Diffusion, Convection and Other problems," *Engineering Analysis with Boundary Elements*, Vol. 14, pp. 349-356, 1994.

- Polyzos, D., G. Dassios and D. E. Beskos, "On the Equivalence of Dual Reciprocity and Particular Integral Approches in the BEM," *Boundary Elements Communications*, Vol. 5, pp. 285-288, 1994.
- Saini, S.S., Bettess, P. and Zienkiewicz, O.C.(1978), "Coupled Hydrodynamic Response of Concrete Gravity Dams Using Finite and Infinite Elements," *Earthquake Engineering and Structural Dynamics*, Vol. 6, pp. 363-374,1978.
- Serafim, J., and J. O. Pedro, "Seismic Study of Arch Dams", *Journal of Structural Division, ASCE*, Vol. 91, No. ST2, April 1965.
- Sharan, S. K., "Finite Element Modeling of Infinite Reservoirs," *Journal of Engineering Mechanics, ASCE*, Vol.111, No. 12, pp. 1457-1469, December 1984.
- Singhal, A. C., "Comparison of Computer Codes for Seismic Analysis of Dams," *Computer and Structure*, Vol. 38, No. 1, pp. 107-112, 1991.
- Tsai, C. S., and G. C. Lee, "Far-Field Modeling in 3D Dam-Reservoir Interaction Analysis," *Journal of Engineering Mechanics, ASCE*, Vol.119, No.8, pp. 1615-1631, August 1993.
- Tsai, C. S., and G. C. Lee, "Method for transient Analysis of Three-Dimensional Dam- Reservoir Interaction," *Journal of Engineering Mechanics, ASCE*, Vol.116, No.10, pp. 2151-2172, October 1990.
- Tsai, C. S., Lee, G. C., and R. L. Ketter, "A Semi-Analytical Method for Time-Domain Analyses of Dam-Reservoir Interactions," *International Journal for Numerical Methods in Engineering*, Vol. 29, pp. 913-933, 1990.
- Vaish, A. K., and A. K. Chopra, "Earthquake Finite Element Analysis of Structure- Foundation Systems," *Journal of Engineering Mechanics Division, ASCE*, Vol. 100, No EM-6, pp. 1101-1116, January 1974.

Weber, B., and H. Bachmann, "Efficient Analysis of Dam-Reservoir Interaction in the Time Domain," *Proceedings of the Tenth European Conference on Earthquake Engineering, Balkema, Rotterdam*, pp. 1957-1962, 1995.

Yamada, T., L. C. Wrobel and H. Power, "On the Convergence of the Dual Reciprocity Boundary Element Method," *Engineering Analysis with Boundary Elements*, Vol. 13, pp. 291-298, 1994.

Zang, Y., Y. Cheng and W. Zhang, "A Higher Boundary Element Method for Three-Dimensional Potential Problems," *International Journal for Numerical Methods in Fluids*, Vol. 21, pp. 311-321, 1995.